SIMULATION AND STABILITY STUDIES OF A FIXED BED CATALYTIC REACTOR IN WHICH COMPLEX REACTIONS OCCUR

o-0-o

A thesis submitted for the degree of

Doctor of Philosophy

in

The University of Leeds

by

John Michael Thornton, B.Sc. (Leeds)

under the direction of

C. McGreavy, B.Sc. (Leeds), M.Eng., D.Eng. (Yale), A.M.I.Chem.E., C.Eng., F.B.C.S.

o-0-o

J. M. Thornton

Department of Chemical Engineering,
Houldsworth School of Applied Science,
The University of Leeds,
LEEDS, LS2 9JT.

August 1970

A man would do nothing if he waited until he could do it so well that no one would find fault with what he has done.

CARDINAL NEWMAN.

ABSTRACT

Steady state and dynamic mathematical models of the fixed bed catalytic reactor have been developed for exothermic (or isothermal) reactions which may involve consecutive and parallel steps. At the steady state, it is shown that a one-dimensional model gives an adequate description of the system for most purposes, provided that the overall effective heat transfer coefficient between the fluid and coolant is suitably evaluated.

The models, which are of the continuum type, take account of the heterogeneous nature of the system by modifying the rates of reaction and heat generation at each point in the bed to allow for the effects of transport processes on the performance of individual catalyst pellets. The models of the catalyst pellet have been formulated initially in a fully distributed form, taking account of transport resistances around and within the particles, and are then simplified by lumping the thermal resistance at the boundary between solid and fluid. These simplified models of the pellet are found to give excellent results over all controlling regimes for practical ranges of the system parameters, and are capable of very rapid solution.

The proposed dynamic model of the reactor is one-dimensional and has been used to examine the basic transient characteristics of the system. It is demonstrated that some unexpected difficulties may arise in attempting to control the reactor. In particular, very high peak temperatures may occur when the inlet temperature is reduced. These are specifically associated with the heterogeneous nature of the model.

A method has been developed which is capable of determining the ranges of fluid conditions over which multiple steady states are possible for the catalyst pellet, and it is shown how this may be extended to enable local and global stability to be related under steady and transient operating conditions. Whereas previous work on non-uniqueness in reacting systems has been concerned either with single catalyst pellets, or with quasi-homogeneous reactors subject to axial diffusion effects, the present work enables, for the first time, reactor stability to be studied in terms of the behaviour of the catalyst pellets, without reference to axial diffusion, which is likely to be unimportant in most practical systems.

ACKNOWLEDGMENTS

I am pleased to take this opportunity to acknowledge the help given by many friends and colleagues. In particular, I am grateful to Dr. C. McGreavy for his patience and advice during the period of this research, and for his helpful comments in the preparation of the manuscript.

I would also like to thank Professor G.G. Haselden, for permitting me to carry out this work in the Department of Chemical Engineering, and the Science Research Council for financial support. Thanks are also due to Mrs. J. Murray of the Houldsworth School Library, and to Mr. L. Bailey for his assistance with some of the computation. This manuscript was typed by Miss S. Toon of the Ceramics Department, to whom I am grateful for the excellence of the final product.

Finally I would like to thank my wife, Bridget, for reading the proofs, and for her constant help and encouragement throughout the many anxious periods of this research.

CONTENTS

LIST OF FIGURES

-x-

LIST OF TABLES

CHAPTER 1

INTRODUCTION AND RESEARCH OBJECTIVES

In recent years an increasing amount of effort has been expended in attempting to simulate chemical processes. Simulation has been made possible by the wider availability of electronic computers and the work has been stimulated by the ever increasing cost of experimental work, which is time-consuming and often gives no real insight into the behaviour of the process being examined. This is particularly true of complex systems when strong interaction occurs between some of the physical or chemical phenomena. Such interaction makes optimisation of the process virtually impossible using experimental data only, and satisfactory control strategies must be developed largely by trial and error.

Mathematical modelling, however, is relatively inexpensive and it is possible to perform many simulations in a relatively short time. Moreover, it is necessary to examine at least some of the underlying effects in the process, and this enables a greater understanding of the system to be developed. In general, the more complex the process, the more benefits are potentially available from a successful mathematical model.

It is unlikely that many processes can be completely and accurately modelled without any experimental work being required. When even a simple mathematical model is available, however, it is possible to use calculations from the model to determine the best way of tackling the experimental work so that the maximum benefit can be obtained from the minimum amount of practical work.

If a mathematical model of a process can be developed which is capable of solution in a very short time, then it may be possible to incorporate it into a control strategy designed to improve the profitability of the system, or into an optimisation procedure at the design stage. In general, the initial models of processes are unsuited to this type of use, since they

are primarily designed to provide information about the way the system works, and to examine the dominant processes involved. Once this has been done, it may be possible to use the results to simplify the model to a stage where it can be solved rapidly enough to meet the requirements necessary for on line control or optimisation. Such model reduction has been attempted in a limited way, and only recently have the results begun to look encouraging.[61] Since these reduced models are primarily designed to be put to practical use, it is essential that they are based on realistic and accurate mechanistic models of the process. The wider use of reduced models will, therefore, tend to increase the number of complex models which are necessary, rather than reduce the demand for them.

In the past, chemical reaction engineering has caused considerable problems in both design and operation and has received a corresponding amount of attention in the development of mathematical modelling techniques. It is on heterogeneous systems in general, and the packed bed catalytic reactor in particular, that much of the attention has been focused.

The packed tubular reactor is particularly useful for carrying out exothermic or endothermic catalytic reactions, and has been in widespread use for many years. The reactor normally consists of a number of small diameter tubes, the external surfaces of which are cooled or heated by a flowing or boiling liquid. In the case of endothermic reactions the heat is necessary to keep the reaction going at an acceptable rate, and hence to keep down the size of reactor required for a given production rate, whereas for exothermic reactions the heat removal is necessary either to minimise the production of unwanted by-products, or to prevent overheating, which may cause damage to the reactor or catalyst. This overheating is commonly referred to as "temperature runaway".

One of the major problems with tubular reactors has been the difficulty of predicting the performance of the reactor from mechanistic models, since

these are necessarily complex, and the system is very sensitive to changes in some of the parameters involved. In particular, the addition or removal of heat through the tube walls may set up severe thermal gradients in the radial direction, and since the chemical rate constants are normally highly non-linear functions of temperature, their values may vary by an order of magnitude across the tube radius. This makes it very difficult to work in terms of radial mean values of the state variables, and initially at least, a two-dimensional model of the reactor is necessary. The heterogeneous nature of the system may also cause difficulties, since there are resistances to heat and mass transfer, both around and within the catalyst pellets and this will generally preclude the use of a quasi-homogeneous type of model for the reactor.

Inclusion of the performance of catalyst pellets into a model of the reactor also introduces problems of stability, since, under some conditions, the pellets may be capable of existing in more than one steady state. In these circumstances, a steady state model is insufficient to predict the performance of the reactor, since the state of each catalyst pellet depends on its previous history, as well as on its environmental conditions.

A mathematical model of the complexity needed to describe the effects which have been mentioned is clearly unsatisfactory for use in either optimisation or control and may well require too much computation even for routine design problems. There are, therefore, many difficulties to be overcome before on-line control becomes feasible for reactors of this type, other than by using the conventional 'black-box' type of model. This is in many ways an unsatisfactory type of approach, however, particularly since there may be internal constraints on the operating conditions, such as the maximum temperature, and also because many of the effects in the system are of a distributed nature and may not be capable of analysis using the lumped parameter model.

To try to discover the exact nature of the problems involved in perfectly general terms, is likely to be an impossibly difficult task, because of the large number of degrees of freedom. A more profitable approach is to conduct a series of case studies which, hopefully, will indicate some general properties. The work reported here covers some aspects of such a study and relates to the oxidation of benzene to maleic anhydride, which has the following reaction scheme:-

$$C_6H_6 + 4O_2 \longrightarrow C_4H_2O_3 + CO + CO_2 + 2H_2O$$

$$2C_4H_2O_3 + 5O_2 \longrightarrow 6CO_2 + 2CO + H_2O$$

$$2C_6H_6 + 13O_2 \longrightarrow 8CO_2 + 4CO + 6H_2O$$

These reactions are all highly exothermic and are normally carried out in the presence of a large excess of air. The object of the control strategy would be to maximise the profitability of the whole process, but this could often involve a sub-optimal problem, such as optimising the production rate or yield of maleic anhydride from the reactor itself.

Since the reactions are carried out in a large excess of air, the rate of each reaction can be treated as a function of the concentration of benzene or maleic anhydride only, and the reaction scheme may be regarded as follows:-

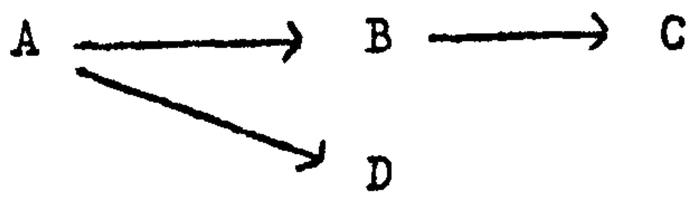

For the reaction scheme previously outlined, it is clear that C and D are the same, but since there may be examples of other reaction schemes where this is not the case, or where B is not the desired product, the scheme shown above will be considered in order to retain as much generality as possible.

The requirements of a mathematical model to be used in design and control are somewhat different. The control model must be capable of very rapid solution, but may only need to be applied over a narrow range of conditions. The design model, however, must have general application over

a wide range of conditions although the solution time is less critical. The control model may be obtained from the design model, using model reduction techniques at present being developed as another aspect of the overall case study.[61]

The basic groundwork for the design model has been done by Cresswell,[35] who confined his attention to developing the numerical techniques suitable for solving the steady state model for the A ——→ B reaction, and to developing some approximation methods for describing the behaviour of catalyst pellets.

The aim of this research is to extend the mathematical models to cover the complex reaction scheme outlined above and to develop a transient model of the reactor. It is also intended to investigate the regions of potential operating difficulties with particular reference to the occurrence of multiple steady states for the catalyst pellet, to determine the conditions under which this can occur, and to examine the implications on the global stability of the reactor.

CHAPTER 2

PREVIOUS WORK AND THE BASIS OF THE PROPOSED MODELS

2.1 General literature

In recent years, a wealth of literature has been published on heterogeneous catalysis and its relevance to reactor design. Among the books covering general aspects of the subject are those by Denbigh[3], Frank-Kamenetskii[53], Thomas and Thomas[54], Satterfield and Sherwood[55], Aris[56], and Petersen[29]. The more notable review articles covering the field are those by Froment[2] and Carberry[57]. A general discussion of the selection and application of mathematical models to chemical reactors has recently been published by Valstar[72].

The methods of obtaining data for the models are not discussed in detail within this thesis, since there have been several excellent reviews published. All the data required in the proposed models (other than kinetic and thermodynamic data) can be found or estimated using information in the books or papers by Satterfield and Sherwood[55], Hougen[1], Beek[62], Carberry[26] and Paris and Stevens[76].

Since the majority of published work has been concerned only with specific aspects of reactor modelling or catalysis, it is convenient to discuss the main body of the work under headings which reveal the structure of the problem and the significance of relevant contributions.

2.2 Single pellet studies

Recent work on the performance of single catalyst pellets has been concerned with non-isothermal systems, particularly those where the rates of reaction are different from those which would be expected from purely kinetic considerations. These variations are normally caused by the transport resistances in the system, and the most general models have been developed to include the following effects:-[35]

(1) A resistance to mass transfer through the pores of the catalyst pellet, expressed by means of an effective pore diffusion coefficient.

(2) A resistance to mass transfer across the boundary layer surrounding the pellet, expressed by means of a film mass transfer coefficient.

(3) A resistance to heat transfer within the pellet, expressed by means of an effective thermal conductivity.

(4) A resistance to heat transfer across the boundary layer surrounding the pellet, expressed by means of a film heat transfer coefficient.

In contrast to these sophisticated models which have become potentially useful since the general availability of electronic digital computers, the early models were relatively simple. The effects of transport phenomena on the performance of catalyst pellets were initially studied to help the experimentalist in his efforts to measure true kinetic rates, so that the kinetic constants might be calculated. It is clearly desirable to measure rates undisturbed by transport effects, and much of the early work was therefore concerned with developing criteria for operating conditions where diffusion is unimportant. It is only comparatively recently that the emphasis has changed towards using models of catalyst pellets in the design of a reactor.

The influence of diffusion (effect (1) above) on the performance of an isothermal catalyst was first examined by Thiele[18] and Zeldowitsch.[19] The studies were extended by Wheeler[19] and by Weisz and Prater[20] who suggested a criterion for avoiding regions where diffusion changed the rate of reaction by more than 5%. Weisz[21,22] also examined non-first order reactions, and developed a criterion for predicting an upper bound on the Thiele modulus, below which the effectiveness factor would vary from unity by loss than a specified amount. These criteria were shown by Schneider and Mitschka[93] to be inappropriate for reactions subject to product inhibition, such as those obeying a Langmuir-Hinshelwood type of rate expression.

However, Hudgins[90] showed that a similar criterion could be developed which is valid for any type of kinetic expression and any order reaction. The criterion reduces to the Weisz-Prater form for first order reactions.

A model of the catalyst pellet which has a non-uniform pore structure was proposed by Mingle and Smith.[82] The pellet was considered to have a system of micro-pores branching from macro-pores, and the authors succeeded in evaluating the effectiveness factor for a single irreversible first order reaction. This type of model is particularly useful for catalysts made by forming powder into pellets. The treatment of Mingle and Smith was extended by Carberry to include reversible[83] and consecutive[84] reaction schemes.

Non-isothermal systems have been studied by a number of authors and in many cases effectiveness factors much larger than unity have been reported (e.g. 26, 30, 33). Wheeler[75] and Prater[23] considered pellets subject to effects (1) and (3) and demonstrated the possible existence of severe thermal gradients. The latter showed that for given surface conditions, the concentration and temperature within the catalyst pellet are linearly related, and that this relationship is independent of pellet geometry and of the form of the kinetic rate expression.

The effect of reaction order in exothermic systems was examined by Tinkler and Metzner[38] who showed that, in general, second order reactions are much less sensitive to temperature than are first order. Østergaard[97] studied the effect of fluid temperature on the apparent reaction rate, and demonstrated that the apparent activation energy can be very sensitive to small changes when the reactions are exothermic. The exothermic case was also studied by Carberry,[26] including for the first time the interphase resistances (effects (2) and (4)). For this work, a numerical procedure was used which was subsequently reported by Carberry and Wendel.[10] The same numerical procedure was also used by Butt[31] in a study of exothermic consecutive reactions in which the interphase resistances were neglected.

The models proposed by Carberry[26] and Butt[31] give rise to simultaneous sets of non-linear two-point boundary value differential equations, the solution of which can only be obtained by finite difference methods. Besides requiring a large amount of computation, the numerical method used to solve the two-point boundary value problems is by no means simple to apply, since convergence of the finite difference representation can only be obtained with care. Neglecting adequate precautions has given rise to the publication of some results of doubtful validity.[31] Even before these models were proposed, it was apparent that a considerable amount of computation would be necessary, and for this reason attempts had already been made to make assumptions which would simplify the model.

The vast majority of published work has been concerned with systems where the interphase resistances (2) and (4) may be ignored. This is unfortunate, since in most practical cases the interphase heat transfer resistance is considerable, and often controls the behaviour of the system. The resistance to mass transfer is relatively small, however,[34] and can often be ignored without serious loss of accuracy. Inclusion of a heat transfer resistance (4) between the phases means that, for most of the published work, it is necessary to find the appropriate surface conditions by an iterative procedure such that they satisfy the boundary condition:-

$$Kp \left.\frac{dTp}{ds}\right|_{s=b} = h(Tf - Tp_{s=b})$$

This clearly adds considerably to the computational effort required to solve pellet models which do not already include this resistance, even if such a solution is feasible. For simple reactions, inclusion of the interphase mass transfer resistance adds no difficulties, since the surface concentration may be found from the heat balance:-

$$h(Tp_{s=b} - Tf) = kc_A(Cf_A - Cp_{A_{s=b}})(-\Delta H_1)$$

Calculation of $Cp_{A_{s=b}}$ (etc.) from $Tp_{s=b}$ for more complex reaction

schemes is not possible, since the rate of heat generation cannot be predicted from one surface concentration. (This point is pursued in Chapters 3 and 4.) In general it can be considered that, for a single reaction, ignoring the interphase resistances means that the proposed pellet model forms only part of a complete model of the pellet and must be solved simultaneously with the appropriate interphase transport equations. In the case of complex reactions, ignoring the interphase transport resistances can only be construed as an attempt at mathematical or model simplification, and must be regarded with suspicion for non-isothermal systems.

Another simplification is to evaluate the performance of the catalyst pellet as if it were isothermal and at the fluid temperature. While such simplifications are not common among the proposers of mathematical models, the results from isothermal cases have been applied to non-isothermal systems,[68,94] without any apparent attempt to use the criterion for negligible heat effects developed by Weisz and Hicks,[30] or indeed any attempt at justification whatsoever.

Several methods of simplification have been proposed, other than the ones mentioned above. Schilson and Amundson[24,25] considered the pellet under non-isothermal conditions, approximating the heat generation function by one or two straight lines. The method was found to be fairly good for the system they considered but is unsuitable for extension to complex reactions where interphase transport resistances are present. Beek[27] considered a system where the interphase heat transport resistance is included. The model can be solved very rapidly, but is based on the assumption that the reaction rate varies linearly with temperature, and this severely restricts the range of application over which the model is valid. Peterson[28,29,92] used the relationship developed by Prater[23] as the basis of an approximation method which is asymptotically valid under conditions of diffusion control, where the reactant concentration falls to zero in the outer layers of the catalyst pellet. This method was extended by McGreavy

and Cresswell[32,33,35] to the case where interphase transport resistances are important. Hatfield and Aris[81] have also used this approach in a general parametric study of the catalyst pellet. Gunn[65] assumed that the temperature profile within the pellet could be represented by a straight line and Tinkler and Pigford[66] allowed for small, but significant, temperature rises by using a perturbation series technique. Both these methods are only useful over a narrow range of conditions.

Numerical computations performed by Cresswell[35] have shown that, over the whole range of practical operating conditions (when the fluid is a gas), the catalyst pellet is essentially isothermal, the temperature rise between fluid and pellet centre being concentrated almost entirely in the interphase region. This result was anticipated by Beek,[27] and also suggested from the results of Hutchings and Carberry.[34] Cresswell[35] proceeded to assume isothermality within the pellet itself, thus allowing analytic solution of the mass transport equation for a first order reaction. This method is attractive, as it was shown to have a wide range of validity and it enables the performance of the pellet to be evaluated very rapidly by solving a single non-linear algebraic equation.

While considerable effort has gone into attempts to simplify description of the single catalyst pellet, a few attempts have been made to relax some of the assumptions on which even the more complex models are based. In particular, the shape of the pellets has received some attention. Most studies reported in the literature have been concerned with spherical pellets, but Aris[40] showed that by using the volume/surface ratio as a characteristic dimension, the asymptotes of effectiveness factor charts (i.e. kinetic control and pore diffusion control) coincided for various shapes. Extensive calculations have been performed by Gunn[41] for finite and hollow cylinders, and by Luss and Amundson[42] for finite cylinders and parallelpipeds. Their results have been summarised and compared by Rester and Aris.[43] Attempts to

simulate the effects of particle shape away from the asymptotes have been made by Rester[44] et al.

Whereas all previous papers had assumed spherical symmetry in the fluid conditions, Copelowitz and Aris[95] considered the behaviour of a pellet situated in steep gradients in the axial direction. Solution of the relevant equations is not straightforward, and introduction of inter-phase transport resistances would increase the difficulty. Moreover, steep axial gradients commonly imply steep radial gradients (in the fluid) and, in this case, not even axial symmetry can be assumed in the fluid phase. It therefore seems unlikely in the foreseeable future that such models will be used in reactor design.

Very little experimental work has been carried out on single catalyst pellets, and the results are somewhat contradictory. This is not surprising since the experimental difficulties are great, particularly in the measurement of intraparticle temperature profiles. Cunningham et al.[85] demonstrated the existence of large temperature differences between the fluid and the pellet centre, and found experimental values of the effectiveness factor as high as 25. Miller and Deans[86] also reported large temperature rises and effectiveness factors greater than unity. Probably the most reliable work on radial temperature gradients was reported by Irving and Butt,[87] who carried out measurements on several pellets using extremely fine thermocouples (0.001 in. diameter). Very large temperature rises across the boundary layer were measured, with relatively small ones occurring within the pellet. This work shows the same features as that of Fulton and Crosser[88] who demonstrated the importance of film resistance by using catalyst pellets of various sizes. They also report the work of Ramaswami,[89] who is alleged to have obtained fluid film temperature rises of up to 420°C.

Transient models of the catalyst pellet have received little attention. McGuire and Lapidus[16] used a transient single pellet model within a transient

model of the reactor. Wei[37] also examined the transient problem and showed that the maximum temperature achieved may be considerably greater than the steady state maximum which is predicted by the Prater[23] relationship.

2.3 Multiple solutions of the catalyst pellet model.

The existence of possible multiple steady states for the catalyst pellet creates considerable difficulties in reactor design and operation, since the performance of the reactor is uncertain unless the history of each pellet is known. The reactor is also likely to be unstable in the transient case, since the pellets tend to change from one state to another under these conditions. Even more important, however, is the fact that the reaction rate at one steady state is often several orders of magnitude greater than at another. This can lead to several undesirable results, such as bad selectivity, catalyst deactivation, or reactor burn-out. The primary motive for determining limits on uniqueness is so that operating conditions can be kept within these bounds, thus avoiding undesirable effects. For models developed which include interphase resistances, there appear to be three possible steady states, of which the middle one is metastable. (Note: There has been evidence published which indicates the possibility of 5 steady states existing.[81] These results lie outside the practical range of operating conditions and occur only over a very narrow range of parameters. In such cases, all the even numbered steady states are metastable.)

As was the case with the single pellet models previously discussed, the vast majority of published literature has been concerned with systems subject to Dirichlet boundary conditions (i.e. no interphase resistances). This is particularly unfortunate, since the results are of no practical use whatsoever. It has already been stated that the Dirichlet formulation of single pellet models is at least potentially useful for single reactions, since this can be solved iteratively to match up with the appropriate

boundary conditions. In the case of multiple solutions predicted by the Dirichlet problem, however, this extension to include boundary effects cannot be done, since each of the steady states corresponds to a different total reaction rate. Now the total reaction rate for a catalyst pellet is given by:-

$$\text{Total rate of consumption of A} = 4\pi b^2 k_{c_A}(Cf_A - Cp_{A_{s=b}}).$$

Each different steady state predicted from the Dirichlet formulation therefore corresponds to a different fluid concentration, and a similar result applies for temperature.

There have been several elegant treatments of the Dirichlet problem but, since they cannot be extended to the Neumann problem, they are of academic interest only. Some of the results obtained from mathematical analyses of the equations are rather surprising. For instance, Copelowitz and Aris[50] have shown that as many as 14 solutions are possible for a first order irreversible reaction, and Horn et al.[96] have shown that some asymmetrical solutions exist in the multiple solution region, even when the pellet is in a constant environment. Aris[39] has reviewed and discussed many of the published criteria in a recent paper.

Of the analyses which have included interphase resistances, Hlavacek[49] et al. considered a system where these were equal for heat and mass transfer (i.e. $Nu' = Sh'_A$). Since the value of Sh'_A/Nu' is commonly of the order of 1000 for real systems, this method is not really of any more use than the solutions of the Dirichlet problem. Cresswell[35] has also worked on the problem where interphase resistances are present, and developed a method for predicting the bounds on the non-unique region for single reactions. The method can be applied to cases where the order of reaction is an integer, or certain fractions for which in integral is tabulated. The method is unsuitable for extension to more complex reaction schemes, and it is not feasible to use it for an analysis of the global stability of the reactor.

2.4 The tubular reactor.

2.4.1 One-dimensional models.

Many of the problems encountered with reactors are due to the high temperature sensitivity of the reaction rate constants. Bilous and Amundson[4] examined the response of an unpacked tubular reactor to a sinusoidal input perturbation, and found that small changes in the system parameters produced large variations in performance. They referred to this phenomenon as 'parametric sensitivity'. The results from a large number of steady state runs were examined by Barkelew, and he suggested that the transient response of the reactor should be stable if the region around the steady state does not display parametric sensitivity. Coste[6] and co-workers examined the sensitivity of the reactor to random fluctuations in the inlet conditions, and defined the sensitivity of the system as the ratio of the standard deviation of the input to that of the output.

Liu and Amundson[7,8] studied the stability of a heterogeneous system in which a reaction occurred on the outer surface of the catalyst pellets. Although account is taken of the transport resistances to the pellet, the model is essentially quasi-homogeneous in character. The reactor was shown to have multiple steady states, and the model was tested to see if the profiles return to their initial steady states after the removal of a perturbation. The models used for these studies were adiabatic, and the latter[8] included the effect of axial mixing. Liu et al.[9] carried out a similar study on the non-adiabatic reactor without axial mixing.

Carberry and Wendel[10] developed a model of the fixed bed reactor which was the first attempt to contain any distributed effects due to the heterogeneous nature of the system. The catalyst model which was used within the reactor model included inter- and intra-phase resistances to mass transfer and an interphase resistance to heat transfer. The results showed that axial diffusion in the reactor is unimportant except for very

short reactors.

A model of the reactor was proposed by Vanderveen et al.,[11] which considered it to be composed of a series of stirred tanks, and the model therefore contains no derivatives in the axial direction. The effect of coupling between pellets was examined. Representing the reactor as a series of stirred tanks is equivalent to writing the differential equations of the continuum model in finite difference form[102] and the continuum and finite stage models can therefore be regarded as intrinsically similar.

The stability of an adiabatic reactor was examined analytically by Crider and Foss,[103] but the reaction was assumed to take place in the gas phase and the packing was considered merely as a heat capacitance. An adiabatic study of stability was also performed by Agnew and Narsimham[104] for a non-catalytic reaction occurring between a solid and a gas. Both these papers[103,104] considered locally linearised rate constants and this, as well as the assumption of adiabatic conditions, severely limits the range of applicability, even for the systems for which they were intended.

2.4.2 Two-dimensional models.

When heat is removed through the walls of a tubular reactor, radial temperature gradients are set up, and these cause radial concentration profiles to develop. The system can therefore only be described in detail by a model which is at least two-dimensional. The first models proposed were concerned with homogeneous or quasi-homogeneous systems. Von Rosenberg[98] described the use of a Crank-Nicholson method for solving the reactor equations and investigated the effect of step sizes in this type of system. Froment[12] also used the Crank-Nicholson method for solving the equations, but in the inlet region a semi-analytic solution was used, to overcome any potential difficulty caused by a singularity at the point $z = 0$, $r = 1$. Beek[62] gives an excellent review of the design of reactors based on quasi-homogeneous models, and also discusses some of the transport effects which

occur in the models. Mickley and Letts[13] extended the model to include multiple reactions with arbitrary rate terms and stoichiometry. An attempt was made to discover the size of yield losses due to radial mixing and failure to withdraw the reactant stream at the points where local yields are at their maximum. A two-dimensional transient model of the homogeneous reactor was solved analytically by Amundson,[79] but since the rate of reaction was assumed to be independent of the concentration and linearly dependent upon temperature, the solution can be considered to be of mathematical interest only.

McGreavy and Cresswell[14,35] proposed a heterogeneous model. The equations describing the behaviour of the system were of a quasi-homogeneous form, but the rate terms were modified at each point in the bed to take account of the influence on the reaction rate of the resistances to heat and mass transfer in and around the catalyst pellets. The results were shown to be significantly different from those predicted by models taking account of pure kinetic rates only. In particular, it was shown that in many cases where the quasi-homogeneous model predicts temperature runaway, the heterogeneous model predicts stable profiles.

In contrast to the continuum models which have been described so far, Deans and Lapidus[15] proposed a mixing cell model in which the reactor is treated as a two-dimensional network of stirred tanks. Each cell has the dimensions of one catalyst pellet and its associated bed voidage. An external surface reaction was assumed. McGuire and Lapidus[16] extended this model to include diffusion and reaction within the catalyst pellets, and the stability with respect to input disturbances was examined. Although this type of model offers certain advantages in the numerical analysis, the computing time was found to be excessive, making it impractical for use on routine problems. Crider and Foss[77] used a mixing cell model to examine a liquid phase non-catalytic reaction occurring under transient inlet

conditions. It was found that sometimes the concentration initially moved in a direction away from the final steady state value. For the system and operating conditions they considered, the effect of axial mixing was found to be small, but radial mixing was almost complete, indicating that a simple one-dimensional continuum model is satisfactory for describing the behaviour of the reactor.

In spite of the apparent differences between the continuum models and the mixing cell models, they are essentially the same, since it may be shown that the latter corresponds to a finite difference representation of the continuum model. Carberry and White[74] considered a two-dimensional model of the reactor for the A $\longrightarrow$ B $\longrightarrow$ C reaction. The model is based on several simplifications relating to the evaluation of the rate of production of the intermediate. In particular, events within the catalyst pellet have been examined in terms of the rate constants evaluated at the fluid conditions, and the heat of reaction of the B $\longrightarrow$ C stage appears to have been ignored. The model is also based on the assumption that radial gradients of concentration do not affect the rate of production of the intermediate, and recent work[61] indicates that there are many cases where this will not hold.

A two-dimensional transient heterogeneous model of the reactor has recently been proposed by Feick and Quon,[99] which is the most comprehensive yet reported in the literature. The model includes radial and axial diffusion of heat and mass in the fluid phase, and resistances to heat and mass transfer in and around the catalyst pellets. Unfortunately the computing time is excessive, about 90 minutes being required on an IBM 360/67. Even this time is optimistic, however, since the step size used in the finite difference network within the catalyst pellet was too large. In fact, the step size was at least eight times as large as that which is required to obtain convergence of the equations under the reactor conditions described,*

* see Appendix 1.

where there was a 200°C temperature difference between the fluid and the pellet centre. The long computing time was unfortunate in that it prevented the authors from carrying out more than one or two runs, and no detailed results are available. At the present time there is therefore little information about the transient behaviour of reactors, except for very special situations, and this information is clearly necessary for a better understanding of the way the system works.

2.5 Concluding comments on previous work.

The widespread use of high speed computers has enabled increasingly sophisticated models of chemical reactors to be solved, and some novel features to be tested. Paris and Stevens[58] have suggested controlling the hot spot by using a cooling jacket in several sections at different temperatures. Calderbank[59] et al. have attempted to optimise the temperature profile through the reactor by diluting the bed with inert pellets. Some of the computations for this were done using a three-dimensional stochastic model, and another stochastic model was proposed by van den Bleek et al.[100]

Although the trend has been towards increasingly complex models, it seems likely that in the future, the emphasis will be on the development of model reduction techniques and the application of models to the design or improvement of practical systems. Hawthorn et al.[101] have shown that it is possible to get good agreement between theory and practice. Model reduction techniques are aimed at reducing the complexity of the system by approximating certain properties by algebraic expressions, while retaining the detailed description which is associated with more complex models. Preliminary attempts have met with some success, and have enabled substantial reductions in computing time to be made.[60,61]

2.6 The assumptions on which the proposed models are based.

(1) The packed bed reactor may be represented by a continuum model.

The packed bed reactor is essentially discrete in character and an exact model would need to describe the fluid on a microscope scale, taking into account the spatial distribution of individual catalyst pellets. A rigorous analysis on this scale, which would take account of the discontinuous nature of the bed, is impossible at the present time. In practice the fluid must follow the random passages in the bed, whereas the chemical reaction occurs only within the catalyst pellets. The problem is therefore best tackled as if the properties of the bed were averaged out to give a pseudo-homogeneous structure. The transport of heat and mass within the bed may then be described in terms of differential equations, using 'effective' transport parameters. (Note: These models are still referred to as heterogeneous, since they distinguish between conditions in the fluid and solid phases. Although the bed properties are space averaged, the equations describing the heat and mass transfer within the catalyst pellet are solved for the actual size of pellet being used.)

(2) The rates of reaction and heat production per unit volume may be calculated at any point in the reactor, as if a catalyst pellet and its associated voidage were acting at that point.

This assumption is necessary as a consequence of assumption (1), although similar assumptions are still necessary for non-continuum models. For example, in the finite stage (mixing cell) models,[15,16] a catalyst pellet is assumed to be situated at the centre of each cell. The assumption implies that every point on the external surface of the catalyst pellet is in contact with fluid of constant composition and temperature and that each point is equally accessible for the purposes of heat and mass transfer.

In practice the concentration and temperature will be non-uniform around individual catalyst pellets, and the resistance to both heat and mass

transfer will increase in the direction of flow. The validity of the assumption is clearly doubtful in the presence of steep gradients, but for most cases it should be a fairly good assumption. If it does not hold, then the profiles within the catalyst pellet will be asymmetrical and solution of the resulting differential equations would be extremely difficult, even if they could be formulated.

(3) The catalyst pellets are assumed to be spherical and of constant size throughout the bed.

If the catalyst pellets are not in fact spherical, it may still be possible to define an effective radius, as is shown by Petersen.[29] If it is not possible to define an effective radius, it may be difficult to set up or solve the appropriate differential equations, particularly if the catalyst pellets have no symmetry.

Having catalyst pellets of non-uniform size present no real problems, provided that each size is known and is confined to a particular section of the bed. For example, it may be desirable to have larger catalyst pellets near the hot spot, since this will tend to slow the reaction down. If the catalyst pellets come in a continuous range of sizes, however, or in a random mixture of specific sizes, greater problems arise, since in general it will be shown that the performance of the reactor is very sensitive to the pellet size. Using the mean value is therefore unlikely to be satisfactory. It may be necessary, in this case, to solve the pellet equations for each size of pellet at each point in the reactor, and then to apply an appropriate weighting factor to each of the results. This process would increase the computation time roughly in proportion to the number of pellet sizes used.

(4) The reactions are irreversible and obey rate expressions of the Arrhenius type:-

$$k_i = A_i \exp\left(-\frac{E_i}{RgTp}\right)$$

This form of the rate expression has been used throughout the present work. There are no problems involved in using other types of rate expression, although it would not be possible to use the simplified pellet model described in Chapter 4, unless the rate of reaction was (approximately) linearly dependent upon concentration.

(5) The reactions may be treated as first order (Chapter 4 only).

This assumption applies only to the method used for simplifying the model of the catalyst pellet, and is not as restrictive as it might appear at first sight. It is only necessary that a pseudo-first order rate constant may be defined, which is valid over the range of concentrations existing within any single catalyst pellet. It is not necessary to define a pseudo-first order rate constant which applies throughout the reactor.

For this reason, all the reactor models have been developed for reactions of any order, whereas the pellet approximation has been developed only for first order reactions.

(6) The rate of reaction along any path depends on the concentration of one reactant only, (i.e. the reactant being consumed in that step), and the reaction scheme may then be represented by:-

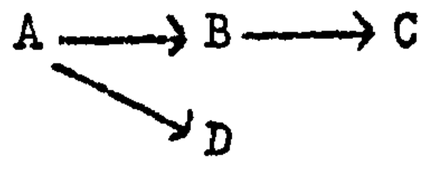

where species A and B are the limiting reactants for the reaction steps in which they are consumed.

This reaction scheme is typical of many reactions of industrial importance. It is often the case that all but one of the reactants involved in a particular step are present in excess. Examples of this are the vapour phase partial oxidation of hydrocarbons, where there may be an explosive (or other) limit on the concentration. (This is often less than 2% in air.)

(7) Diffusion of heat and mass in the axial direction may be neglected.

Carberry and Wendel[10] showed that axial dispersion could be ignored if the bed length is greater than 50 particle diameters, and a similar result was obtained by Marek and Hlaváček.[51] If this assumption is relaxed, the

computational effort required to solve the reactor model increases considerably.

(8) Radial heat transfer within the bed is due only to convection caused by mixing of the fluid stream.

The components which make up the effective radial conductivity of packed beds have been identified by Yagi and Kunii.[70] Kunii and Smith[36] analysed the static components, such as conduction between pellets at the point of contact, and radiation. They developed a complex expression for the total effect of the static components, but this is small compared with the dynamic contribution[1] for conditions found in industrial catalyst beds.

Where temperature runaway is predicted by the models, it is possible that radiation may become important. Since one of the reasons for developing models of the reactor is to help to avoid conditions which lead to temperature runaway, it is not essential to be able to predict exactly what does happen in this case. It is usually sufficient to know that the resulting conditions are undesirable.

(9) All physical and chemical properties are independent of position, concentration and temperature.

This is a fairly common assumption to make in systems of this nature, since in general any errors caused by neglecting variations in the properties are small when compared with the overall errors due to uncertainty in the data. In practice, relaxation of this assumption would introduce few problems for parameters such as the heats of reaction, but more serious problems would arise if the pressure were allowed to vary, since the mass and heat balances must be accompanied by a momentum balance.

There is also some doubt about the validity of assuming constant bed voidage, and if this is not constant, then the velocity, radial conductivity and radial diffusivities will also vary. Thierney[71] has shown that for regularly shaped pellets, the porosity is greatest at about two pellet diameters from the tube wall. The exact distribution of the voidage was

shown to be very dependent upon the ratio of pellet/tube diameters, tho exact shape of the pellets, and tho way in which the tube was packed. For a given mass flowrate the velocity profile will be deformed, since the flow will tend to take place along preferred directions (i.e. where the voidage is highest), and the velocity is reduced in the region of the tube axis. As this is the hottest part of the tube, it is to be expected that in real systems tho conversion will be greater than that predicted using the assumption of plug flow. Valstar[72] imposed a velocity profile on a model of the reactor and suggested that the results were sufficiently different from those obtained for plug flow to warrant further investigation. In the absence of satisfactory data on the actual radial velocity profile likely to arise in any given situation, it is not possible at present to draw any positive conclusions as to the best way to approach this problem. This is particularly true in the presence of heat generation, since this also tends to alter tho velocity profile, as the fluid nearest the axis of the tube expands most. This would tend to counteract the variation in the bed voidage, but since even the order of magnitude of these effects are unknown, any cancellation of errors in this way cannot be relied on. In the light of present knowledge, however, there seems to be little alternative to using the assumption of plug flow.

(10) The coolant temperature is constant along the length of the reactor.

This assumption commonly applies in practice, particularly when the coolant is flowing perpendicular to-the tube axis or when it is a boiling liquid. Relaxation of this assumption introduces no new difficulty, however, since any (known) coolant profile can easily be incorporated into the finite difference solution of the reactor model. When cooling is by co-current flow, a heat balance must be carried out on the coolant, and the same applies to countercurrent-flow, but in the latter case an iterative process is needed, since it is then necessary to assume a coolant temperature

at the reactor inlet ($z = 0$) and then to match the inlet coolant temperature with its known value at the reactor exit ($z = 1$).

(11) In the transient models it is assumed that the catalyst properties are independent of time.

This assumption of no catalyst deactivation etc. would hold well under normal operating conditions, since the transient changes predicted by the model take place over a period of minutes, whereas deactivation usually occurs over a period of days, months or years. An exception to this might be where the model predicts temperature runaway. In this case there is a possibility of rapid deactivation occurring, but it is probably sufficient to know that temperature runaway has occurred and that the transient change which brought it about is undesirable.

2.7 The effect of relaxing the assumptions.

In the event of sufficient information being available, it is clearly possible to relax some or all of the assumptions which have been made in the formulation of the models. In general, dropping each of the assumptions makes the model more complex and increases the computational effort required to reach a solution. An even more important consideration, however, is the large additional quantity of data which is required as the model becomes more complex.

At the present time, very little of the data which would be necessary is available in any general form and much of the information would be extremely difficult to acquire even for specific systems. This may be seen by considering the two examples outlined below.

1. The velocity profile. For a specific system, it may be possible to determine the velocity profiles fairly well over a wide range of conditions and hence to develop some form of algebraic representation. Any results obtained in this way would only apply to the system under consideration and would have no general applicability.

2. The mass transfer coefficient. For a single pellet situated in a flowing fluid, the mass transfer coefficient would be expected to vary around the surface, since there is no reason why the boundary layer should have the same thickness at each point. In general, it could be anticipated that the value would be lower on the downstream side of the pellet, but it would be extremely difficult to devise an experiment to measure the variation in this parameter. It would be practicelly impossible to do so in the presence of other pellets, and a comprehensive model of the pellet would need to take into account such things as variations in flow patterns around the points of contact with other pellets.

The second example is, perhaps, rather extreme but it indicates the kind of difficulties which could arise. Even if the relaxation of assumptions were restricted to parameters or properties which could be measured experimentally for a specific system (such as the radial velocity profile), then the greatest advantage of using mathematical modelling techniques would be lost, since these are primarily designed to reduce the amount of costly experimental work which needs to be done in order to achieve a desired result.

CHAPTER 3

A FULLY DISTRIBUTED STEADY STATE MODEL OF THE CATALYST PELLET

3.1 Introduction.

The equations describing the behaviour of catalyst pellets in terms of the kinetic and transport parameters have been solved for various reaction schemes and boundary conditions. The models originally proposed were for isothermal systems and single first order reactions.[17,18] The isothermal treatment was also applied to more complex reaction schemes,[19] but recently most attention has been focused on non-isothermal systems, since it is for these cases that the tubular reactor is particularly well suited. Among the more recent workers, Butt[31] considered a system of two consecutive exothermic reactions with Dirichlet boundary conditions (i.e. surface conditions are the same as adjacent fluid conditions) and Cresswell[35] considered a single reaction where Neumann (i.e. flux) boundary conditions were used. It was shown by Cresswell that the interphase transport resistances, particularly that for heat transfer, exerted a strong influence on the behaviour of the particle.

All the models of catalyst pellets so far reported in the literature have been inadequate for describing many reactions of industrial importance, either because they have been restricted to simple reaction schemes or have used inappropriate boundary conditions which induce misleading conclusions. The treatment which follows will deal with a reaction scheme of the type:

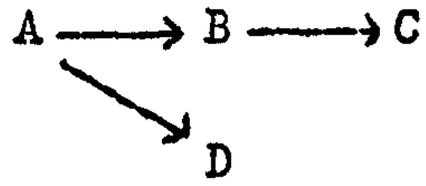

and will include flux boundary conditions.

When the reaction rate constants obey an Arrhenius type rate expression (or any other non-linear form), the resulting mathematical model comprises a set of non-linear differential equations which must be solved by finite

difference techniques. It is to be expected that the solution obtained in this way will require considerable computational effort, and may therefore be too time-consuming to use on a routine basis within a mathematical model of the reactor itself. Nevertheless, the finite difference solution is the only method which can produce an 'exact' solution and must therefore be solved as a standard against which simpler and more approximate methods can be judged.

3.2 Formulation of the Equations.

For the reaction scheme $A \longrightarrow B \longrightarrow C$, $A \longrightarrow D$, three differential equations describing independent heat and mass balances must be solved to determine the behaviour of the system. They are:-

$$\frac{1}{s^2} Dp_A \frac{d}{ds}\left(s^2 \frac{dCp_A}{ds}\right) - k_1 Cp_A^{n_1} - k_3 Cp_A^{n_3} = 0 \qquad (3.1)$$

$$\frac{1}{s^2} Dp_B \frac{d}{ds}\left(s^2 \frac{dCp_B}{ds}\right) + k_1 Cp_A^{n_1} - k_2 Cp_B^{n_2} = 0 \qquad (3.2)$$

$$\frac{1}{s^2} Kp \frac{d}{ds}\left(s^2 \frac{dTp}{ds}\right) + (-\Delta H_1) k_1 Cp_A^{n_1} + (-\Delta H_2) k_2 Cp_B^{n_2} + (-\Delta H_3) k_3 Cp_A^{n_3} = 0 \qquad (3.3)$$

where $k_i = A_i \exp\left(-\frac{E_i}{RgTp}\right)$

These equations are subject to the boundary conditions:-

$$\frac{dCp_A}{ds} = \frac{dCp_B}{ds} = \frac{dTp}{ds} = 0 \quad \text{at } s = 0 \qquad (3.4)$$

$$\left.\begin{aligned} k_{c_A}(Cf_A - Cp_A) &= Dp_A \frac{dCp_A}{ds} \\ k_{c_B}(Cf_B - Cp_B) &= Dp_B \frac{dCp_B}{ds} \\ h(Tf - Tp) &= Kp \frac{dTp}{ds} \end{aligned}\right\} \text{at } s = b \qquad (3.5)$$

Solution of these equations gives the radial profiles of Tp, Cp_A and Cp_B. If it is required to know the total rate of production of species C

or D, this may be obtained by integrating the rate of production throughout the pellet. For example:

$$\text{Rate of production of C} = 4\pi \int_0^b k_2 \, Cp_B^{n_2} s^2 \, ds \qquad (3.6)$$

Once equations (3.1), (3.2) and (3.3) have been solved, k_2 and Cp_B are known functions of position within the catalyst pellet, and this integral may be evaluated by any of the normal methods, such as Simpson's Rule.

Equations (3.1) to (3.3) are most conveniently solved in dimensionless form. They may be rewritten as follows:-

$$\frac{d^2 c_A}{dy^2} - \frac{2}{1-y}\frac{dc_A}{dy} - \phi_1^{*2} c_A^{n_1} - \phi_3^{*2} c_A^{n_3} = 0 \qquad (3.7)$$

$$\frac{d^2 c_B}{dy^2} - \frac{2}{1-y}\frac{dc_B}{dy} + \beta \phi_1^{*2} c_A^{n_1} - \beta \phi_2^{*2} c_B^{n_2} = 0 \qquad (3.8)$$

$$\frac{d^2 t}{dy^2} - \frac{2}{1-y}\frac{dt}{dy} + H(\phi_1^{*2} c_A^{n_1} + H_2 \phi_2^{*2} c_B^{n_2} + H_3 \phi_3^{*2} c_A^{n_3}) = 0 \qquad (3.9)$$

$$\frac{dc_A}{dy} = \frac{dc_B}{dy} = \frac{dt}{dy} = 0 \quad \text{at } y = 1 \qquad (3.10)$$

$$\left.\begin{aligned} \frac{dc_A}{dy} &= \frac{Sh_A'}{2}(c_A - C_A) \\ \frac{dc_B}{dy} &= \frac{Sh_B'}{2}(c_B - C_B) \\ \frac{dt}{dy} &= \frac{Nu'}{2}(t - T) \end{aligned}\right\} \quad \text{at } y = 0 \qquad (3.11)$$

where the dimensionless parameters are defined by:-

$$c_A = \frac{Cp_A}{C_o} \qquad C_A = \frac{Cf_A}{C_o}$$

$$c_B = \frac{Cp_B}{C_o} \qquad C_B = \frac{Cf_B}{C_o}$$

$$t = \frac{RTp}{E_1} \qquad T = \frac{RTf}{E_1}$$

$$y = 1 - s/b$$

$$H = \frac{(-\Delta H_1)\ Dp_A\ C_o\ Rg}{Kp\ E_1}$$

$$\phi_i^{*2} = \theta_i^2 \exp\left(-\frac{E_i}{E_1} \cdot \frac{1}{t}\right)$$

$$\theta_i^2 = b^2 \frac{A_i}{Dp_A} C_o^{n_i - 1}$$

$$Sh_A' = \frac{2bk_{c_A}}{Dp_A} \qquad Sh_B' = \frac{2bk_{c_B}}{Dp_B}$$

$$Nu' = \frac{2bh}{Kp} \qquad \delta = \frac{Dp_A}{Dp_B}$$

$$H_2 = \frac{(-\Delta H_2)}{(-\Delta H_1)} \qquad H_3 = \frac{(-\Delta H_3)}{(-\Delta H_1)}$$

C_o is an arbitrary reference concentration. For the steady state study of the single pellet, this is often the fluid concentration of component A, making $C_A = 1$, whereas for reactor studies it would normally be the inlet concentration of component A.

3.3 Selection of the dimensionless groups.

If approximations to the generalized model are to be used, they must be shown to have validity over a wide range of operating conditions. For complex reaction schemes, the number of variables is clearly too large to enable the whole range of each parameter to be studied. Butt[31] examined a consecutive reaction scheme for which he assumed Dirichlet boundary conditions (i.e. $Nu' \simeq Sh_A' = Sh_B' = \infty$). Even so, the number of parameters made it difficult to draw any general conclusions. With the system of three reactions considered here, and with Neumann boundary conditions, the number of parameters is even greater. The preferred method of approach is to consider specific systems over a wide range of operating conditions.

In the literature, most attention has been given to single first order reactions, and results have normally been presented in terms of the groups

$$\gamma_1 = \frac{E_1}{Rg\ Tf}$$ - the activation factor

$$\beta_1 = \frac{(-\Delta H_1) Dp_A\ Cf_A}{Kp\ Tf}$$ - the thermicity factor

$$\phi_1 = b\sqrt{\frac{A_1 \exp(-\gamma_1)}{Dp_A}}$$ - the Thiele modulus

It may be seen that this is not a very convenient set of parameters for the examination of specific systems, since variation of Tf and Cf_A causes all three dimensionless parameters to change. The extension to the complex reaction scheme is even more unsatisfactory, since 9 dimensionless parameters, ϕ_i, β_i, γ_i (i = 1, 2, 3), vary simultaneously as Tf, Cf_A and Cf_B change.

Using the set of dimensionless parameters suggested in the previous section, the maximum number of parameters is fixed by specifying the catalyst, reaction rate expressions and transport coefficients. This means that for a given reactor operating at a particular flowrate, it would only be necessary to examine the effect of 3 variables, C_A, C_B and T. It will be shown later that the use of θ instead of ϕ has particular advantages in stability analysis.

3.4 Numerical solution of the equations.

Equations (3.7), (3.8) and (3.9) represent a highly non-linear system. The equations are coupled through the exponential dependence of the rate constants on temperature, and the dependence of the rate of production of intermediate, B, on the rate of reaction of species A. Carberry and Wendel[10] demonstrated a method for the solution of equations of this type, in which the derivative terms in both the equations and the boundary conditions are replaced by their central difference approximations. Expressing equations (3.7), (3.8) and (3.9) in this way result in three sets of simultaneous non-linear algebraic equations each having a tridiagonal matrix of coefficients. Matrices of this type may be efficiently inverted by the well known Thomas method described by Bruce.[63]

The non-linear terms are included in the matrix by defining (dimensionless) pseudo-first order rate constants k^*_i (e.g. $\phi_1^{*2}\ c_A^{n_1-1}$) which are allowed to lag one iteration, and the final solution is obtained by iterating on an initial assumed solution. If the reactions are first order it is only necessary to assume a temperature profile. The finite difference solution is examined in detail in Appendix 1.

Great care must be taken in the solution, since it is found that the step size and type of finite difference network necessary to obtain a converged solution depend on the form of the profiles. This means that the problem must be solved twice. The initial solution is an approximate one and in the light of the results an appropriate form of the finite difference network can be chosen. The method is therefore time-consuming and it is not easy to devise an efficient automatic procedure for calculating the correct results.

3.5 The effectiveness factor and selectivity.

The effectiveness factor is defined as the ratio of the actual rate of reaction in the pellet to the kinetic rate calculated at the fluid conditions. For any order reaction this may be written as:-

$$\eta = \frac{1.5\ Sh'_A\ (C_A - c_{A_s})}{\phi_1^2\ C_A^{n_1} + \phi_3^2\ C_A^{n_3}} \qquad (3.12)$$

where $\phi_i^2 = \theta_i^2 \exp\left(-\frac{E_i}{E_1 T}\right)$ (3.13)

and $c_{A_s} = c_{Ay=0}$

The selectivity for reactant B may be defined as the ratio of the rate at which B is produced to the rate at which A is consumed:-

$$\Psi = \frac{Sh'_B\ (c_{B_s} - C_B)}{\delta\ Sh'_A\ (C_A - c_{A_s})} \qquad (3.14)$$

where $c_{B_s} = c_{By=0}$

It has been customary to define η and Ψ in terms of gradients at the pellet surface[31] instead of the interphase transport rates used here. The two forms are equivalent, since they represent opposite sides of the boundary conditions, but evaluation of the gradients introduces additional convergence problems (see Appendix 1) and great care must be taken to ensure that the correct answers are obtained. In general the forms used in equations (3.12) and (3.14) are more convenient to evaluate and since they produce more accurate answers, they will be used throughout the following work.

3.6 Prediction of maximum temperature.

In many practical situations there is a constraint on the maximum temperature which can be allowed to exist within a catalyst pellet. This is usually imposed by the properties of the catalyst itself, such as the conditions under which a phase or chemical change occurs, resulting in deactivation. It is therefore necessary to be able to predict the temperature rise which occurs between the fluid and the pellet centre. Although the actual temperature rise must be calculated from the numerical solution of the differential equations, it is possible to obtain bounds on the maximum temperature rise by inspection of the differential equations and boundary conditions. This has been done for the $A \longrightarrow B$ reaction by Prater[23] who showed that concentration and temperature within the catalyst pellet are related by:-

$$t = t_s + H(c_{A_s} - c_A) \qquad (3.15)$$

For the case where the interphase resistances to heat and mass transfer are zero (i.e. $Nu' = \infty$, $Sh_A' = \infty$), then $c_{A_s} = C_A$, $t_s = T$ and equation (3.15) becomes:-

$$t = T + H(C_A - c_A) \qquad (3.16)$$

This is a maximum when $c_A = 0$,

$$\text{i.e.} \quad t_{max} = T + HC_A \qquad (3.17)$$

Cresswell[35] combined equation (3.15) with a heat balance between the catalyst pellet and the surrounding fluid giving:-

$$t = T + HC_A \frac{Sh'_A}{Nu'} - Hc_A - Hc_{A_s} \left(\frac{Sh'_A}{Nu'} - 1 \right) \qquad (3.18)$$

This expression suffers from the disadvantage that it is required to know c_{A_s} if $Nu' \neq Sh'_A$. This can only be obtained from a numerical solution of the differential equations and any advantage which may be gained from being able to use an expression such as eq. (3.18) is therefore lost. The maximum possible temperature which can be reached is given by:

$$t_{max} = T + HC_A \frac{Sh'_A}{Nu'} \qquad (3.19)$$

It is not possible to extend the relationship between concentration and temperature to cover the system of combined series and parallel reactions, since the ratio of the rates of reaction along the paths A $\longrightarrow$ B and A $\longrightarrow$ D will vary through the pellet as the temperature changes, depending on the point values of ϕ_1^{*2} and ϕ_3^{*2}.

If there are series reactions only (i.e. $\phi_3^* = 0$) it is possible to extend the treatment as follows. The heat and mass balances are described by the equations:

$$\nabla^2 c_A + \phi_1^{*2} c_A = 0 \qquad (3.20)$$

$$\nabla^2 c_B + \phi_2^{*2} c_B - \phi_1^{*2} c_A = 0 \qquad (3.21)$$

$$\nabla^2 t - \phi_1^{*2} c_A H - \phi_2^{*2} c_B H H_2 = 0 \qquad (3.22)$$

These equations can be combined to give:-

$$\nabla^2 (H(1 + H_2) c_A + H H_2 c_B + t) = 0$$

If the concentration and temperature are constant at all points on the external surface, then by the maximum-minimum property[63]:-

$$H(1 + H_2)c_A + HH_2 c_B + t = \text{constant.}$$

i.e. $$t = t_s + H(1 + H_2)(c_{A_s} - c_A) + HH_2(c_{B_s} - c_B) \qquad (3.23)$$

If the interphase transport resistances are zero, then $c_{A_s} = C_A$, $c_{B_s} = C_B$, and $t_s = T$, and equation (3.23) becomes:

$$t = T + H(1 + H_2)(C_A - c_A) + HH_2(C_B - c_B) \qquad (3.24)$$

The maximum value of t occurs when $c_A = 0$ and $c_B = 0$:-

$$t_{max} = T + H(1 + H_2)C_A + HH_2 C_B \qquad (3.25)$$

If the interphase transport resistances are not zero, then equation (3.23) can be combined with a heat balance on the catalyst pellet giving

$$t = T + \frac{Sh'_A}{Nu'} C_A H(1 + H_2) + \delta \frac{Sh'_B}{Nu'} HH_2 C_B - H(1 + H_2)c_A$$

$$-H(1 + H_2)c_{A_s}\left(\frac{Sh'_A}{Nu'} - 1\right) - HH_2 c_B - HH_2 c_{B_s}\left(\delta \frac{Sh'_B}{Nu'} - 1\right) = 0 \qquad (3.26)$$

This equation suffers from the same disadvantage as equation (3.18), namely that the surface concentrations are unknown. These would need to be evaluated numerically if $\frac{Sh'_A}{Nu'} \neq 1$ and $\delta \frac{Sh'_B}{Nu'} \neq 1$. It is, however, possible to calculate an upper bound on the temperature as:-

$$t_{max} = T + \frac{Sh'_A}{Nu'} C_A H(1 + H_2) + \delta \frac{Sh'_B}{Nu'} HH_2 C_B \qquad (3.27)$$

For the combination of series and parallel reactions modified forms of equations (3.25) and (3.27) can be used to give a conservative estimate of the upper bound. They are respectively

$$t_{max} = T + HH^* C_A + HH_2 C_B \qquad (3.28)$$

and $$t_{max} = T + \frac{Sh'_A}{Nu'} C_A HH^* + \frac{\delta Sh'_B}{Nu'} HH_2 C_B \qquad (3.29)$$

where H* is the larger of $(1 + H_2)$ and H_3. In practice, products C and D are often the same, in which case $1 + H_2 = H_3$ and these values of t are

not conservative.

The derivation of the equations in this section involved no assumptions about the pellet geometry, and the results therefore apply to particles of any shape.

3.7 Discussion of the Results.

Fig. 3.1 shows how the effectiveness factor varies with fluid temperature for two typical cases. In region (1) the reaction is kinetically controlled, and as the temperature is increased, the diffusional resistance within the pellet assumes increasing importance (2). For some ranges of parameters (i.e. at high rates of heat generation), it is possible for a region of multiple solutions to exist, in which case the solution in region (3) is metastable and cannot, therefore, be regarded as a solution of any practical importance. At high temperatures, and hence high values of the rate constant, it is possible for the reaction rate to be limited by film mass transfer as shown in region (4). In this region, the surface concentration of reactant falls towards zero and the limiting value of the effectiveness factor may be obtained from equation (3.12) as

$$\eta = \frac{1.5\, Sh'_A C_A}{\phi_1^2\, C_A^{n_1} + \phi_3^2\, C_A^{n_3}} \qquad (3.30)$$

The numerical solution shows that the effectiveness factor does in fact approach very closely to this value in the mass transfer controlled region, and the maximum temperatures agree with the values predicted by the equations in section (3.6). These temperatures are not likely to be realised in practice, however, since the value of t_{max} is often so high that the assumption that radiation can be ignored no longer holds. Nevertheless, an approximate knowledge of t_{max} is useful since it would at least enable the importance of radiation to be assessed, or regions of undesirable operating conditions to be determined.

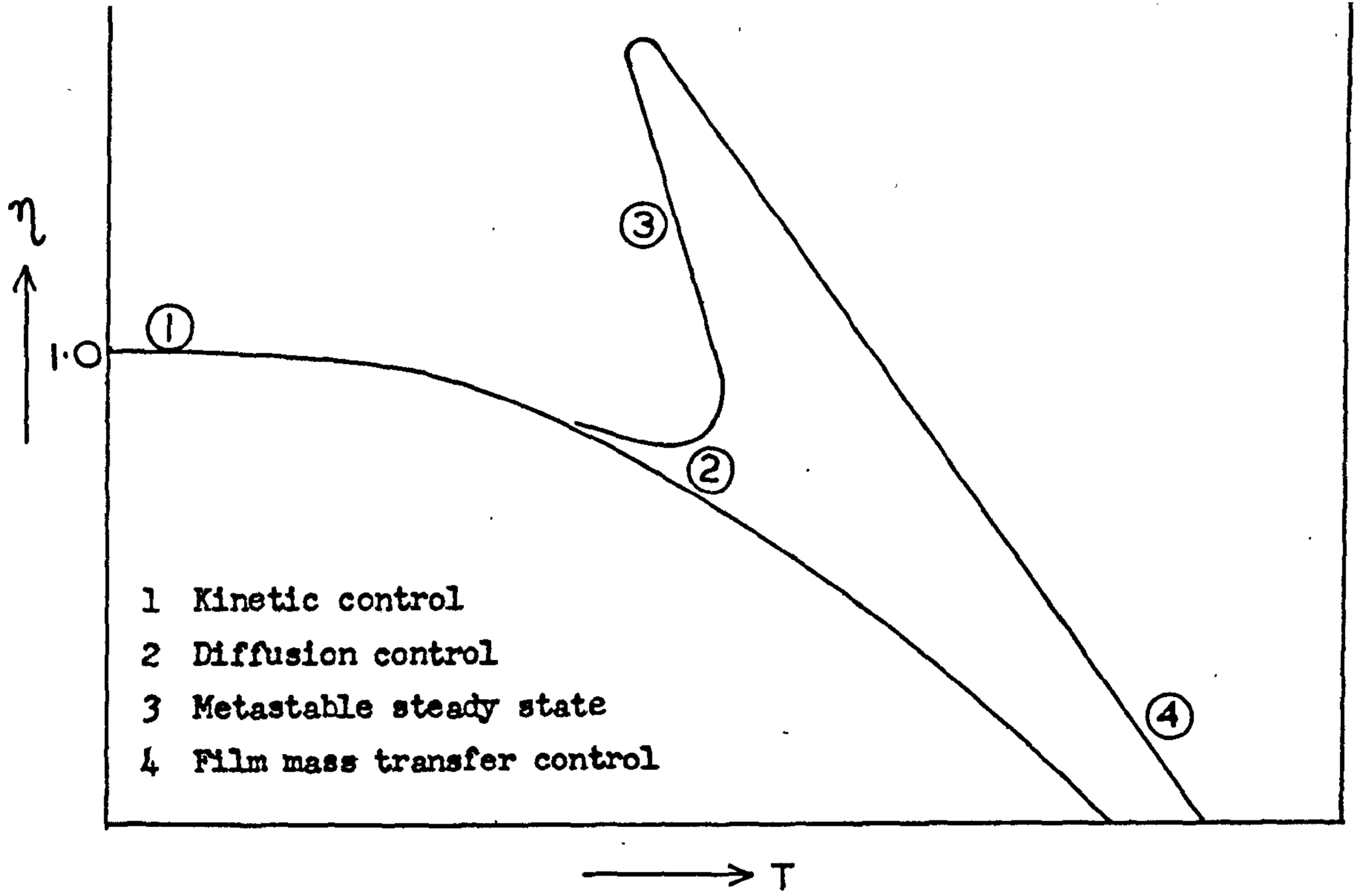

FIG. 3.1 Schematic diagram showing typical relationships between effectiveness factor and fluid temperature for large and small heat effects.

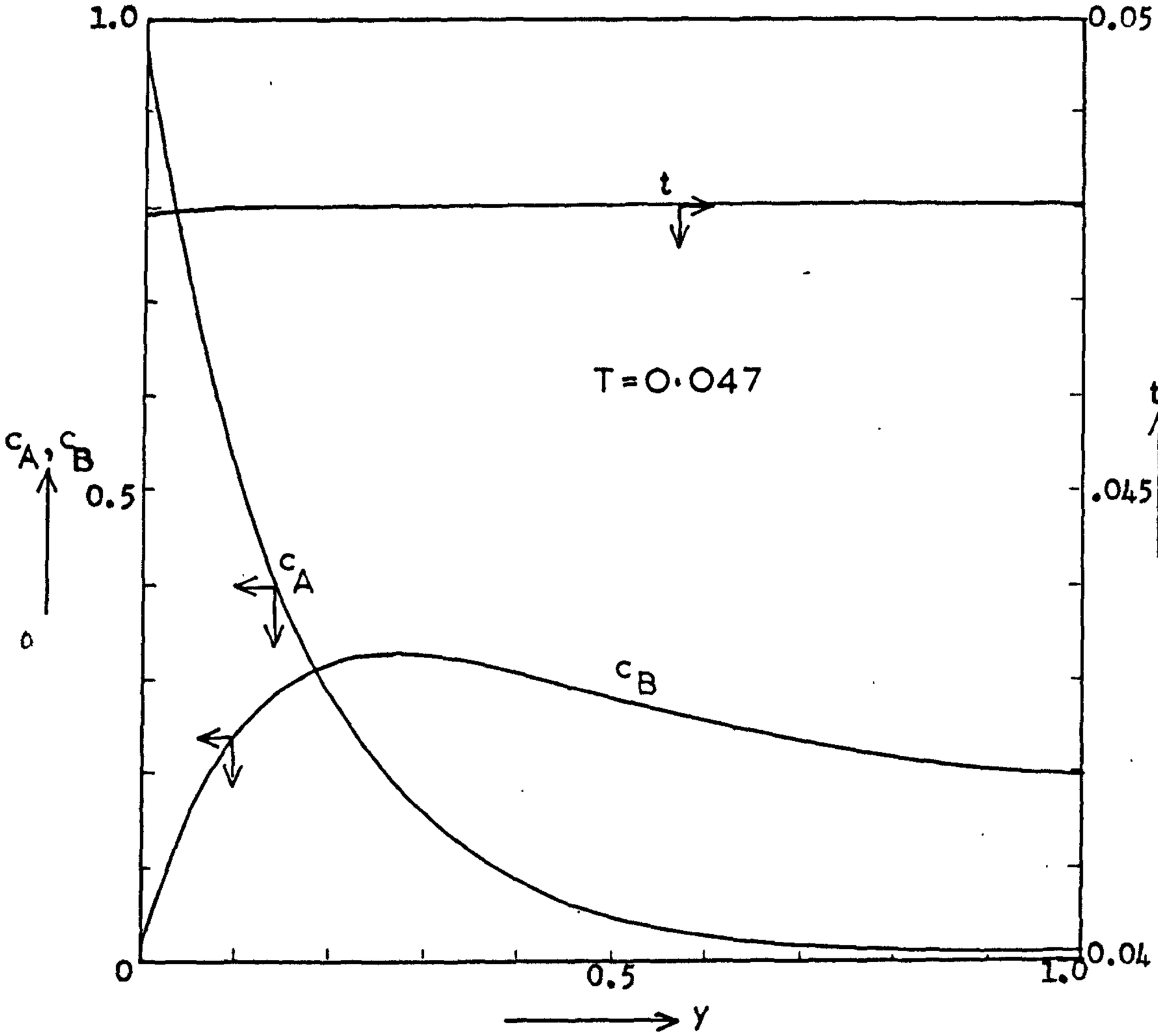

FIG. 3.2 Radial concentration and temperature profiles within the catalyst pellet. Data as given in Table 3.1.

n_i	1.0			
A_1	3.64×10^9	sec^{-1}	θ_1	2.09×10^5
A_2	7.99×10^5	"	θ_2	3.10×10^3
A_3	1.60×10^5	"	θ_3	1.39×10^9
E_1	32	kcal/g.mole	H	6.27×10^{-5}
E_2	21	"	H_2	0.695
E_3	18	"	H_3	1.695
$(-\Delta H_1)$	367	"	E_2/E_1	0.656
$(-\Delta H_2)$	255	"	E_3/E_1	0.563
$(-\Delta H_3)$	622	"	Nu'	1.0
Dp_A, Dp_B	3.66×10^{-3}	cm^2/sec	Sh'_A	500
kc_A, kc_B	4.36	cm/sec	Sh'_B	500
Kp	5.04×10^{-4}	cal/cm/sec/°K	δ	1.0
h	1.2×10^{-3}	$cal/cm^2/sec/°K$	C_A	1.0
C_o	3.82×10^{-7}	$g.moles/cm^3$	C_B	0.0
b	0.21	cm	B_o (1)	6.27×10^{-5}
ρ^* (2)	1.0	g/cm^3	K_T (2)	15.5 ? 1.55 secs.
e^*	0.4			
C_p^*	0.177	cal/g/°K	K_c	4.95 secs.

TABLE 3.1 A typical set of data used in the solution of the catalyst pellet models.

(1) Used in Chapter 4

(2) Used in Chapter 7.

Typical concentration and temperature profiles are shown in Figure 3.2 for the data in Table 3.1. As would be expected, the concentration of species A falls as the distance from the surface increases, whereas the concentration of B rises to a maximum value and then declines. The concentration of B falls since, in the centre of the pellet, species B is reacting to form C but is only being replenished slowly due to the low concentration of A. The temperature is almost constant throughout the pellet, due to the high interphase resistance to heat transfer, and this forms the basis of a simplified model which is discussed in the following chapter.

The simplified model will be shown to give good agreement with the fully distributed model, and to be capable of solution many times faster. It is clearly unprofitable in terms of computer time to pursue an investigation of pellet performance using the more complex model, and this will therefore be deferred until Chapter 4 where the simplified model is developed.

CHAPTER 4

A LUMPED THERMAL RESISTANCE APPROXIMATION TO THE FULLY DISTRIBUTED STEADY STATE MODEL OF THE CATALYST PELLET

4.1 Introduction.

The finite difference solution of the steady state pellet model described in the previous chapter is very time-consuming, requires an excessive amount of computer storage, and involves computational difficulties. The possibility of using an approximation to the fully distributed model is therefore very attractive and several alternatives have been used in the past. Most of the methods have been applied to systems in which the interphase resistances to heat and mass transfer were neglected (i.e. $Sh'_A = Sh'_B = Nu' = \infty$). Schilson and Amundson[24,25] approximated the heat generation function by one or two straight lines, while Gunn[65] assumed that the temperature profile in the pellet could be represented by a straight line. Tinkler and Pigford[66] allowed for small, but not negligible, temperature rises by using a perturbation series technique. Petersen[29] developed an asymptotic method which applies when the reaction is confined to a region near the external surface of the catalyst pellet.

It is clear that the methods used by Gunn and Tinkler and Pigford are only of limited applicability, since in general the heat effects may be large and the system is usually highly non-linear. The method of Schilson and Amundson involves iteration, and if the method is extended to include interphase transport resistances, another unknown quantity (i.e. the surface concentration) enters the problem. Petersen's asymptotic method, however, has been extended[35] to include interphase resistances. For the $A \longrightarrow B$ reaction the temperature and concentration within the pellet can be related in terms of the fluid conditions and the unknown surface concentration. (This has previously been shown - see equation 3.18). The surface concentration may then be obtained by iteration. The method is unsuitable for

either consecutive or parallel reactions. For consecutive reactions there are two unknown concentrations at the surface, and in the case of parallel reactions the concentration and temperature cannot be related since the heat generated at any point within the pellet will depend on the relative magnitudes of the rate constants. An alternative method of approximation has been suggested by Cresswell[35] which is based on the magnitudes of the interphase transport resistances likely to arise in practice. For a typical case, Hutchings and Carberry[34] noted that:

$$\frac{k_{cA}}{Dp_A} \eqsim 1000 \frac{h}{Kp}$$

This implies that most of the resistance to mass transfer is within the catalyst, whereas the heat transfer resistance is concentrated around the pellet, which is then almost isothermal. This has been shown in Figure 3.2. The value of the pellet conductivity, Kp, which was used, is at the lower end of the practical range of values[67] and higher values would make the pellet even closer to isothermality. The effect of varying Kp is shown in Figure 4.1, from which it is apparent that the pellet is isothermal over the whole range of pellet conductivities likely to arise in practice. If the temperature within the catalyst pellet is constant and the reactions are assumed to be first order, then the differential equations describing mass transport within the pellet are linear and may be solved analytically.

An additional assumption is therefore made, namely that the reactions are assumed to be first order with respect to the main reactant at each step, or are capable of being approximated by a first order expression over the range of conditions existing within a single catalyst pellet.

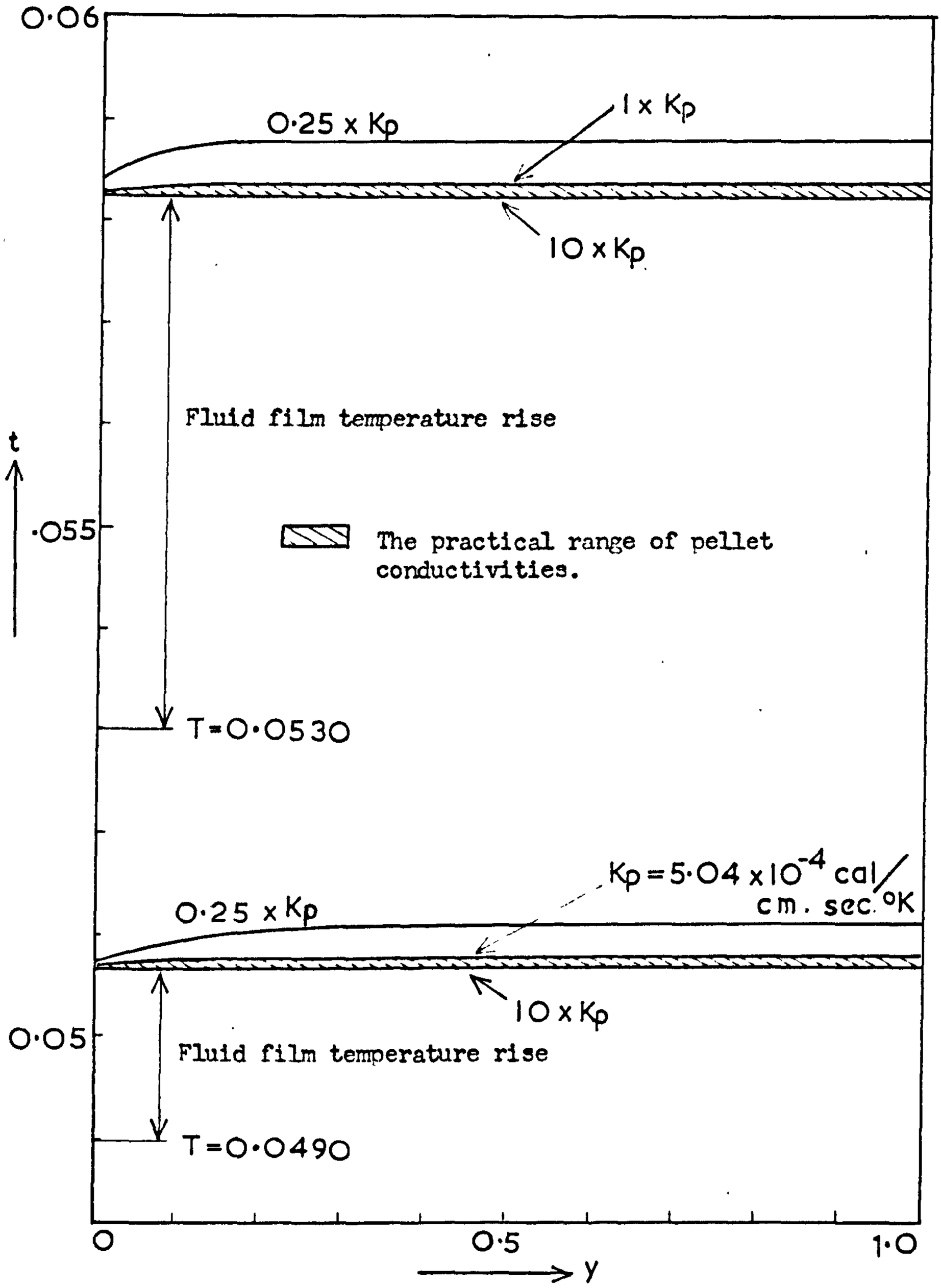

FIG. 4.1. The effect of pellet conductivity on the temperature profile within the catalyst particle. Data as given in Table 3.1.

4.2 The modified equations.

For first order reactions, equations (3.7) and (3.8) become:

$$\frac{d^2c_A}{dy^2} - \frac{2}{1-y}\frac{dc_A}{dy} - (k_1^* + k_3^*)c_A = 0 \qquad (4.1)$$

$$\frac{d^2c_B}{dy^2} - \frac{2}{1-y}\frac{dc_B}{dy} + \delta k_1^* c_A - \delta k_2^* c_B = 0 \qquad (4.2)$$

Subject to the boundary conditions

$$\frac{dc_A}{dy} = \frac{dc_B}{dy} = 0 \quad \text{at } y = 1 \qquad (4.3)$$

$$\left.\begin{aligned} \frac{dc_A}{dy} &= \frac{Sh'_A}{2}(c_A - C_A) \\ \frac{dc_B}{dy} &= \frac{Sh'_B}{2}(c_B - C_B) \end{aligned}\right\} \text{ at } y = 0 \qquad (4.4)$$

where $k_i^* = \theta_i^2 \exp\left(-\frac{E_i}{E_1 t}\right) = \phi_i^{*2}$

If the temperature throughout the pellet is constant, then k_i^* is constant, and the equations are linear and may be solved analytically. The solution gives the concentration profiles in terms of the unknown temperature t, which must be obtained by choosing a value to satisfy a heat balance on the pellet:-

$$B\left(Sh'_A\left(1 - \frac{c_{As}}{C_A}\right)\left(\frac{k_1^*}{k_1^* + k_3^*}(1 + H_2) + \frac{k_3^*}{k_1^* + k_3^*}H_3\right) - Sh'_B\left(\frac{c_{Bs}}{C_A} - \frac{C_B}{C_A}\right)H_2\right) - t + T = 0 \qquad (4.5)$$

where $B = B_o \times C_A$

$$B_o = \frac{(-\Delta H_1)C_o D p_A R g}{2bhE_1}$$

$$c_{A_s} = c_{A_{y=0}}, \quad c_{B_s} = c_{B_{y=0}}$$

4.3 The analytic solution for the concentration profiles.

Defining the variable:-

$$z_A = c_A(1 - y) \qquad (4.6)$$

equation (4.1) may be written as:-

$$\frac{d^2 z_A}{d(1-y)^2} = (k_1^* + k_3^*)\, z_A \qquad (4.7)$$

subject to the boundary conditions

$$z_A = 0 \quad \text{at} \quad y = 1 \qquad (4.8)$$

and

$$\frac{dz_A}{d(1-y)} = \frac{Sh_A'}{2} c_A - z_A \left(\frac{Sh_A'}{2} - 1\right) \qquad (4.9)$$

The general solution of equation (4.7) is

$$z_A = P \sinh\left(\sqrt{k_1^* + k_3^*}\,(1-y)\right) + Q \cosh\left(\sqrt{k_1^* + k_3^*}\,(1-y)\right) \qquad (4.10)$$

where P and Q are arbitrary constants. Applying the boundary conditions (4.8) and (4.9), and rearranging, the solution for c_A may be obtained:-

$$c_A = \frac{F_1}{(1-y)} \frac{\sinh\left(\sqrt{k_1^* + k_3^*}(1-y)\right)}{\sinh\sqrt{k_1^* + k_3^*}} \qquad (4.11)$$

where $$F_1 = \frac{\frac{Sh_A'}{2} c_A}{\frac{Sh_A'}{2} - 1 + \sqrt{k_1^* + k_3^*} \coth\sqrt{k_1^* + k_3^*}} \qquad (4.12)$$

Defining the variable

$$z_B = c_B(1-y) \qquad (4.13)$$

and substituting the r.h.s. of equation (4.11) for c_A, equation (4.1) becomes

$$\frac{d^2 z_B}{d(1-y)^2} - \delta k_2^* z_B = -\delta k_1^* F_1 \frac{\sinh\left(\sqrt{k_1^* + k_3^*}(1-y)\right)}{\sinh\sqrt{k_1^* + k_3^*}} \qquad (4.14)$$

subject to the boundary conditions

$$z_B = 0 \quad \text{at} \quad y = 1 \qquad (4.15)$$

and

$$\frac{dz_B}{d(1-y)} = \frac{Sh_B'}{2} c_B - z_B \left(\frac{Sh_B'}{2} - 1\right) \qquad (4.16)$$

Equation (4.14) is a non-homogeneous linear differential equation. The solution may be obtained by adding a particular solution of the non-homogeneous equation to the general solution of the homogeneous part. The particular solution may be obtained from standard mathematical tables[80]:

$$z_B = - \frac{\delta k_1^* F_1 \sinh\left(\sqrt{k_1^* + k_3^*}(1 - y)\right)}{(k_1^* + k_3^* - \delta k_2^*) \sinh \sqrt{k_1^* + k_3^*}} \qquad (4.17)$$

The general solution of the homogeneous equation is

$$z_B = P \sinh\left(\sqrt{\delta k_2^*}(1 - y)\right) + Q \cosh\left(\sqrt{\delta k_2^*}(1 - y)\right) \qquad (4.18)$$

Adding the right hand sides of equations (4.17) and (4.18), applying the boundary conditions (4.15) and (4.16), and rearranging, we obtain

$$c_B = \frac{1}{(1-y)} \left(F_3 \frac{\sinh\left(\sqrt{\delta k_2^*}(1 - y)\right)}{\sinh \sqrt{\delta k_2^*}} - F_2 \frac{\sinh\left(\sqrt{k_1^* + k_3^*}(1-y)\right)}{\sinh \sqrt{k_1^* + k_3^*}}\right) \qquad (4.19)$$

where $$F_2 = \frac{\delta k_1^* F_1}{k_1^* + k_3^* - \delta k_2^*} \qquad (4.20)$$

$$F_3 = \frac{\frac{Sh'_B}{2} C_B + F_2\left(\left(\frac{Sh'_B}{2} - 1\right) + \sqrt{k_1^* + k_3^*} \coth \sqrt{k_1^* + k_3^*}\right)}{\left(\frac{Sh'_B}{2} - 1\right) + \sqrt{\delta k_2^*} \coth \sqrt{\delta k_2^*}} \qquad (4.21)$$

Although equation (4.19) represents the most general form for c_B, it is not suitable for handling all values of the system parameters, since the denominator of F_2 will be zero if $\delta k_2^* = k_1^* + k_3^*$. By applying Lhôpital's rule, equation (4.19) may be manipulated to give:

$$c_B = \frac{F_5}{(1-y)} \frac{\sinh\left(\sqrt{k_1^* + k_3^*}(1-y)\right)}{\sinh \sqrt{k_1^* + k_3^*}} - F_4 \frac{\cosh\left(\sqrt{k_1^* + k_3^*}(1-y)\right)}{\cosh \sqrt{k_1^* + k_3^*}} \qquad (4.23)$$

where $$F_4 = \frac{\delta k_1^* F_1}{2\sqrt{k_1^* + k_3^*} \tanh \sqrt{k_1^* + k_3^*}} \qquad (4.24)$$

and $$F_5 = \frac{\frac{Sh'_B}{2} C_B + F_4 \left(\frac{Sh'_B}{2} + \sqrt{k_1^* + k_3^*} \tanh \sqrt{k_1^* + k_3^*}\right)}{\left(\frac{Sh'_B}{2} - 1\right) + \sqrt{k_1^* + k_3^*} \coth \sqrt{k_1^* + k_3^*}} \qquad (4.24)$$

It may be seen that

$$c_{A_s} = F_1 \tag{4.25}$$

$$c_{B_s} = F_3 - F_2 \text{ when } k_1^* + k_3^* \neq \delta k_2^* \tag{4.26}$$

or $$c_{B_s} = F_5 - F_4 \text{ when } k_1^* + k_3^* = \delta k_2^* \tag{4.27}$$

These expressions may now be substituted in equation (4.5), the overall heat balance on the pellet. The root of this equation can be found by the Newton-Raphson procedure or by the method of false position. The differentiation of equation (4.5) is rather tedious so the latter method would be preferable. However, the derivative of this equation is required for the work on stability (see Appendix 5), and it is therefore convenient to use the Newton-Raphson method, which in general has better convergence characteristics than the method of false position.

4.4 Comparison of models of the catalyst pellet.

Figures 4.2 to 4.5 show how the lumped thermal resistance model, and two other models which have been commonly used in the past, compare with the fully distributed model described in the previous chapter. These graphs show the effect of fluid temperature on the effectiveness factor and selectivity. The first two are drawn for $C_B = 0$ and the second two for $C_B = 1$.

It is apparent that the curves, numbered (1) on the graphs, which correspond to overall isothermality, and the curves, numbered (2), which correspond to no interphase heat or mass transfer resistances ($Nu' = Sh_A' = Sh_B' = \infty$) show completely different characteristics from curves (4) which are obtained from the solution of the fully distributed model. The curves numbered (3), however, show very close agreement with (4) over the whole range of regimes from kinetic control to film mass transfer control.

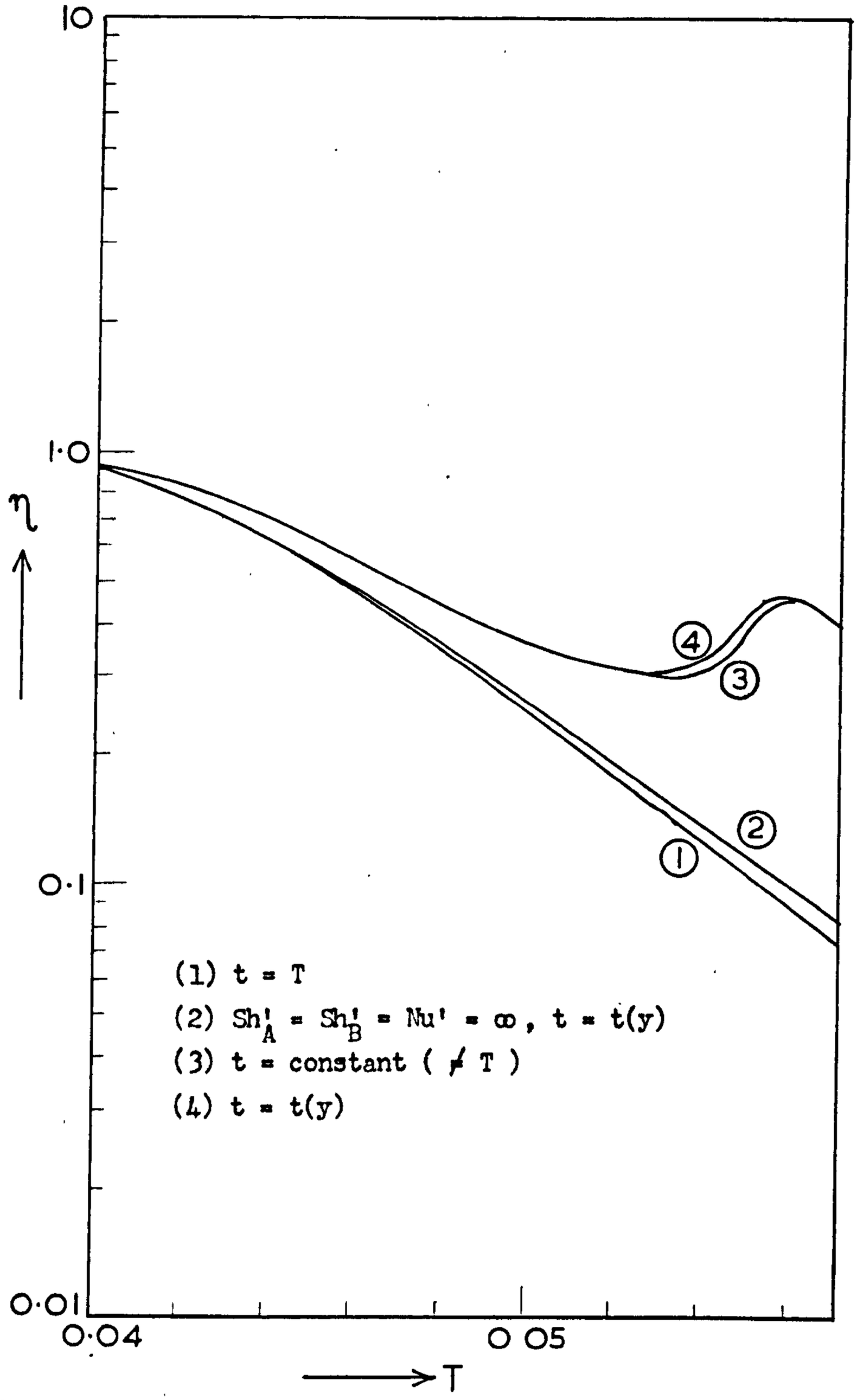

FIG. 4.2. Comparison of effectiveness factor predicted from various models of the catalyst pellet. Data as given in Table 3.1. $C_B = 0$.

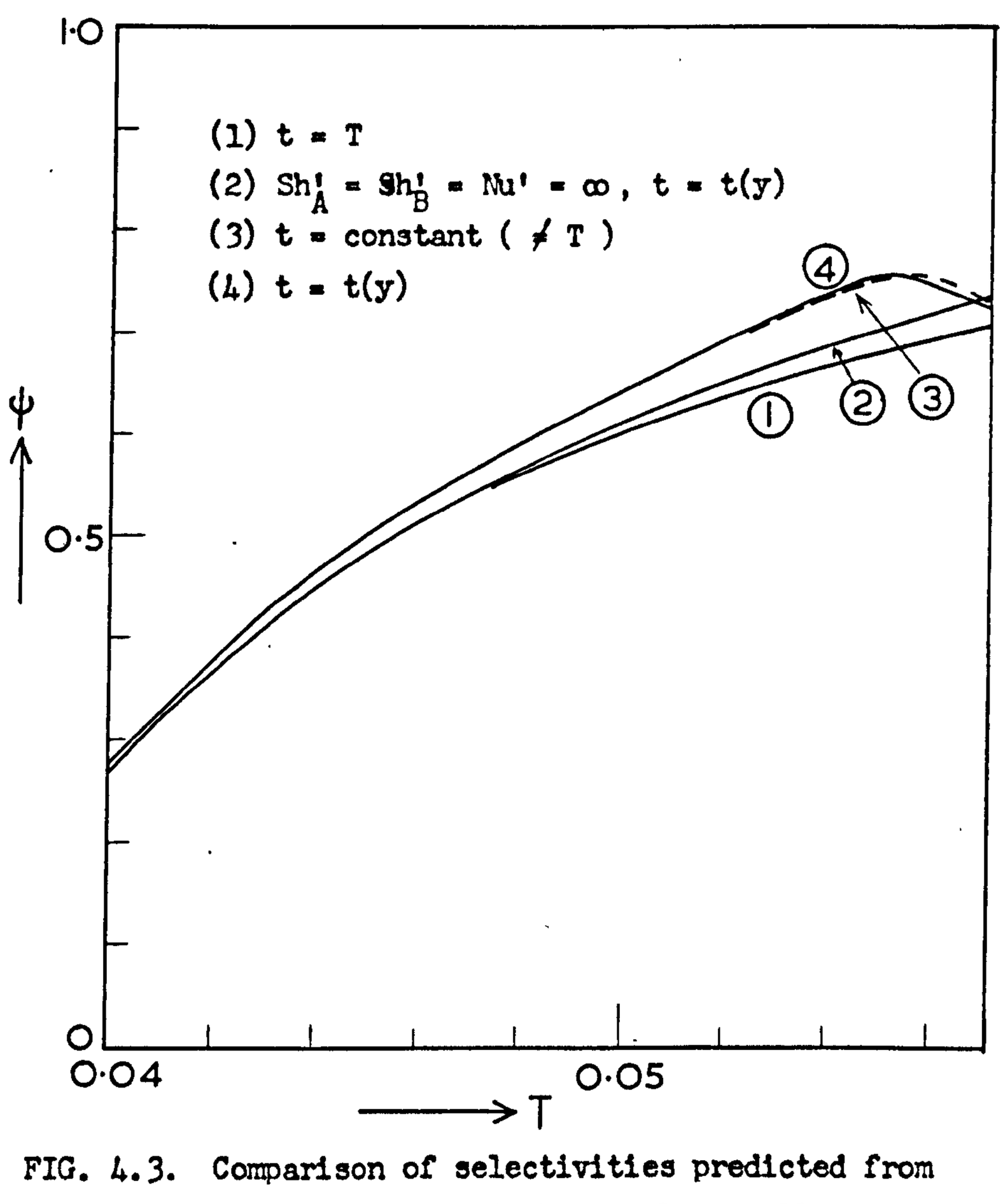

FIG. 4.3. Comparison of selectivities predicted from various models of the catalyst pellet. Data as given in Table 3.1. $C_B = 0$.

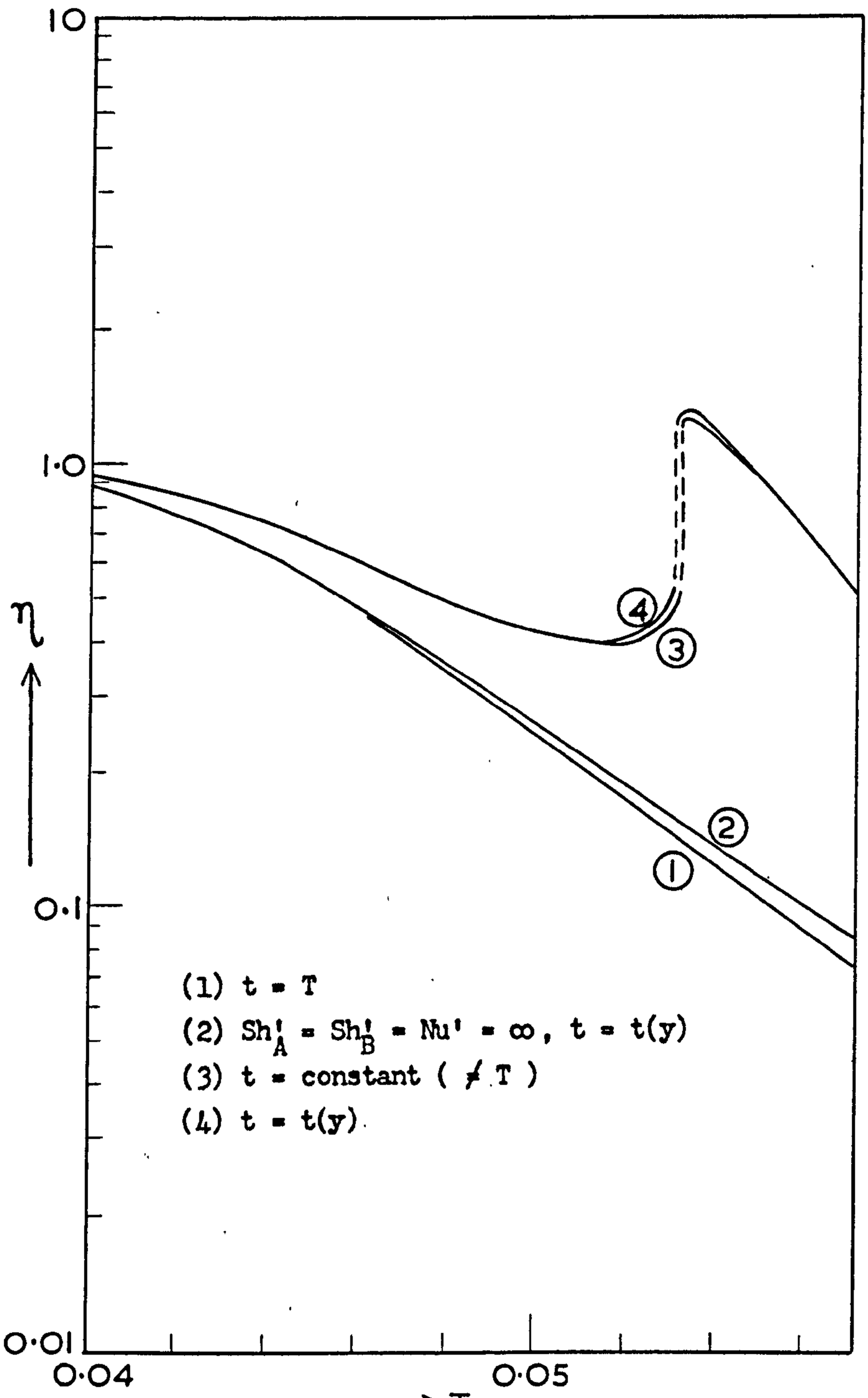

FIG. 4.4. Comparison of effectiveness factors predicted from various models of the catalyst pellet. Data as given in Table 3.1. $C_B = 1.0$.

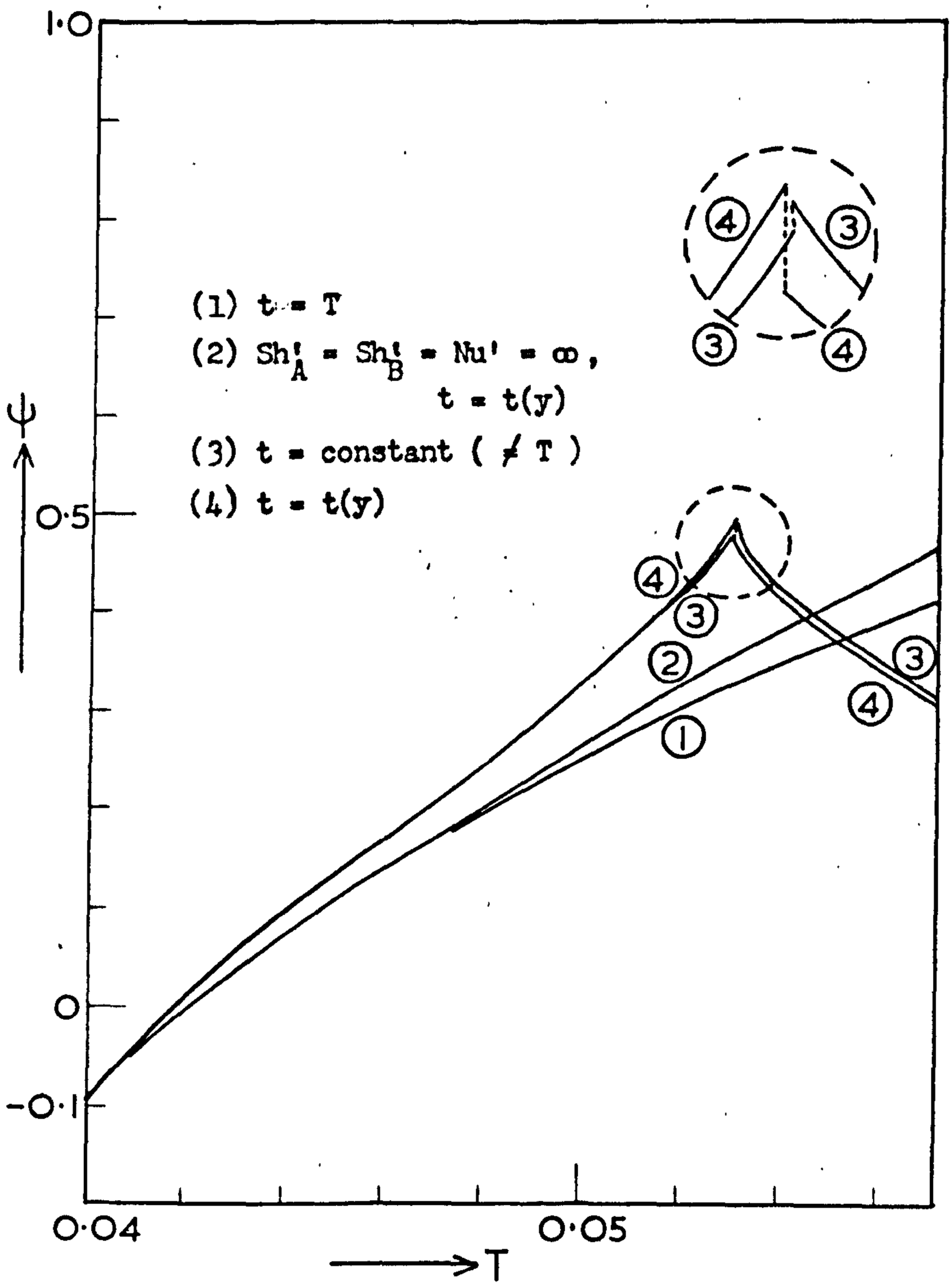

FIG. 4.5. Comparison of selectivities predicted from various models of the catalyst pellet. Data as given in Table 3.1. $C_B = 1.0$.

Not only is the lumped thermal resistance model simple to use, in that there are no numerical difficulties, but the method also has the additional advantages of being capable of solution in a very short time (about one fortieth of the time required for the fully distributed model), and of requiring only a small amount of computer storage.

(Note: There may be no apparent justification for including the overall isothermal model (curves (1)) in a critical comparison with other models, since it has never been directly stated that this model could be used for exothermic systems. Nevertheless, results for isothermal models have been quoted[68] in justifying the conclusions drawn from kinetic experiments and these curves are therefore included for the sake of completeness. Models corresponding to curves (2) have been used in the majority of published literature.)

4.5 The influence of transport resistances on the behaviour of the catalyst pellet.

When a reaction is occurring within a catalyst pellet, the reactant must be replenished by transfer from the surrounding fluid. This process occurs by diffusion across the boundary layer and through the catalyst pores, and can only occur in the presence of a concentration gradient. The concentration within the pellet is therefore always lower than in the fluid phase and this tends to cause the reaction rate to fall below the value calculated at the fluid conditions. At low temperatures (and hence low reaction rates) the decrease in concentration is small, but as the temperature increases, so does the concentration gradient and the actual reaction rate tends to deviate from the kinetic rate by an increasing amount. In Figure 4.6, this effect causes the kinetic or quasi-homogeneous curve (1) to change to a position corresponding to curve (2). (As is normal in work of this kind, the actual rate is most conveniently expressed using the effectiveness factor (η) which is the ratio of the actual rate to the

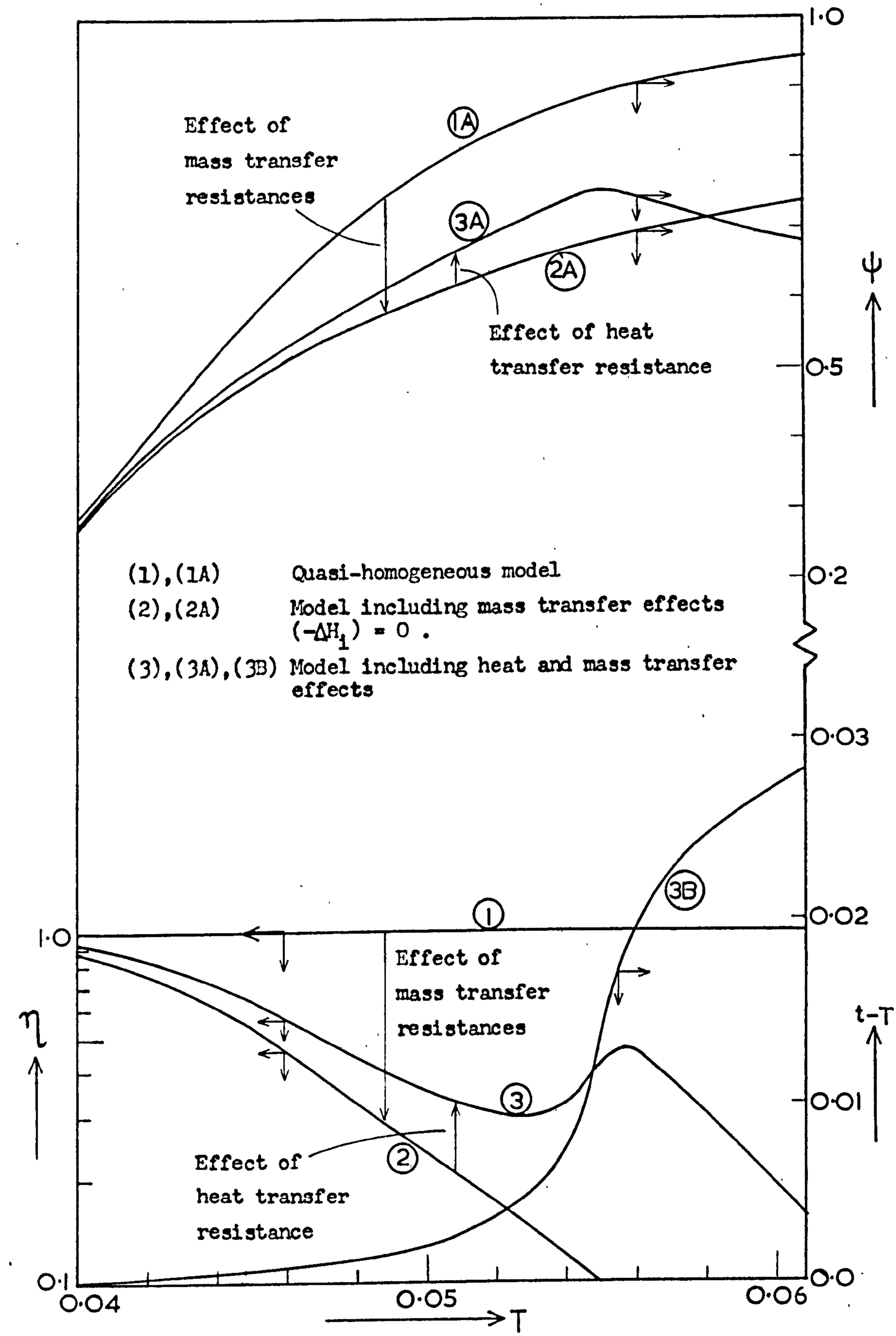

FIG. 4.6. An example of the influence of heat and mass transfer effects on the behaviour of the pellet at various fluid temperatures. Data as given in Table 3.1 .

kinetic rate - see Equation 3.12.)

In the case of exothermic reactions, a temperature difference must be set up so that heat can be removed from the pellet. This increase in temperature, to a value above that existing in the fluid phase, tends to cause the reaction rate to rise above the value calculated at the fluid conditions. These concentration and temperature effects therefore act in opposite directions and it is found that either may predominate, depending on the parameters in the system. In Figure 4.6 for example the temperature effects cause curve (2) to change to a value corresponding to curve (3).

The selectivity for species B is decreased by the presence of mass transfer resistances, since these will hinder the escape of B into the surrounding fluid and some will then be destroyed by reaction. This causes curve (1A) in Figure 4.6 to change to (2A). The effect of the heat transfer resistance on the selectivity is not quite as straightforward, however, since even the quasihomogeneous selectivity may increase or decrease as the temperature changes, depending on the relative magnitudes of the activation energies for the different reaction steps. The quasihomogeneous selectivity is defined by the expression

$$\psi = \frac{k_1' C_A - k_2' C_B}{(k_1' + k_3') C_A}$$

If the values of the activation energies are such that an increase in temperature tends to increase the quasihomogeneous selectivity (as is the case in Figure 4.6), then the inclusion of a heat transfer effect will also increase the selectivity over some of the temperature range. Beyond a certain temperature, however, (corresponding to strong diffusion influence, or external mass transfer control), the thermal resistance reduces the selectivity. In this region the increasing temperature does not provide any more of species B since A is already reacting as fast as it can be supplied across the surrounding fluid film, but the rate constant for the

consumption of B continues to rise and less can therefore escape from the catalyst pellet before reacting to give the undesirable product C. This is illustrated by curve (3A) in Figure 4.6.

If the values of the activation energies are such that an increase in temperature reduces the quasihomogeneous selectivity, then inclusion of the heat transfer resistance will always reduce the selectivity below the isothermal value.

As would be expected, the temperature difference between the pellet and surrounding fluid increases as the fluid temperature increases. This is shown by line (3B) of Figure 4.6. It is apparent that in the region of maximum selectivity the pellet temperature is very sensitive to changes in fluid temperature. In practice, there will often be a constraint on the maximum permissible pellet temperature and this may limit the range of operating conditions and the maximum selectivity that can be obtained in specific systems.

4.6 The influence of some of the parameters of the model.

In models such as the one considered here, it is difficult to draw general conclusions about how the system behaves, since many of the effects are coupled together, and they may operate in opposite directions. The highly non-linear nature of the kinetic rate expressions, as given by the Arrhenius type of equation, means that the dominant effects may change rapidly with small changes in the system parameters, and it is therefore hazardous to attempt to extrapolate results, and in some cases it may even be dangerous to interpolate. However, since there are so many parameters involved in the model, it is essential to attempt to examine the behaviour of the system in some methodical way which does not involve covering all possible sets of values of the dimensionless groups. This examination is best carried out using the 'case study' approach, where a realistic set of parameters is chosen and the behaviour predicted by the model is examined

as one or more dimensionless group is varied at a time. The advantage of this approach is that only a finite amount of computing is necessary, and provided that care is taken, both in the selection of the data and in physical consideration of the system, it should be possible to demonstrate most of the phenomena which could occur if all possible sets of data were to be run. Although it is normal to investigate the influence of state variables and physical parameters separately, this is not convenient for the present study, since in particular B is a combination of a state variable and physical parameters.

Figure 4.7 shows the effect of varying parameter B when $C_B = 0$. Now $B = \frac{(-\Delta H_1)\, Cf_A\, DpA\, Rg}{2\, b\, h\, E_1}$, and since all its constituents, besides Cf_A and h, occur in other dimensionless groups, changing B alone amounts to examining the effect of $\frac{Cf_A}{h}$. In physical terms, this means that the same pellet temperature, t, would result if either the amount of heat available were doubled or if the resistance to heat escaping (i.e. $\frac{1}{h}$) doubled.

The graph shows that over some parts of the range of B, the pellet performance is very sensitive to changes in any of the parameters of the system. At high values of B there is also a tendency for multiple solutions of the pellet model to exist over certain ranges of fluid temperature. These effects are undesirable at any point in a reactor since if multiple steady states exist, a steady state reactor model is insufficient to predict the performance of the reactor, which would then also depend upon the history of each of the catalyst pellets. This problem is discussed in more detail in Chapter 9. The existence of multiple solutions and regions of high sensitivity are clearly due to the increasing difference between the temperatures of pellet and fluid, caused by increasing Cf_A or decreasing h, since in an isothermal system the effectiveness factor is independent of concentration.

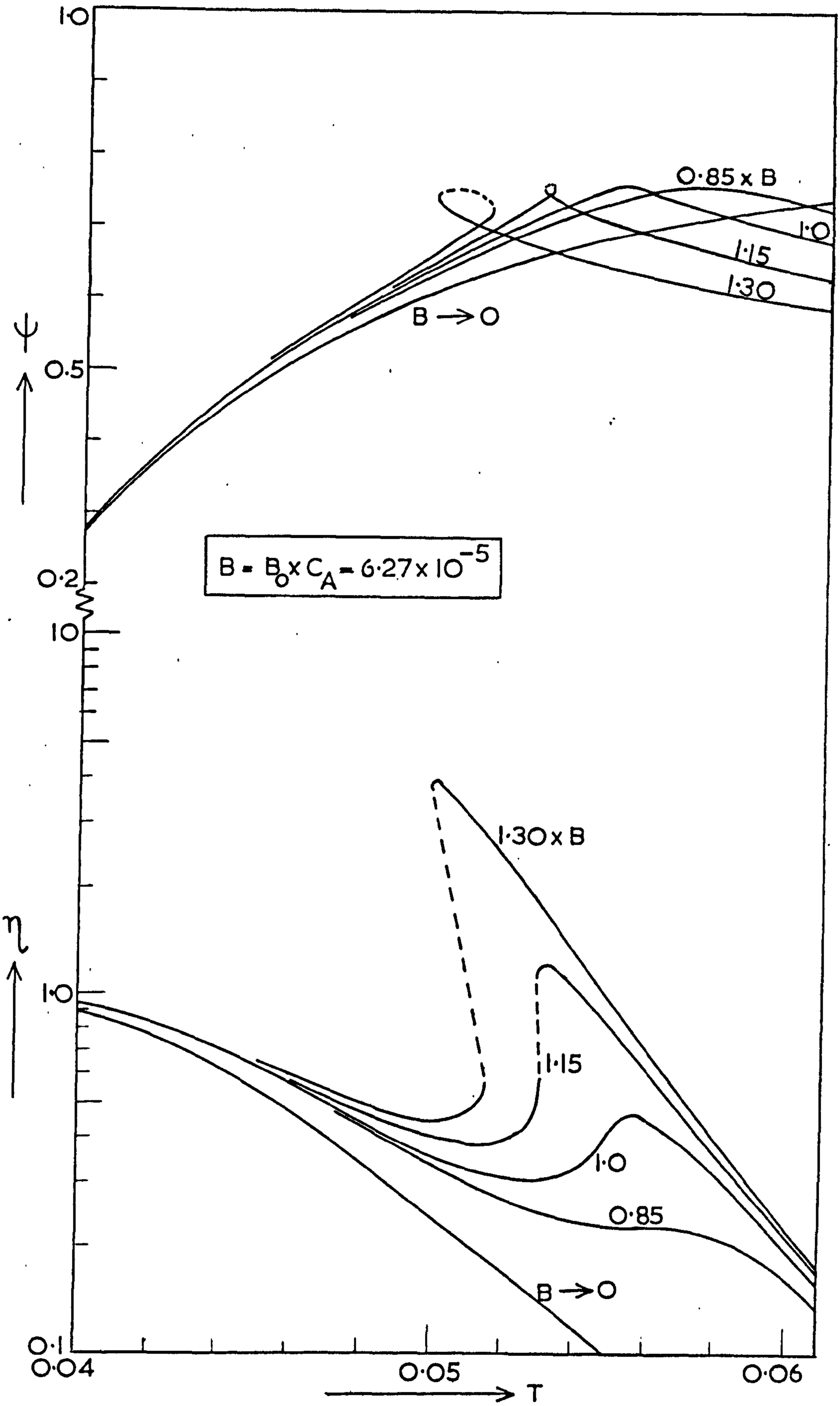

FIG. 4.7. The effect of the value of parameter B on the effectiveness factor (η) and selectivity (ψ) at various fluid temperatures. Data as given in Table 3.1 .

In the kinetically controlled region (i.e. at low fluid temperatures) a high value of selectivity is favoured by increasing the temperature, and therefore increases as parameter B increases. In the higher range of fluid temperatures, where the conversion rate of species A is controlled by interphase mass transfer limitations, changes in the pellet temperature have no effect on the rate at which A is consumed, whereas the rate constant for the consumption of B rises with increasing pellet temperature. This means that a decreasing proportion of B then manages to escape into the fluid phase before further reaction occurs giving the undesired product C. The selectivity therefore falls as the value of B increases.

Since, over much of the range of T, the behaviour of the pellet is sd sensitive to B (and hence to h), it appears to be necessary to obtain the value of the heat transfer coefficient to a much better accuracy than is generally available from correlations in the literature. Whether this is in fact necessary will depend upon the conditions existing in the reactor and on the part of the curve on which these conditions lie. Clearly under conditions of kinetic or mild diffusion control the value of η is not very sensitive to B and the normal correlations may be sufficiently accurate. This aspect will be discussed in the chapter on the one-dimensional steady state reactor model.

Figure 4.8 shows the effect of an increase in the concentration of species B in the fluid phase. If the reaction B $\longrightarrow$ C was isothermal, the effectiveness factor would be independent of C_B, and any change in η which does occur in the non-isothermal case is therefore initiated by the additional heat produced by this reaction. The heat generated by this reaction would, in fact, increase the heat generated by all the reactions since each of the reaction rates would be increased by the higher pellet temperature. It can be seen from the graph that increasing C_B raises the sensitivity of the system and also makes the existence of a multiple solution

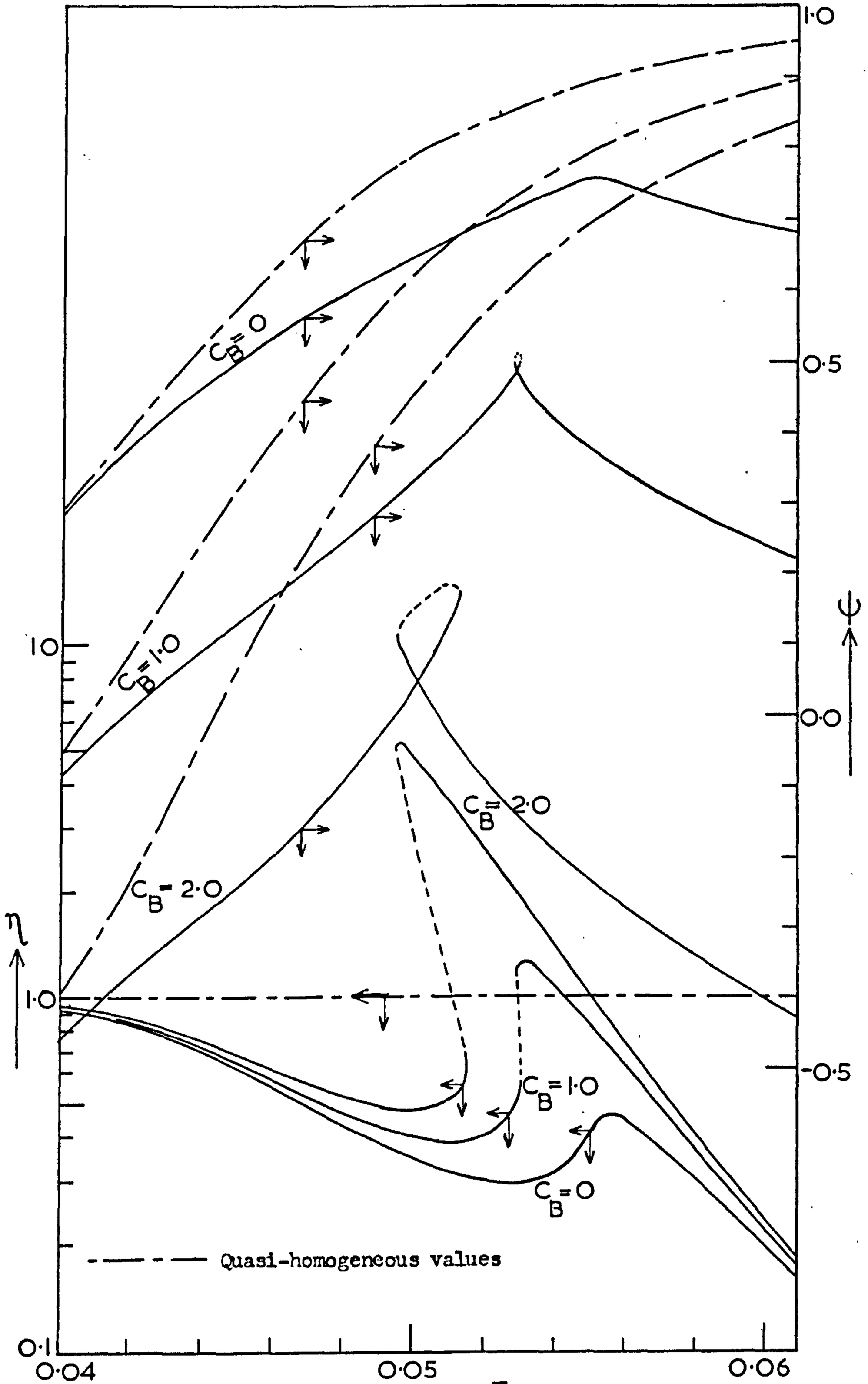

FIG. 4.8. The effect of the concentration of species B on the effectiveness factor (η) and selectivity (ψ) at various fluid temperatures. Data as given in Table 3.1.

region more likely.

Whereas the effectiveness factor is exclusively a reflection of the heterogeneous effects in the system, the selectivity is not, since its value arises also as a consequence of the kinetic and concentration effects in the system. In Figure 4.8 the broken lines for ψ show these quasi-homogeneous effects, and the continuous lines are drawn for the heterogeneous model. The distance between the broken and continuous lines is therefore a measure of the effect of heterogeneity on the selectivity. As was previously the case, the selectivity is adversely affected by the heterogeneous effects and this becomes increasingly so as the fluid temperature rises. In the quasi-homogeneous case, high concentration of B leads to poor selectivity and this is also true in heterogeneous systems. Moreover, increasing concentration of B lead to higher temperature differences across the fluid film at the pellet surface, and interphase mass transfer control occurs at decreasing fluid temperatures, again resulting in poor selectivity.

The effect of the external film resistances to mass transfer (i.e. $\frac{1}{Sh'_A}$, $\frac{1}{Sh'_B}$) is illustrated in Figure 4.9. As would be expected, the lower the value of Sh'_A and Sh'_B, the lower the temperature at which they become important. In the mass transfer controlled region, the quantity of heat generated within the catalyst pellet is increased by increasing the Sherwood numbers, and this makes the pellet less sensitive to changes in the fluid temperature. As a result, high values of Sh'_A, Sh'_B stabilise the film mass transfer controlled region, which can then exist at lower fluid temperatures. This also has the effect of making the existence of multiple steady states more likely. The effect of Sh'_A and Sh'_B on the selectivity appears to be small unless the values are very low in which case ψ is decreased due to the difficulty which species B has in escaping into the fluid phase before reacting along the path B ——→ C.

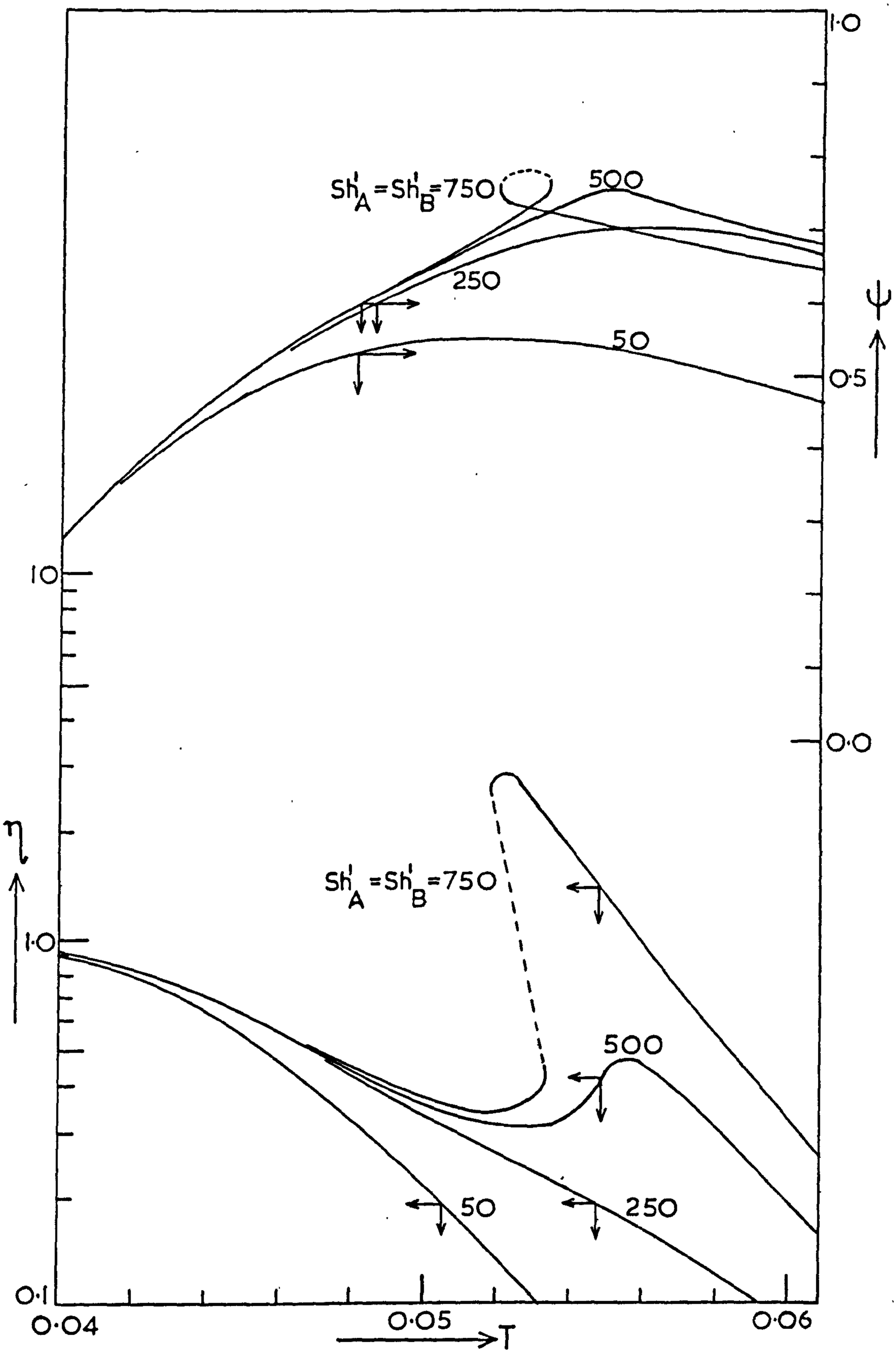

FIG. 4.9. The effect of the interphase mass transfer resistances on the effectiveness factor (η) and selectivity (ψ) at various fluid temperatures. Data as given in Table 3.1 .

Figure 4.10 shows the influence of the value of δ, which is the ratio of the intraparticle diffusivities $\frac{D_{pA}}{D_{pB}}$. The variation of δ from a value of unity would normally be a consequence of the relative molecular weights of reactant and product. The primary effect of a change in δ is to change the selectivity, but since this also changes the amount of heat produced, the effectiveness factor also changes slightly. In practice it seems unlikely that δ would vary from 1.0 by an amount large enough to cause any significant variations in the behaviour of the catalyst pellet.

4.7 Conclusions.

A method has been described for reducing the complexity of the single pellet model of the catalyst pellet to an extent which makes it feasible to incorporate it into a model of the fixed bed reactor. The simplifications apply to reactions which can be represented by first order rate expressions and arise out of the high interphase resistance to heat transfer which occurs in real systems. This enables the catalyst pellet to be treated as isothermal, with the temperature rise being concentrated across the fluid film surrounding the pellet. Agreement with the fully distributed model has been shown to be good over all controlling regimes, and there appear to be no numerical -difficulties.

The main effects occurring in the system have been examined, and the sensitivity of the model to some of the parameters investigated. The model exhibits high parametric sensitivity over some ranges of conditions, and this is usually found to be associated with a change in the controlling mechanism.

Parametric sensitivity is commonly encountered with systems of this type, and implies that the availability of accurate physical and chemical data may be a critical factor in the successful application of the mathematical model. This aspect of the problem cannot be examined in isolation, but is best studied when the pellet model is used within a model of the packed bed reactor. It is then possible to see what interaction there is in the system, and whether operating conditions are such that accurate data for the pellet model is essential.

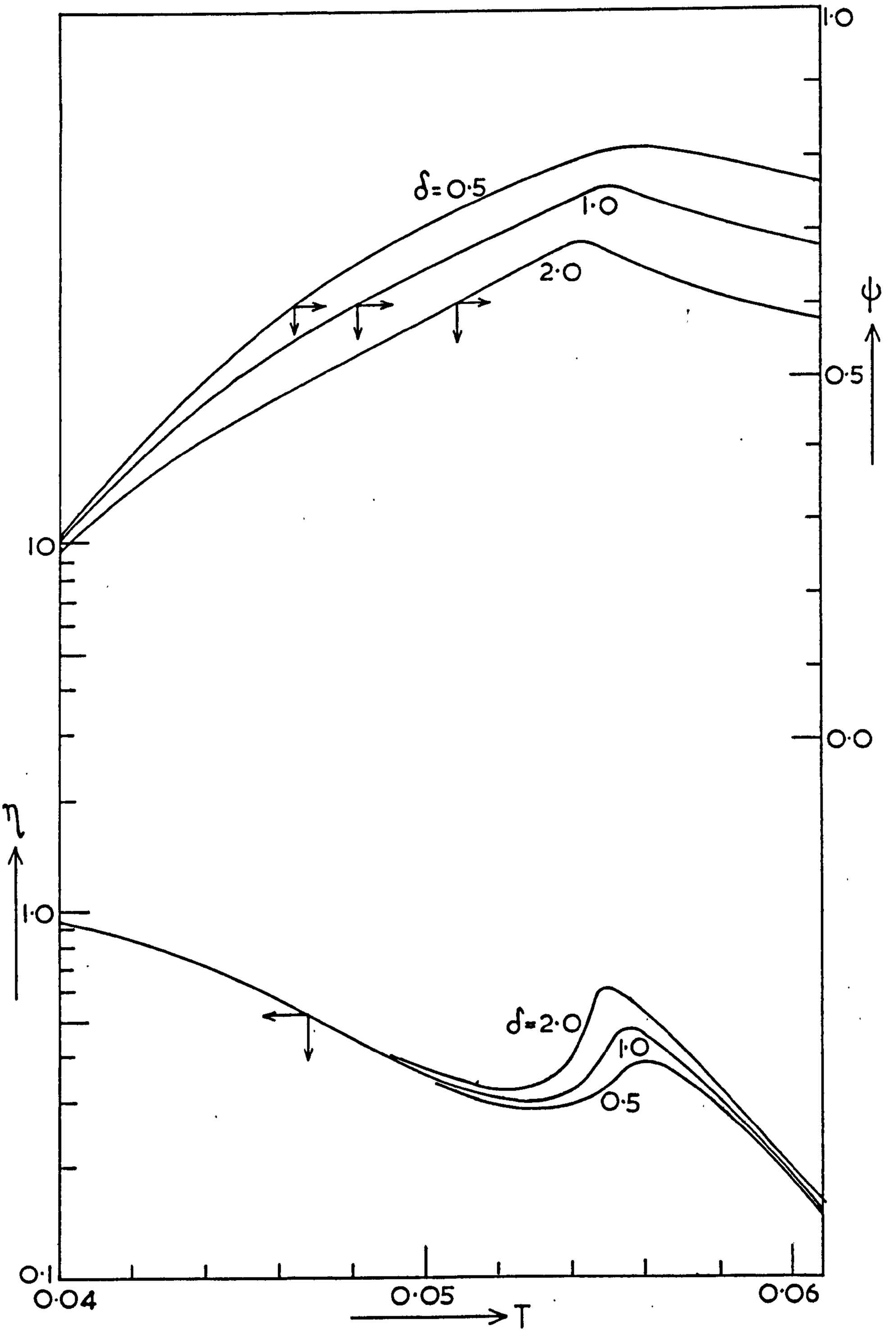

FIG. 4.10. The effect of the ratio of the intra-particle diffusivities on the effectiveness factor (η) and selectivity (ψ) for various fluid temperatures. Data as given in Table 3.1 .

CHAPTER 5

A TWO-DIMENSIONAL STEADY STATE MODEL OF THE REACTOR

5.1 Introduction.

The amount of published work on mathematical modelling of fixed bed catalytic reactors has been steadily increasing in recent years. The models which have been proposed may conveniently be divided into two groups: those models which include intraparticle effects, known as heterogeneous models, and those which do not. The latter type of model is commonly referred to as quasi-homogeneous, and this name will be used to cover true homogeneous systems and heterogeneous systems which are treated as homogeneous. In general the results obtained from quasi-homogeneous models may easily be predicted from heterogeneous models by letting the values of the effectiveness factor and selectivity approach their values under kinetic control:-

$$\eta = 1, \quad \psi = \frac{\phi_1^2 C_A^{n_1} - \phi_2^2 C_B^{n_2}}{\phi_1^2 C_A^{n_1} + \phi_3^2 C_A^{n_3}}$$

It is therefore unnecessary to consider quasi-homogeneous reactors as a class on their own, although in practice it would be preferable to formulate as a quasi-homogeneous model any system which behaves in this way, since the computer storage requirements and solution time are less than those required for the heterogeneous model. Many catalytic systems of industrial importance, however, do involve transport effects which cause appreciable alteration to the reaction rate under normal operating conditions, and heterogeneous models are therefore essential.

The heterogeneous models which have been considered in the literature have been expressed in two forms: continuum models, which have been the most widely used, and finite stage models, also referred to as mixing cell models. If radial temperature gradients occur across the reactor tube, a two-dimensional model is necessary which must be solved either by finite

difference methods, or by applying model reduction techniques. Finite stage models have been proposed by Lapidus and co-workers[11,15,16] and are essentially similar to the finite difference representation of the continuum model, except that the step size is the pellet diameter, whereas for continuum models the step size is reduced until the solution converges to a constant result.

For the following work, a continuum model is proposed which includes heat and mass transport in the radial direction as well as the intraparticle effects which have been discussed in the previous chapters.

5.2 Formulation of the equations.

The heat and mass balances at a point within the bed are described by the equations:-

$$Df_A \frac{1}{x} \frac{\partial}{\partial x}\left(x \frac{\partial Cf_A}{\partial x}\right) - u \frac{\partial Cf_A}{\partial l} - \frac{(1-e)}{e}\left(k_1 Cf_A^{n_1} + k_3 Cf_A^{n_3}\right)\eta = 0 \qquad (5.1)$$

$$Df_B \frac{1}{x} \frac{\partial}{\partial x}\left(x \frac{\partial Cf_B}{\partial x}\right) - u \frac{\partial Cf_B}{\partial l} + \frac{(1-e)}{e}\left(k_1 Cf_A^{n_1} + k_3 Cf_A^{n_3}\right)\eta\psi = 0 \qquad (5.2)$$

$$Kf \frac{1}{x} \frac{\partial}{\partial x}\left(x \frac{\partial Tf}{\partial x}\right) - \rho u C_p \frac{\partial Tf}{\partial l} + \frac{(1-e)}{e} \frac{3h}{b}(T_s - Tf) = 0 \qquad (5.3)$$

subject to the boundary conditions

$$\frac{\partial Cf_A}{\partial x} = \frac{\partial Cf_B}{\partial x} = \frac{\partial Tf}{\partial x} = 0 \quad \text{at} \quad x = 0,\ l > 0 \qquad (5.4)$$

$$\left.\begin{aligned} \frac{\partial Cf_A}{\partial x} = \frac{\partial Cf_B}{\partial x} = 0 \\ \frac{\partial Tf}{\partial x} + \frac{U}{e\,Kf}(Tf - Tc) = 0 \end{aligned}\right\} \quad \text{at } x = R,\ l > 0 \qquad (5.5)$$

and the initial conditions:

$Cf_A = Cf_A(r)$, $Cf_B = Cf_B(r)$ and $Tf = Tf(r)$ at $l = 0$, $0 \leqslant x \leqslant 1$

These equations are most conveniently expressed in dimensionless form as follows:-

$$\frac{\partial^2 C_A}{\partial r^2} + \frac{1}{r}\frac{\partial C_A}{\partial r} - G_1 \frac{\partial C_A}{\partial z} - G_1 G_2 \eta \left(\phi_1^2 C_A^{n_1} + \phi_3^2 C_A^{n_3} \right) = 0 \qquad (5.6)$$

$$\frac{\partial^2 C_B}{\partial r^2} + \frac{1}{r}\frac{\partial C_B}{\partial r} - G_1 \Delta \frac{\partial C_B}{\partial z} + G_1 G_2 \Delta \eta \psi \left(\phi_1^2 C_A^{n_1} + \phi_3^2 C_A^{n_3} \right) = 0 \qquad (5.7)$$

$$\frac{\partial^2 T}{\partial r^2} + \frac{1}{r}\frac{\partial T}{\partial r} - G_3 \frac{\partial T}{\partial z} + G_3 G_4 (t - T) = 0 \qquad (5.8)$$

the boundary conditions being

$$\frac{\partial C_A}{\partial r} = \frac{\partial C_B}{\partial r} = \frac{\partial T}{\partial r} = 0 \quad \text{at} \quad r = 0, \quad z > 0 \qquad (5.9)$$

$$\left.\begin{aligned} &\frac{\partial C_A}{\partial r} = \frac{\partial C_B}{\partial r} = 0 \\ &\frac{\partial T}{\partial r} + Nu_W (T - T_c) = 0 \end{aligned}\right\} \text{ at } r = 1, \quad z > 0 \qquad (5.10)$$

The inlet conditions are

$C_A = C_A(r)$, $C_B = C_B(r)$ and $T = T(r)$ at $z = 0$, $0 \leqslant r \leqslant 1$

The additional dimensionless quantities which have been introduced are defined as follows:-

$$r = {}^{x}/_{R} \qquad z = {}^{l}/_{L}$$

$$G_1 = \frac{R^2 u}{Df_A L} = \frac{R^2}{2bL} Pe_M \qquad G_2 = \frac{(1-e)\, L\, Dp_A}{b^2\, ue}$$

$$G_3 = \frac{R^2 \rho C_p U^*}{Kf\, L} = \frac{R^2}{2bL} Pe_H \qquad G_4 = \frac{(1-e)\, 3hL}{b \rho\, ue\, C_p}$$

$$\Delta = \frac{Df_A}{Df_B} \qquad Nu_W = \frac{RU}{eKf} = \frac{RUPe_H}{2b \rho\, ueC_p}$$

$$T_c = \frac{TcRg}{E_1} \qquad Pe_M = \frac{2bu}{Df_A} \qquad Pe_H = \frac{2bu \rho C_p}{kf}$$

The groups G_1, G_3 and Nu_W have been expressed above in two forms. In general they are most conveniently evaluated in the second of the forms, using the Peclet numbers for radial heat and mass transfer, since the radial heat and mass transfer coefficients are related to the velocity in such a way that Pe_M and Pe_H remain constant,[78] having a value of approximately 10. Moreover

it may also be assumed that the radial diffusivities are equal for each component in the fluid phase, making $\Delta = 1$. This occurs because dispersion is caused mainly by mechanical disturbance of the streamlines under conditions of turbulent flow.

5.3 Solution of the equations.

The solution of the equations may be obtained using an iterative Crank-Nicholson method. The finite difference approximation to the differential equations is described in detail in Appendix 2. The solution is accomplished as follows.

1. Assume radial profiles for C_A, C_B and T at the first (or next) axial position.
2. Using these values, solve the single pellet model at each node of the finite difference network to obtain η, ψ and t.
3. Use these values to evaluate the non-linear terms in the differential equations (5.6) to (5.8) at each node.
4. Solve the algebraic equations for C_A, C_B and T consecutively using the method described in Appendix 2.
5. Testfor convergence by comparing values with those used in step (2). If unsatisfactory, repeat from step (2) using the new values of the state variables.
6. If satisfactory repeat from step (1) while $z < 1$.

No difficulties are usually encountered in obtaining the solution in this way. Step (1) of the above scheme is carried out by projecting the values of the state variables from the previous two axial positions. (This cannot be done for the first step in the reactor, in which case the assumed values are those at the inlet.) In this way, a fairly good initial estimate is obtained, and only one iteration is required through most of the reactor, although in the region of the hot spot this may rise to between two and five iterations.

Tests on typical sets of data indicated that 200 axial and 20 radial steps are sufficient to ensure convergence, and for this size of network, a solution time of 10 - 15 minutes on an ICL KDF9 computer is to be expected.

5.4 Discussion of the Results.

In the next chapter, a simpler model of the reactor is proposed, for which the computing time is considerably less than for the present two-dimensional model. It is therefore more efficient, in terms of computer time, to carry out most of the examination of reactor performance using the simpler model, which is one-dimensional and works in terms of radial mean values of the state variables. This model is unable to predict anything about the radial variations in concentration, effectiveness factor and so on, but the model does depend upon an assumed radial temperature profile. In this section, therefore, discussion of the results will be confined to examination of features which relate specifically to the radial direction, and a consideration of other phenomena is included in Chapter 6.

For the reasons discussed in Chapter 4 with reference to the single pellet model, the general characteristics of the system are best examined by considering a specific set of data and using this to assess the importance of each of the parameters. This basic set of data is given in Table 5.1. The solution takes the form shown in Figures 5.1 to 5.3, where the radial concentration and temperature profiles have been plottod at various longitudinal positions. It is apparent that the concentration gradients in the radial direction are fairly mild and that radial mixing is sufficiently rapid to keep the concentration difference across the tube small. In the case of temperature, however, the profile is often steep. This is caused by the removal of heat through the wall of the reactor, and by the non-linear nature of the chemical rate expression which tends to increase the

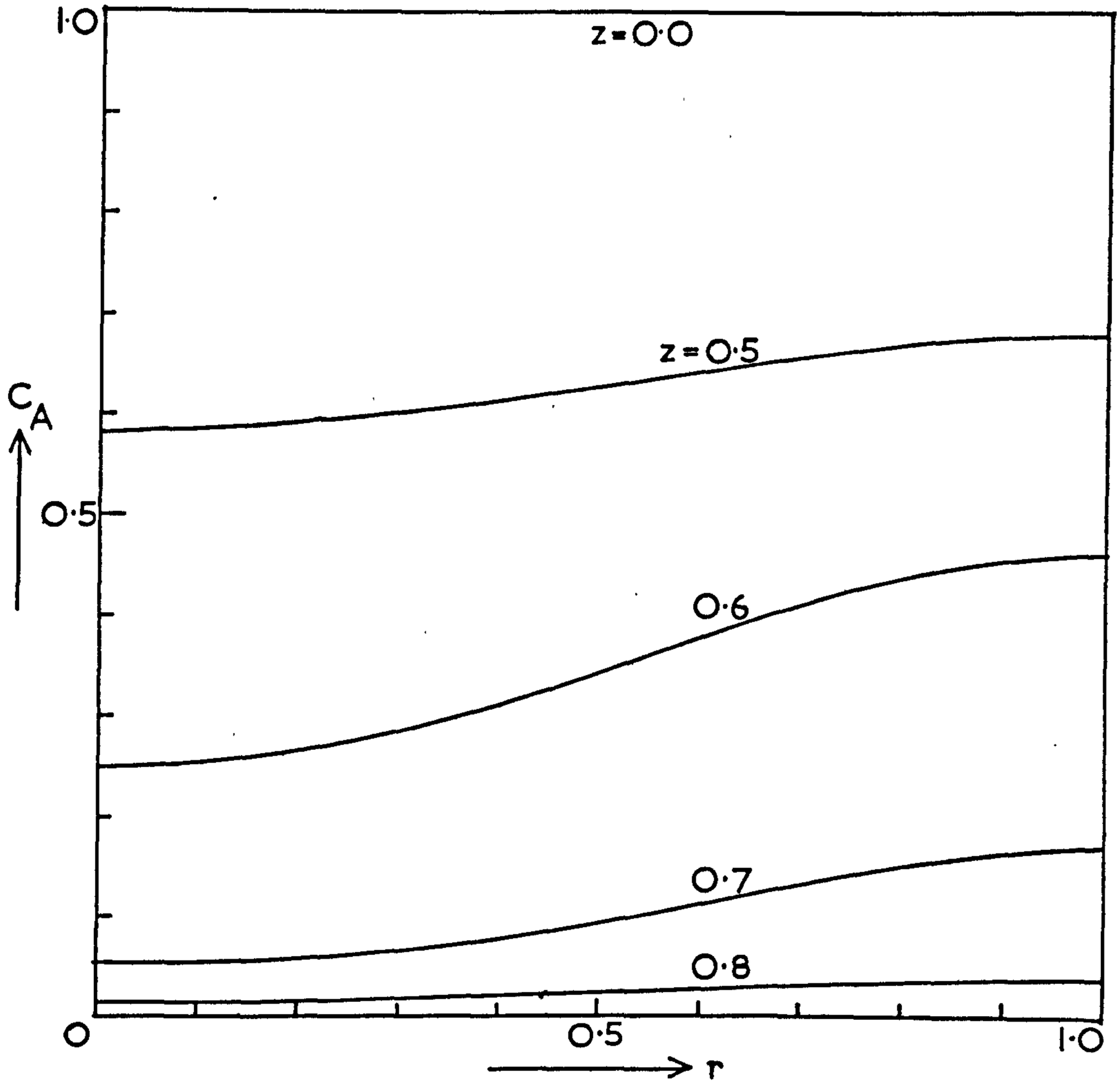

FIG. 5.1 Radial concentration profiles for species A at various axial positions. Data as given in Table 5.1.

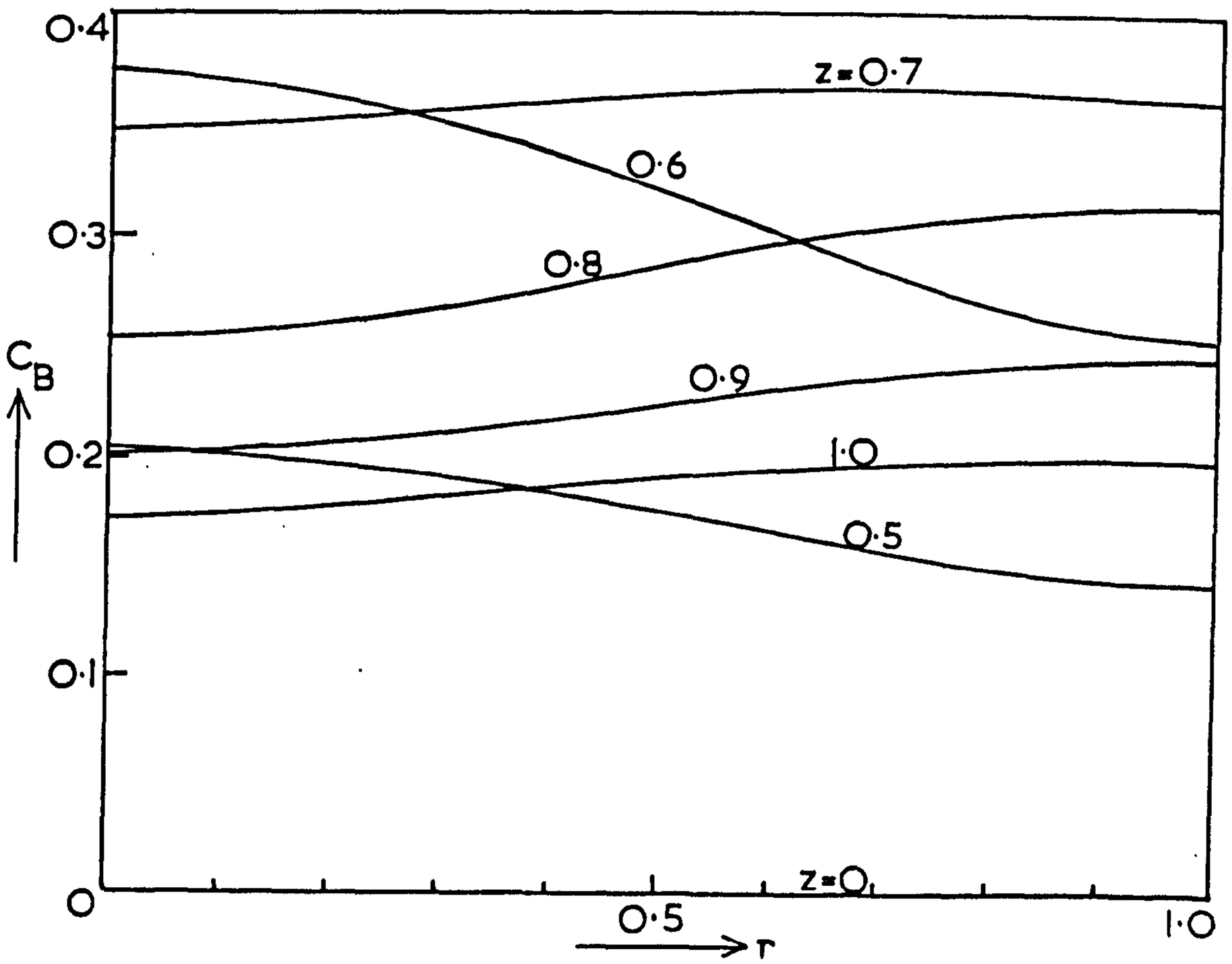

FIG. 5.2 Radial concentration profiles for species B at various axial positions. Data as given in Table 5.1.

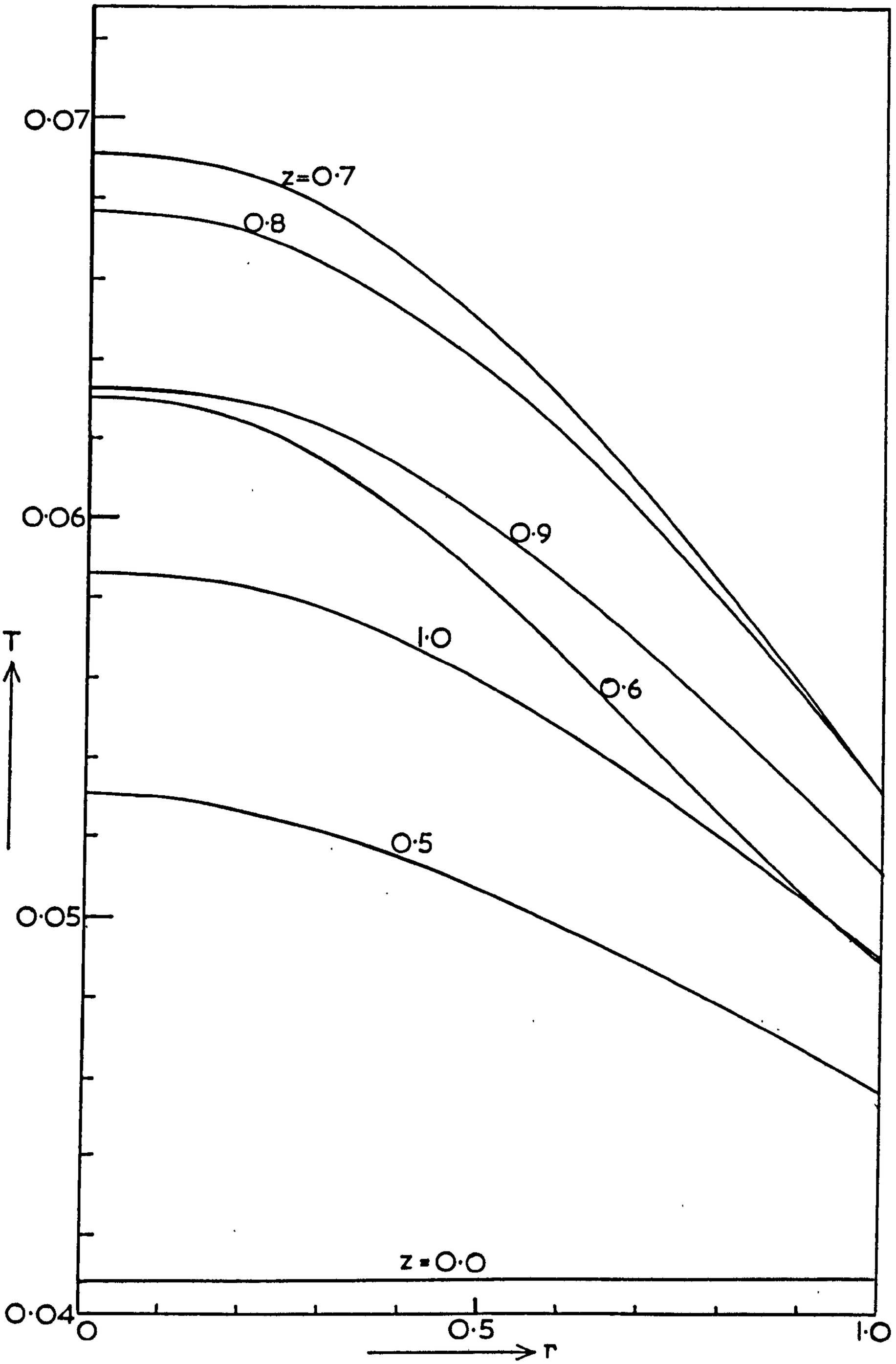

FIG. 5.3 Radial temperature profiles at various axial positions. Data as given in Table 5.1.

fluid temperature at points where it is already high. The presence of steep thermal gradients implies that a simplified model which takes no account of them is unlikely to be satisfactory. The difficulty may be overcome by assuming an algebraic form for the temperature profile, which leads to a modification of the wall Nusselt number, as will be seen in section 6.3.

Figure 5.4 shows a comparison of the concentration and temperature profiles predicted by the heterogeneous and quasi-homogeneous models. The profiles obtained from the two models are completely different, and quasi-homogeneous model predicting temperature runaway, while the heterogeneous results show no sign of such instability. This may be explained by examining Figures 5.5 and 5.6 which show the radial profiles of effectiveness factor and selectivity at various positions in the reactor. The values of the effectiveness factor show that the diffusional resistances to mass transfer within the catalyst pellet cause a reduction in the actual rate of reaction to a value well below the kinetic rate. The effectiveness factor becomes even smaller as the fluid temperature rises since the relative importance of the diffusional resistance increases as the kinetic rate increases. Thus diffusion limits the rate at which reactant is consumed and also the rate at which heat is produced, whereas in the quasi-homogeneous case there is no such limitation and the predictions therefore diverge at an increasing rate as the reaction proceeds.

From Figure 5.5 it may be seen that the effectiveness factor begins to rise again after the temperature peak has been passed, and if the reactor were long enough, it would eventually rise to a constant value across the radius. This value would be that for an isothermal system existing at the coolant temperature, which in the case considered here is such that $\eta = 0.84$. This can be seen from Figure 4.7 for the curve where the concentration tends to zero (i.e. $B \longrightarrow 0$).

A_1	3.62×10^9	sec^{-1}	θ_1	2.09×10^5
A_2	7.99×10^5	sec^{-1}	θ_2	3.10×10^3
A_3	1.60×10^5	sec^{-1}	θ_3	1.39×10^3
E_1	32	kcal/g.mole	B_o	5.01×10^{-5}
E_2	21	kcal/g.mole	H_2	0.695
E_3	18	kcal/g.mole	H_3	1.695
$(-\triangle H_1)$	367	kcal/g.mole	E_2/E_1	0.656
$(-\triangle H_2)$	255	kcal/g.mole	E_3/E_1	0.563
$(-\triangle H_3)$	622	kcal/g.mole	Sh'_A	500
Dp_A, Dp_B	3.66×10^{-3}	cm^2/sec	Sh'_B	500
			Nu'	1.0
k_{c_A}, k_{c_B}	4.36	cm/sec	δ	1.0
			$\triangle$	1.0
h	1.2×10^{-3}	$cal/cm^2 sec\,^oK$	G_1	0.84
b	0.21	cm	G_2	0.0949
L	125	cm		
Kp	5.04×10^{-4}	$cal/cm/sec/^oK$	G_3	0.84
u	164	cm/sec	G_4	76.85
R	2.1	cm	Nu_w	2.0
U	6.7×10^{-4}	$cal/cm^2/sec/^oK$	C_A (inlet)	1.0
e	0.4		C_B (inlet)	0.0
C_p	0.25	$cal/g/^oK$	T (inlet)	0.0408
C_o	3.05×10^{-7}	$g.moles/cm^3$	T_c	0.0408
Tf (inlet)	660	^oK	Nu_w * (1)	1.33
Tc	660	^oK		
Pe_H, Pe_M	10		K_T (2)	1.55 secs.
ρ *(2)	1.0	g/cm^3	G_5	0.64 secs.
C_p *	0.177	$cal/g/^oK$	G_6	0.64 secs.

TABLE 5.1 A typical set of data used in the solution of the reactor models.

(1) Used in Chapter 6

(2) Used in Chapter 8.

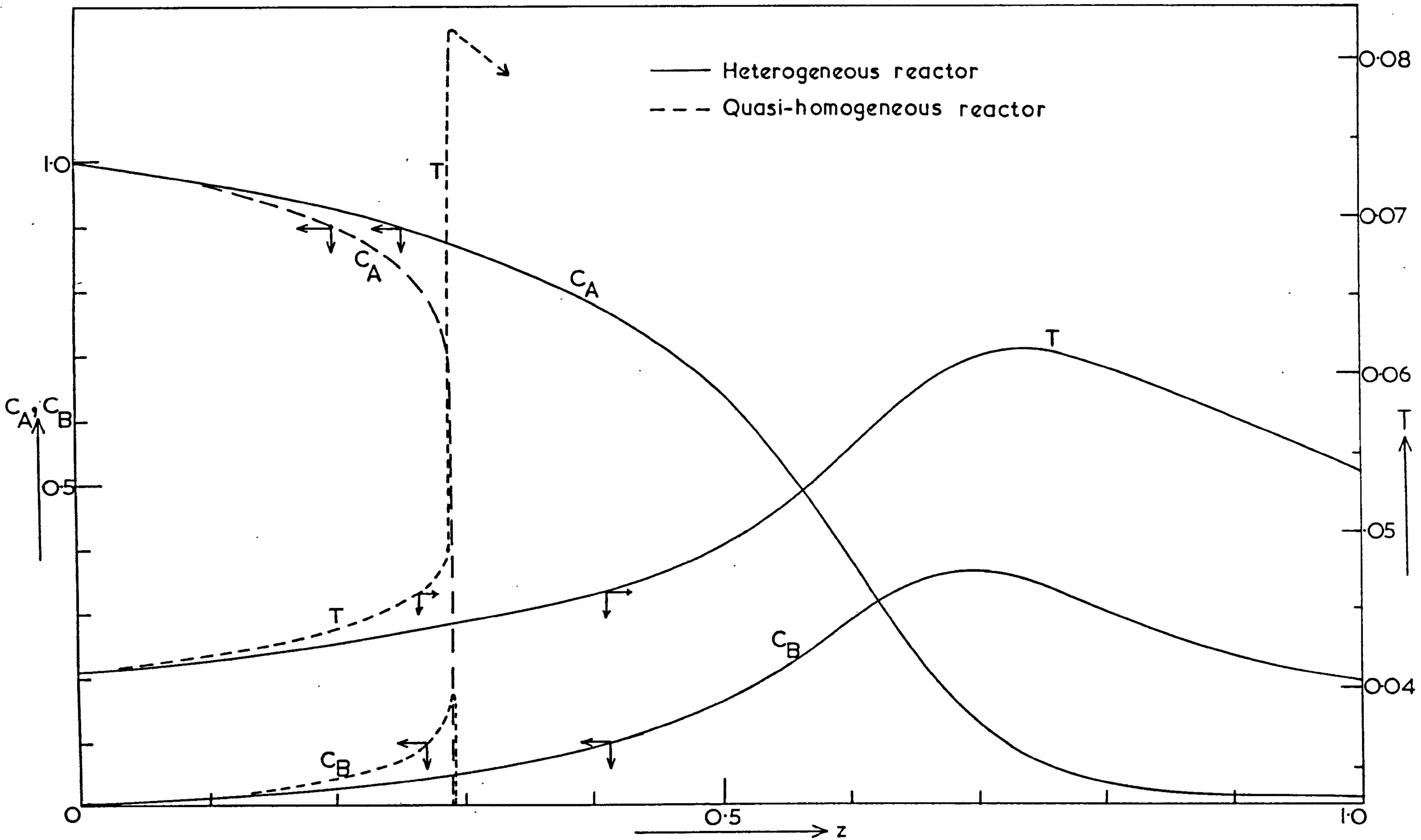

FIG. 5.4. Comparison of radial mean concentration and temperature profiles for heterogeneous and quasi-homogeneous models of the reactor. Data as given in Table 5.1.

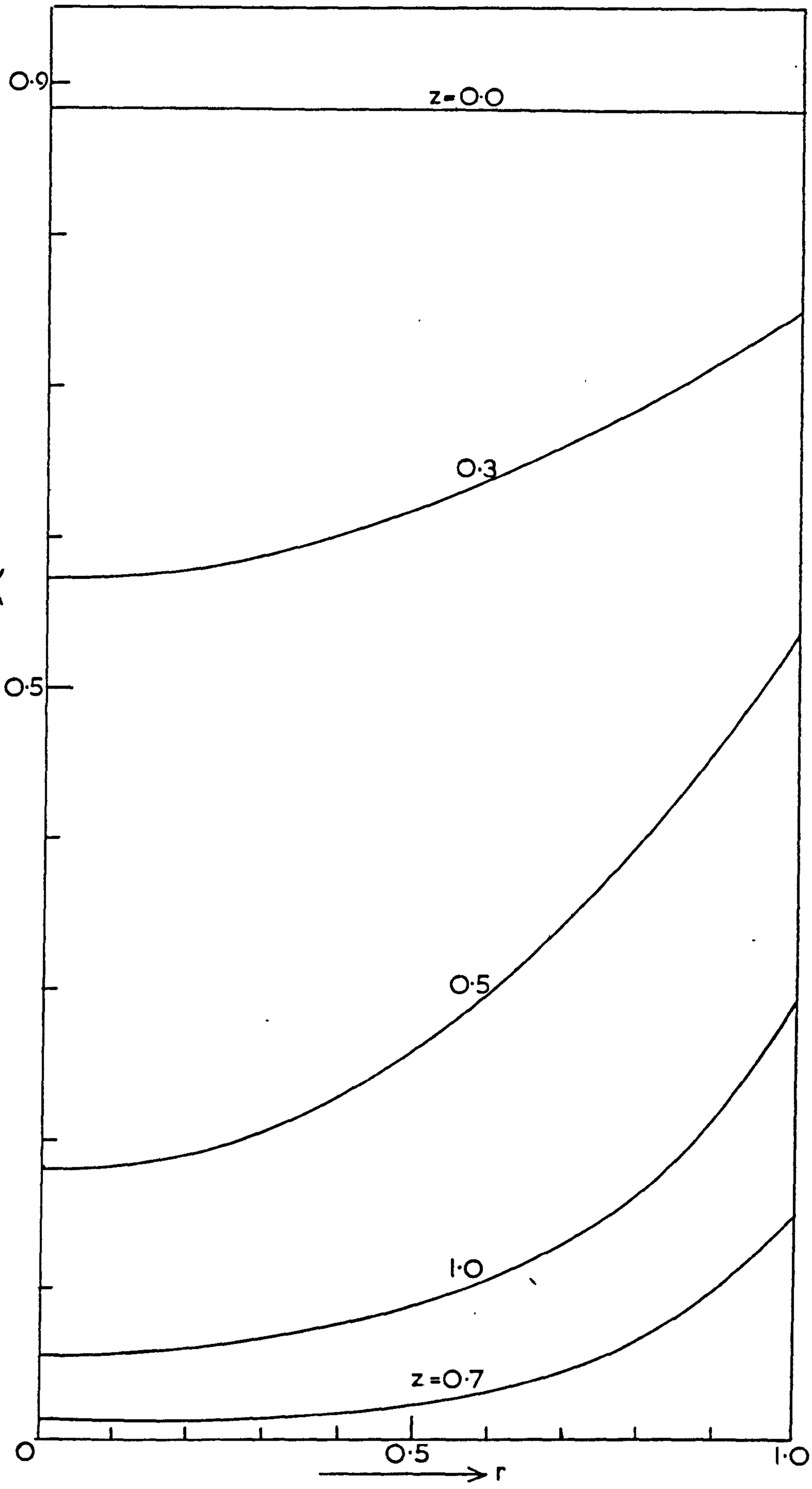

FIG. 5.5 Radial profiles of the effectiveness factor at various axial positions. Data as given in Table 5.1.

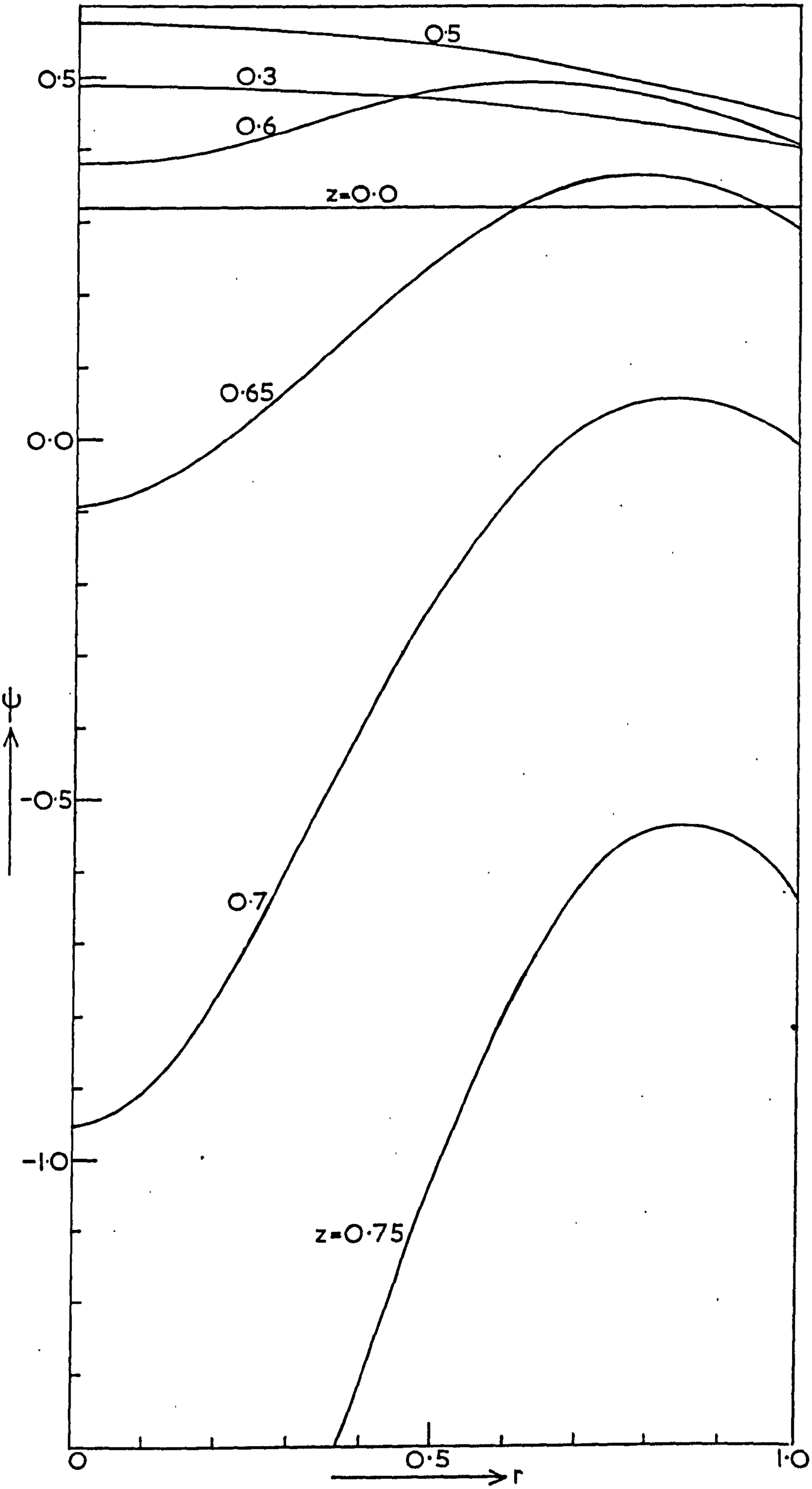

FIG.5.6 Radial profiles of selectivity at various axial positions.
Data as given in Table 5.1.

Figure 5.6 shows the radial profiles of selectivity at various longitudinal positions. Near the beginning of the reactor the selectivity is higher on the tube axis, and this is to be expected in the present system, since it has already been shown in Figure 4.7 that high temperature tends to increase the selectivity under conditions of kinetic or diffusion control. It has also been shown in Figure 4.8, however, that a high concentration of species B lowers the selectivity. (This is also apparent from kinetic considerations.) The effects of variations in T and C_B therefore act in opposite directions and gradually the effect of C_B increasing becomes dominant. At some point in the reactor this causes the selectivity to become negative and species B begins to be consumed faster than it is produced. This situation would clearly be undesirable if B was the desired product, and in practice the reactor would terminate at a point corresponding to $z \simeq 0.7$ for the given data.

The effect of radial mixing is shown in Figure 5.7. For fixed bed reactors the value of the radial Peclet numbers for heat and mass transfer is normally approximately 10, with the possible range being $8 \longrightarrow 11$. (Perfect mixing occurs when $Pe_H = Pe_M = 0$). The results show that the performance of the reactor is relatively insensitive to the Peclet number within the practical range, and the assumed value of 10 is therefore likely to give results well within the accuracy to be expected from other data.

Letting $Pe_H = Pe_M \longrightarrow 0$ effectively reduces the model to a one-dimensional form and this results in profiles which differ considerably from the curve for $Pe_H = Pe_M = 10$. The equivalent one-dimensional model is based on the assumption of flat radial concentration and temperature profiles, and is clearly inappropriate for systems where heat is removed through the reactor wall. An alternative to this assumption of flat profiles based on a modified wall heat transfer coefficient is discussed in the following chapter.

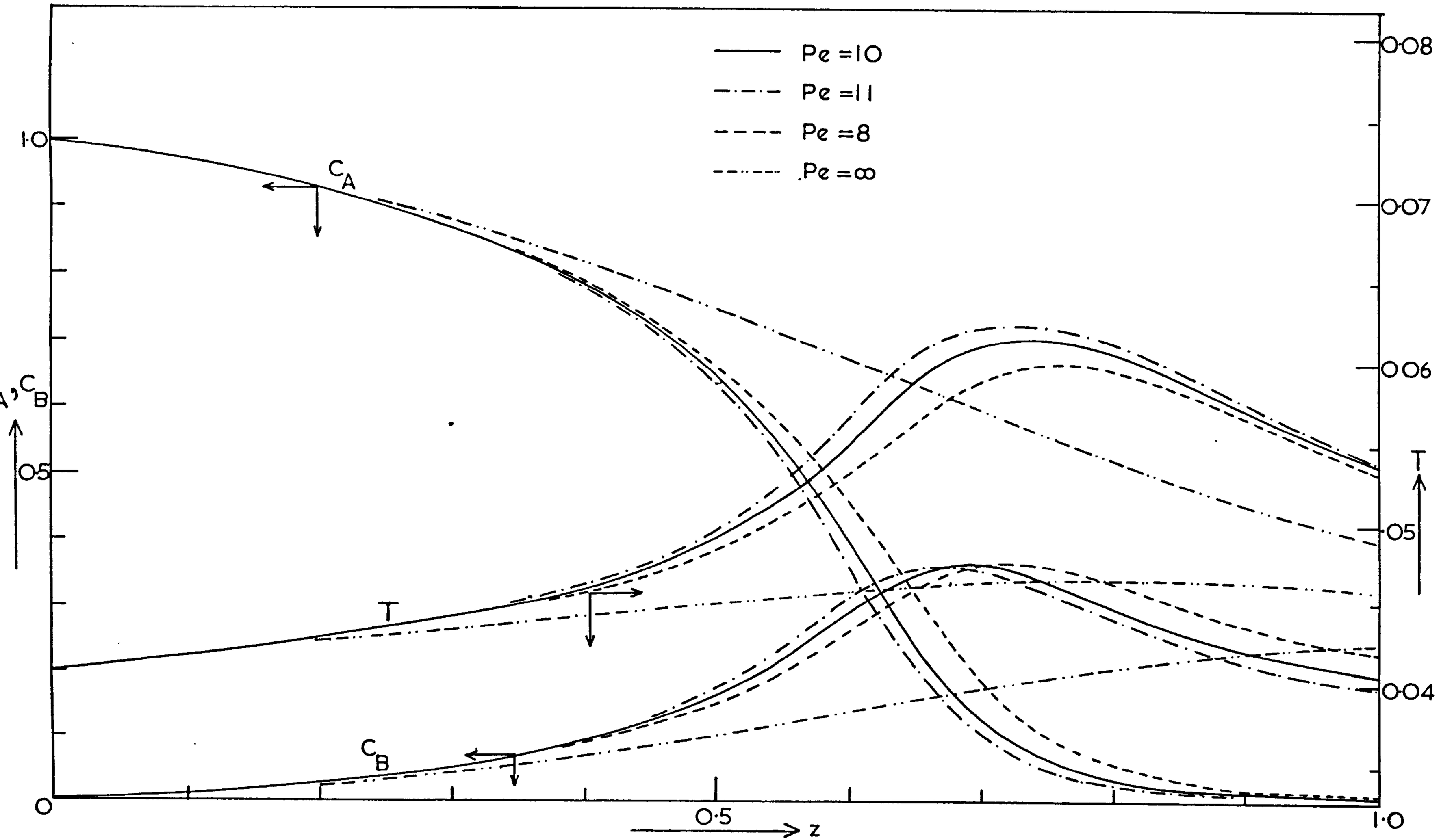

FIG.5.7 The effect of radial mixing on the performance of the reactor, showing radial mean concentration and temperature profiles. Data as given in Table 5.1. ($Pe = Pe_H = Pe_M$).

5.5 Conclusions.

A model of the fixed bed catalytic reactor has been developed which takes account of radial and longitudinal gradients in the fluid phase, and radial gradients within the catalyst pellet. The parameters of the model are physical, chemical and thermodynamic quantitios which are readily identifiable and can be obtained from simple experiments or correlations in the literature. For a finite difference network with 200 steps in the axial direction and 20 in the radial direction, about 15 minutes computing time is required on an ICL KDF9 computer. For all sets of data run for the heterogeneous system, the numerical procedure was found to converge quickly, although for the quasi-homogeneous reactor difficulties can be encountered in cases where temperature runaway occurs.

For many purposes, a computing time of 15 minutes is quite unacceptable, particularly for optimisation or control studies. Also, since dynamic models tend to involve a series of pseudo-steady state solutions, the dynamic model based on this steady state version would require a prohibitive amount of time for solution, as 15 minutes computing would be required for each time step. An alternative model is required which is capable of solution in a considerably shorter time than the present two-dimensional model. Preliminary runs on the latter model have shown that neither an assumption of quasi-homogeneity nor one of perfect radial mixing leads to results which are sufficiently close to those from the complex model to enable these assumptions to be used as the basis of a simpler model. This is in agreement with previous published work. The main difficulty is apparently caused by the pronounced thermal gradients which occur across the reactor radius, and it appears that any simplification will need to take account of these.

CHAPTER 6

A ONE-DIMENSIONAL STEADY STATE MODEL OF THE REACTOR

6.1 Introduction.

While some mathematical modelling of fixed bed catalytic reactors has been carried out as an aid to the experimentalist working on kinetic problems, the main attraction has been the possibility of using the models in the design, optimisation and control of reactors. In the previous chapter a two-dimensional model of the reactor was described, which required about 15 minutes for solution on an ICL KDF9 digital computer. This is clearly excessive for any of the uses outlined above, except perhaps for a design problem which involved no optimisation. It is therefore desirable to develop either a more rapid method of computation or a simpler model of the reactor. More efficient computing techniques, while always desirable, are unlikely to reduce the computing time sufficiently, and attention must, therefore, be given mainly to developing an alternative mathematical model. Before attempting this development, however, it is worthwhile setting down some of the desired features to be aimed for in the new model.

In many catalytic systems there are constraints. These are often imposed for example, by the explosive limit on the concentration of reactant, or by the maximum operating temperature for the catalyst, above which deactivation occurs. Another constraint might be that fluid conditions, which lead to multiple solutions of the single pellet model, must be avoided. Although concentration restrictions are usually easy to overcome, because they can be applied to the inlet conditions, the constraints involving temperature are internal, as the maximum temperature generally occurs between the inlet and outlet of the reactor. The main implication of this is that a "black box" type of model is basically unsuitable for describing the behaviour of the reactor, since it is unable to predict any of the distributed

characteristics of the system. The other main disadvantage of this type of model is that all the parameters must be determined by means of curve-fitting techniques, using the results obtained from experiments or computed from the two-dimensional model. Because of the highly non-linear nature of the system, these parameters will only apply over a narrow range of conditions and it would, therefore, be necessary to switch from one parameter set to another, as the operating conditions change. A major advantage of the mechanistic type of model over the black box model is that it is much easier to obtain a physical understanding of the way the system behaves and this is likely to make further simplification of the model easier.

The question of how accurate the model should be depends very much on the use to which the results will be put, and on the accuracy of the available data. Probably the best approach is to develop a model and then to assess any limitations on its use, or to suggest possible ways of using it to its best advantage in any given situation. This aspect will be considered in more detail later in the chapter.

At this point it is worth considering the general characteristics upon which selection of the appropriate model might depend. Clearly, it is not profitable to employ a mathematical model which is more elaborate than is necessary to satisfy the minimum requirements of accuracy and description in any given situation. Two considerations are relevant here. The first of these is the discrepancy between solutions obtained from different models of the system. For example, where only longitudinal gradients of concentration and temperature are considered (in the steady state), the system will be represented by a set of ordinary differential equations. Where radial gradients are included, partial differencial equations result. However if the results do not differ significantly over the practical range of operating conditions, then the simpler model should be used, provided that the necessary parameters can be satisfactorily predicted. The second

consideration is the need to relate the parameters of the model to physically identifiable processes. This is usually possible in complex models, but in the case of simpler models, the parameters may not be readily identifiable.

While approximations have often been made, they tend to be the result of mathematical convenience. Froment[2] has demonstrated, by defining a suitable wall heat transfer coefficient, that the difference between the one and two-dimensional quasi-homogeneous models is small over a wide range of operating conditions, but that the one-dimensional model is inadequate in regions near temperature runaway. Physical interpretation of models is of particular importance and McGreavy and Cresswell[14] have shown that the major differences between models are between quasi-homogeneous and heterogeneous, rather than between one and two-dimensional models. (Note: The distinction here is essentially one of degree. Clearly all fixed bed reactors are heterogeneous. When the conditions inside the catalyst pellet are assumed not to differ significantly from those in the fluid phase, it is normal to treat each element of reactor volume as quasi-homogeneous. However when there are appreciable differences between conditions in the bulk fluid and catalyst pellet and these are included in the model, the term heterogeneous is used.)

If the reactor behaves in a quasi-homogeneous manner, it is possible to make considerable savings in the computing time required for solution of the model, since it is then unnecessary to solve the pellet equations and the selectivity can be obtained explicitly. However, this simplification cannot be used as a general method of approach, as can be seen from Figure 5.4, where the profiles of concentration and temperature predicted by the quasi-homogeneous and heterogeneous models are compared for a typical set of data.

Since it is essential to retain the description of the reactor in the longitudinal direction, the simplified model which is proposed is one-

dimensional and takes account of the radial temperature profile by assuming an algebraic form for it. This results in a modification of the Nusselt number for heat transfer at the wall and the heat removed through the wall can then be expressed in terms of an overall driving force based on the radial mean temperature.

6.2 Formulation of the equations.

Using the same nomenclature as for the two-dimensional model, the equations become:-

$$\frac{dC_A}{dz} + G_2 \eta \left(\phi_1^2 \, C_A^{n_1} + \phi_3^2 \, C_A^{n_3} \right) = 0 \qquad (6.1)$$

$$\frac{dC_B}{dz} - \Delta G_2 \eta \psi \left(\phi_1^2 \, C_A^{n_1} + \phi_3^2 \, C_A^{n_3} \right) = 0 \qquad (6.2)$$

$$\frac{dT}{dz} - G_4 (t - T) + 2 \frac{Nu^*_w}{G_3} (T - T_c) = 0 \qquad (6.3)$$

subject to the initial conditions

$$T = T_{z=0} \qquad C_A = C_{A_{z=0}} \qquad C_B = C_{B_{z=0}}$$

where Nu^*_w is an effective overall wall Nusselt number which enables the heat removed to be calculated from the mean fluid temperature. The way in which Nu^*_w is obtained will be discussed in the next section.

It should be noted that the state variables occurring in equations (6.1) - (6.3) are all radial mean values. The reaction rates are also radial mean values and this is likely to raise problems of evaluation, since for non-linear functions the radial mean value is not the same as the value at the radial mean conditions. Methods of tackling this difficulty are discussed later in the chapter, but as an initial policy, the rate may be evaluated by solving the catalyst pellet model at the radial mean conditions. This is clearly the most desirable method of evaluating the mean rate and is the one which has been used exclusively in the literature.

6.3 Solution of the equations.

Equations (6.1) to (6.3) all have the form

$$\frac{df}{dz} + R'f + R'' = 0$$

In finite difference form this becomes

$$\frac{f - xf}{k} + (1 - Q)\,xR'\,xf + (1 - Q)\,xR'' + QR'f + QR'' = 0$$

where Q is a constant $0 < Q \leqslant 1$,

and the prefix 'x' denotes the value of a variable at the previous axial position, i.e. it is known.

In this equation, the unknowns are f, R' and R''. Solution is accomplished by working from the inlet to the outlet as follows.

1) Assume values of f for $f \equiv C_A$, C_B, T at the first (or next) position where they are unknown.
2) Use these values to solve the catalyst pellet model (giving η, Ψ and t) and thus evaluate the non-linear terms.
3) Calculate the new values of C_A, C_B and T.
4) Test against the previous value (used at step (2)) for satisfactory convergence. If unsatisfactory, repeat from step (2).
5) If satisfactory and $z < 1$, repeat from step (1).

It can be seen from section 5.3 that the method of solution is basically the same as for the two-dimensional model, but no simultaneous equations arise from radial derivatives and the solution is therefore more straightforward. As for the two-dimensional case, the initial assumed values of the state variables used in step (1) were obtained by extrapolation from the previous axial position.

6.4 Evaluation of the effective overall wall heat transfer coefficient.

The mean temperature of the fluid in the radial direction is given by

$$T_m = 2\int_0^1 T r\,dr \qquad (6.4)$$

Integrating twice by parts

$$T_m = T_{r=1} - \frac{1}{3}\left(\frac{dT}{dr}\right)_{r=1} + \int_0^1 \frac{r^3}{3}\,\frac{d^2T}{dr^2}\,dr \qquad (6.5)$$

Now the boundary conditions on the two-dimensional model are

$$\left(\frac{dT}{dr}\right)_{r=0} = 0$$

$$\left(\frac{dT}{dr}\right)_{r=1} = -Nu_w(T_{r=1} - T_c) \qquad (6.6)$$

The simplest polynomial which will fit the boundary conditions is a quadratic of the form

$$T = T_a - ar^2$$

and hence

$$\left(\frac{dT}{dr}\right)_{r=1} = \frac{d^2T}{dr^2} = -2a \qquad (6.7)$$

The integral in equation (6.5) can now be evaluated

$$\int_0^1 \frac{r^3}{3}\,\frac{d^2T}{dr^2}\,dr = \frac{1}{12}\left(\frac{dT}{dr}\right)_{r=1} \qquad (6.8)$$

Therefore equation (6.5) becomes

$$T_m = T_{r=1} - \frac{1}{4}\left(\frac{dT}{dr}\right)_{r=1} \qquad (6.9)$$

An overall wall Nusselt number can be defined such that

$$Nu^*_w(T_m - T_c) = Nu_w(T_{r=1} - T_c) \qquad (6.10)$$

Equations (6.6) and (6.10) can be combined to give

$$\left(\frac{dT}{dr}\right)_{r=1} = \frac{Nu_w Nu^*_w}{Nu_w - Nu^*_w}(T_{r=1} - T_m)$$

Substituting this in equation (6.9) yields the result

$$Nu^*_w = \frac{4Nu_w}{4 + Nu_w} \qquad (6.11)$$

Although this result is similar to that obtained by Froment[2], who considered the transfer of heat in a heat exchanger (i.e. no heat generation), it is important to recognise the significantly different interpretation to be placed on the results. In the case of heat transfer with no reaction, the value of the wall Nusselt number is over-estimated[60], and the prediction of the radial mean temperature profile is only approximate. The extension to a system where reaction is occurring is difficult to justify, since in this case, heat is being generated within the solid phase, and is being transmitted to the surrounding fluid at a rate which is determined by the inter-phase temperature difference. Even if this temperature difference were constant, which would correspond to a fixed rate of heat generation at each point across the radius, considerable distortion of the heat exchanger temperature profiles would occur. In real systems, however, the rate of heat transfer to the fluid commonly varies by an order of magnitude (or more) across the tube radius. For example, consider the radial temperature profile for z = 0.6 in Figure 5.3, where the temperatures of the fluid on the axis and at the wall are approximately 0.063 and 0.049 respectively. At these temperatures, the rate constants for the A $\longrightarrow$ B reaction are considerably higher than those for the A $\longrightarrow$ C stage, and the relative rate constants for the consumption of species A at the tube axis and wall are given by:

$$\frac{k_1 \text{ (axis)}}{k_1 \text{ (wall)}} \simeq \frac{\exp\left(-\frac{1}{0.063}\right)}{\exp\left(-\frac{1}{0.049}\right)} \simeq 90$$

The effectiveness factor at the tube wall is about five times the value on the axis, so that the effective rate constants are in the ratio of approximately 1:18. Taking into account the concentration variation across the radius (Figure 5.1), the ratio of the rates of reaction becomes about 1:10, and since the selectivity is almost constant at z = 0.6 (Figure 5.6), the rates of heat production are also in the ratio of approximately 1:10.

A variation of this order of magnitude in the rate of heat generation could make the temperature profile vary greatly from the type of profile obtained for heat transfer only. This makes it hazardous, in the absence of other information, to apply results obtained for systems with no heat generation to those where heat is being generated. Although the assumption made by Froment leads to the same result as that which is produced on the basis of a parabolic temperature profile, the assumptionson which the latter are based are clearly defined, whereas, in the former case, conceptual difficulties arise when the reacting system is examined in detail.

6.3 Reconstruction of the radial temperature profile.

Since the radial temperature was assumed to have the form

$$T = T_a - ar^2$$

this may be substituted in equation (6.4) and the integral evaluated giving

$$T_m = T_a - \frac{a}{2} \qquad (6.12)$$

From equations (6.6), (6.7) and (6.10)

$$Nu^*(T_c - T_m) = \left(\frac{dT}{dr}\right)_{r=1} = -2a$$

Using this relationship to substitute for a in equation (6.12) gives

$$T_a = T_m + \frac{Nu^*_w}{4} (T_m - T_c) \qquad (6.13)$$

Combining equations (6.12) and (6.13) gives an expression for the radial temperature profile in terms of the mean temperature:

$$T = T_m + \frac{Nu^*_w}{4} (T_m - T_c) - \frac{Nu^*_w}{2} (T_m - T_c)r^2 \qquad (6.14)$$

This result clearly indicates the advantage of assuming a temperature profile, rather than extending the solution of the heat exchanger problem, since with the latter approach it is impossible to draw any conclusions about the temperature profile or to predict what the maximum temperature will be.

6.6 Comparison of the models and improvement of the one-dimensional model.

6.6.1 General comments.

It was found that in all cases where models were compared, good agreement between the temperature profiles resulted in good agreement between the concentration profiles, and similarly for poor agreement. For this reason, when models are being compared, only the mean temperatures will be used.

The results from the one-dimensional model, which is proposed here, show moderately good agreement with those obtained from the two-dimensional model, as shown by lines numbered (2) in Figure 6.1. For many purposes this order of accuracy may be sufficient, since it shows all the qualitative features of the two-dimensional model and in quantitative terms it may be well within the accuracy of available experimental data. However, in some cases better agreement may be required, particularly when working close to constraints or in the region of optimum operating conditions. If an attempt is to be made to improve the prediction of the model, it is first necessary to understand some of the ways in which errors can arise.

From Figure 6.1 it is apparent that either the reaction rate is being underestimated or the heat removal is being overestimated, or both. Since the two cases are likely to lead to similar effects, it appears that the model can be improved by adjusting either one of them in a suitable way.

6.6.2 Improvement of the evaluation of rate terms.

Since the kinetic rate expressions are highly non-linear functions of temperature, the reaction rate evaluated at the mean conditions is lower than the true mean rate. Within the main reaction zone of the reactor, the results for the simple model therefore represent a lower bound on the possible temperature profiles. In order to improve the estimate, it is necessary to make some broad assumptions, namely that the mean concentration exists over

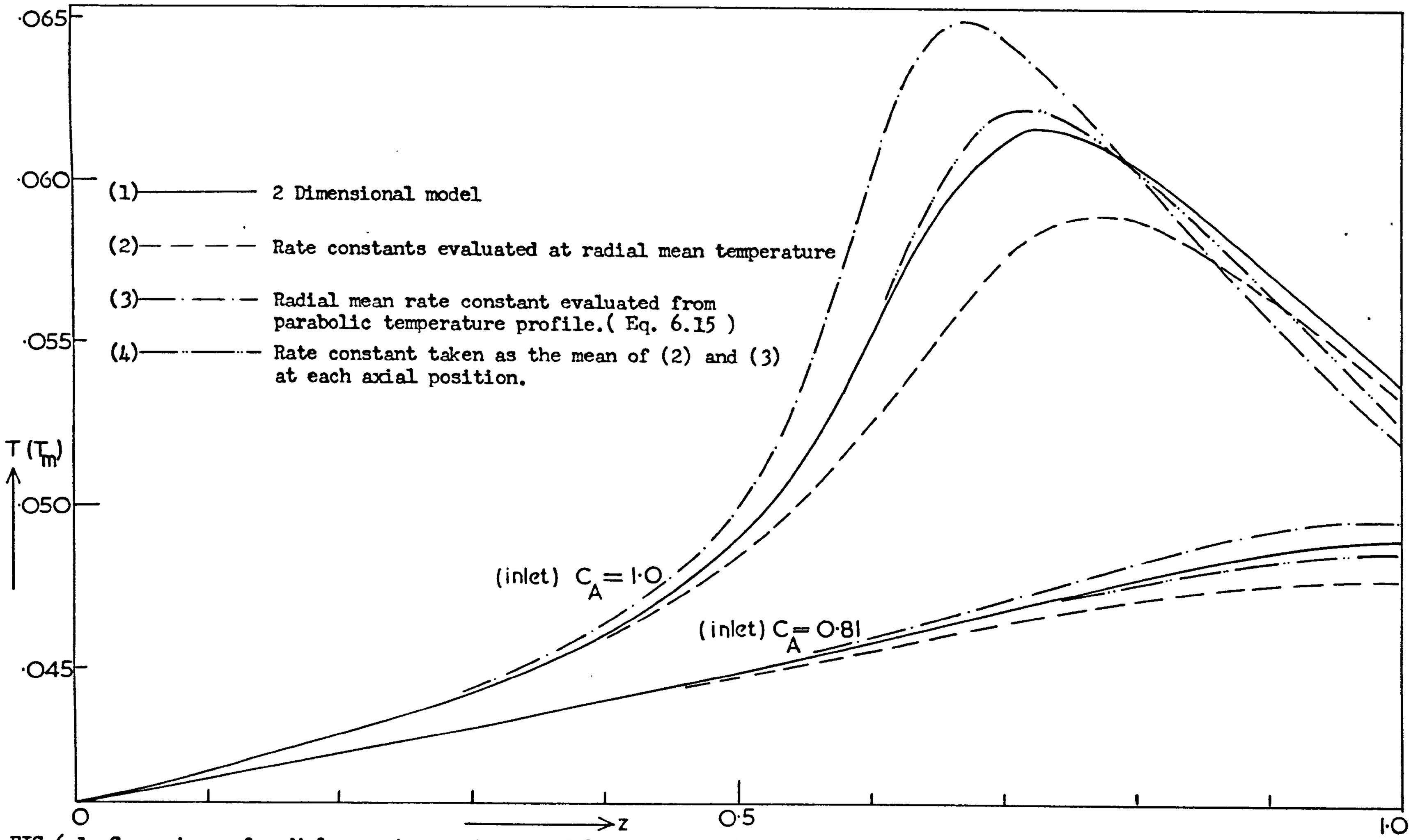

FIG.6.1 Comparison of radial mean temperature profiles computed from the two dimensional reactor model and various forms of the one dimensional model. Data as given in Table 5.1.

the whole of the radius and that the effectiveness factor and selectivity are also constant over the radius, at a value calculated at the mean conditions.

The mean rate term for the conversion of species A is then

$$\int_0^1 2\eta\left(\phi_1^2 C_A^{n_1} + \phi_3^2 C_A^{n_3}\right) r\, dr$$

$$= \int_0^1 2\eta\left(\theta_1^2 \exp\left(-\frac{1}{T}\right) C_A^{n_1} + \theta_3^2 \exp\left(-\frac{E_3}{E_1 T}\right) C_A^{n_3}\right) r\, dr \qquad (6.15)$$

and since T is a known function of r, as given by equation (6.14), the integral can be evaluated numerically. This may be conveniently done by applying Simpson's rule at each axial step through the reactor.

The results obtained using this method are shown as lines (3) in Figure 6.1. The temperature profiles give higher values than those predicted from the two-dimensional model, and in fact this is to be expected from an examination of the assumptions mentioned above. The dimensionless rate constants (i.e. ϕ_i) can vary across the tube radius by an order of magnitude, as has already been shown. The highest rates and therefore the most critical values of concentration and effectiveness factor occur on the tube axis. In fact, it has been demonstrated that at this point the concentration and effectiveness factor are considerably lower than the mean values (see Figures 5.1 and 5.5) and within the main reaction zone the results obtained from the model may, therefore, be regarded as an upper bound on the temperature profile.

The one-dimensional model is thus capable of giving both an upper bound and a lower bound on the longitudinal temperature profile within the reactor. The next logical step is to use a value between these two, and in fact the mean of the two rates taken at each axial step, gives the curves numbered (4) in Figure 6.1. It can be seen that agreement with the two-dimensional model is very good, and this was found to be so for all cases tested. If good agreement could be guaranteed as a general rule, the method would be

attractive, since it requires very little more computational effort than the simple one-dimensional model. However the method is not based on a rigorous foundation, and it would therefore be dangerous to say that it is generally applicable. Nevertheless it could be very useful if applied with discretion.

(Note: In discussing the upper and lower bounds on the temperature profile, it has been emphasised that these apply within the main reaction zone. It is necessary to specify this, since the temperature profiles obtained from different models of a given system almost invariably cross one another when the reaction of species A is (almost) complete. This is to be expected, since the model which predicts the fastest reaction rate gives the highest peak temperature and the greatest rate of heat transfer to the coolant. In each of the temperature profiles of Figure 6.1 which have a maximum (i.e. those for $C_A = 1.0$) the total production of heat is almost constant, and the variation in exit temperature thus reflects only the amount of heat removed by the coolant. Therefore, a model which overestimates the temperature in the region of the peak will give a low estimate of the exit temperature, and can only be said to provide an upper bound on the temperature profile as far as some unspecified point beyond the peak.)

6.6.3 Improvement of the modified wall Nusselt number.

It has been shown by McGreavy and Turner[60] that for heat transfer in the absence of reaction, the effective overall wall Nusselt number is overestimated. If this is also the case when reaction is occurring, it could well lead to the kind of discrepancy between the two models which has been shown. It is therefore possible that for any system, a suitable value of Nu^*_w can be found by comparing the results from the two models for various values of Nu^*_w and then choosing the one which gives the best agreement. The results of this type of trial and error experiment are shown in Figure

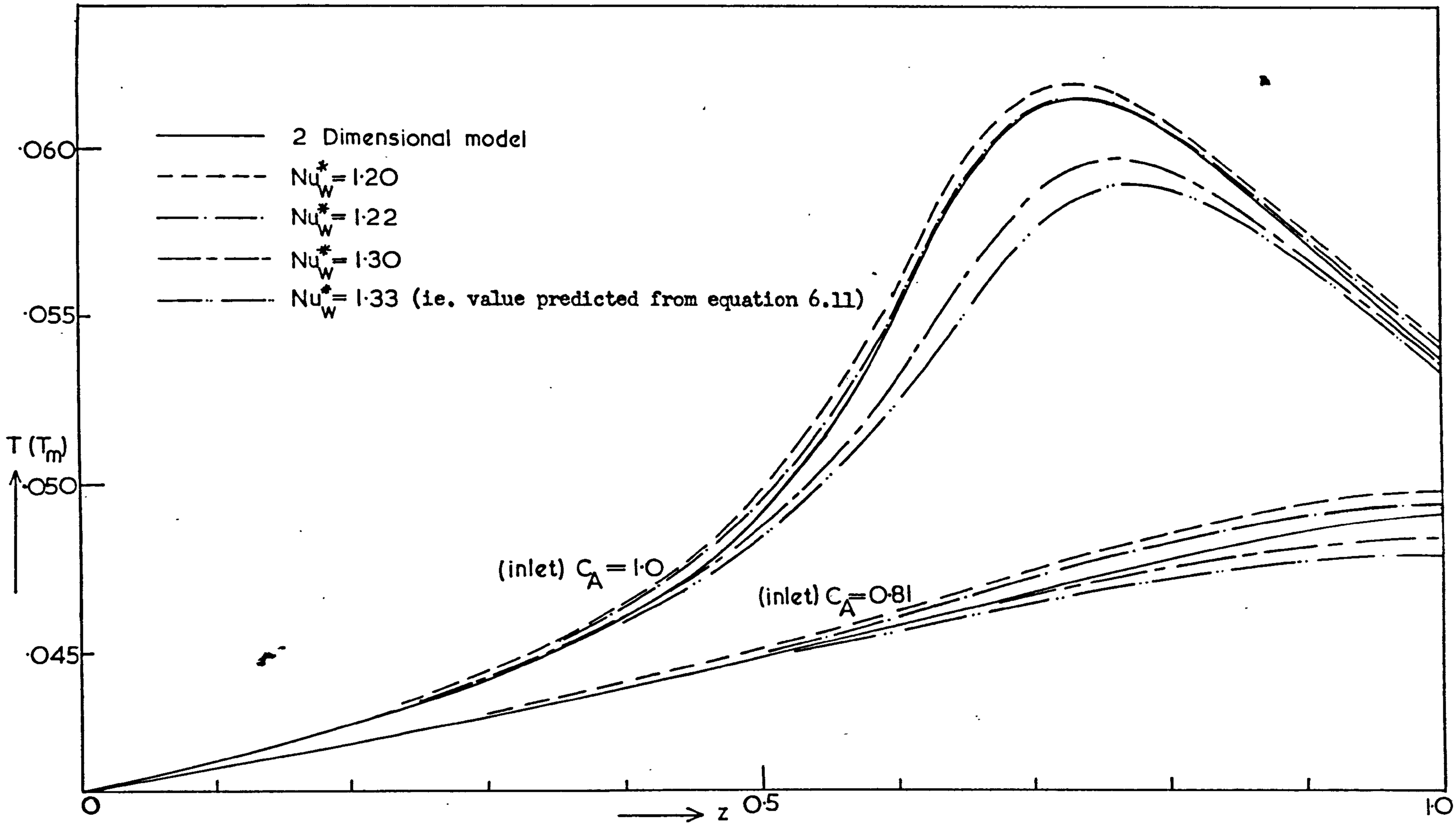

FIG.6.2 Comparison of radial mean temperature profiles computed from the two dimensional model and the one dimensional model using various values of the effective overall wall Nusselt number. Data as given in Table 5.1.

6.2. It can be seen that a value of $Nu^*_w = 1.22$ gives good agreement for both inlet concentrations using the given set of data.

This approach suffers from the disadvantage that, for a given system, some results from a two-dimensional model must be available. The method is not a particularly elegant one, but is attractive since it is easy to use and gives excellent results. The development of the modification to Nu^*_w, as presented here, is not very rigorous and in the absence of other information, it could not be considered generally applicable. However Turner[61] has shown that it is always possible to correct Nu^*_w to give good agreement with the two-dimensional model, and has developed a technique for calculating the correction term without reference to any results for the more complex model.

6.6.4 Comparison of radial temperature profiles and maximum temperatures.

Figure 6.3 shows comparisons, at two longitudinal positions, of the radial temperature profiles predicted by the two-dimensional model with the parabolic profiles predicted from equation (6.14). The parabolic profiles (in this figure only) are based on the mean temperature obtained from the two-dimensional model and have been constructed for two values of the effective overall wall Nusselt number (Nu^*_w). It appears to be fairly general, for exothermic reactions, that the parabolic profile gives a flatter shape for the temperature than is actually the case, and that the radial temperature profile is fairly insensitive to the value of Nu^*_w for a given mean temperature, T_m. (In the reactor, however, T_m will be very dependent on Nu^*_w since this determines how much heat is removed through the wall.) One result of the flattening of the radial temperature profile is that the value of the axial temperature (T_a) predicted by equation (6.13) is too low, and therefore the value of T_a would be in error even if T_m could be estimated exactly.

Figure 6.4 shows the longitudinal profiles of T_a predicted by the two-dimensional model and by using equation (6.13) with various forms of the

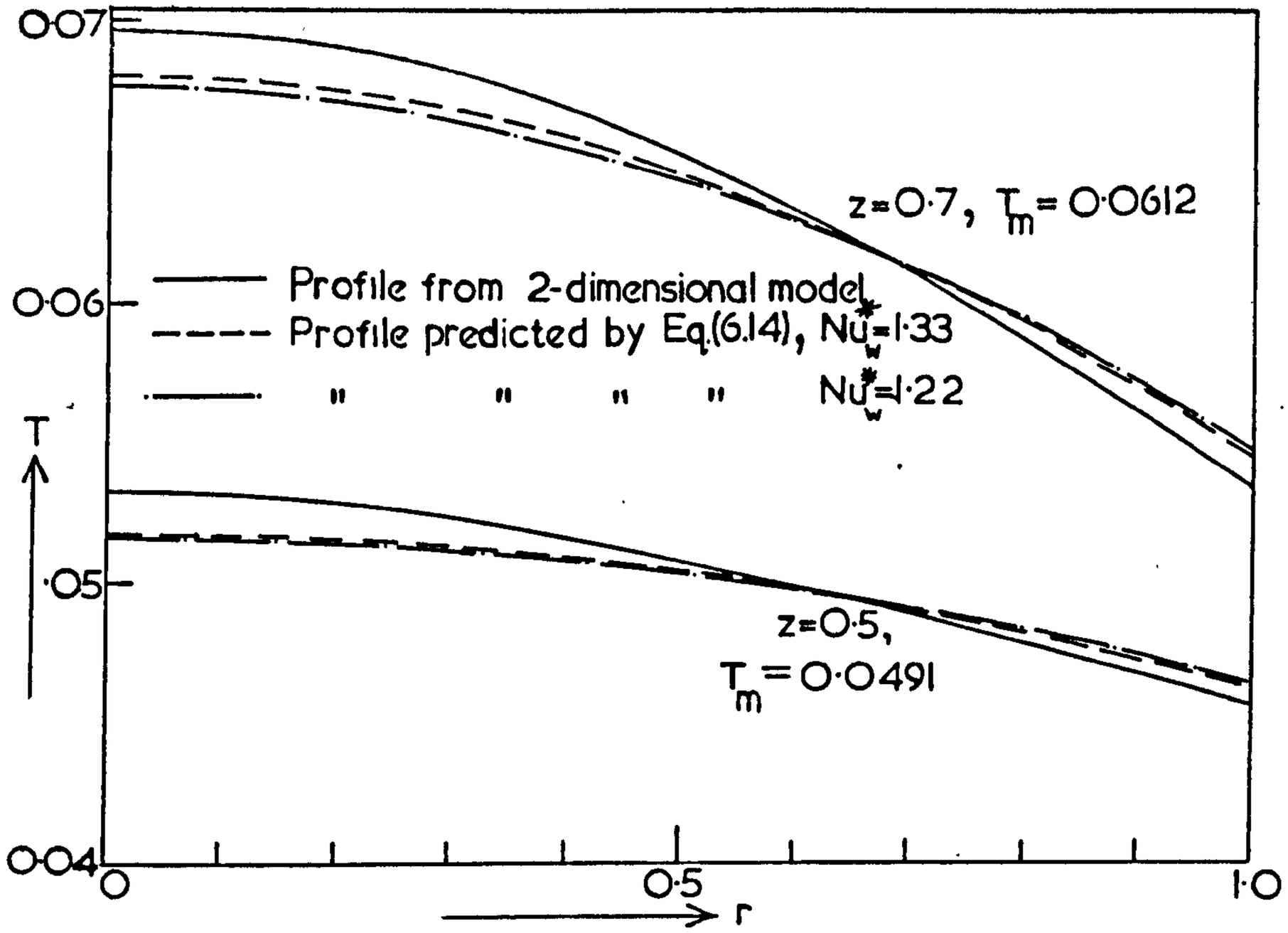

FIG.6.3 Comparison of radial temperature profiles predicted by the two dimensional model with those predicted by equation (6.14) using the same mean temperature (T_m). Data as given in Table 5.1.

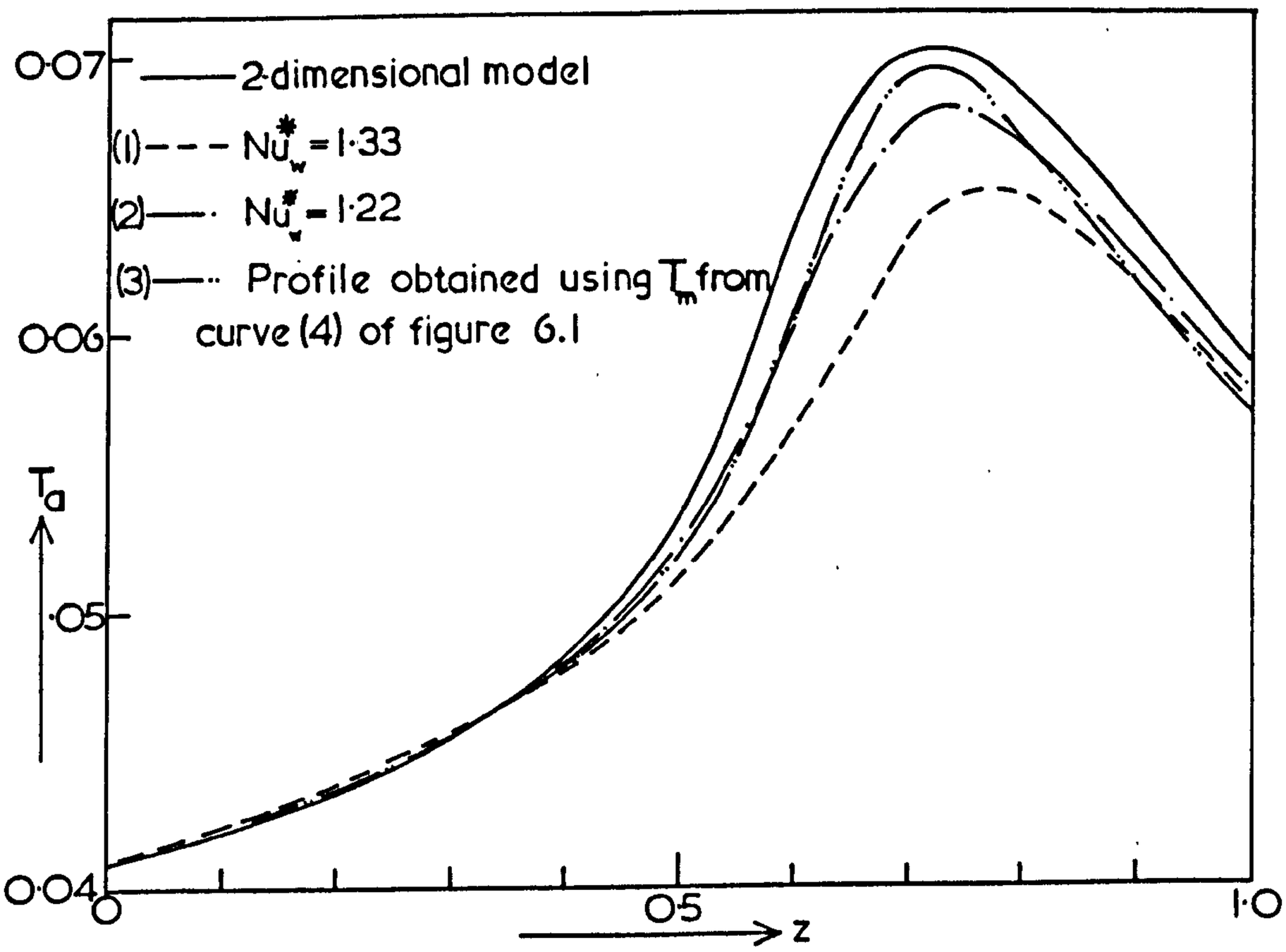

FIG.6.4 Comparison of axial temperatures (r=0) predicted by various forms of the one dimensional model using equation (6.13) with that predicted by the two dimensional model. Data as given in Table 5.1.

one-dimensional model. The 'basic' one-dimensional model (in which $Nu^*_w = \frac{4\ Nu_w}{4 + Nu_w}$ and the reaction rate is evaluated at the mean temperature) considerably underestimates the value of T_a throughout the main reaction zone (curve 1), but this could have been anticipated since it has been shown in Figures 6.1 and 6.2 that the mean temperature itself is underestimated. The improvements to the basic model, which were suggested in sections 6.6.2 and 6.6.3, give better estimates of T_a, the best estimate being given by the modification suggested in section 6.6.2, where the rate constants are altered to take account of the parabolic temperature profile. Since the maximum temperature, for a given T_m, is relatively insensitive to Nu^*_w, the difference between curves (2) and (3) of Figure 6.4 is clearly a reflection of the difference in the values of T_m predicted by the two models. Comparing curve (4) in Figure 6.1 with that for $Nu^*_w = 1.22$ in Figure 6.2, it can be seen that the former overestimates the radial mean temperature in the region of the hot-spot and this to some extent cancels out the underestimation of the axial temperature by equation (6.13).

In Figure 6.4, therefore, the better fit given by curve (3), compared with curve (2), is caused by a fortuitous cancellation of errors and in general this cannot be guaranteed. Since the errors could be cumulative instead of cancelling (as they would be for an inlet concentration of 0.81 (see Figure 6.1)), the method represented by curve (2) is more reliable for general use.

6.7 Discussion of the Results.

6.7.1 General comments.

In discussing the results, a case study approach is again used for the reasons outlined in previous chapters. The results were computed using a value of $Nu^*_w = 1.33$. This value arises from the data used in the previous chapter ($Nu_w = 2.0$) if it is assumed that the exact form of the expression

for Nu^*_w holds:

$$Nu^*_w = \frac{4\,Nu_w}{4 + Nu_w}$$

Alternatively 1.33 may be regarded as the true value of Nu^*_w, which has been chosen as the best one for a particular reactor, using the results from the two-dimensional model. The way in which this value of Nu^*_w is viewed is, in a sense, unimportant in the present context, since for the purposes of a case study, any realistic value would be satisfactory.

For most of the profiles considered, the conversion of species A was almost complete. It was found that in this case the higher the peak temperature, the lower the exit temperature, indicating that the exit temperature is useless as a means of predicting what happens to the temperature profile at other points in the bed. Another interesting feature of the profiles is that the peak temperature always occurred after the peak in C_B. A large number of sets of data were run, varying all the parameters of the model, but providing the exothermity of the B ⟶ C reaction was of the same order of magnitude as that for the A ⟶ B reaction, it was not found possible to get the peak of T in front of that for C_B. This indicates that under optimum conditions, where the peak in C_B occurs at the reactor exit, the maximum temperature will also be at the reactor exit, and any constraint on the temperature can therefore be applied to the outlet conditions.

6.7.2 The effect of some of the parameters of the model.

Although it is very convenient to formulate models and examine their behaviour in terms of dimensionless groups, it is important to remember that these groups are made up of physical, chemical and thermodynamic data which must be supplied before the model is of any use for describing specific systems. (An exception to this is the Peclet number, which has been discussed earlier.) At this stage, therefore, it is worthwhile to examine the importance of some of the individual items of data, and to attempt to assess the accuracy required so that any potential sources of difficulty may be

identified.

Since one of the main attractions of mathematical modelling is to reduce the amount of experimental work which is required to produce a desired result, attention will be given primarily to those parameters which must be estimated from correlations or chosen in an appropriate way. Clearly, some experimental work is always necessary to determine the kinetic data and catalyst characteristics, but much of the benefit of simulation will be lost if it is also necessary to measure properties such as transport coefficients. Many of these are fairly well correlated in the literature, but have often been obtained under idealised conditions such as in isothermal or non-reacting systems, and some of the results may not be reproducible (such as those obtained for randomly packed beds). It is therefore desirable to know how important each parameter is, in order to assess whether the available method for obtaining data is adequate.

Studies on single catalyst pellets do not always provide sufficient information on which to base such an assessment, since, in the end, it is only the effect on the overall performance of the reactor which is important, and this is the result of interactions between the kinetic and heat and mass transport phenomena. The effects of some of the parameters of the model have already been discussed, such as the radial Peclet numbers for heat and mass transport, and the overall effective wall Nusselt number, and these will therefore not be discussed further.

Figure 6.5 shows the influence of pellet radius on reactor performance, and the system is clearly very sensitive to the value of b. It is necessary to include pellet radius in the list of 'uncertain' data, since it will often be the case that the pellets are not perfect spheres of constant radius. It is quite likely that, in practice, the pellets will be cylinders, irregularly shaped, or in a range of sizes. Whatever is the case, it is obviously essential to get a very good estimate of the effective pellet

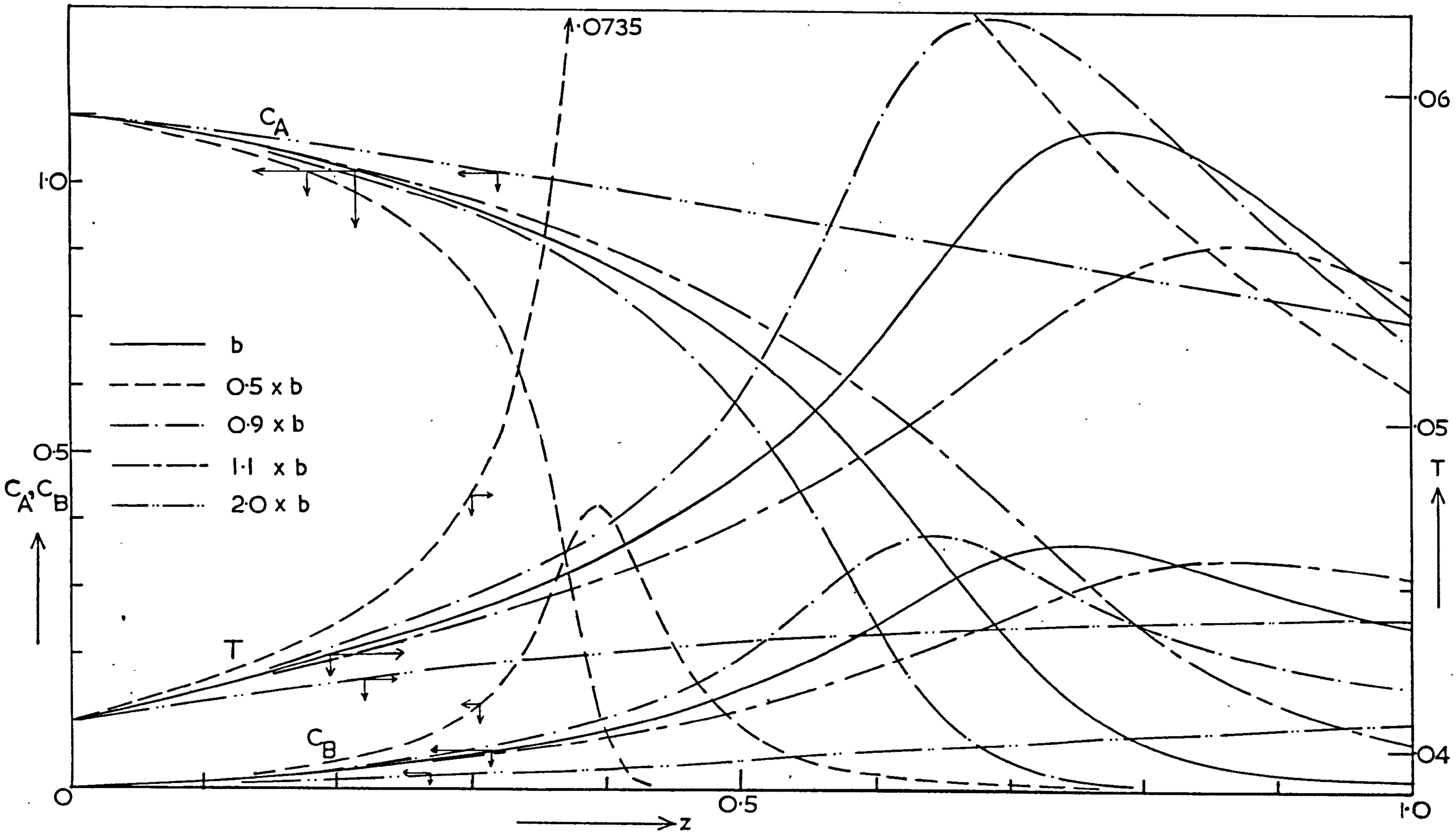

FIG.6.5 The effect of pellet radius on the concentration and temperature profiles within the reactor. Data as given in Table 5.1.

radius. Aris[40] has shown that it is possible to define an effective radius for catalyst pellets subject to Dirichlet boundary conditions, but no such analysis has been carried out for Neumann boundary conditions. The reason for the high sensitivity of the present system to the pellet radius is that the operating conditions lie within the region of appreciable pore diffusion influence (see Figure 5.5) and in this region increasing the radius merely increases the amount of the pellet which is wasted, since very little reactant can diffuse through the outer layers of catalyst before reacting. This lowering of the effectiveness factor is also caused by reducing the effective pore diffusion coefficient for similar reasons (see Figure 6.6). In isothermal systems the effectiveness factor under diffusion control is proportional[29] to $\frac{1}{b^2} \frac{Dp_A}{k_1 + k_3}$ and it is therefore to be expected that the reactor is more sensitive to pellet radius than to diffusivity. This is confirmed by Figures 6.5 and 6.6. It is apparent that the diffusivity must be estimated fairly accurately, although for any permissible error in the performance of the reactor the error in diffusivity can be about twice that which would be acceptable in the pellet radius. As Dp_A increases, there is an increasing tendency towards temperature runaway, and this once again emphasises the need for using heterogeneous models.

Figure 6.7 shows the effect of varying the bed voidage while keeping the superficial velocity (u x e) constant. Any variation in performance is then a reflection only of the volume of catalyst in the bed (per unit length). Since the performance is fairly sensitive to voidage it is necessary to estimate e by weighing the catalyst before packing the tube, rather than using the correlations for voidage which are given in the literature.

The sensitivity of reactor performance to changes in the heat transfer coefficient at the pellet surface is rather less than might be anticipated from single pellet studies, as is shown in Figure 6.8. Although the

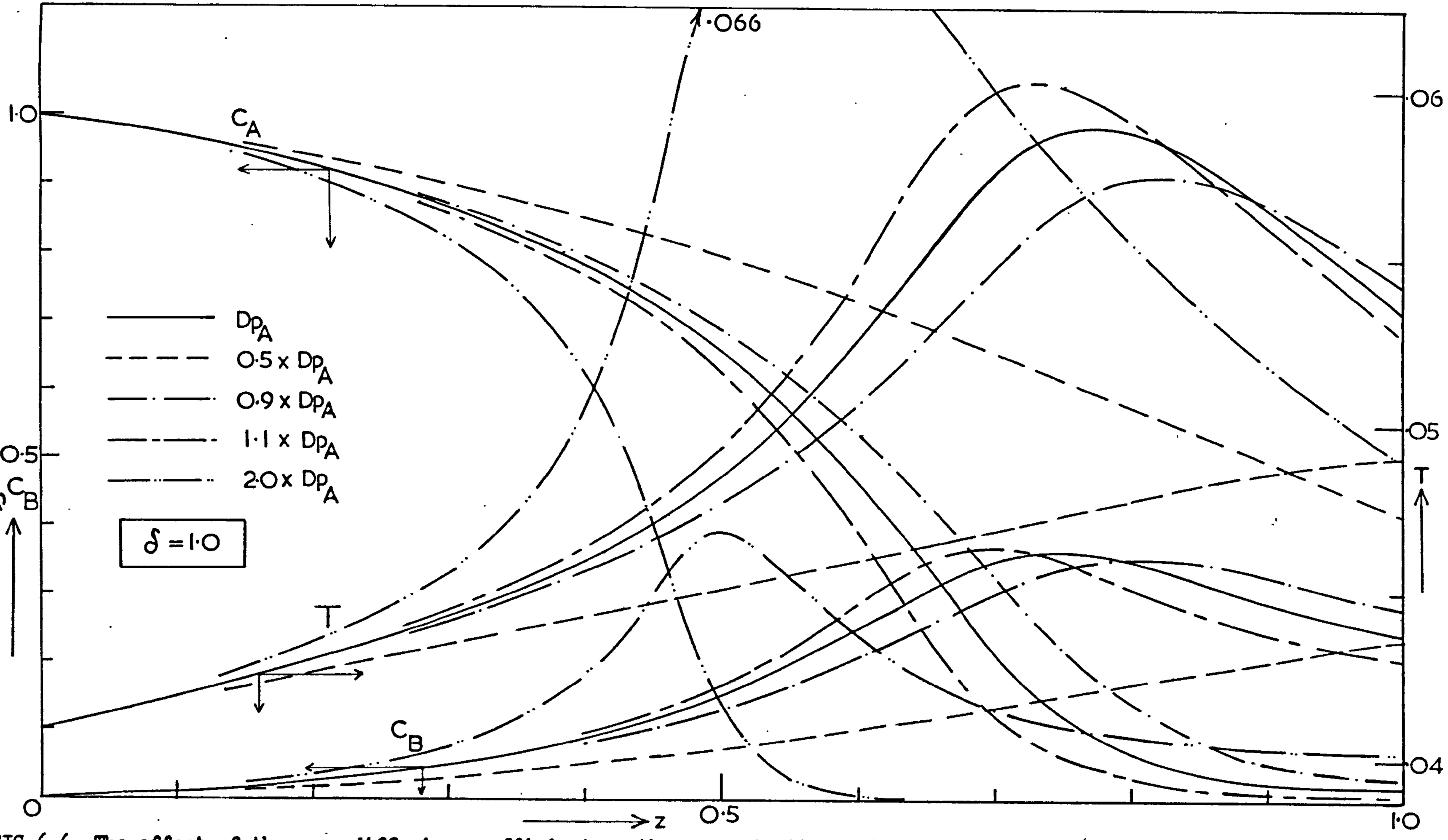

FIG.6.6 The effect of the pore diffusion coefficient on the concentration and temperature profiles within the reactor. Data as given in Table 5.1.

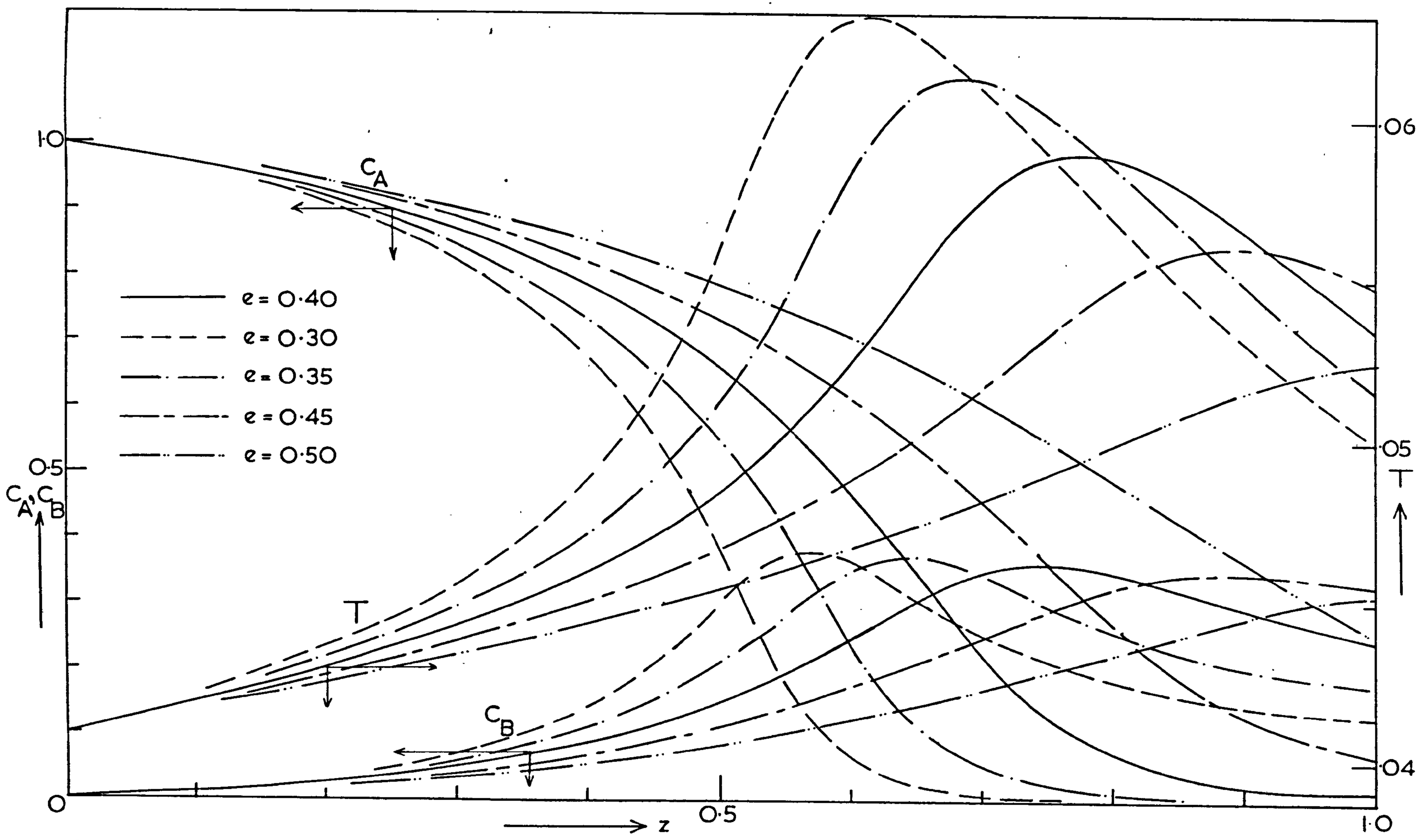

FIG.6.7 The effect of bed voidage on the concentration and temperature profiles within the reactor. The superficial velocity (u x e) is constant. Data as given in Table 5.1.

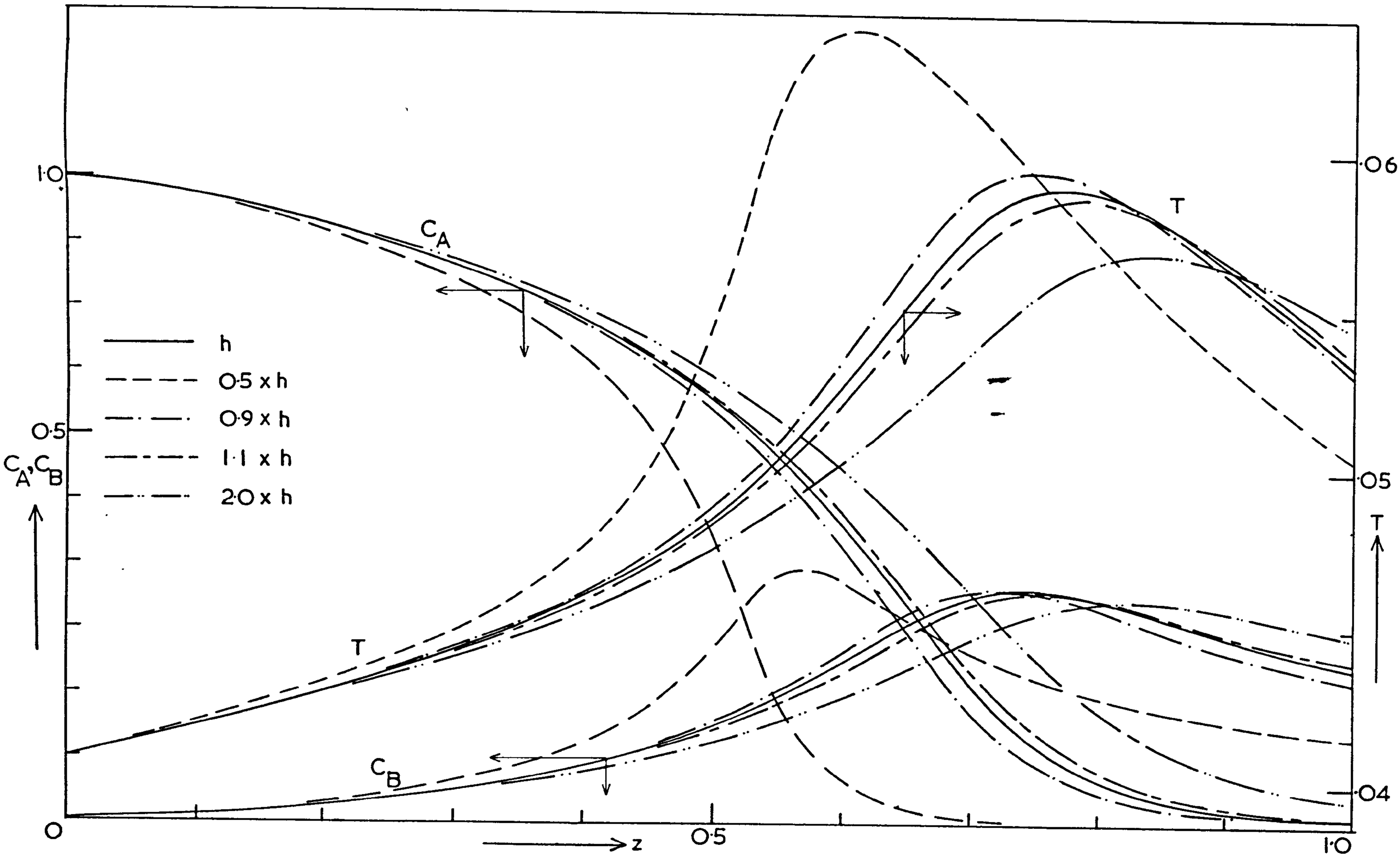

FIG.6.8 The effect of the interphase heat transfer coefficient on the concentration and temperature profiles within the reactor. Data as given in Table 5.1.

temperature difference between pellet and fluid is inversely proportional to Nu', so is the difficulty of heat removal, and the amount of heat leaving the pellet is unaffected for a given reaction rate. Clearly in a real system, an increase in pellet temperature caused by reducing Nu' also increases the reaction rate and the amount of heat generated. In general, however, the temperature rises across the film are only a few degrees, except in regions near temperature runaway, and the reaction rate therefore does not change greatly. Figure 6.8 indicates that for the present data a 10% error in h would probably be acceptable.

Since the effectiveness factor profiles given in Figure 5.5 show that the operating conditions are well away from regions where film mass transfer is controlling, it is to be expected that the reactor performance would not be very sensitive to the mass transfer coefficients (kc_A, kc_B) at the pellet surface, and this is confirmed by Figure 6.9. A 100% change in these parameters only changes the temperature rise by about 7% and putting $kc_A = kc_B = \infty$ changes the temperature rise by about 10%. It appears that no problems are likely to arise in obtaining sufficiently accurate values of these coefficients.

6.7.3 The effect of the inlet conditions.

Raising the inlet temperature or concentration increases the maximum temperature and brings the peaks in the temperature and concentration of B nearer to the reactor inlet. Apart from this the profiles are very similar to those which have already been drawn. In the optimisation of reactor performance, it is often desirable to optimise the yield or concentration of species B, and for a given reactor, this would most conveniently be done by adjusting the inlet conditions. For the data given in Table 5.1 it is found that increasing T and C_A increases the maximum value of C_B over a wide range of both these parameters, but since species A is likely to be expensive, it might be desirable to optimise the yield

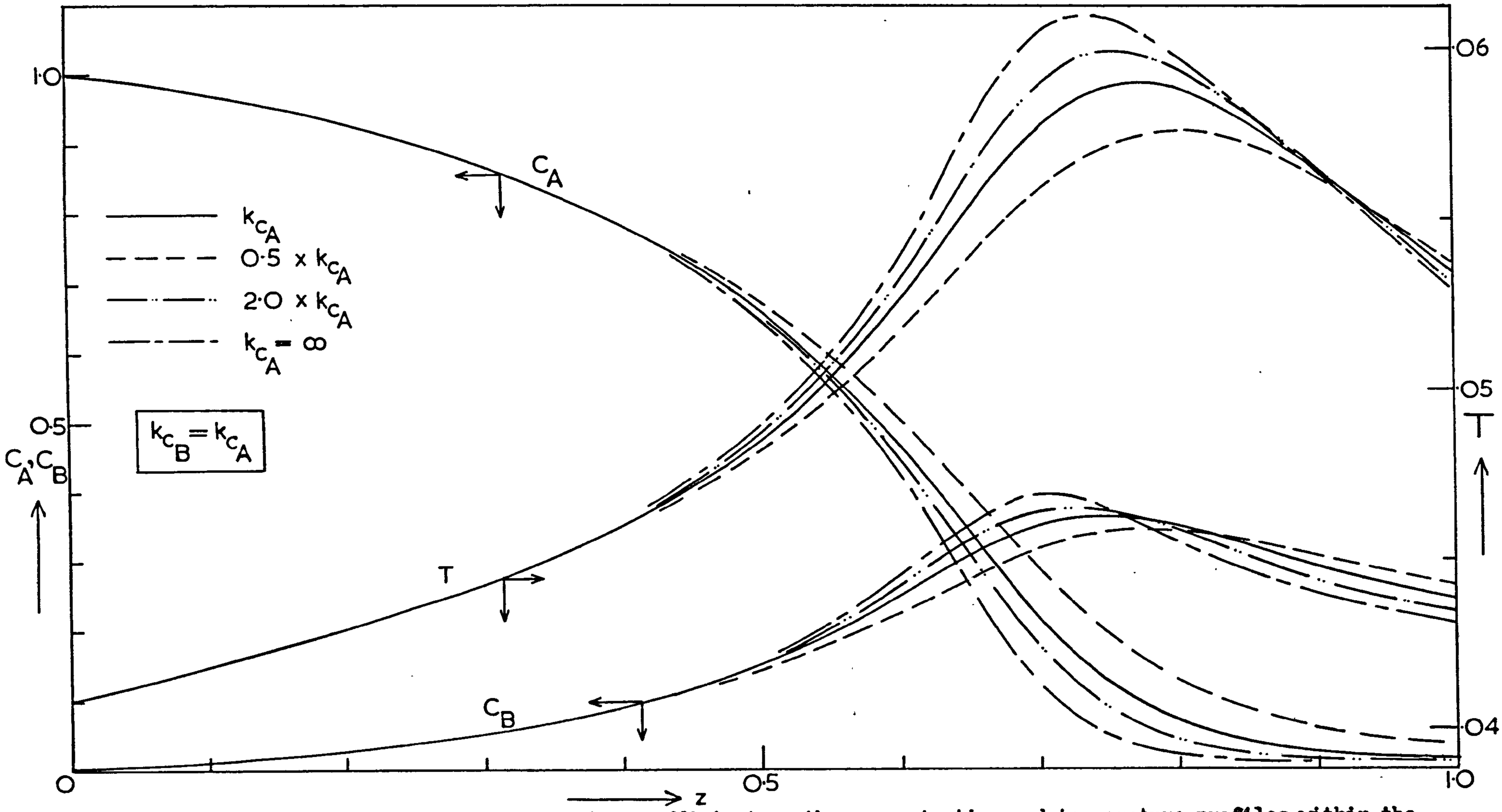

FIG.6.9 The effect of the interphase mass transfer coefficient on the concentration and temperature profiles within the reactor. Data as given in Table 5.1.

$\frac{C_{B(max)}}{C_{A(inlet)}}$. This is realistic at the design stage of the reactor, because the reactor length could be chosen so that $C_B(max)$ coincided with the outlet, $z = 1$. The coolant temperature is clearly another possible control variable, but for simplicity it will be assumed that this is adjusted so that the inlet and coolant temperatures are equal. Figure 6.10 shows the yield of species B as a function of T and C_A at the inlet. These curves are not accurate, since the maximum occurs between two of the finite difference nodes, but they give a good indication of the way the system behaves. For any inlet temperature, there is an optimum inlet concentration, but the yield in this system generally increases as the temperature increases while simultaneously decreasing the concentration. Some of the contours of constant $\frac{C_{B(max)}}{C_{A(inlet)}}$ are shown in Figure 6.11. It is apparent that the best yields will be obtained at high temperatures and low concentrations. Figure 4.1 indicates that yields of around 0.7 could possibly be obtained at high enough inlet temperatures, but in general the resulting temperature profiles are likely to violate constraints on the system.

It therefore appears that an unconstrained optimisation is impossible for the present system and that the optimum performance would be obtained by working as near to the temperature constraint as possible.

6.8 Conclusions.

A one-dimensional model has been developed which predicts the reactor behaviour in fairly good agreement with the two-dimensional model. Modifications to the one-dimensional model are possible which can give even better agreement. The simplifications are based on an assumed parabolic temperature profile which enables the maximum radial temperature to be predicted, and this also agrees fairly well with the two-dimensional prediction. The major advantage of the one-dimensional model is the relatively small amount of

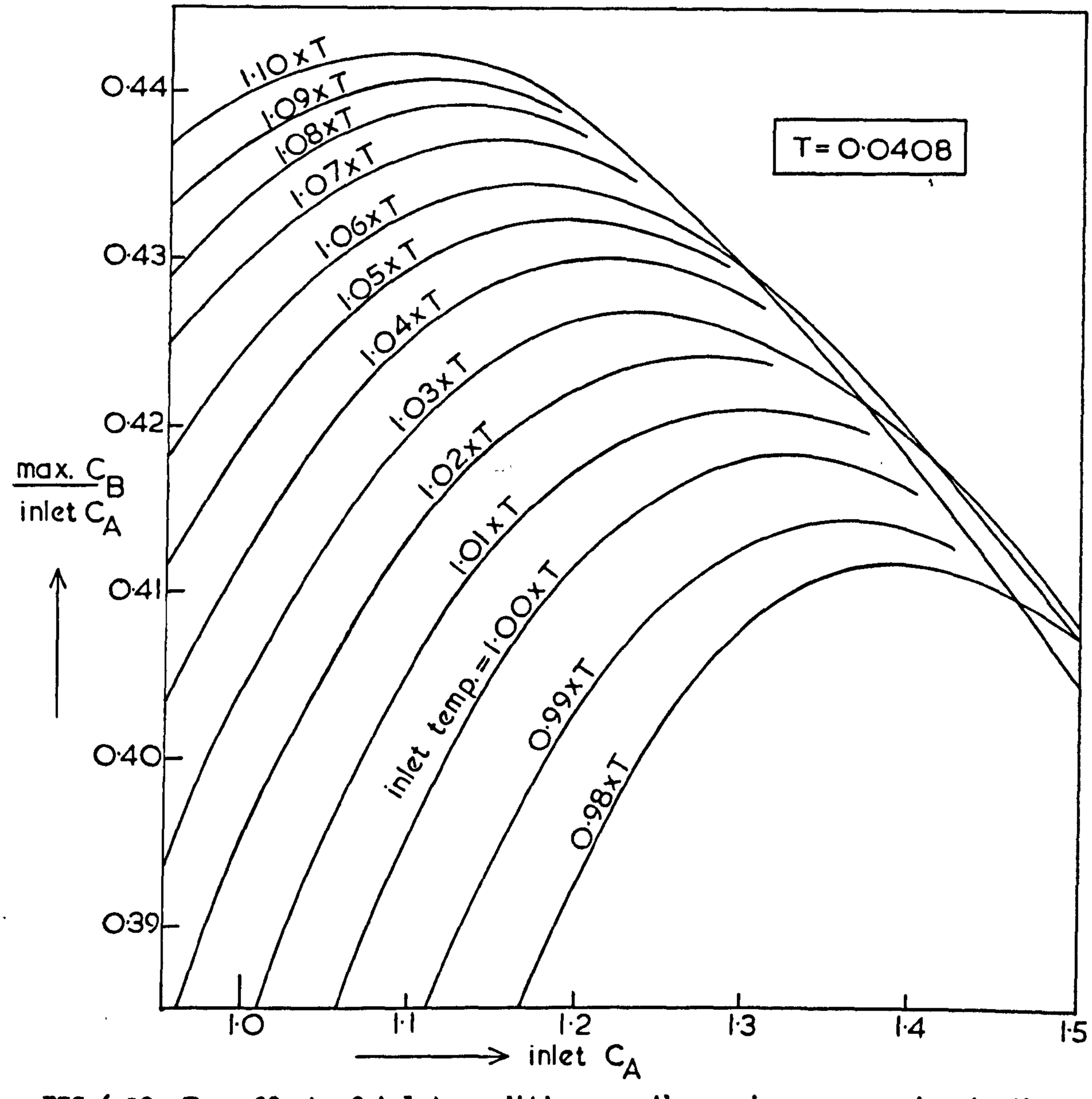

FIG.6.10 The effect of inlet conditions on the maximum conversion to the desired product, B. The coolant temperature is taken to be equal to the inlet temperature in each case. Data as given in Table 5.1.

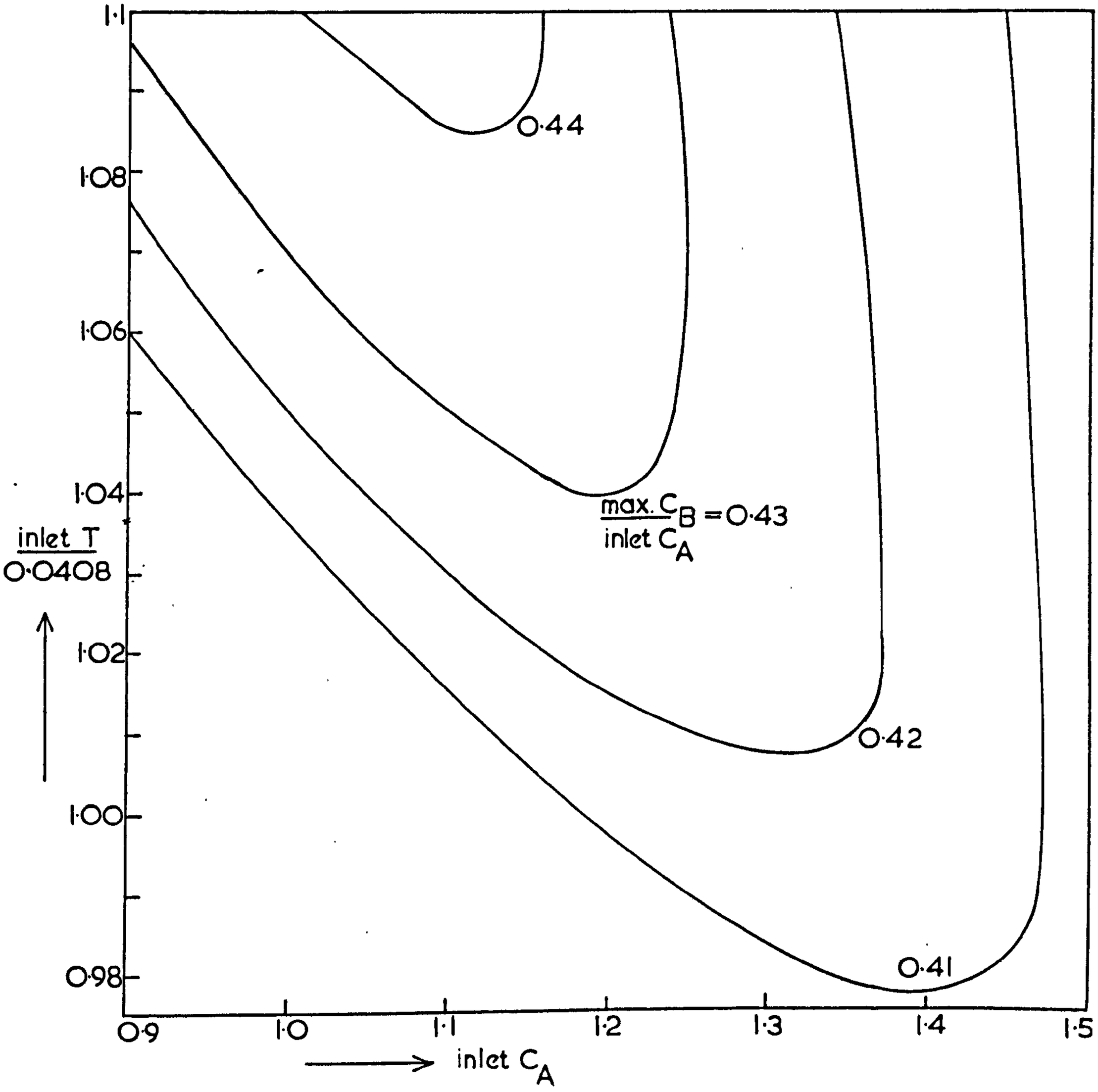

FIG.6.11 Lines at constant maximum conversion to species B, taken from the curves in Figure 6.10.

computation which is required for solution - about one twentieth of that required for the solution of the two-dimensional model.

The model has been used to examine the performance of the reactor, particularly regarding the sensitivity to some of the parameters. It appears that very good estimates are required of the effective pellet radius, the pore diffusion coefficient and the effective overall wall Nusselt number, but that other parameters are less critical. In particular, the performance is relatively insensitive to the interphase mass transfer coefficient.

The model displays the expected parametric sensitivity in most ways, but this is less extreme than is the case for quasi-homogeneous systems. The results also indicate that unconstrained optimisation would be unsatisfactory for the system considered, and that this could also be true for other systems where the desired product is destroyed by further reaction, particularly if the activation energy for the A $\longrightarrow$ B reaction is high, making high temperature operation desirable for a good selectivity.

Since the optimal performance of the reactor is likely to be realised when operating very close to constraints, it is apparent that accuracy of the mathematical model is essential in the region of the optimum. Great advantage can clearly be gained by using the correct approach to the optimisation, particularly with regard to the use of one- and two-dimensional models. The best strategy would appear to be to use the one-dimensional model to locate the optimum within some predetermined limits, and then to use the two-dimensional model to refine the estimate as required. Used in this way, absolute accuracy of the one-dimensional model is not of paramount importance. It is the time of solution which is critical in this context.

CHAPTER 7

DYNAMIC MODELS OF THE SINGLE CATALYST PELLET

7.1 Introduction.

In order to develop a dynamic mathematical model of the heterogeneous catalytic reactor, it is first necessary to have available a dynamic model of the single catalyst pellet. McGuire and Lapidus[16] proposed such a model of the catalyst pellet, ignoring the interphase resistances to heat and mass transfer. This type of model has been shown to be inappropriate for the steady state modelling of exothermic reactions, and it is therefore also unsatisfactory for dynamic modelling.

In this chapter a dynamic model of the catalyst pellet will be developed which includes the interphase resistances to heat and mass transfer. It will be seen that the dynamic model can be simplified in a similar way to that used for the steady state model, and that the behaviour of the pellet may be predicted from the solution of one first-order ordinary differential equation.

It has been shown in Chapter 4 that the selectivity is no more sensitive to changes in the system parameters than is the effectiveness factor, and this means that any simplifications which can be developed for the A $\longrightarrow$ B reaction can equally well be applied to the more complex reaction scheme. It is therefore proposed to examine initially a system in which only one reaction is occurring, and then to extend the results to the set of consecutive and parallel reactions.

7.2 The fully distributed model for the A $\longrightarrow$ B reaction.

7.2.1 Formulation of the equations.

Using the same nomenclature as in the previous chapters, the equations describing the heat and mass balances on an element of the pellet become

$$\frac{\partial^2 c_A}{\partial y^2} - \frac{2}{1-y}\frac{\partial c_A}{\partial y} - \phi_1^{*2} c_A^{n_1} = K_c \frac{\partial c_A}{\partial \tau} \qquad (7.1)$$

$$\frac{\partial^2 t}{\partial y^2} - \frac{2}{1-y}\frac{\partial t}{\partial y} + H\phi_1^{*2} c_A^{n_1} = K_T \frac{\partial t}{\partial \tau} \qquad (7.2)$$

(Note: y = dimensionless distance from the pellet surface, 1 - s/b).

Subject to the following boundary and initial conditions:

$$\frac{\partial c_A}{\partial y} = \frac{\partial t}{\partial y} = 0 \quad \text{at} \quad y = 1, \quad \tau \geq 0$$

$$\left.\begin{aligned} \frac{\partial c_A}{\partial y} &= \frac{Sh'_A}{2}(c_A - C_A) \\ \frac{\partial t}{\partial y} &= \frac{Nu'}{2}(t - T) \end{aligned}\right\} \quad \text{at} \quad y = 0, \quad \tau \geq 0$$

$$\left.\begin{aligned} t &= t_{\tau=0} \\ c_A &= c_{A_{\tau=0}} \end{aligned}\right\} \quad \text{at } \tau = 0, \quad 0 \leq y \leq 1$$

where

$$K_c = \frac{b^2 e^*}{Dp_A}$$

$$K_T = \frac{\rho^* b^2 C^*_p}{Kp}$$

The external variables causing disturbances may be concentration, temperature and flowrate, making C_A, T, Nu' and Sh'_A functions of time (τ).

7.2.2 Solution of the equations.

Equations 7.1 and 7.2 may be solved using the same method as for the two-dimensional steady state reactor model, since the form of the differential equations is basically the same in each case. The main differences between the two finite difference formulations are that, for the transient pellet, a finite difference network containing two step sizes must be used, and the external conditions and boundary transport coefficients may change with time. (In the tubular reactor case, this would correspond to a variation in the

coolant temperature and wall heat transfer coefficient along the length of the reactor.) The varying external or boundary phenomena cause no computational problems, however, and can easily be incorporated into the finite difference formulation of the equations, as shown in Appendix 3.

The solution of the differential equation may be accomplished using a procedure similar to that for the two-dimensional reactor model, except that the non-linear terms can be obtained explicitly, whereas for the reactor it is first necessary to obtain η and ψ by solving the pellet model at each node of the finite difference network. In the latter case, the computation also has a specific end (i.e. when $z = 1$) whereas for the transient pellet it is continued as long as required. Subject to these differences, the equations can be solved using steps 1 and 3 - 6 in section 5.3, replacing 'axial' by 'time' and 'C_A, C_B and T' by 'c_A, t'. As for the tubular reactor, the profiles assumed at step (1) were obtained by a linear projection of the two previous profiles, except at the first time step, where the assumed profile is the initial boundary condition.

7.2.3 Modification of the model.

Before computing any results from the model, it is possible to draw some conclusions about the characteristics of the system from a further examination of the differential equations. Equations (7.1) and (7.2) may be written in the form:-

$$\nabla^2 c_A - \phi_1^{*2} c_A^{n_1} = K_c \frac{\partial c_A}{\partial \tau} \qquad (7.3)$$

$$\nabla^2 t + H\phi_1^{*2} c_A^{n_1} = K_T \frac{\partial t}{\partial \tau} \qquad (7.4)$$

In order to examine the magnitudes of the terms in these equations on a comparable basis, it is convenient to multiply equation (7.3) by H giving:-

$$H\nabla^2 c_A - H\phi_1^{*2} c_A^{n_1} = HK_c \frac{\partial c_A}{\partial \tau} \qquad (7.5)$$

Equations (7.4) and (7.5) now have a term in common, $H \phi_1^{*2} c_A^{n_1}$, and since the equations apply under all conditions, it may be postulated that the terms in each of the equations have the same order of magnitude. The dynamic characteristics of the equations are then comparable and

$$\left| K_T \frac{\partial t}{\partial \tau} \right| \sim H K_c \frac{\partial c_A}{\partial \tau} \qquad (7.6)$$

where $\sim$ has been used to indicate an order of magnitude relationship.

From equation (7.6)

$$\left| \frac{dc_A}{dt} \right| \sim \frac{K_T}{H K_c}$$

i.e.

$$\frac{\frac{dc_A}{c_A}}{\frac{dt}{t}} \sim \frac{K_T t}{H K_c c_A} > \frac{K_T T}{H K_c C_A} = \frac{1}{\beta} \frac{K_T}{K_c} \qquad (7.7)$$

In practice the upper bound on β is 10^{-2} and is more commonly 10^{-3}. $\frac{K_T}{K_c}$ is typically around 0.3. Equation (7.7) therefore implies that, on a relative basis, the concentration changes at least 30 times faster than temperature. Within the catalyst pellet $t > T$ and $c_A < C_A$ making this estimate very conservative in many cases.

This result conflicts with the basic assumption which led to equation (7.6) and the dynamic characteristics of the two equations are not of comparable magnitudes. In a system where two coupled transient effects are occurring, as is the case here, it is only necessary to consider both phenomena if the relative rates of change are of the same order of magnitude. If this is not the case, then the faster change will enable one of the variables to reach a pseudo-steady state, and the response will depend only on the transient event having the longest time constant.

In the case considered here, the relative rates of change of concentration

and temperature are such that the concentration change is very fast compared with the change in temperature, and can be regarded as being at a pseudo-steady state which depends only on the instantaneous temperature profile.

As an example of the rate at which the concentration changes, consider the case of an isothermal reaction, where the concentration is constant ($= C_o$) throughout the pellet at $\tau = 0$. In the period immediately following $\tau = 0$, there will be no radial gradients in concentration and equation (7.1) becomes, for a first order reaction

$$K_c \frac{dc_A}{d\tau} = -k_1^* c_A \qquad (7.8)$$

where $c_A = 1$ at $\tau = 0$

This equation will only apply over an infinitesimal time after $\tau = 0$, since concentration gradients will immediately begin to develop when the imposed concentration profile is relaxed due to diffusion of reactant into the pellet from the surrounding fluid. Nevertheless, equation (7.8) can be used to give some indication of the response over a limited period, the solution being:

$$c_A = \exp(-\frac{k_1^*}{K_c} \delta\tau)$$

Expanding this and neglecting high order terms:

$$c_A = 1 - \frac{k_1^*}{K_c} \delta\tau + \frac{1}{2} (\frac{k_1^*}{K_c} \delta\tau)^2 \qquad (7.9)$$

If the initial gradient $\left.\frac{dc_A}{d\tau}\right|_{\tau = 0}$ was used in assessing the concentration after time $\delta\tau$, the value of c_A would be given by:

$$c_A = 1 - \frac{k_1^*}{K_c} \delta\tau \qquad (7.10)$$

The error caused by using equation (7.10) is therefore

$$\frac{1}{2} (\frac{k_1^*}{K_c} \delta\tau)^2$$

and the rate of growth of the error is

$$\frac{1}{2}\left(\frac{k_1^*}{K_c}\right)^2 \delta\tau \times 100 \text{ per cent per unit time} \qquad (7.11)$$

Taking typical values of $k_1^* = 3$, $K_c = 4.95$ seconds and imposing an upper limit of 0.1% per second on the rate at which the error is permitted to grow, equation (7.11) gives the required $\delta\tau$ as

$$\delta\tau \leq 5.4 \times 10^{-3} \text{ seconds.}$$

This is clearly a very short step to take, and a one second response using only 100 radial increments in the pellet would require about five times as much time as the whole quasi-homogeneous steady state reactor model (i.e. about 30 minutes on an ICL KDF9 computer). The method used to derive $\delta\tau$ is clearly not very rigorous, since it is in fact based on an impossible initial condition, and in practice it is found that the result is optimistic, particularly for an exothermic reaction. It is usually found necessary to use step sizes in the range 10^{-4} to 10^{-6} seconds to obtain satisfactory convergence.

Assuming that the concentration profile reaches a pseudo-steady state, the equations describing the transient response of the pellet become

$$\frac{\partial^2 c_A}{\partial y^2} - \frac{2}{1-y}\frac{\partial c_A}{\partial y} - \phi_1^{*2} c_A^{n_1} = 0 \qquad (7.12)$$

$$\frac{\partial^2 t}{\partial y^2} - \frac{2}{1-y}\frac{\partial t}{\partial y} + H\phi_1^{*2} c_A^{n_1} = K_T \frac{\partial t}{\partial \tau} \qquad (7.13)$$

The boundary conditions and method of solution are the same as those for equations (7.1) and (7.2), although it is of course unnecessary to specify an initial concentration profile. A time step of 0.1 seconds is usually sufficient to ensure convergence of the solution of these equations, confirming the conclusion that equation (7.7) is conservative.

Although the computation time required to solve equations (7.12) and

(7.13) shows considerable improvement over that which would be required to solve equations (7.1) and (7.2), it is still too long to enable incorporation of the pellet model into a dynamic model of the reactor, and this is likely to be true of any fully distributed model of the pellet.

7.3 The lumped thermal resistance model for the A ⟶ B reaction.

A typical solution of equations (7.12) and (7.13) is displayed in Figure 7.1, where the radial temperature profiles have been drawn, showing the effect of a step change in the fluid temperature from 0.0408 to 0.045. (For an activation energy of 32,000 cal/g.mole, this would represent about 68°C increase in temperature.) It is apparent from the diagram that, for a short time, the step change induces a significant thermal gradient at the pellet surface (y = 0). After 0.5 seconds the gradient has flattened considerably, and after 1.5 seconds the pellet is again almost isothermal.

These profiles indicate that a lumped thermal resistance model is again likely to be useful, especially in real systems, where step changes in temperature are uncommon. The assumption of a lumped thermal resistance implies that the pellet is isothermal, and the differential equations describing the mass transport can be solved analytically. The solution of equation (7.12) has been given in Chapter 4 for the complex reaction scheme, and the solution for the single reaction can be found by putting $k_3^* = 0$ in equation (4.11).

If t is constant throughout the pellet, equation (7.13) may be replaced by a heat balance on the whole pellet:

$$T - t + B_o Sh'_A (C_A - c_{A_s}) = \frac{1}{3} \frac{K_T}{Nu'} \frac{dt}{d\tau} \qquad (7.14)$$

subject to the initial condition

$$t = t_{\tau = 0}$$

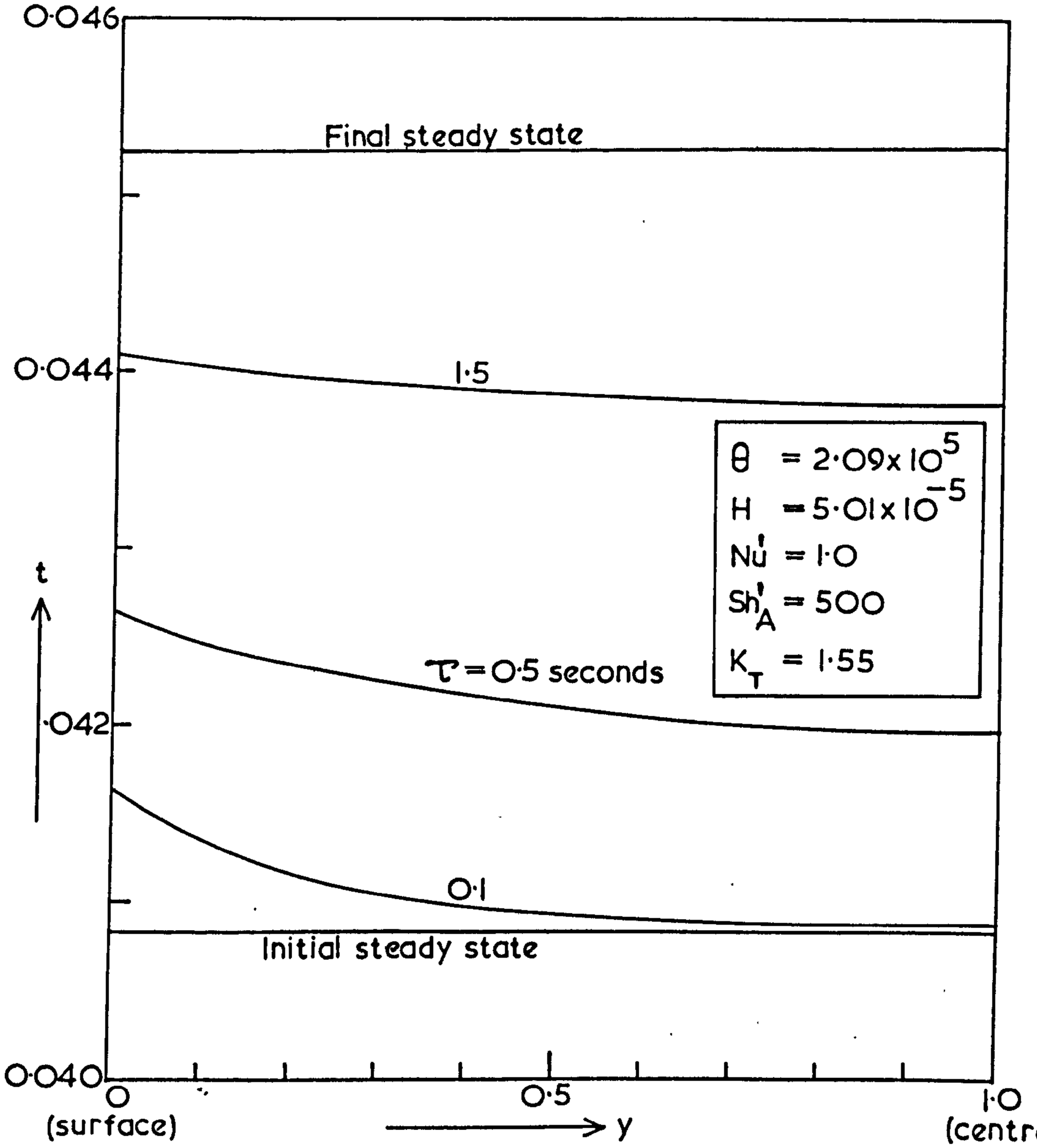

FIG.7.1 The radial temperature profiles within the catalyst pellet in response to a step change in the dimensionless fluid temperature from 0.0408 to 0.045 .

where

$$c_{A_s} = \frac{\frac{Sh'_A}{2} c_A}{(\frac{Sh'_A}{2} - 1) + \sqrt{k_1^*} \coth \sqrt{k_1^*}} \quad \text{(from equation 4.11)}$$

$$k_1^* = \phi_1^{*2}$$

Equation (7.14) may be solved by any of the normal techniques. For the following work, the solution was actually accomplished using the Runge-Kutta-Merson algorithm which is available as a library program.[69]

Figure 7.2 shows a comparison of the temperatures and effectiveness factors predicted by the distributed and lumped parameter models. Comparison of the models, in terms of temperature, is not straightforward in the period immediately following the step change, since the actual temperature profile is not flat, and therefore no single temperature characterises the performance of the pellet in the distributed case. In the diagram, the maximum and minimum temperatures, at the surface and centre, are shown. Even using the mean temperature would not be a satisfactory method of judging how good the agreement is between the two models, since the importance of the temperature at any point is related to the concentration at that point. This problem is not difficult to overcome, however, because the effectiveness factor itself provides a complete representation of the performance of the pellet, since it is effectively an integration of the rate of reaction throughout the pellet. This can therefore be regarded as the means of judging the overall performance of the pellet, and it is clear that agreement between the two models is excellent.

It is not surprising that the lumped thermal resistance model gives good agreement with the distributed model, since the relative magnitudes of the resistances to heat transfer inside and outside the pellet are the same as for the steady state, and a similar accuracy of the models could therefore be expected.

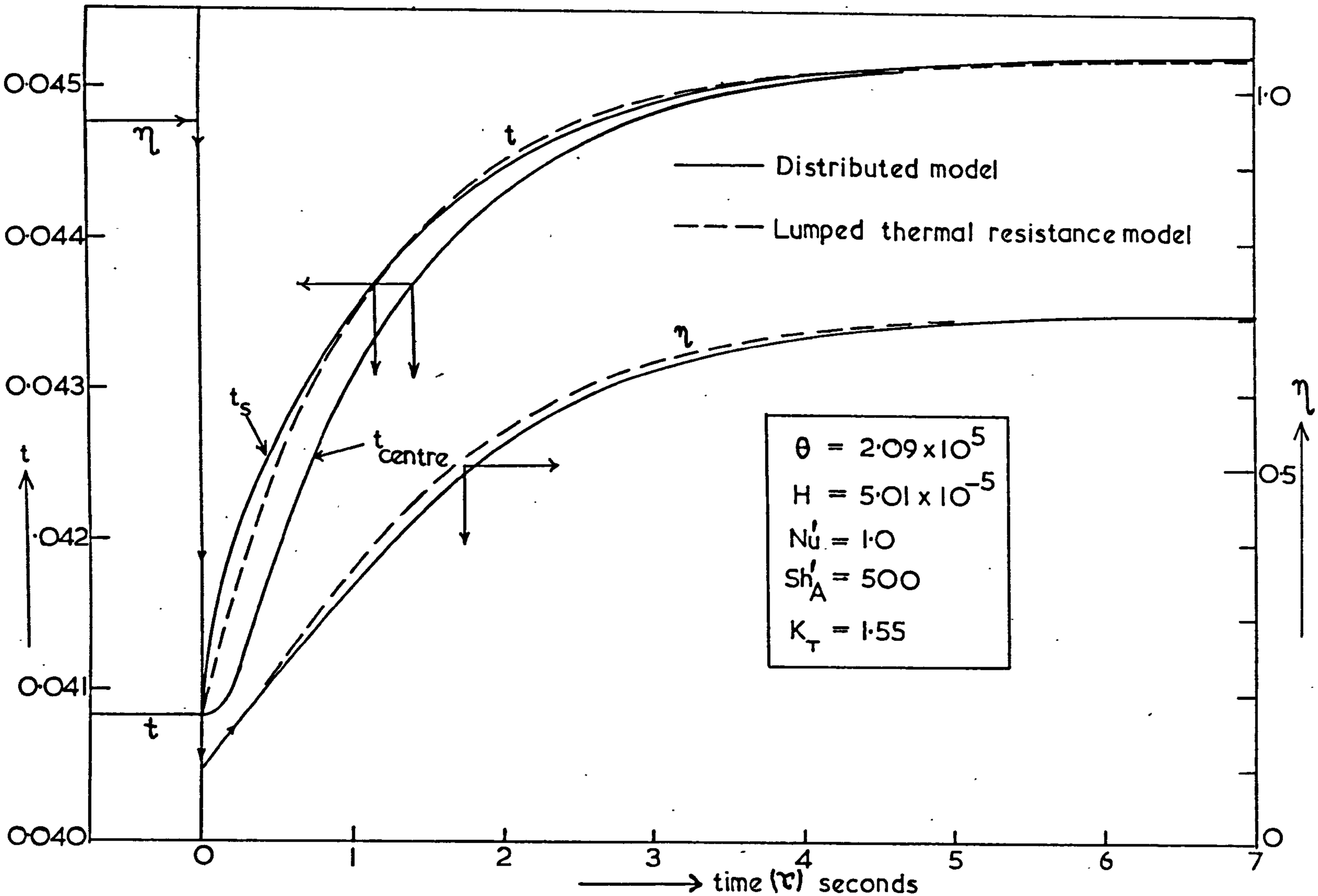

FIG.7.2 Comparison of pellet temperatures and effectiveness factors predicted by the distributed and lumped thermal resistance models in response to a step change in the dimensionless fluid temperature from 0.0408 to 0.045 .

7.4 The lumped thermal resistance model for the complex reaction scheme.

Equation (7.14) may easily be extended to the case where complex reactions are occurring, since a heat balance on the catalyst pellet gives:-

$$B\left(Sh'_A\left(1 - \frac{c_{A_s}}{C_A}\right)\left(\frac{k_1^*}{k_1^* + k_3^*}(1 + H_2) + \frac{k_3^*}{k_1^* + k_3^*}H_3\right) - Sh'_B\left(\frac{c_{B_s}}{C_A} - \frac{C_B}{C_A}\right)H_2\right) - t + T = \frac{2}{3}\frac{K_T}{Nu'}\frac{dt}{d\tau} \quad (7.15)$$

(cf. equation (4.5)).

The expressions for c_{A_s} and c_{B_s} are given by equations (4.25) to (4.27). Equation (7.15) may be solved in the same way as equation (7.14). The computation is very rapid, and may often be faster than the steady state solution, since the latter involves an iterative process which requires several evaluations of the left hand side of equation (7.15). The solution time is therefore short enough for the model to be incorporated into a dynamic model of the reactor such as that proposed in Chapter 8.

Some typical transient responses are indicated in Figure 7.3, which shows the response to ramp changes in T occurring at three different rates. For an activation energy of E_1 = 32,000 cal/g.mole, the initial temperature of T = 0.04 corresponds to 646°K and the temperature on the right hand side of the graph is 924°K. For the three responses, the temperature rise across the graph (278°C) was allowed to take place over periods of 100, 10 and 1 seconds. It can be seen that the responses are very different, the slowest change naturally giving rise to a response which is closest to the steady state curves. The pellet appears to be capable of following a transient change of about 3°C per second so that the pellet performs as if it were at steady state. Even if this could be applied as a general rule, however, there would be no advantage in solving the steady state pellet

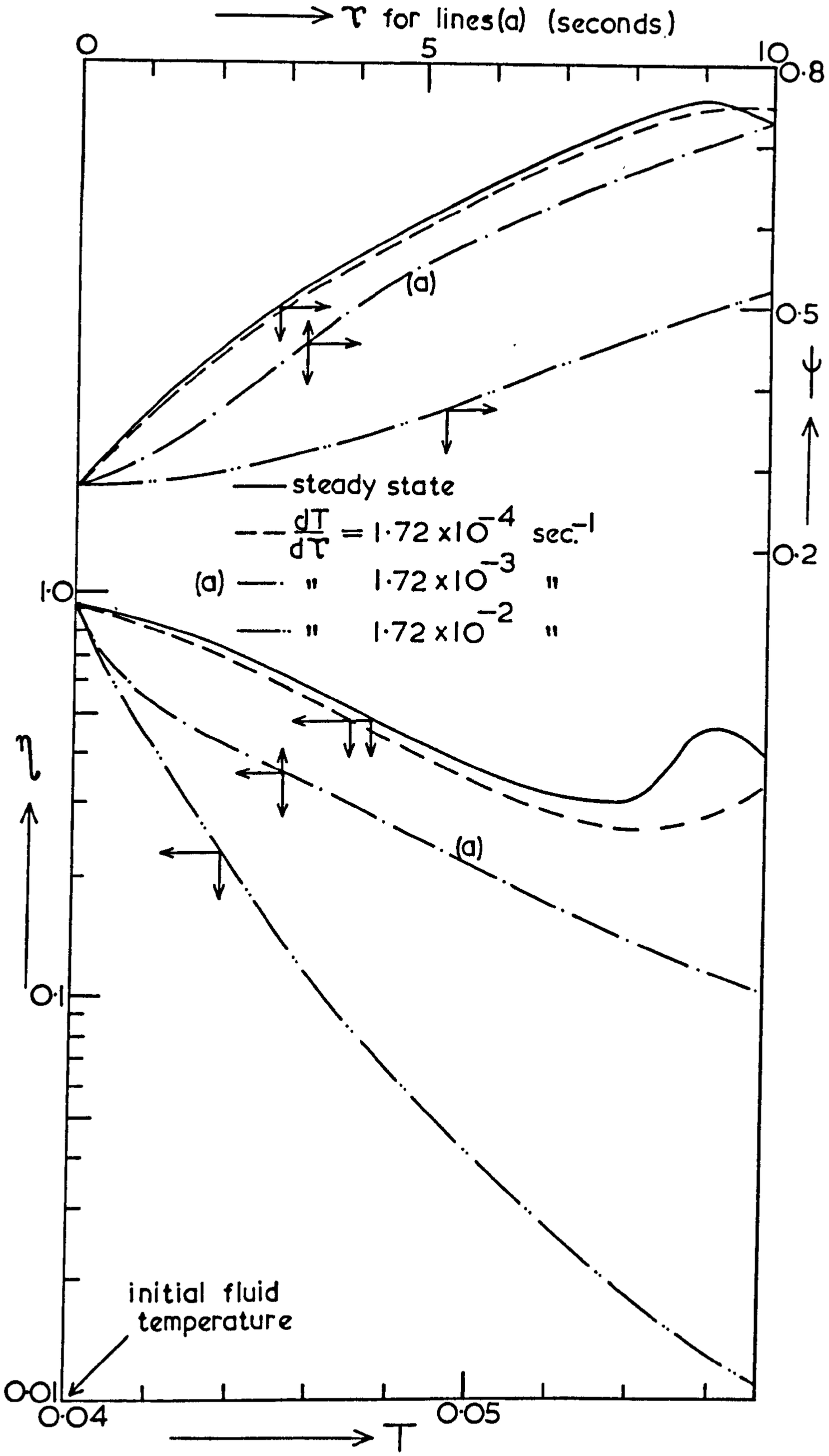

FIG.7.3 The effectiveness factor and selectivity in response to a ramp change in fluid temperature. Data as given in Table 3.1 .

model instead of the transient model since it has already been stated that the transient pellet model can be solved at least as rapidly as the steady state model. Moreover, it is the small deviations from the steady state which give the reactor its dominant transient characteristics as will be seen in the following chapter.

CHAPTER 8

A ONE-DIMENSIONAL DYNAMIC MODEL OF THE REACTOR

8.1 Introduction.

There has been relatively little work done on dynamic modelling of fixed bed catalytic reactors, compared to that which has been done on steady state modelling and most has been concerned with quasi-homogeneous systems (e.g. 7, 8, 9, 79).

Heterogeneous dynamic models have been proposed by McGuire and Lapidus[16] and by Feick and Quon;[99] but in each case the models were two-dimensional and required such a great amount of computational effort that no detailed examination of the reactor performance was possible. In the absence of any useful information on the characteristics of the dynamic behaviour, it would be instructive to carry out a case study of the reactor and to examine the response under transient conditions. The reactor model which is proposed is one-dimensional and may be regarded as being based on the assumption of an effective overall wall heat transfer coefficient. Although this gives an excellent prediction of steady state performance, there is no prior reason to presume that it will remain valid in the transient case, but it should nevertheless be possible to obtain satisfactory estimates of reactor performance and hence to obtain an understanding, which is lacking at the present time, of the dynamic characteristics of packed bed tubular reactors.

8.2 Formulation and solution of the equations.

Using the same nomenclature as for the one-dimensional steady state model of the reactor, the equations representing heat and mass balances may be written in dimensionless form as follows:

$$\frac{\partial C_A}{\partial z} + G_2 (\phi_1^2 C_A^{n_1} + \phi_3^2 C_A^{n_3}) \eta + \left(\frac{G_5}{G_1}\right) \frac{\partial C_A}{\partial \tau} = 0 \qquad (8.1)$$

$$\frac{\partial C_B}{\partial z} - G_2 (\phi_1^2 C_A^{n_1} + \phi_3^2 C_A^{n_3}) \eta \psi + \left(\frac{G_5}{G_1}\right) \frac{\partial C_B}{\partial \tau} = 0 \qquad (8.2)$$

$$\frac{\partial T}{\partial z} + 2\left(\frac{Nu_W^*}{G_3}\right)(T - T_c) - G_4(t - T) + \left(\frac{G_6}{G_3}\right) \frac{\partial T}{\partial \tau} = 0 \qquad (8.3)$$

where $G_5 = \frac{R^2 e}{2bu} P_{e_M} \left(= G_1 \frac{Le}{u}\right)$ seconds

$$G_6 = \frac{R^2 e}{2bu} P_{e_H} \left(= G_3 \frac{Le}{u}\right) \text{ seconds}$$

The initial conditions are:

$$C_A = C_A(\tau), \quad C_B = C_B(\tau), \quad T = T(\tau) \quad \text{at } z = 0 \quad \tau \geqslant 0$$

$$C_A = C_A(z), \quad C_B = C_B(z), \quad T = T(z) \quad \text{at } \tau = 0 \quad z \geqslant 0$$

The equations may be solved by a marching technique, starting from the reactor inlet and working through to the outlet at each time step, using the finite difference formulation described in Appendix 4. This appendix also contains a check on the accuracy of the integration for an adiabatic reactor under transient conditions.

The finite difference formulation involves the values of C_A, C_B, T, t, η and ψ at four nodes of the network. Two of these nodes are at the previous time step, for which the complete axial profiles (and hence t, η and ψ) are known, and one node is at the time step under consideration. This node is at the previous axial position for which C_A, C_B, T, t, η and ψ are also known. The only unknowns, therefore, are C_A, C_B etc. at the axial and time node under consideration and the solution can be obtained as follows:-

(1) Assume values of C_A, C_B and T at the first (or next) axial position where they are unknown.

(2) Integrate the equations describing the transient behaviour of the catalyst pellet (Equation 7.15) to give t, η and ψ at this position.

(3) Evaluate C_A, C_B and T at the position where they are unknown and compare the values with those used in step (1). If agreement is satisfactory, continue to step (4), otherwise repeat from step (2).

(4) Repeat from step (1) while $z \leqslant 1$ (i.e. until the reactor outlet is reached).

(5) Repeat the whole computation for the next time step and continue as long as necessary.

Step (2) can be accomplished using the Runge-Kutta-Merson algorithm which is available as a standard library procedure.[69] For the purposes of this algorithm it is necessary to be able to specify the values of the state variables, at points other than the starting and finishing points, within any given time step. This is done by assuming that the changes in fluid conditions are linear over one time step and that the pellet is effectively subject to a ramp change in fluid conditions. This is a reasonable assumption to make since the finite difference representation of the differential equation is based on the assumption that any changes are linear over one step. The only point where this representation is not used is at the reactor inlet, if the reactor is subject to a step change in inlet conditions. In this case the transient pellet model can be solved for the exact change which is occurring.

8.3 Discussion of the results.

Despite the fact that the postulated model represents the simplest case which is typical of the class of highly exothermic homogeneous reactors, it is still not possible to give a perfectly general solution which will cover all possible types of behaviour. Even by confining attention to the

practical ranges for the dimensionless groups occurring in the differential equations, it is only feasible to attempt to investigate the kind of response for particular problems and to try to find some pattern or special features which will characterise the system. This is the kind of information which is useful in deciding on the control strategy to be used, (i.e. what variables will be manipulated, measured and controlled). Furthermore, any unusual behaviour will be invaluable when deciding how near to the limit of stability the reactor can work. In short, the simulation should provide a basis for knowing what effects to take into account when designing a reactor.

A simple reactor model such as the one considered here, although rigorous in identifying the rate limiting processes, is not necessarily accurate in detail, particularly with regard to the radial temperature profile which can be reconstructed from the assumption of a parabolic form (see equation 6.14). In the following discussion most attention will be paid to the longitudinal temperature profiles, because this is the major variable which limits the long term behaviour of the system and the safety and satisfactory operation of the fixed bed catalytic reactor.

Table 5.1 gives the values of the data and the corresponding values of the dimensionless groups used in the simulation discussed here. Even with this limited set of parameter values, which are based on data for benzene oxidation, the general problems can be demonstrated well, and particularly the dangers of relying on intuition based on a superficial analysis.

Preliminary computed results indicate that the capitance of the fluid to absorb heat and mass is negligible in comparison with the thermal capacity of the catalyst pellets. In other words, the transient response of the reactor is slow compared to the residence time and the fluid equations can be solved as if they were at a pseudo-steady state. This may be seen from Figure 8.1 where the temperature profiles are compared at two times in response

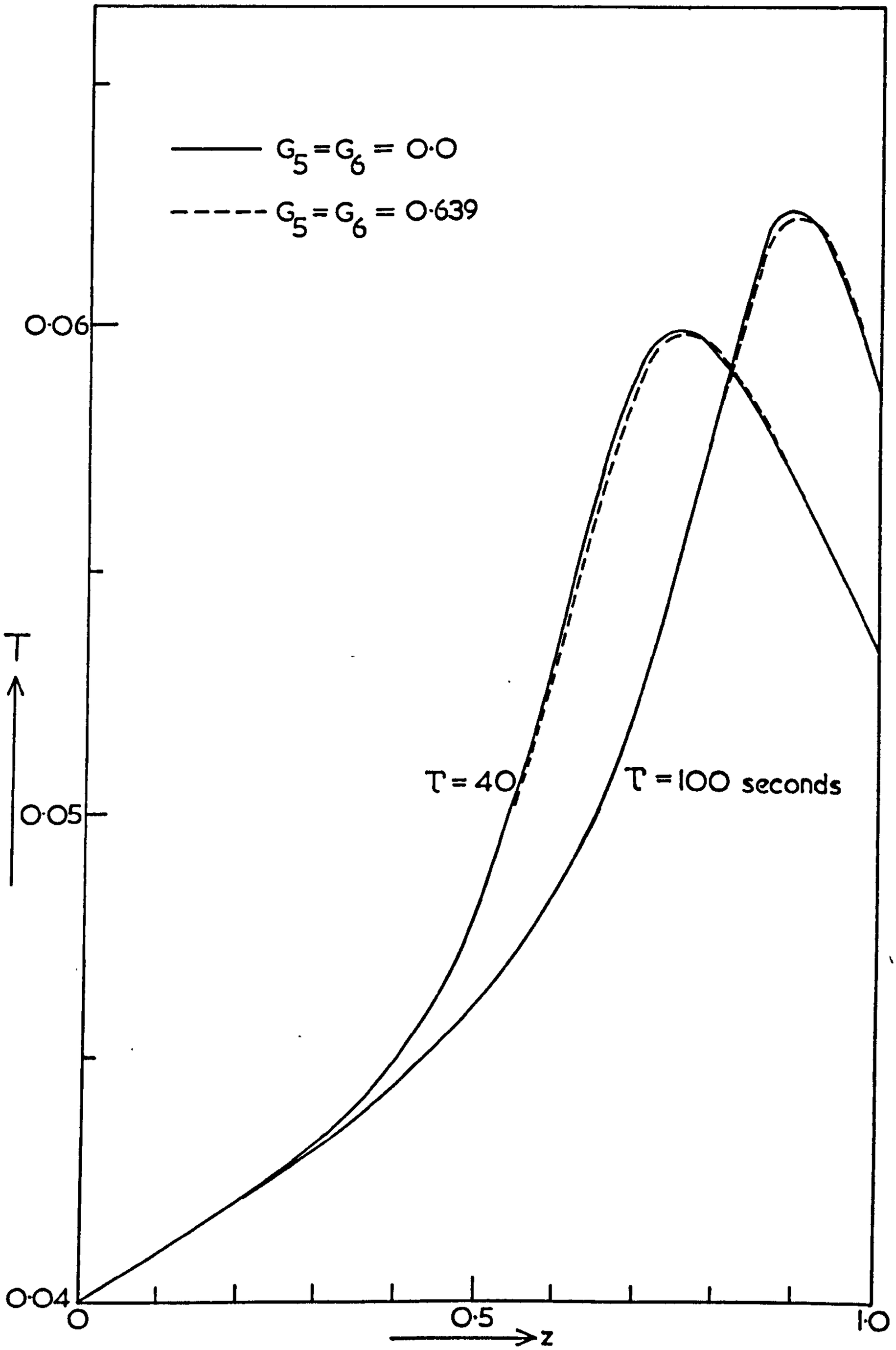

FIG. 8.1 The effect of parameters G_5 and G_6 on the temperature profiles in the reactor following a step decrease of 0.0008 in the dimensionless inlet temperature. Data as given in Table 5.1. For the given E_1 this change represents approximately 13°C.

to a step decrease in the inlet temperature for $G_5 = G_6 = 0$ and $G_5 = G_6 = 0.639$. The difference between the curves is negligible in comparison with the magnitude of the changes which are occurring. Treating the reactor fluid as being at a pseudo-steady state enables great savings in computational effort to be made, particularly when step changes in concentration occur at the inlet, since it would then be necessary to take very small steps in the time direction to follow the disturbance through the reactor. Normally time steps of 0.25 to 5 seconds are sufficient to ensure convergence of the solution, but to follow a step change in concentration through the reactor when $G_5 = G_6 \neq 0$ would require a step size at least two orders of magnitude smaller than this.

The danger of relying on a lumped parameter element to represent the reactor in the control loop is illustrated in Figure 8.2, which shows the response of the reactor following decrease in the inlet temperature. This change causes the outlet temperature to fall slightly for a time, followed by a large rise to a value which overshoots the final steady state and then the temperature falls to its final value. However, the most surprising thing is the behaviour of the peak temperature inside the reactor. In the early stages it moves towards the entrance, increasing in magnitude, then moves back towards the position of the original steady state peak temperature, still continuing to increase and finally settles down to a lower peak value nearer the reactor exit.

At first sight this is most unexpected, but on closer examination is perfectly reasonable, as can be seen by reference to Figure 8.3 and comparison with Figure 8.2. In the period immediately following the initial drop in the inlet temperature, the most important effect is the resulting fall in temperature of the catalyst pellets in the inlet region, caused by the cooling effect of the gases entering the reactor. This

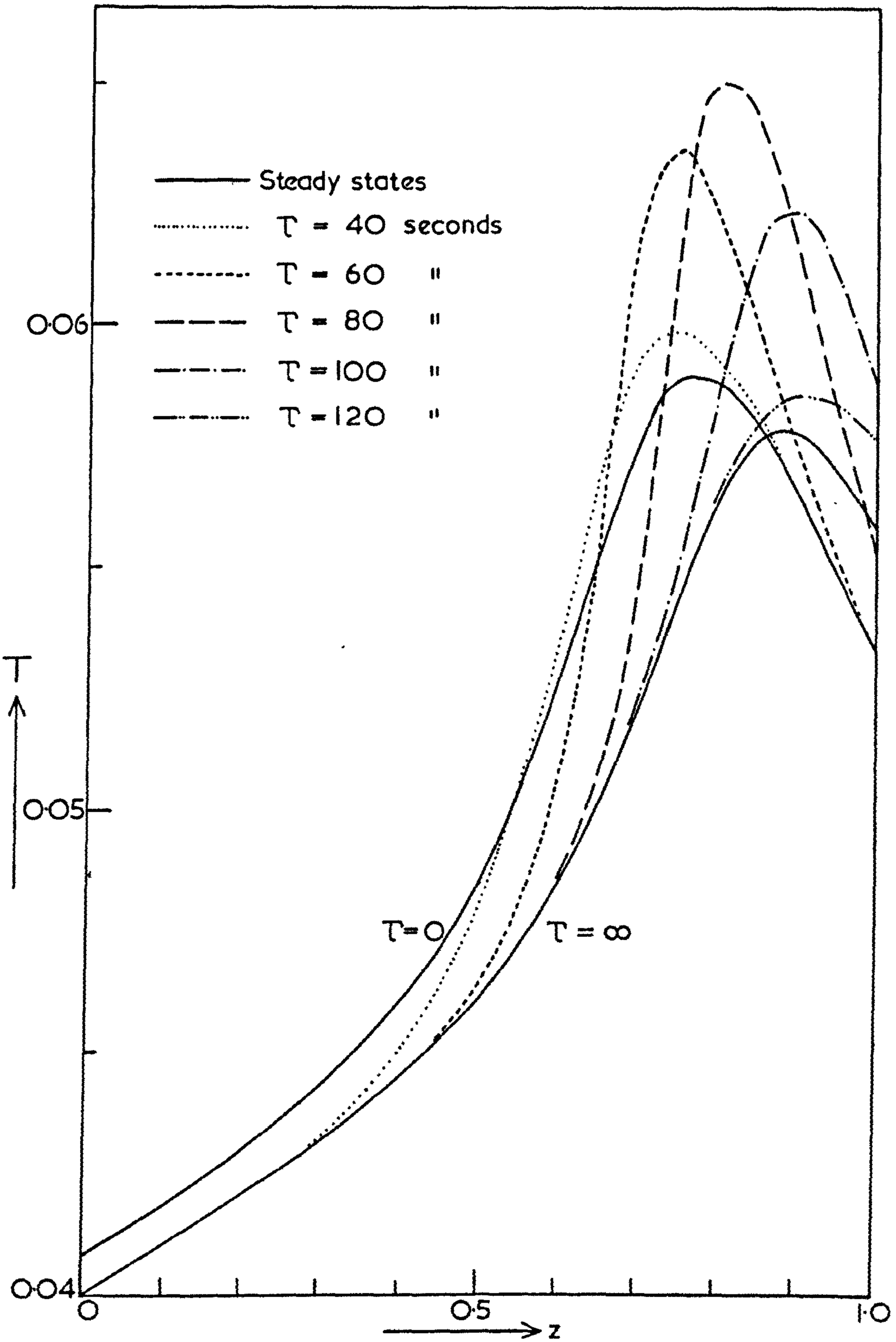

FIG. 8.2 The temperature profiles in the reactor following a step decrease of 0.0008 in the dimensionless inlet temperature. Data as given in Table 5.1. For the given E_1 this change represents approximately 13°C.

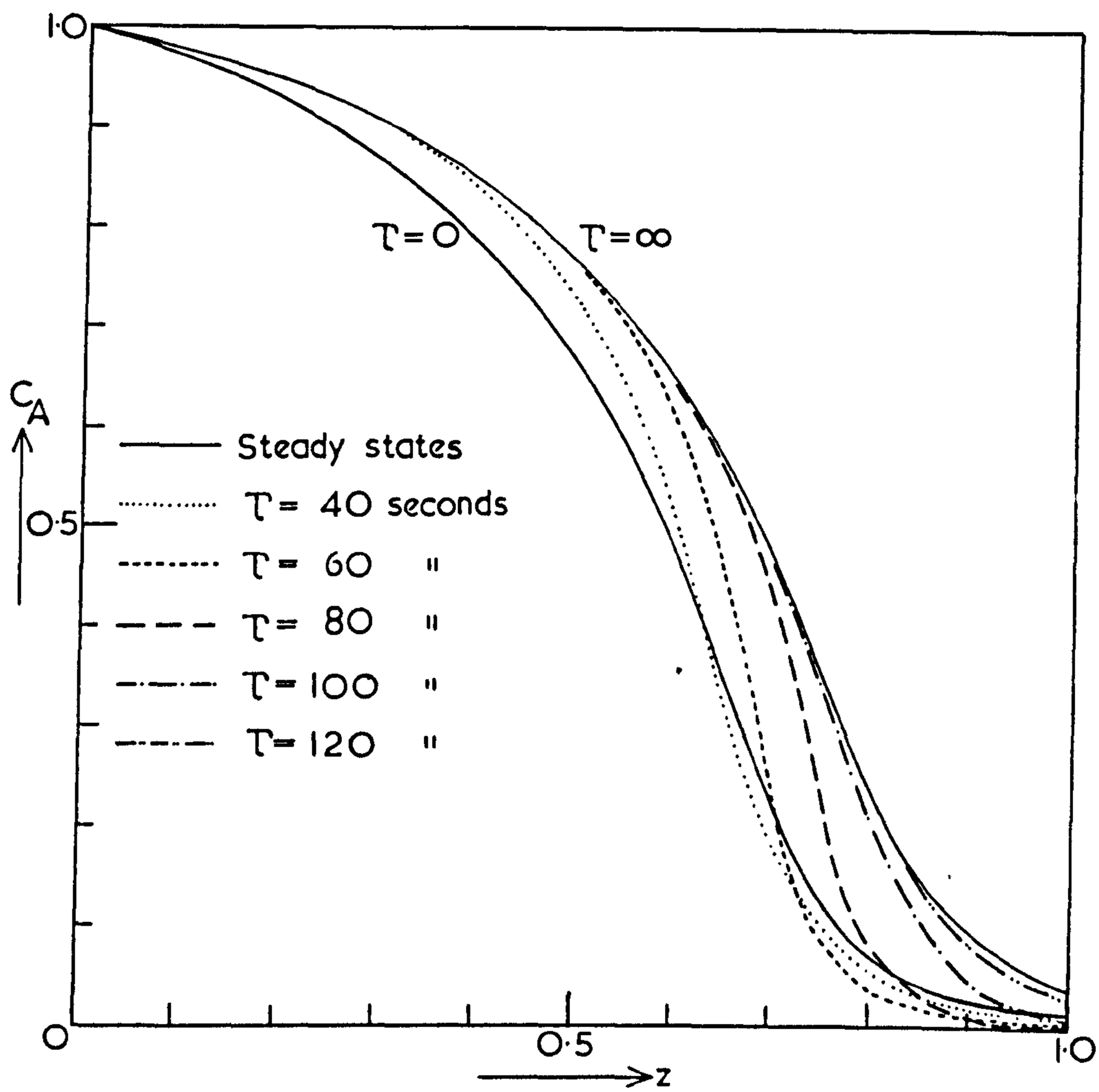

FIG. 8.3 The concentration profiles corresponding to the temperature profiles of Figure 8.2.

results in less of the reactant being consumed until it reaches the section of the bed which has not yet been cooled but where the initial temperature profile was beginning to rise sharply towards the peak. A situation thus arises where an increasing concentration is reaching parts of the bed which are already hot, so that the temperature begins to rise rapidly. As the cooled region in the reactor inlet gradually moves into the bed, the balance between reaction and heat removal is adjusted until the final steady state is reached.

This type of response is an excellent demonstration of the distributed parameter effect and of how an apparently safe action, i.e. reduction of the inlet temperature, may give rise to conditions which result in catalyst damage from excessively high temperatures.

A step increase in the inlet temperature could be equally misleading if the peak temperature alone is monitored, as can be seen from Figure 8.4. The effect of an increase in the inlet temperature is to cause a new temperature peak to begin to form nearer to the inlet than the old peak, while the latter begins to decay and move towards the reactor outlet. As would be expected, the final peak temperature is greater than the initial value. Some oscillation of the outlet temperature is found, although in general the movement of temperature is in the opposite direction to the input. However, this depends on the length of the reactor, and in a shorter one the outlet temperature could increase monotonically. Although monitoring the peak could induce misleading conclusions, the response to a step increase in inlet temperature is basically what would be expected from intuitive considerations. Closer examination of the temperature differences between pellet and fluid, as shown in Figure 8.5, indicates some effects resulting from the thermal capacitance. At the exit of the bed, most of the reaction has taken place so it is largely heat transfer

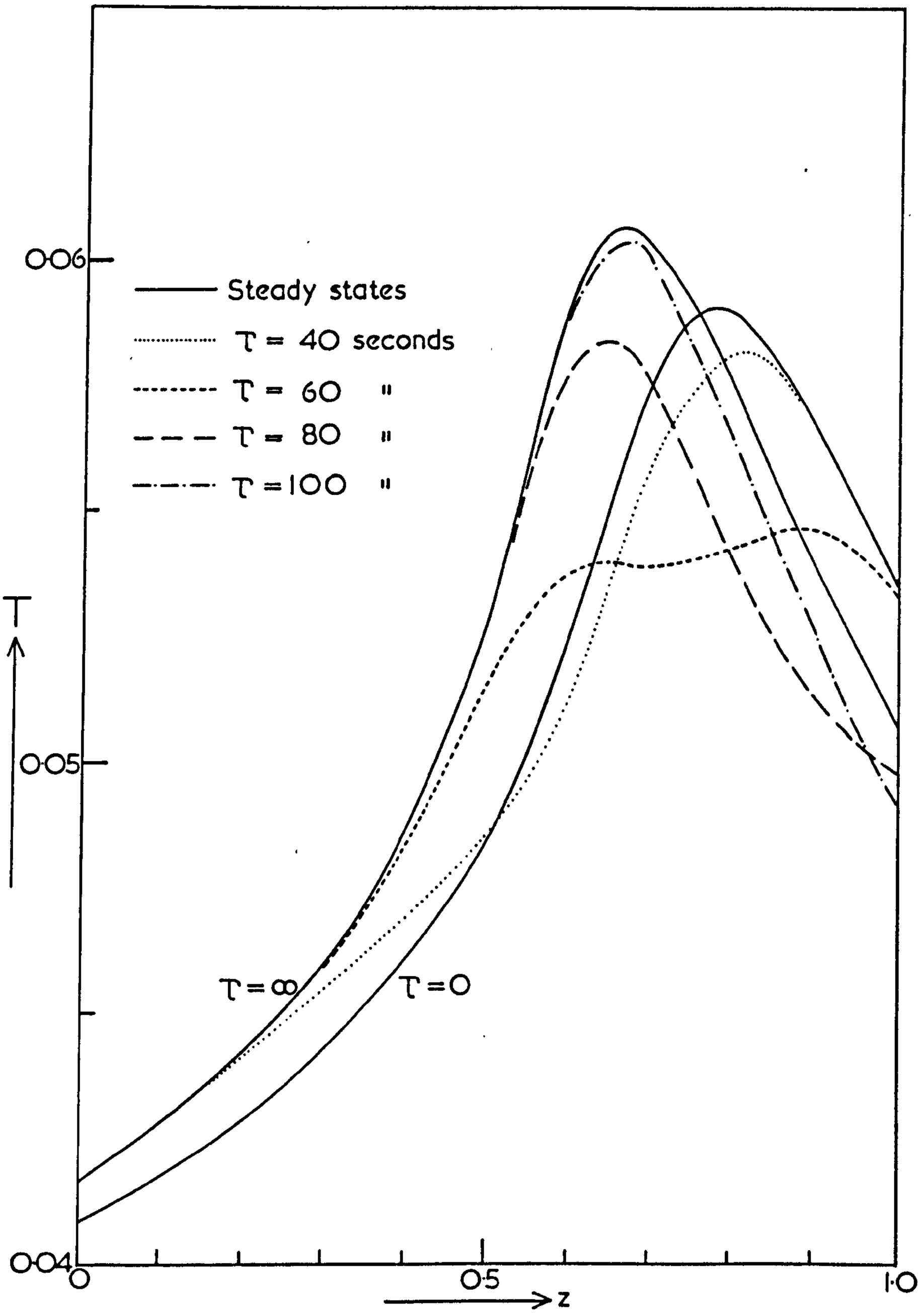

FIG. 8.4 The temperature profiles in the reactor following a step increase of 0.0008 in the dimensionless inlet temperature. Data as given in Table 5.1. For the given E_1 this change represents approximately 13°C.

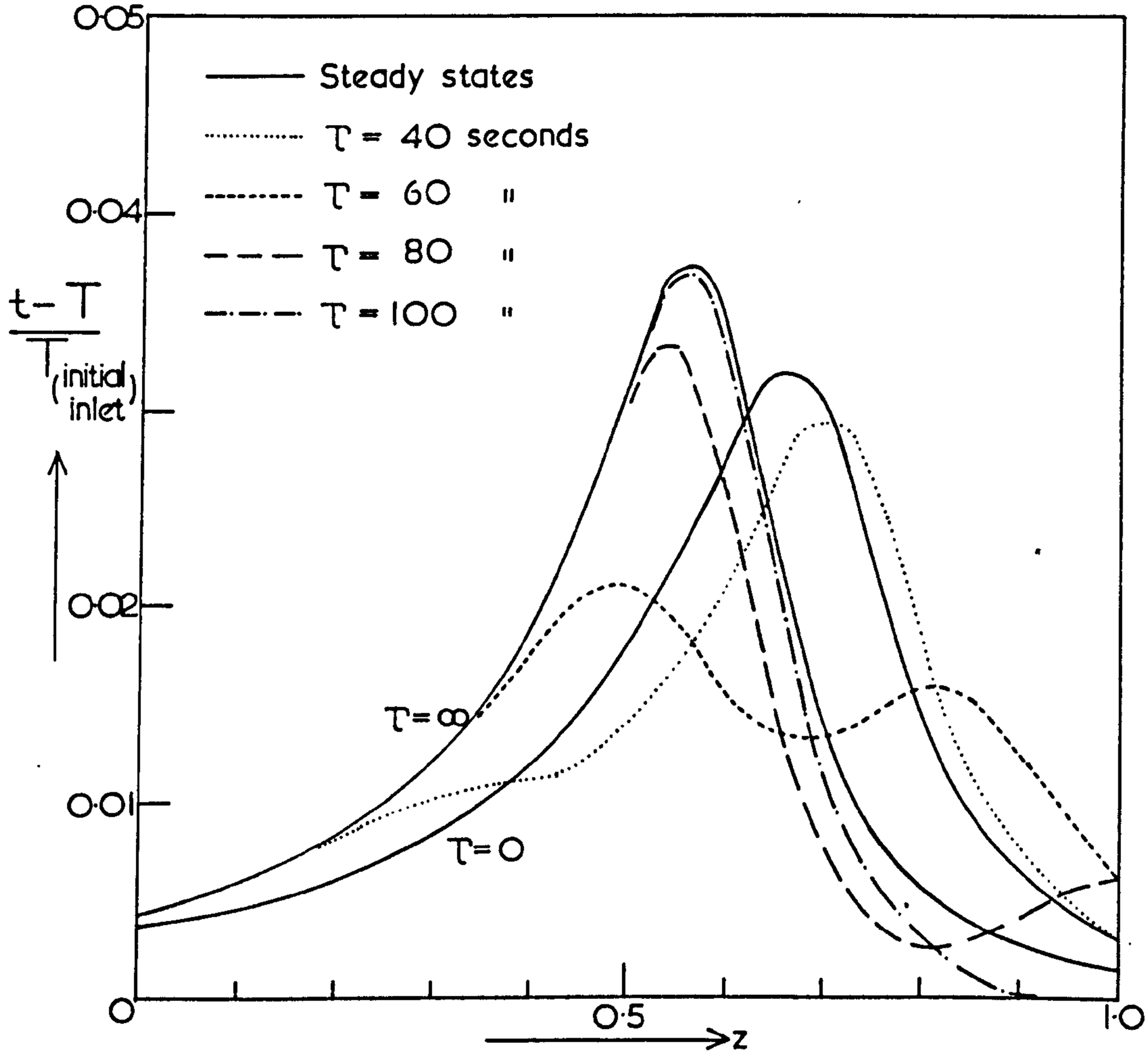

FIG. 8.5 Profiles of the relative film temperature rise corresponding to the temperature profiles in Figure 8.4.

between pellet and fluid, and fluid and coolant, which determines the dynamic behaviour here. This figure again indicates the way that dominant processes are distributed within the system. In one region it is the heat generation from chemical reaction and heat transfer from fluid to the coolant; in another region it is the residual heat being transferred from pellets, which were at the reactor hot spot, into the fluid and heat transfer to the coolant, and in the exit region it is mainly a balance between heat transfer effects from the fluid to pellet and coolant. Generally, the relative importance of each effect varies with time as well as with position.

A step change is obviously extreme so it is useful to see how the behaviour just examined is modified by less drastic disturbances. The effect of a ramp decrease in the inlet temperature is shown in Figure 8.6. The non-linear character of the system means that it would not be reasonable to expect the behaviour to be the same as a sequence of step changes. Nevertheless, the same qualitative features are apparent. A wave of the peak temperature, of increasing amplitude, passes along the bed and finally out. There is no general trend towards the inlet but the peak temperature may become very high before leaving the reactor. The response to a much slower ramp change is found to be generally smoother, since the system has effectively more time to settle down after each infinitesimal change, resulting in a gradual monotonic decline in the temperature peak which moves towards the reactor exit and eventually out of the reactor. In this case, the outlet temperature rises monotonically as the temperature peak approaches the reactor outlet and then declines monotonically after the peak passes out.

Further evidence of the necessity of incorporating allowance for all relevant transport effects is provided by examination of the result of an increasing ramp input temperature as shown in Figure 8.7. At first, the

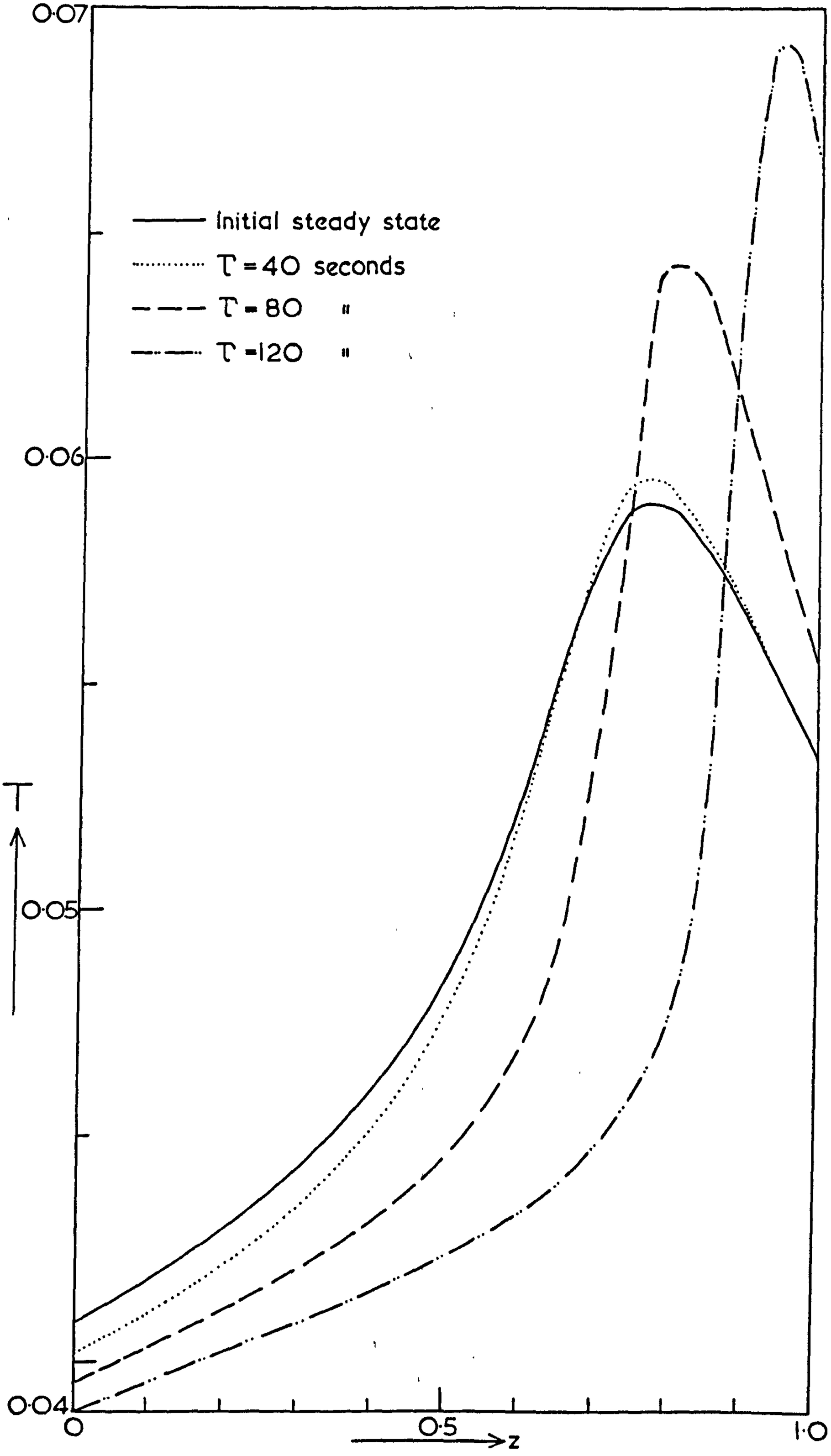

FIG. 8.6 The temperature profiles in the reactor caused by a ramp decrease in the dimensionless inlet temperature of 1.6×10^{-5} per second. Data as given in Table 5.1. For the given E_1 this change represents approximately $0.25^{\circ}C$ per second.

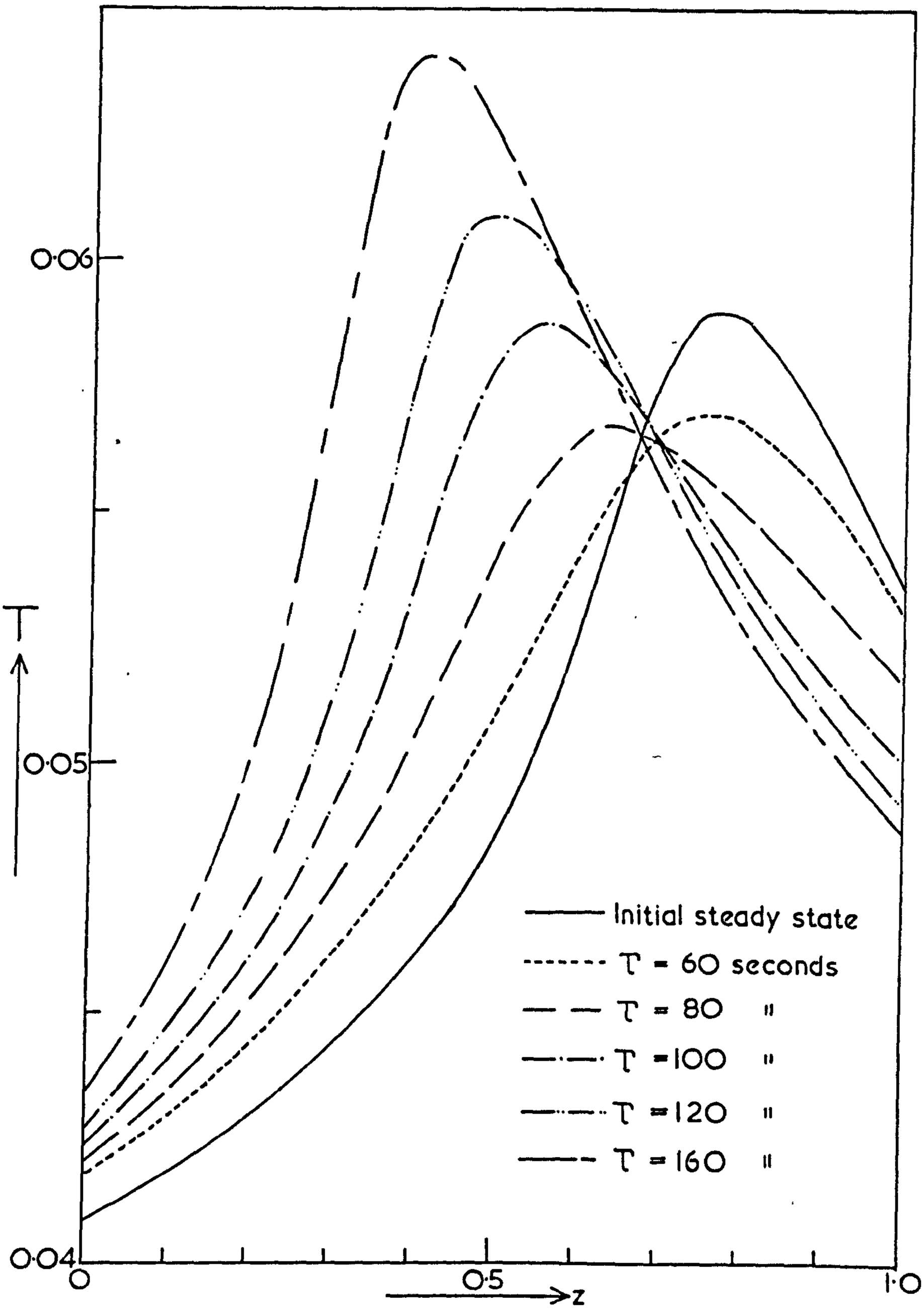

FIG. 8.7 The temperature profiles in the reactor caused by a ramp increase in the dimensionless inlet temperature of 1.6×10^{-5} per second. Data as given in Table 5.1. For the given E_1 this change represents approximately $0.25^{\circ}C$ per second.

peak temperature decreases, then moves towards the inlet and begins to increase until it is appreciably higher than the initial steady state peak. For the case shown in Figure 8.7, the outlet temperature falls monotonically, but cases have been found where it rises before falling, so it is not merely related to the input and is not easily incorporated into a simple control strategy.

Changing the inlet concentration leads to the type of response which might be expected on intuitive grounds. In general, increasing the concentration causes a monotonic increase in the peak temperature and a movement of the peak towards the inlet. Decreasing the concentration reduces the temperature monotonically and moves the peak towards the outlet. Manipulating the concentration therefore represents a much more attractive way of controlling the system, when compared with using the temperature, since the responses are largely monotonic and in general behave much more predictably than responses to temperature changes. However, increasing the inlet concentration does tend to reduce the outlet temperature, confirming the conclusion reached in Chapter 6 that this is an unreliable indication of reactor performance.

8.4 Conclusions.

The results from the dynamic model of the reactor indicate clearly the necessity for a detailed investigation of the system under consideration. In general the behaviour of the reactor is controlled by a combination of chemical and thermal effects, the relative magnitudes of which may change considerably with time and position in the bed. This results in dynamic responses which are not easily predicted without extensive simulation. The complex interactions which are present emphasise the importance of the multivariable approach, especially when deciding on the structure of a control system.

It is important to note that many of the unexpected responses arise from the distinction between the solid and the fluid phases, i.e. they are caused by the heterogeneous nature of the system. A quasi-homogeneous model would not take into account the resistance-capacitance stage for the solid to fluid heat transfer, which causes thermal effects to be delayed and irregular behaviour of the temperature profiles to occur.

The proposed model is suitable for preliminary investigations in stability and control studies, since the computational load is not excessive and it is therefore reasonable to expect to be able to carry out extensive simulations on any particular system being studied.

CHAPTER 9

MULTIPLE SOLUTIONS AND THEIR EFFECT ON STABILITY

9.1 Introduction.

It is well known that the solution of the steady state model of a catalyst pellet can exhibit multiple solutions under certain conditions. Since such conditions indicate potential instability, considerable effort has been expended in the examination of these problems as a first step in the stability analysis of the reactor as a whole. Most of the work has been done on systems with Dirichlet boundary conditions, assuming that the conditions at the pellet surface are the same as those in the surrounding fluid. This type of problem was discussed by Aris[39] who reviewed and compared some of the criteria which have been developed. In all practical systems, the interphase transport resistances are important, but no satisfactory method has yet been developed which enables the range of operating conditions, over which multiple solutions can occur, to be determined. Cresswell[52] has examined the phenomenon of multiple solutions using a model with flux boundary conditions, but the criterion which was developed is unsuitable for application to specific systems. This is discussed in greater detail in section 9.5. At the present time there is no method available for relating the local and global stability within reactors, and one reason for this may be that the problem has invariably been studied in a way which is basically unsuitable for solving the problem.

A major source of difficulty has been the fact that the usual form of effectiveness chart, as expressed in terms of the Thiele modulus (ϕ), the thermicity factor (β) and the activation factor (γ), only applies under one set of conditions. This means that the existence of multiple solutions can only be investigated by considering each point in the reactor individually. Analysis in terms of these groups has not been achieved satisfactorily even

for the reaction A ⟶ B. In the case of more complex reactions the problem is even more formidable using comparable dimensionless groups, since the values of an even larger number of these groups change simultaneously as the temperature and concentration vary.

The analysis which follows in this chapter deals only with the single first order reaction A ⟶ B, since general conclusions may be drawn which apply to all appropriate systems. The extension to complex reaction schemes and non-first order reactions is given in Appendix 5.

9.2 Calculation of the bounds on the non-unique region.

For the single reaction A ⟶ B, equation (4.5), the heat balance on the catalyst pellet, reduces to

$$T = t - B_o Sh'_A (C_A - c_{A_s}) \qquad (9.1)$$

and from equations (4.11) and (4.12), for first order, or pseudo-first order reactions

$$c_{A_s} = \frac{Sh'_A}{2} C_A \left(\frac{g}{(\frac{Sh'_A}{2} - 1)g + r^*} \right) \qquad (9.2)$$

where $r^* = \sqrt{k_1 *} = \theta_1 \exp(-\frac{1}{2t})$

$g = \tanh(r^*)$

Substituting for c_{A_s} in equation (11.1):-

$$T = t - B\, Sh'_A \frac{r^* - g}{(\frac{Sh'_A}{2} - 1)g + r^*} \qquad (9.3)$$

where

$$B = B_o \times C_A \quad (= \frac{(-\Delta H_1) C f_A Dp_A Rg}{2bhE_1})$$

Equation (9.3) is a condition for the steady state to occur and for any value of t, a steady state exists at some value of T, the dimensionless fluid temperature. Fig. 9.1 shows graphically the relationship between t and T for three typical sets of reaction parameters. As would be expected,

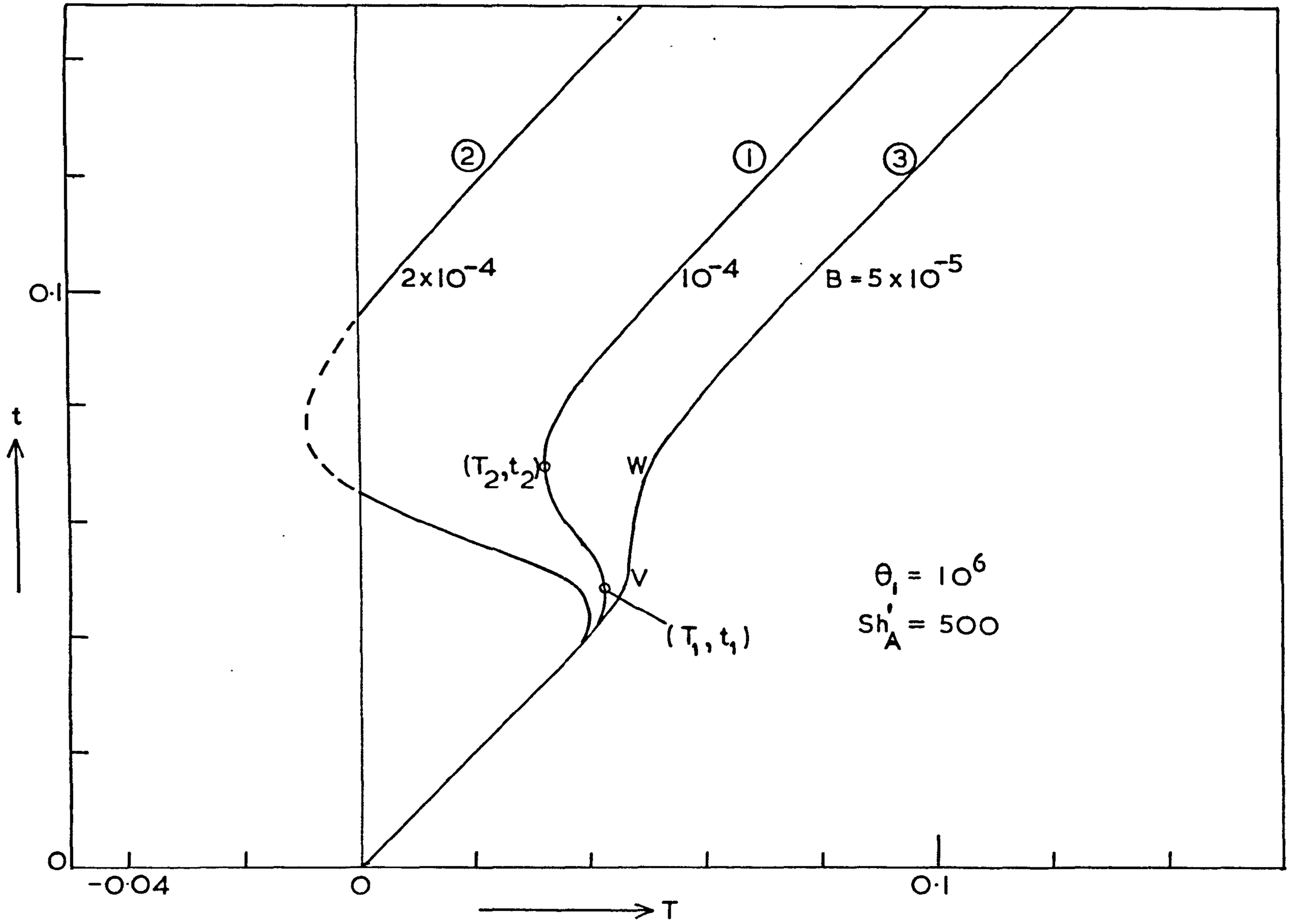

FIG.9.1 The steady state relationship between the temperatures of the pellet (t) and fluid (T) for typical sets of the system parameters, obtained by solving equation (9.3).

a region of three steady states may exist in some cases, the middle one being metastable. It is apparent from considering Figure 9.1 that if a region of multiple steady states does exist, then the bounds on the fluid temperature, T, within which the multiple solutions lie, may be found from the solution of the equation

$$\frac{dt}{dT} = \infty \cdot$$

or in a more convenient form

$$\frac{dT}{dt} = 0 \qquad (9.4)$$

Differentiating equation (9.3) and using equation (9.4) gives the condition for a bound on the non-unique region:-

$$1 - \frac{B Sh'^2_A}{t^2} \frac{r^{*2} g^2 - r^{*2} + r^* g}{\left(\left(\frac{Sh'}{2}A - 1\right)g + r^*\right)^2} = 0 \qquad (9.5)$$

This equation may easily be solved by any of the standard procedures such as the Newton-Raphson method.

9.3 Characteristics of the multiple solution region.

The solutions of equation (9.5) take the form shown in Figure 9.2, where the results are given for a range of the parameter B. The lines (1), (2) and (3) correspond to the lines of the same number in Figure 9.1. For case (1), starting at point A, the pellet temperature, t, will increase slowly as T increases until T reaches a value just above T_1 when the pellet temperature will rise to a high value corresponding to interphase mass transfer control. This occurs when the surface concentration falls almost to zero, and from equation (9.1) we obtain:-

$$t \simeq T + B Sh'_A \qquad (9.6)$$

If the fluid temperature T is now reduced, equation (9.6) will hold until T falls below T_2, when the pellet will again be in a region of unique solutions, and the reaction rate will once more be controlled by a mixture

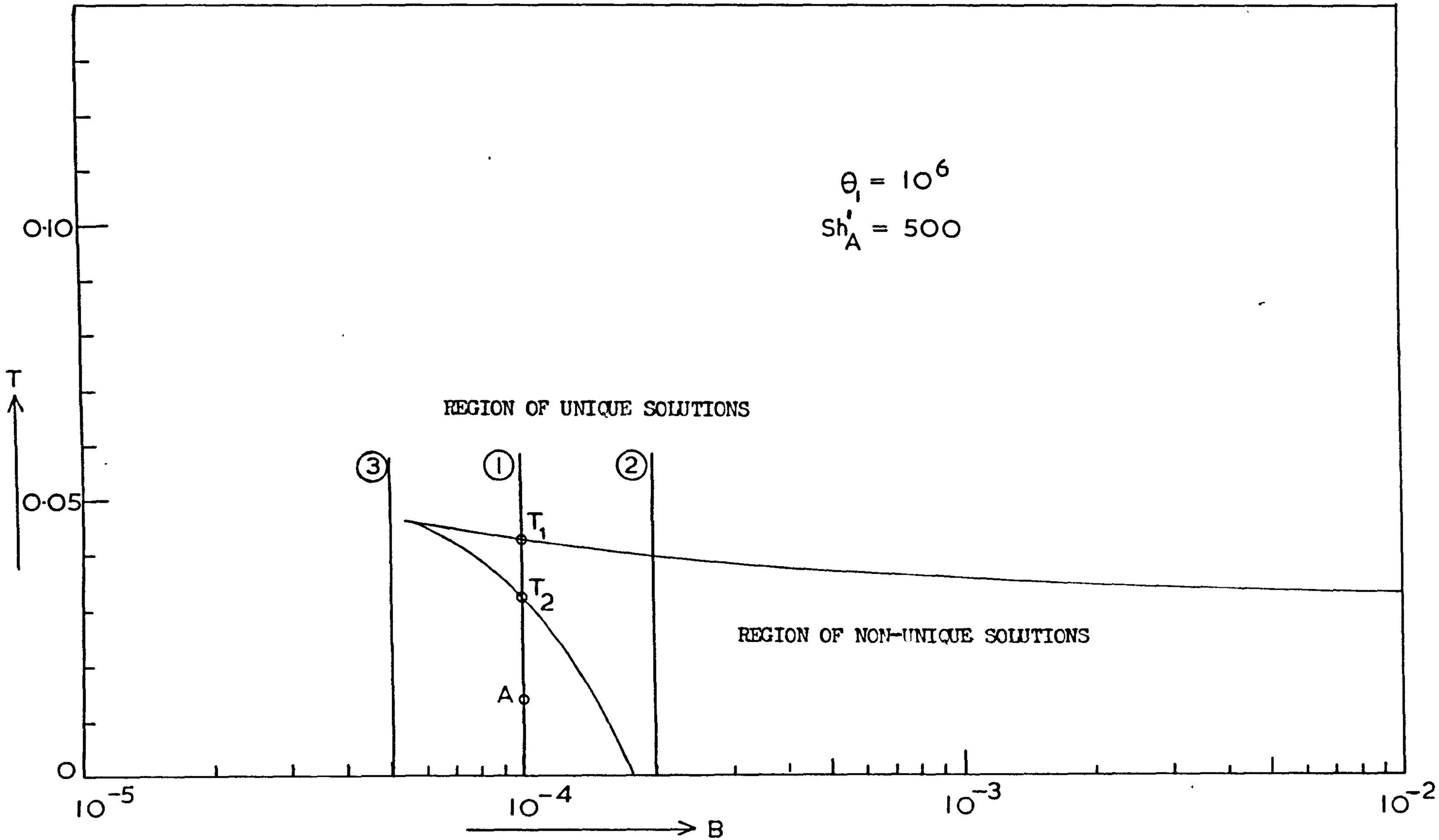

FIG.9.2 The unique and non-unique regions predicted by equation (9.5), showing the relationship to the curves of Figure 9.1 .

of kinetics and pore diffusion. In case (2) it is apparent that the lower steady state cannot be obtained from the upper steady state by reducing the temperature alone. Case (3) is unique at all temperatures and equation (9.4) therefore has no real solution for this value of B.

Figures 9.3 and 9.4 show the effect of varying θ_1 and Sh'_A respectively. In a given reactor θ_1 is constant and Sh'_A can only vary between fairly narrow limits, since the mass transfer coefficient k_{c_A} (and hence Sh'_A) is proportional to the square-root of the flowrate. A set of curves similar to those in Fig. 9.4 will therefore cover all possible operating conditions for a given reactor, but since the range of values of Sh'_A in any one system is very restricted, a single curve will usually be sufficient. This is particularly true because the upper arm of the curve is almost independent of Sh'_A over most of the range. This is much more important than the lower arm since, in the multiple solution region, it determines when the pellet moves from its lower value to the value predicted by equation 9.6. The insensitivity of the upper portion of the curves to changes in Sh'_A is expected from physical considerations, since this represents a region of significant internal diffusion resistance. Therefore, provided that the external mass transfer coefficient is not low, it would not be expected to have much influence.

Figure 9.5 was formed by plotting lines similar to the dotted lines of Figures 9.3 and 9.4 for various values of θ_1 and Sh'_A. The value of this graph is that it gives an immediate indication of a limit on the concentration (i.e. on B) below which non-unique solutions cannot exist at any temperature. Only if it was required to design a reactor to operate to the right of the appropriate point on this graph would it be necessary to continue to investigate the non-unique region in more detail.

It is interesting to note that for almost the whole practical range of B, no multiple solutions can exist for $T > 0.125$ (i.e. $\gamma_1 < 8$ in the

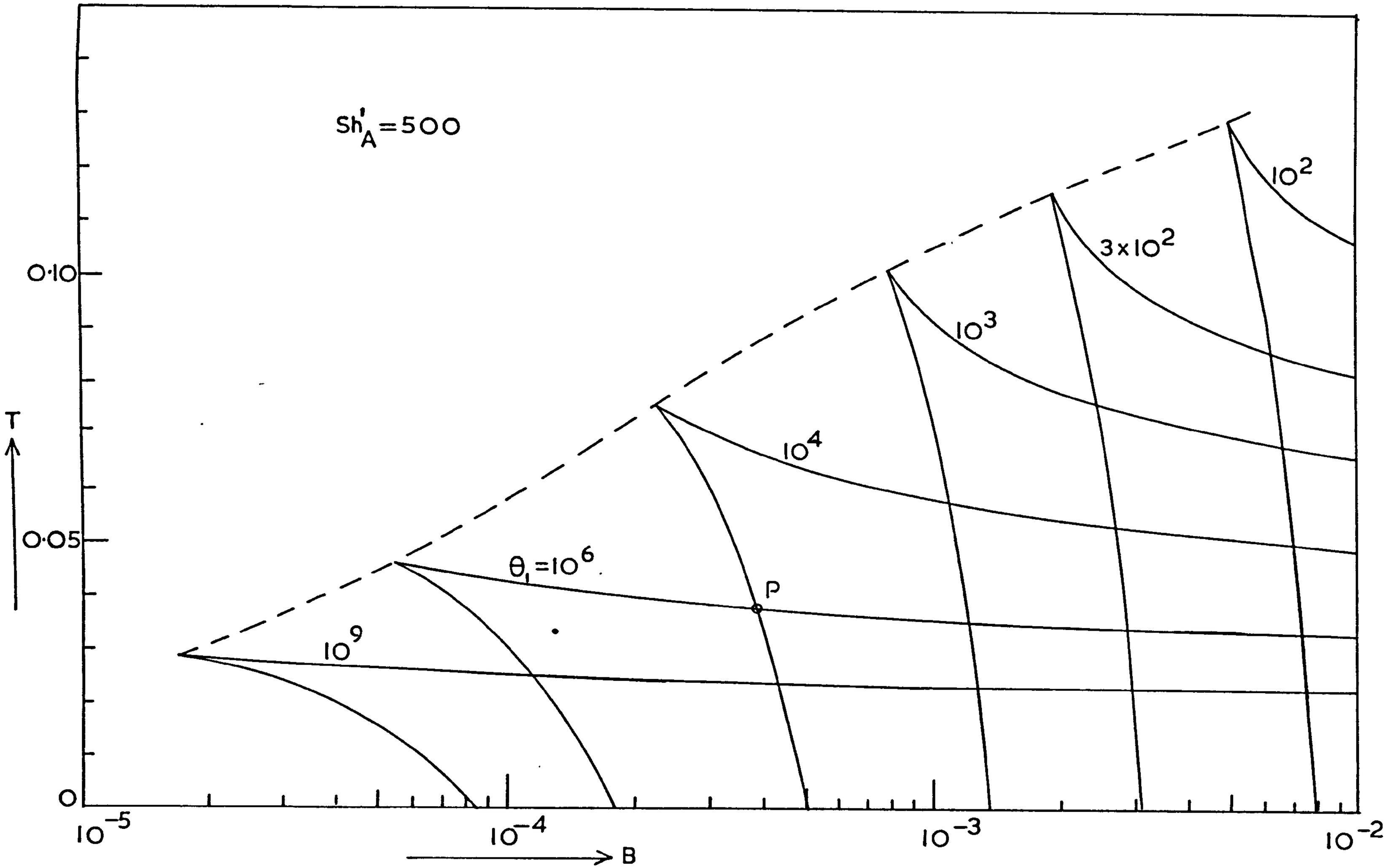

FIG.9.3 The effect of parameter θ_1 on the non-unique region.

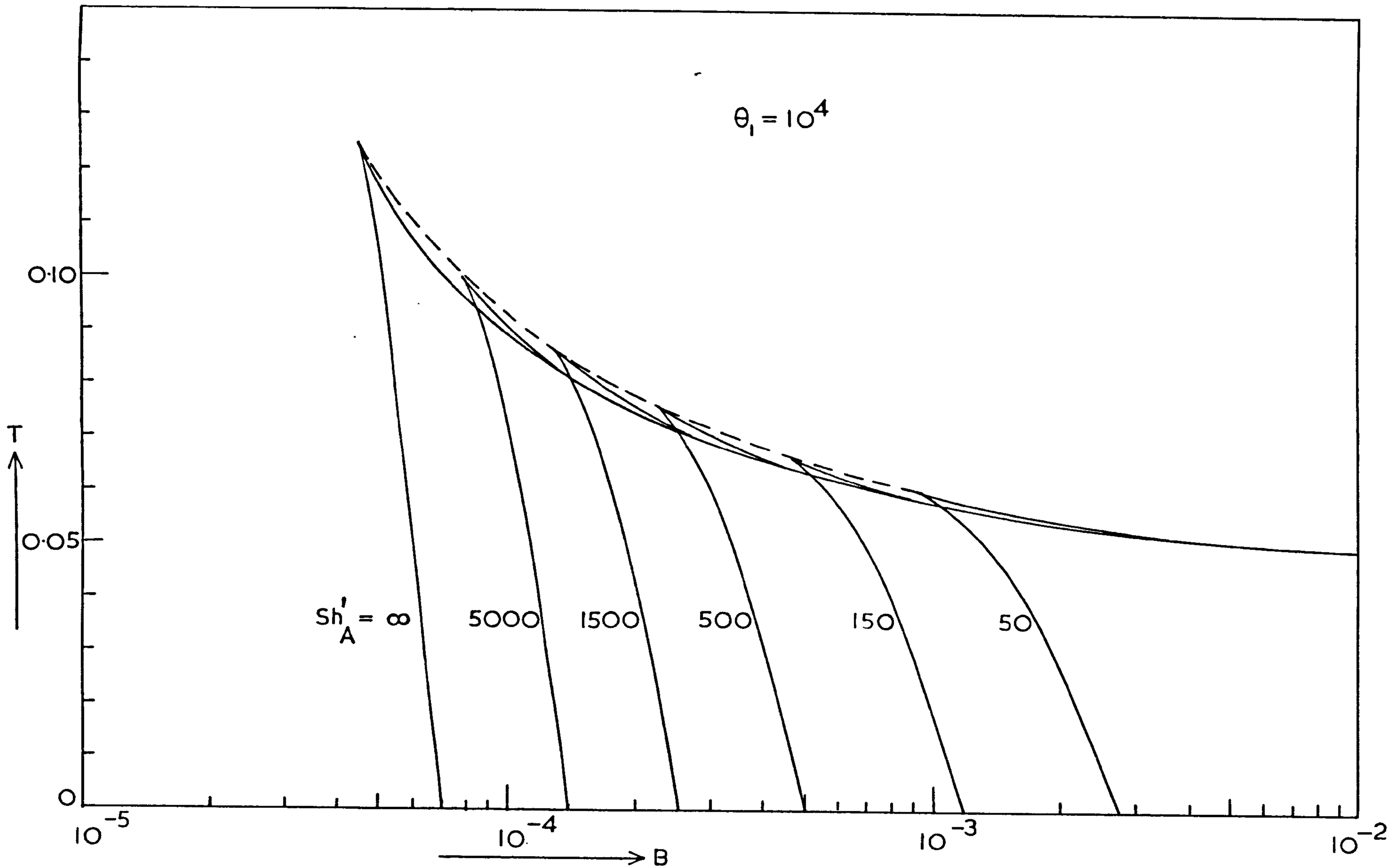

FIG.9.4 The effect of the modified Sherwood number (Sh_A') on the non-unique region.

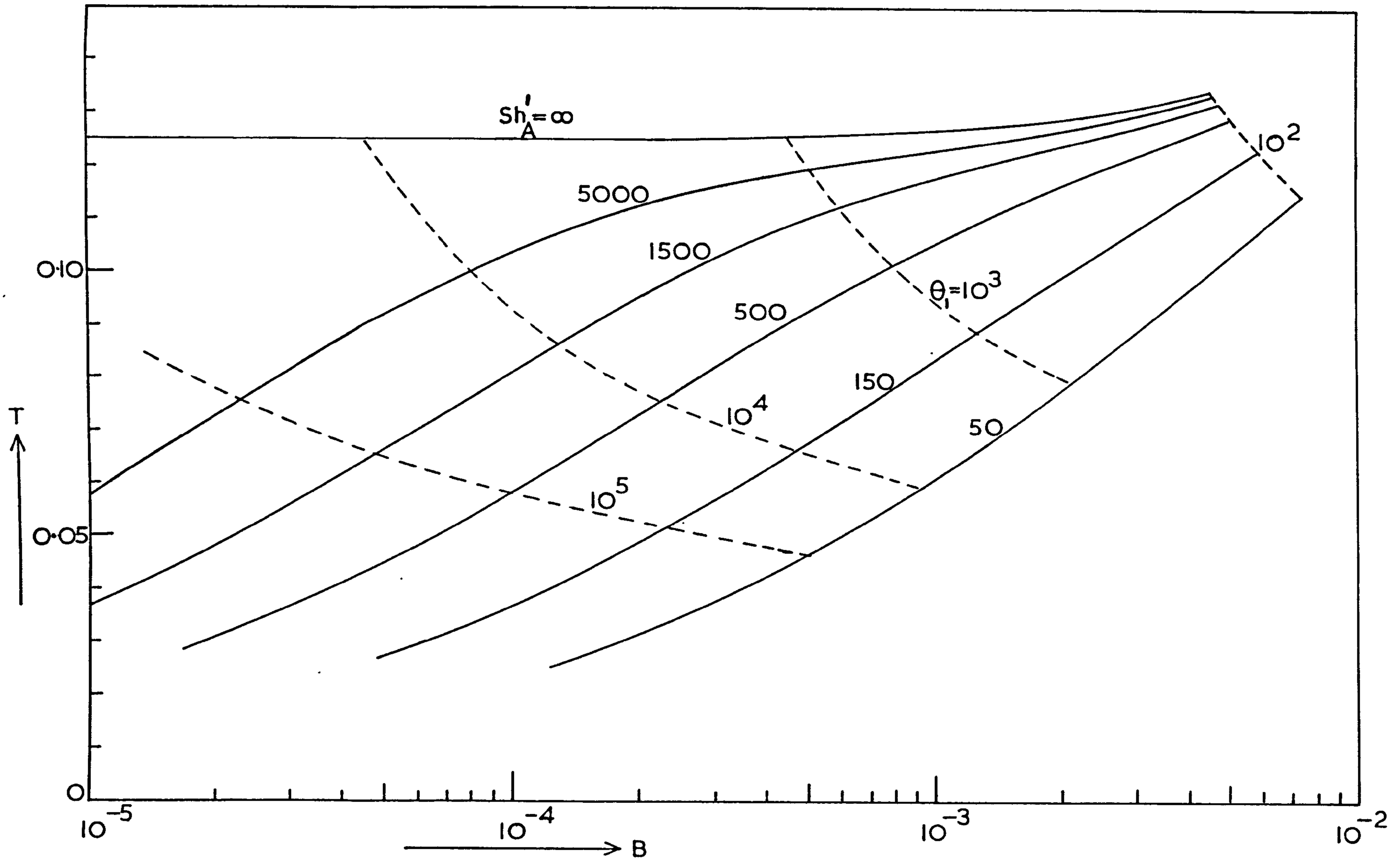

FIG.9.5 The loci of the cusps of the non-unique region for various values of θ_1 and Sh'_A .

conventional notation). This result has recently been confirmed by Cresswell[52] using a different method of analysis from that suggested here.

In practice it is not only desirable to avoid regions of multiple solutions, but also regions of high sensitivity. In Figure 9.1 for instance, curve (3) corresponds to a region just beyond the cusp of the non-unique region, as is shown in Figure 9.2. Although this curve has a unique value of t for each value of T, there is clearly a region between V and W where the system is likely to exhibit extreme parametric sensitivity, since the pellet temperature increases rapidly for small changes in the fluid temperature. In Figure 9.4, it is found that beyond the cusp for any particular value of Sh'_A, the curve for $Sh'_A = \infty$ continues to predict regions of high sensitivity. It may well be desirable in practice, therefore, to use the curves for $Sh'_A = \infty$ in all cases, since they enable all regions of potential difficulty to be avoided. In Figure 9.6 these curves have been plotted for a wide range of values of θ_1.

It has already been mentioned that in the normal effectiveness factor chart, η is plotted against ϕ_1, the Thiele modulus evaluated at the fluid conditions. Cresswell[52] has developed a method for calculating the bounds on ϕ_1 between which non-unique solutions occur. From the method suggested in this chapter, it is also possible to calculate these bounds if required. This may be accomplished by taking points at constant T from curves similar to those in Figure 9.3. Typical results obtained in this way are shown in Figure 9.7 for $Sh'_A = 500$. The bounds on ϕ_1 obtained from Figure 9.7 may be used to check the accuracy of the method, since these bounds may also be obtained by plotting the results from the numerical solution of the fully distributed model of the catalyst pellet described in Chapter 3. A comparison of the results is shown in Table 9.1. Agreement is better than 6% in all cases, but since ϕ_1 is exponentially dependent upon temperature, the accuracy of the predicted bounds on temperature is much better than 6%.

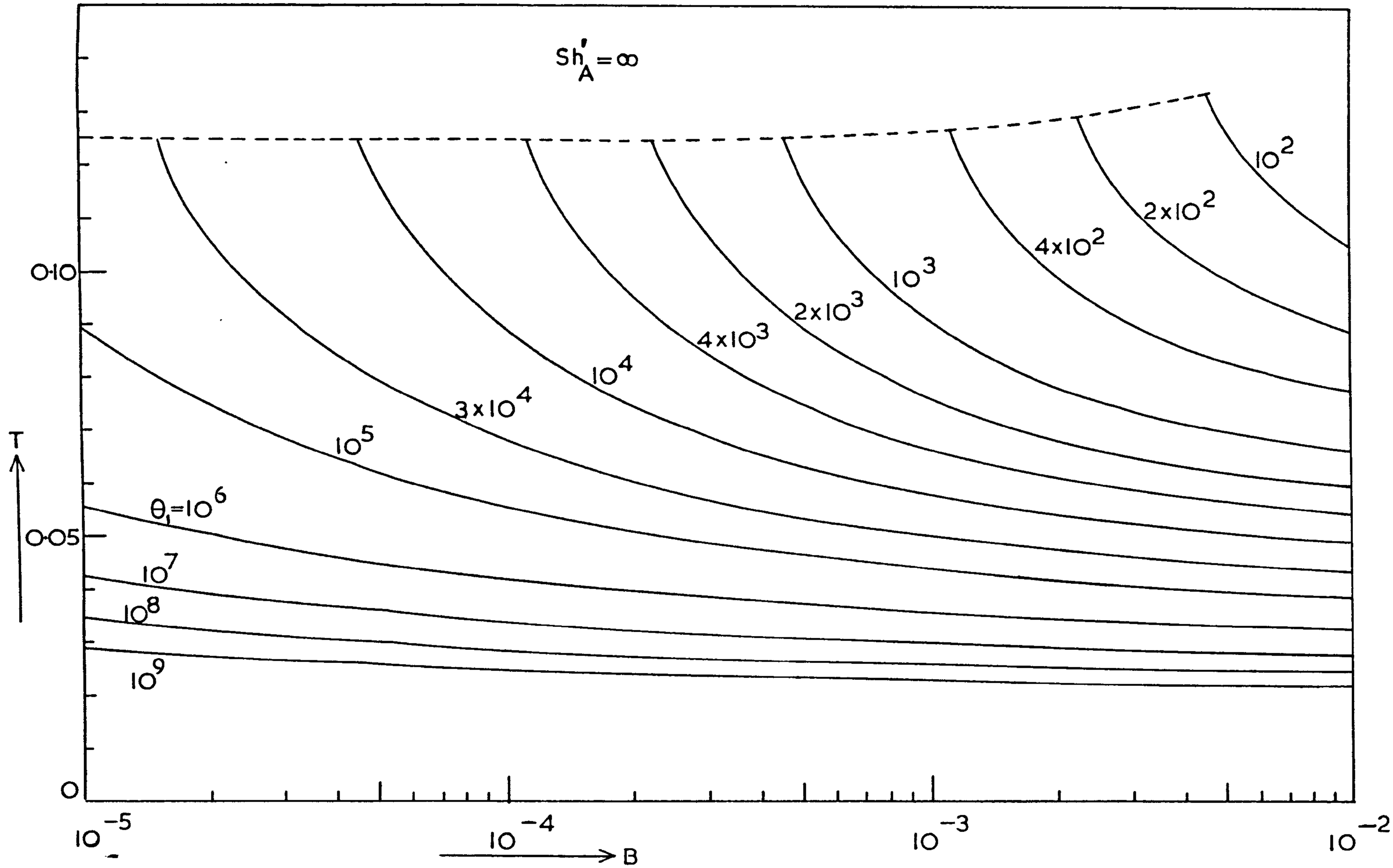

FIG.9.6 The upper curves of the non-unique region for $Sh'_A=\infty$, plotted at various values of θ_1.

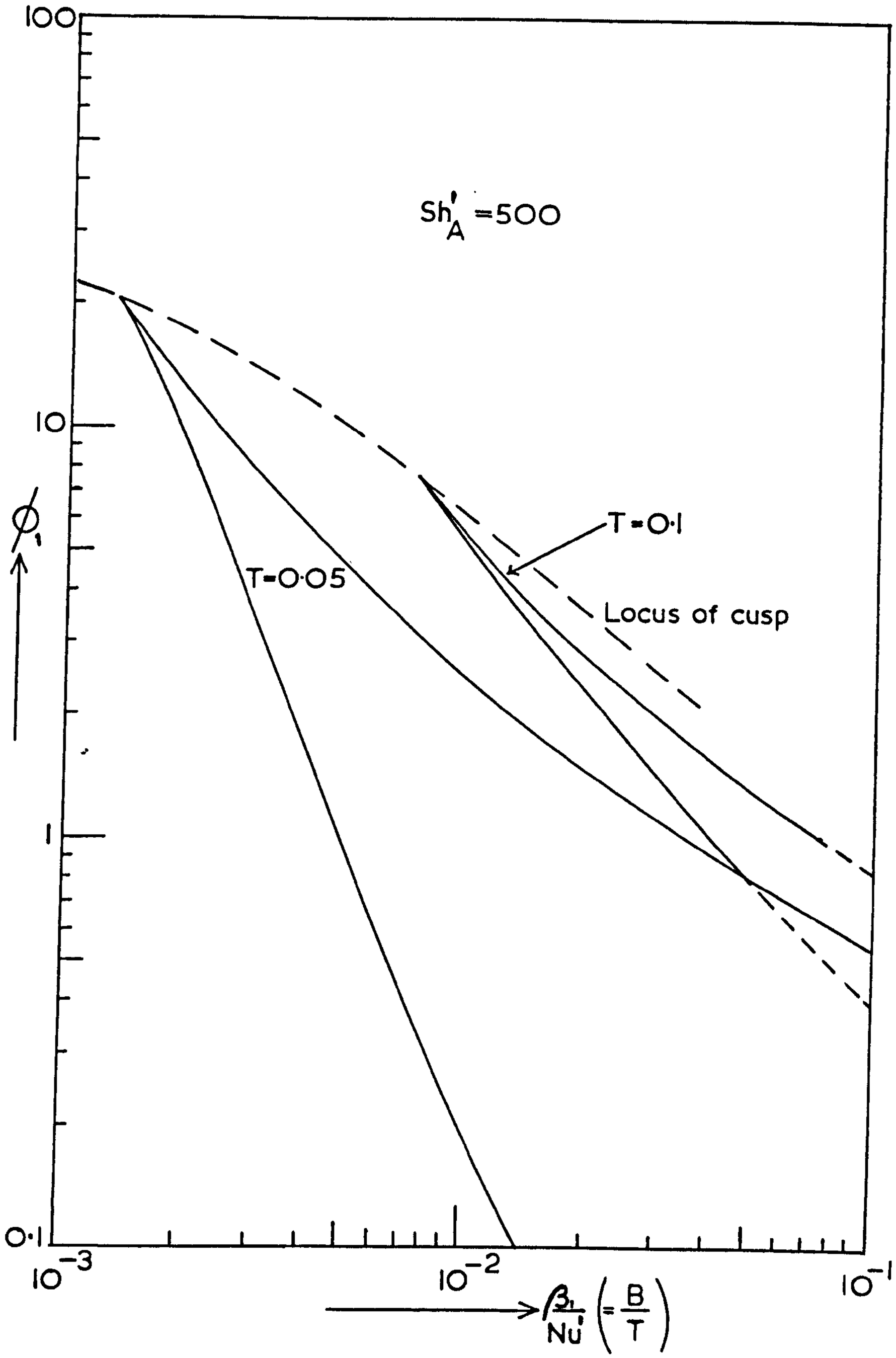

FIG.9.7 The bounds on ϕ_1 for non-uniqueness.

β_1	γ_1	Nu'	B	ϕ_1 (upper bound)		ϕ_1 (lower bound)	
				Exact	From Fig. 9.7	Exact	From Fig. 9.7
0.05	10	1	0.005	1.26	1.32	0.82	0.81
0.01	10	0.2	0.005	1.32	1.32	0.81	0.81
0.01	20	1	0.0005	2.45	2.45	0.19	0.20
0.02	20	10	0.0001	11.8	12.5	9.0	8.0

Table 9.1 Comparison of exact bounds on ϕ_1, between which non-unique solutions occur, with those obtained from Figure 9.7. The exact bounds are obtained from the numerical solution of the fully distributed model of the pellet described in Chapter 3 ($Sh'_A = 500$).

An advantage of the method suggested here for determining the bounds of non-unique solutions is the simple way in which it can be extended to more complex reactions such as the $A \longrightarrow B \longrightarrow C$, $A \longrightarrow D$ reaction scheme. This arises because for complex reactions an equation similar to equation (9.3) can be obtained (see Chapter 4) and the required bounds on the non-unique region can again be calculated by solving equation (9.4).

9.4 The relationship between local and global stability.

Analyses of multiple solutions in connection with stability in tubular reactor systems have tended to deal with either the quasi-homogeneous reactor or with the behaviour of single particles. In the heterogeneous reactor there is an interaction between the two which inevitably restricts the degrees of freedom in specifying the state variables, and which may tend to limit the development of instabilities. This interaction is particularly difficult to investigate using the conventional dimensionless groups for the pellet (ϕ, β, γ), but the problem is more amenable to analysis using the groups θ, B and T. A plot of the fluid temperature, T, against the

group B is characteristic of a set of operating conditions and the non-unique region can be drawn for a given system as shown in Figure 9.2, where the region of non-unique solutions is indicated. If the equations describing the heterogeneous two-dimensional catalytic reactor are solved, it is possible to plot the longitudinal trajectories for particular radial positions on the same chart. Only if any of the curves pass through the multiple solution region will the reactor tend to have multiple solutions at some point, and therefore by potentially unstable.

Typical trajectories along the reactor axis (r = 0) are shown in Figure 9.8. The influence of coolant temperature is indicated, values greater than about 480°K indicating possible instability for the data in Table 9.2.

Figure 9.9 shows longitudinal trajectories for various radial positions for a coolant temperature of 488°K. No complete radial profile lies in the multiple solution region, so it is possible that instabilities will be clamped down. It is apparent from this graph that it may often be necessary to use a two-dimensional model when examining stability, since it is required to know the radial temperature and concentration profiles.

Besides indicating where a reactor will tend to be unstable by virtue of trajectories passing through the non-unique region, it is possible to obtain some idea of how the reactor will behave outside but close to this region. In the course of numerical solutions, the criteria provided by these charts makes it fairly simple to assess whether undesirable operating conditions have been presented. Where the reactor model is part of an optimisation procedure, this is very useful.

For the complex reaction scheme, it is also possible to examine the global stability, since instead of obtaining one line which defines the non-unique region and depending on θ_1 and Sh'_A only, a set of lines will result, one for each value of C_B. The loci of these lines will also depend

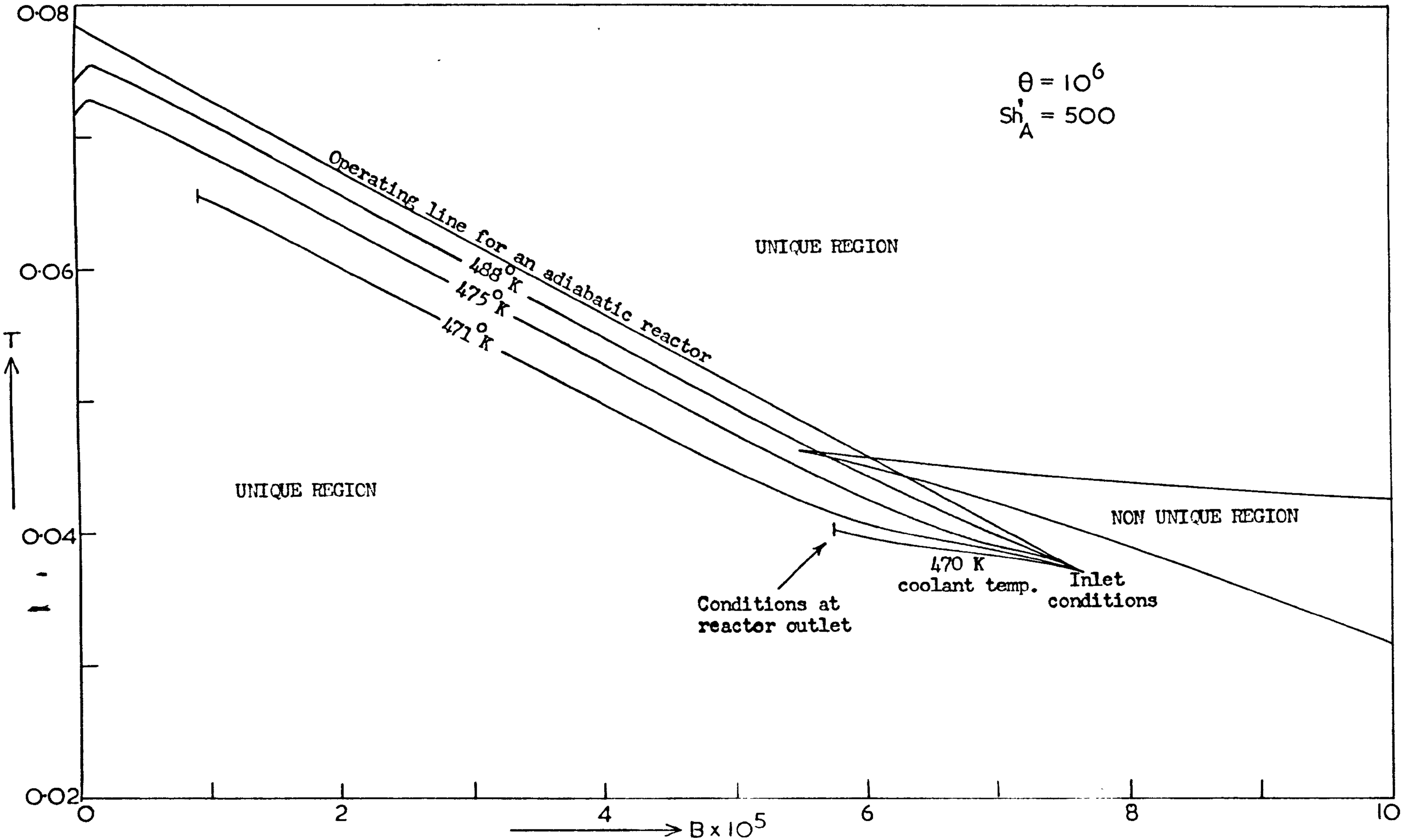

FIG.9.8 The effect of coolant temperature on axial (r=0) trajectories of B and T in the reactor. Data as given in Table 9.2 .

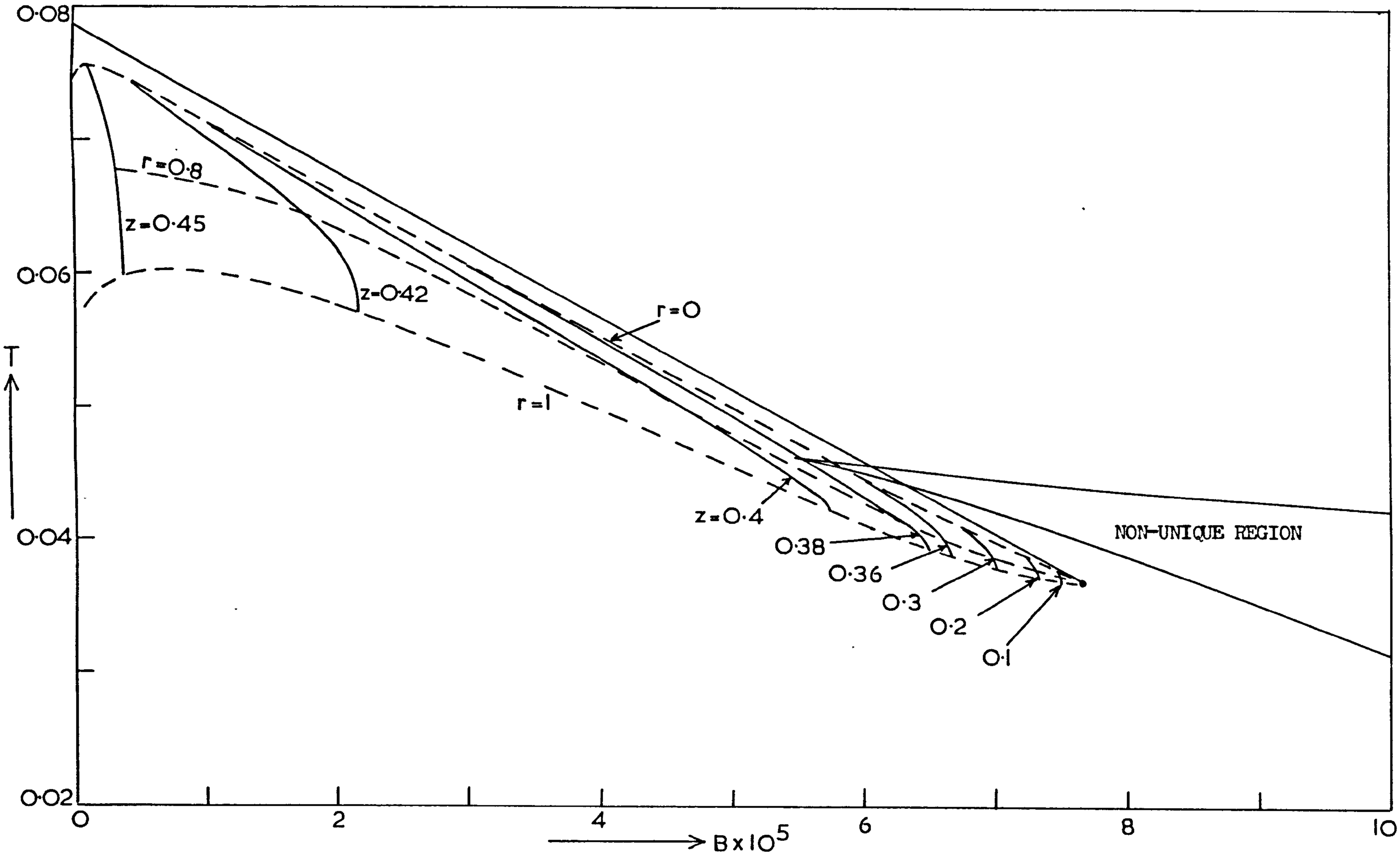

FIG.9.9 Profiles of B and T at various radial and longitudinal positions. Data as given in Table 9.2. T_c=0.0363 which corresponds to 488°K for the given activation energy, E_1 .

A_1	8.29×10^{10}	sec^{-1}	θ_1	1.0×10^6
E_1	26.6	Kcal/g.mole	B	7.67×10^{-5}
$(-\Delta H_1)$	500	Kcal/g.mole	Sh'_A	500
Dp_A	3.66×10^{-3}	cm^2/sec	Nu'	1.0
k_{c_A}	4.36	cm/sec	G_1	0.84
h	1.20×10^{-3}	$cal/cm^2/sec/^oK$	G_2	0.0949
b	0.21	cm	G_3	0.84
L	125	cm	G_4	76.85
u	164	cm/sec	G_5	0.84 secs
R	2.1	cm	G_6	0.84 secs
U	6.7×10^{-4}	$cal/cm^2/sec/^oK$	Nu_W	2.00
e	0.4		Nu_W^*	1.33
C_p	0.25	$cal/g/^oK$	K_T	1.55 secs
C_o	2.84×10^{-7}	$g.moles/cm^3$	T (inlet)	0.0372
Tf (inlet)	500	^oK		
Pe_H, Pe_M	10			
ρ^*	1.0	g/cm^3		
C_p^*	0.177	$cal/g/^oK$		
Kp	5.04×10^{-4}	$cal/cm/sec/^oK$		

TABLE 9.2. Data used for the reactor models in Chapter 9. Coolant temperatures are as specified in individual graphs.

on θ_2, θ_3, E_2/E_1, E_3/E_1, H_2, H_3, Sh'_B and δ, each of which is constant for a particular reaction on a given catalyst. It is therefore possible to monitor the numerical solution of the reactor model as before, by plotting the reactor trajectories in the B - T plane, and to test for multiple solutions on one graph, although this is slightly more difficult than for the A $\longrightarrow$ B reaction. The details of this are given in Appendix 5.

9.5 The relationship of the present method to that proposed by Cresswell.

In his recent paper, Cresswell[52] developed a criterion for the absence of multiple solutions in the single pellet, using a model which included the interphase resistances to heat and mass transfer, as well as intra-particle effects. A method was also suggested for determining the bounds on the non-unique region, if one existed. Since the notation and grouping of the parameters are similar to that which has commonly been used in the past (i.e. different from the grouping proposed here), it is interesting to examine exactly what the methods are capable of predicting, and relationship to the current work.

The criterion for the absence of multiple solution can be rewritten in the present notation as:

$$B < \frac{8T^2}{Sh'_A} + 8BT$$

If this equation is solved as an equality, it predicts the locus of the dotted line in Figure 9.3, and the region in which the inequality applies is clearly above and to the left of this line. The criterion is therefore very conservative for any given system, for which θ_1 would be fixed. This is particularly important since it excludes the desirable range of conditions to the left of the lower curve defining the non-unique region for the relevant value of θ_1. For example, the inlet conditions

shown in Figure 9.8 would violate the criterion and could therefore not be regarded as permissible, even though in fact the profiles are shown to be completely stable for appropriate values of the coolant temperature. Cresswell's criterion predicts the upper limit on B as $\sim 3 \times 10^{-5}$ for T = 0.0372, and this is only about 40% of the concentration which has been shown in Figure 9.8 to give a satisfactory trajectory in the B, T plane.

It can be seen that the criterion, given above, approaches $T > 0.125$ as Sh'_A tends to infinity, confirming the results shown in Figure 9.6.

When multiple solutions do occur, Cresswell devised a method for determining the bounds on the non-unique region in terms of upper and lower values of ϕ_1, for fixed values of Sh'_A, Nu', β_1 and γ_1.

$$\text{Now} \quad B = \frac{\beta_1}{\gamma_1 Nu'}, \quad \text{and} \quad T = \frac{1}{\gamma_1}$$

so fixing the parameters suggested by Cresswell defines a point in the B - T plane, such as point P in Figure 9.3, and since

$$\phi_1 = \theta_1 \exp(-\frac{0.5}{\gamma_1}) = \theta_1 \exp(-0.5T)$$

the method actually predicts the two values of θ_1 (i.e. different systems) for which the curves intersect at this point, namely $\theta_1 = 10^4$ and 10^6. Examination of non-uniqueness in this way is clearly inconvenient for any given system where the value of θ_1 would be fixed, and since the method cannot be worked in reverse, it is not easy to use it for an examination of the global stability of the system.

9.6 Transient effects relating to non-uniqueness.

The results obtained from the transient reactor model have shown that it is possible to have high concentrations and high temperatures existing at some point in the reactor for finite periods of time. Since this may drive the reactor into a non-unique region, or across the upper bound of the non-unique region, it is necessary to examine how individual

pellets behave when subject to transient external conditions, particularly those which occur near the bound of the non-unique region.

For the reaction A ——→ B, the equation describing the transient response of the pellet is:-

$$\frac{2}{3Nu'}K_T \frac{dt}{d\tau} = T - t + B_o Sh'_A (C_A - c_{A_s}) \qquad (9.7)$$

Combining equations (9.2) and (9.7) to eliminate c_{A_s} gives

$$\frac{2}{3Nu'}K_T \frac{dt}{d\tau} = T - t + B\, Sh'_A \left(\frac{r^* - g}{(\frac{Sh'_A}{2} - 1)g + r^*} \right) \qquad (9.8)$$

where $B = B_o \times C_A$

Equation (9.8) is an initial value problem which can be solved by a Runge-Kutta procedure. The starting value of t is obtained from the steady state solution at the initial conditions.

Figure 9.10 shows an enlarged view of part of the non-unique region, together with the pellet temperatures associated with the bounds on non-uniqueness. It can be seen by comparing this graph with Figure 9.1 that the pellet tends to change its state whenever the pellet temperature enters the region enclosed by the dotted lines.

Figure 9.11, for example, shows the response to a step change in the fluid temperature which takes the value of T to a point just above T_1. Initially the normal type of stable response is evident, with the pellet temperature apparently approaching asymptotically towards a new steady state value. Just before this steady state is reached, however, the pellet temperature passes the critical value, t_1, and begins to rise with increasing rapidity until interphase mass transfer controls the reaction rate. The temperature of the pellet is then at a value which is predicted by equation (9.6), and in a reactor this would result in temperature runaway, with all its associated undesirable effects such as catalyst deactivation and poor selectivity.

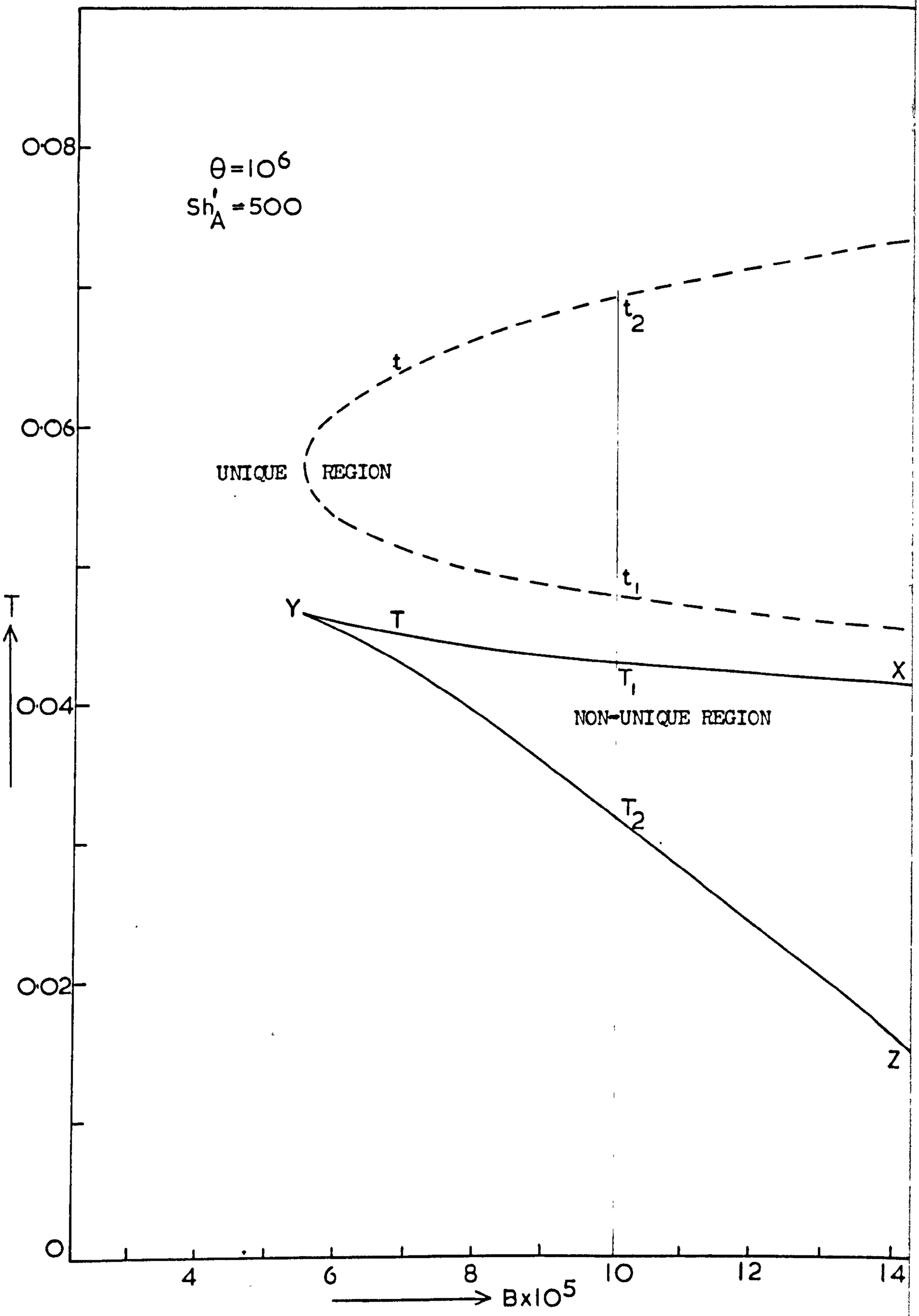

FIG.9.10 An enlarged view of part of the non-unique region, showing the pellet temperatures associated with the bounds on the region.

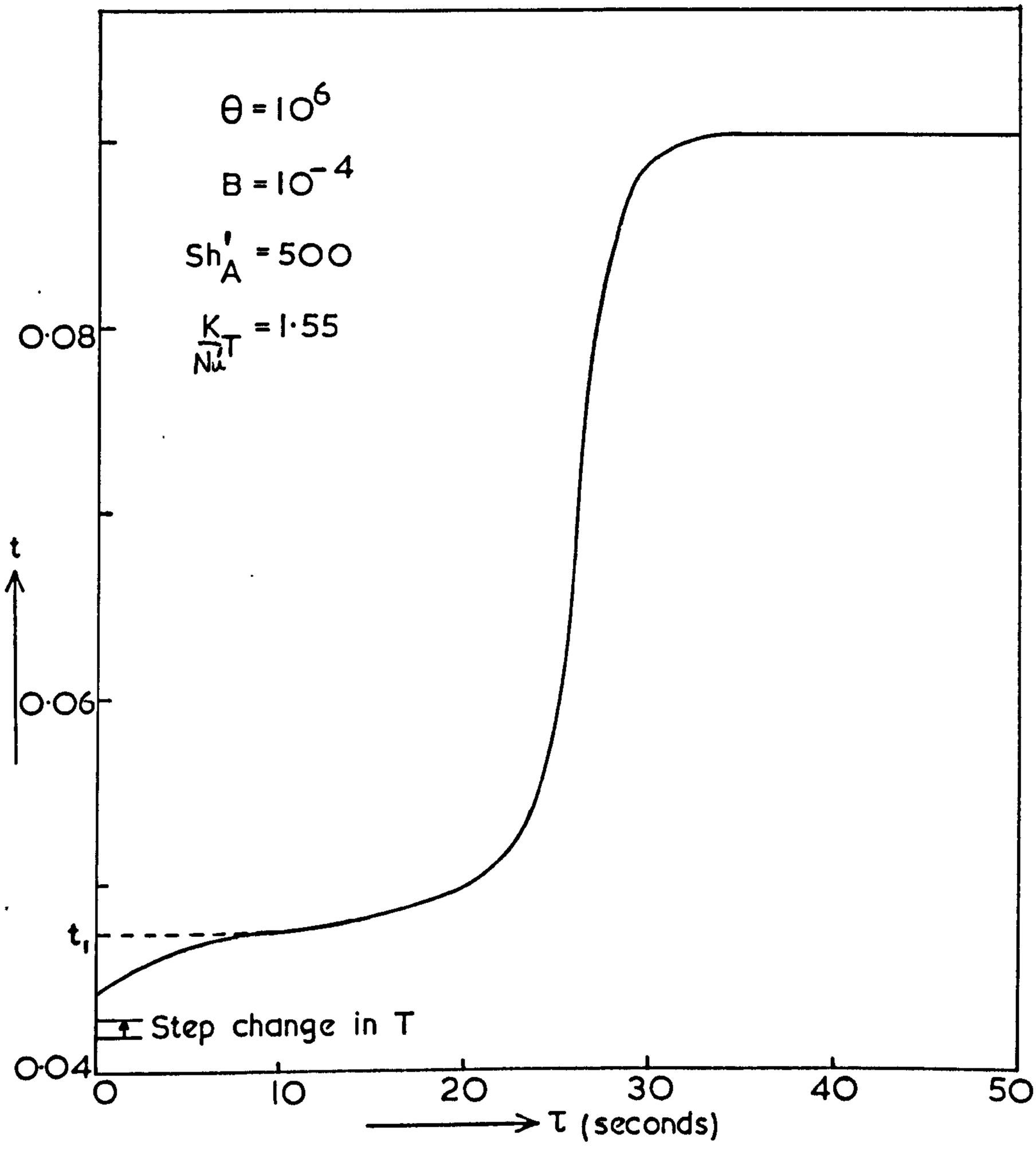

FIG.9.11 The response of the pellet to a step change in the fluid temperature which crosses the upper bound of the non-unique region.

It is possible, however, to pass transiently beyond the limit of non-uniqueness if the time in the runaway region is sufficiently short. This is best seen by considering the frequency response to a sinusoidal perturbation. Figure 9.12 shows the effect of perturbing the fluid temperature which crosses and recrosses the non-unique bound T_1. The curves have been drawn for various periods of oscillation. Not unexpectedly, the response to the perturbation with the highest frequency shows the smallest amplitude, the least distortion, and has the greatest relative time lag. As the frequency is reduced, longer periods are spent above the line XY and the pellet becomes less stable. The distortion of the response also becomes more noticeable and is due to the highly non-linear effect of temperature on the reaction rate causing higher peaks in pellet temperature as the fluid temperature rises. At very low frequencies the fluid temperature remains above T_1 long enough for the pellet temperature to run away, and interphase mass transfer control results. In this state, the pellet is unaffected by any decrease in temperature which might follow, unless T falls below T_2.

Figure 9.13 shows the effect of perturbing the concentration sinusoidally. (This has been shown as a perturbation in B since $B = B_o \times C_A$). The curves are rather similar to those previously discussed for an oscillating temperature. However, this perturbation was sufficiently large to cross both the XY and YZ lines of Figure 9.10 and the pellet therefore reaches the lower steady state each time the concentration falls, even after temperature runaway has occurred.

The factors which actually determine which pseudo-steady state is reached under oscillating conditions may be examined by plotting the response on a graph such as that shown in Figure 9.14. The continuous lines are an enlargement of curve (1) in Figure 9.1. It is apparent from Figure 9.14 that the lower steady state could be recovered even after temperature runaway

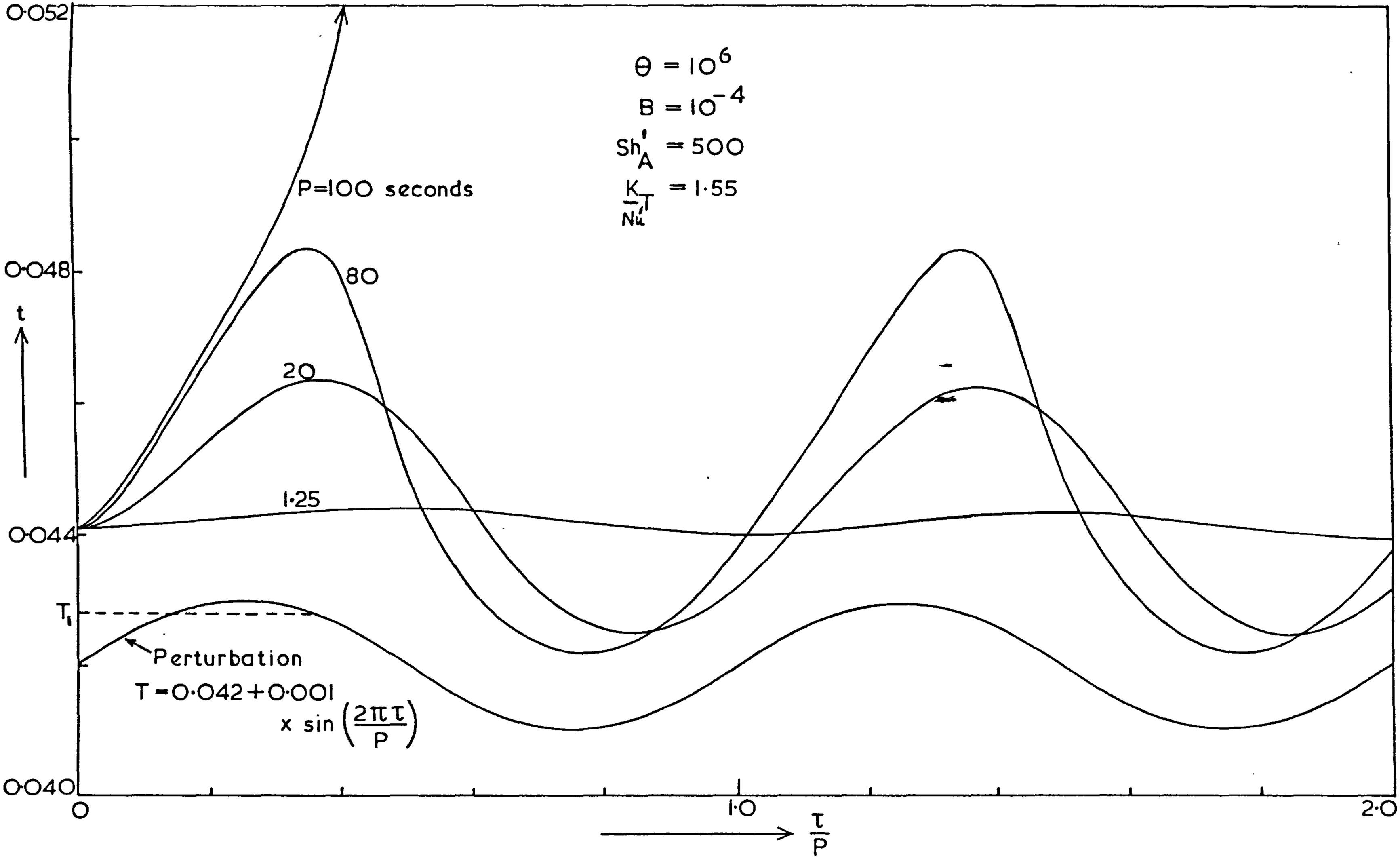

FIG.9.12 The response of the pellet to an oscillating fluid temperature which crosses the upper bound of the non-unique region.

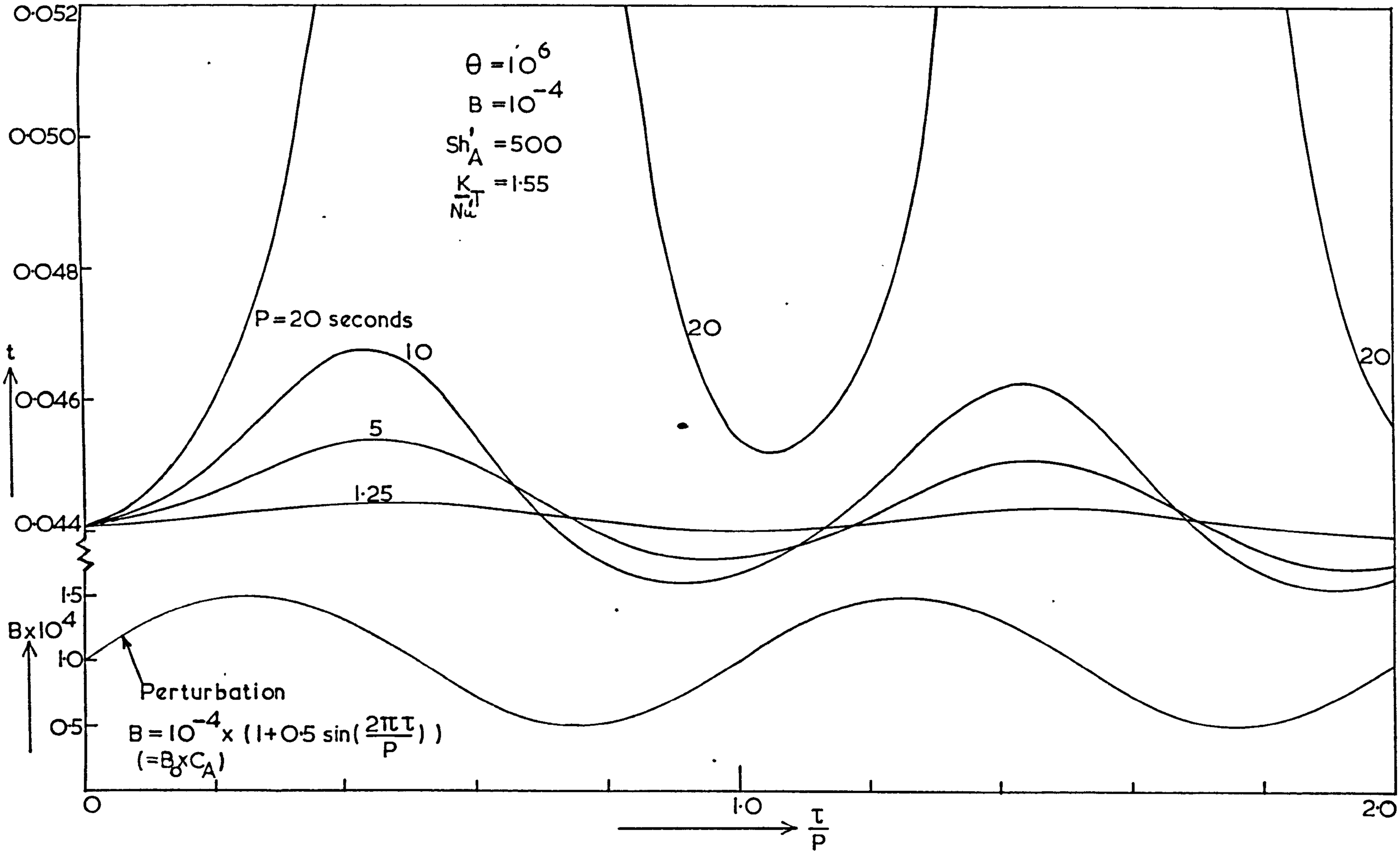

FIG. 9.13 The response of the pellet to an oscillating fluid concentration which crosses both bounds of the non-unique region.

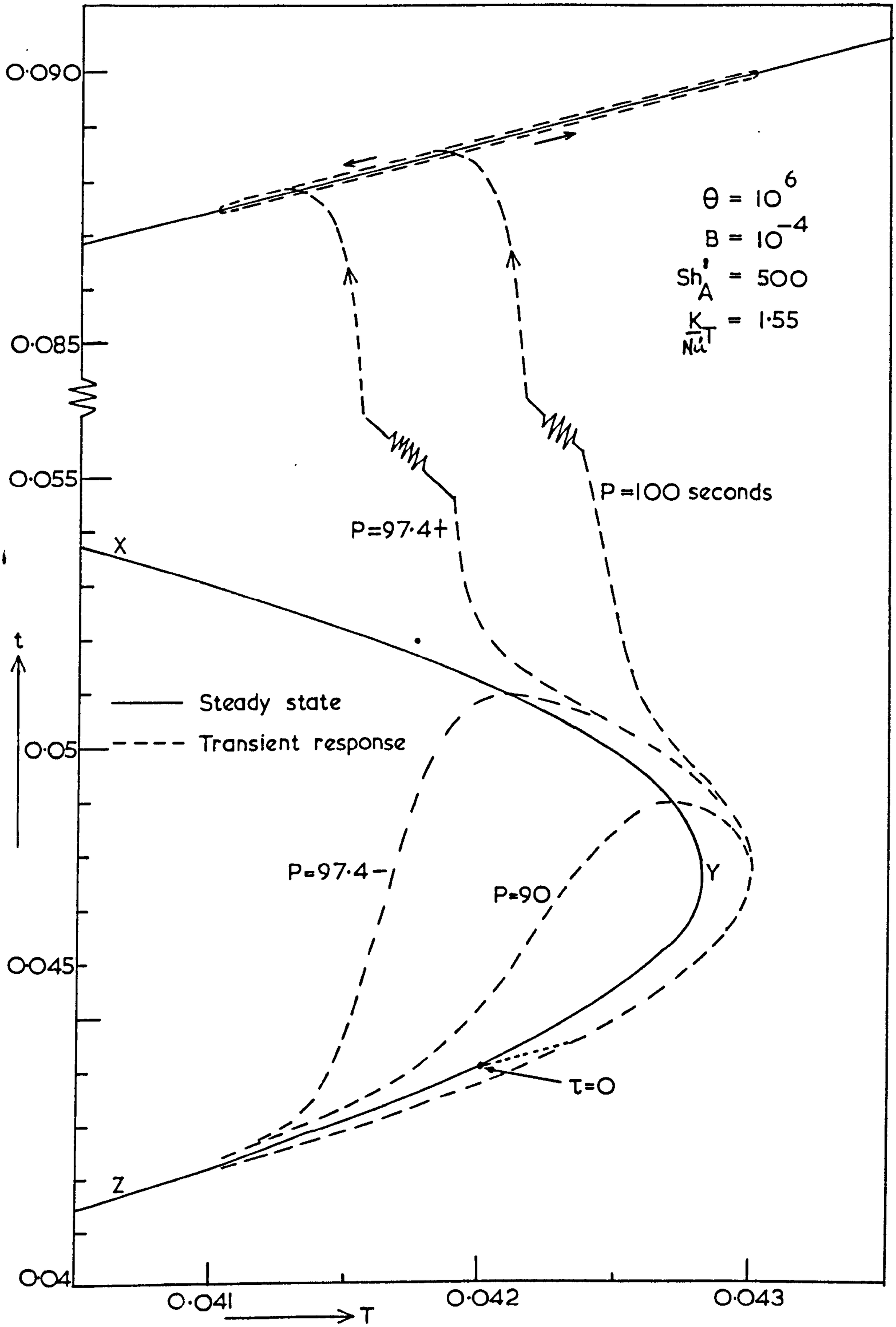

FIG.9.14 Phase plane plot of pellet temperature against fluid temperature in response to an oscillating fluid temperature at various frequencies.

has begun, provided the values of T and t are made to come within the line XYZ. This could be done either by changing T very rapidly, or by changing the concentration to give a different value of B for which the new locus of XYZ would envelop the current point (T, t).

From the way these responses occur, it is clear that if it were possible to obtain an analytic solution of equation (9.8), the benefits would be great, since the locus of the response could be examined in relation to the steady state solution of the pellet model (i.e. the continuous lines of Figure 9.14). If the response intersected the metastable steady state line XY, the response would be stable since the heat generated would be greater than that removed and the pellet would return to its initial state. It would then be possible to determine the critical amplitudes and frequency of the perturbation for which the response was just stable. However it was found that all attempts to linearise equation (9.8), or to convert it into a non-linear form amenable to analysis, resulted in the loss of the important characteristics of the response and at the present time, numerical solution seems to be the only satisfactory method.

The effect of the time lag on the stability of the reactor may also be examined in terms of the effectiveness factor, shown in Figure 9.15 for the steady state and a typical transient case. The two curves are obviously very different, and while the steady state effectiveness factor is multiple values over most of the range, the transient value is unique at this frequency. In the region of mass transfer control the effectiveness factor in the steady state is given by

$$\eta = \frac{3Sh'_A}{2\theta_1^2 \exp(-\frac{1}{T})}$$

which in the case considered here gives values between 9.4 and 29.4. However for clarity only the smaller values have been included in Figure 9.15.

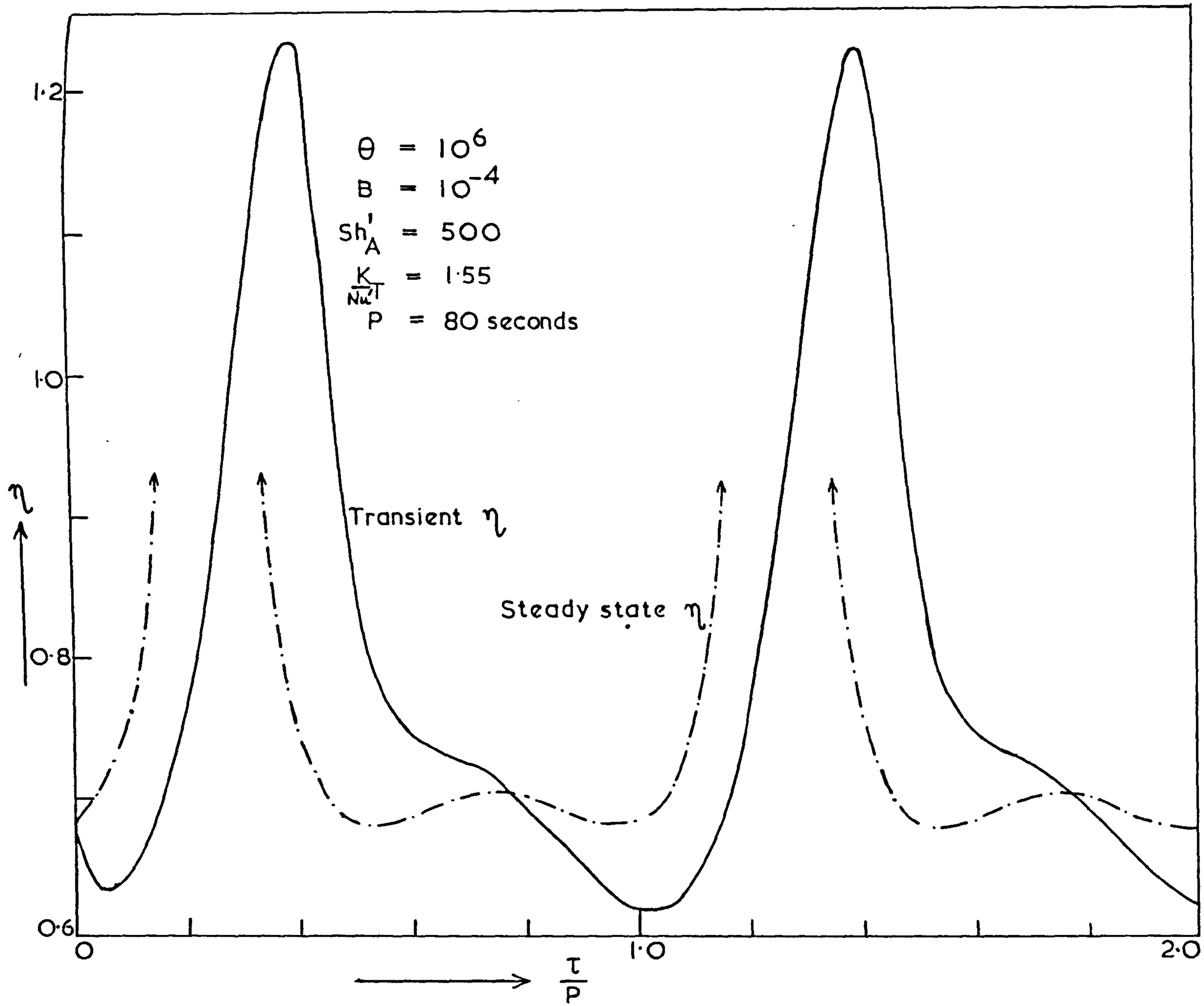

FIG.9.15 Comparison of steady state and transient effectiveness factors when the pellet is subject to an oscillating fluid temperature which crosses the upper bound of the non-unique region.

The extended troughs in the transient curve are due to the time lag when the fluid temperature has begun to rise steeply while the pellet temperature is still near its minimum value. The frequency of the perturbation clearly has a strong influence on the transient effectiveness factor, since when the temperature oscillates at high frequencies the kinetic rate also oscillates strongly but the actual rate remains almost constant since the pellet temperature hardly changes.

9.7 General comments.

A method has been developed for determining the range of fluid conditions over which it is possible for a catalyst pellet to exist in more than one steady state. If the profiles of temperature and concentration should enter this region, a steady state model on its own is not capable of predicting the performance of the reactor, since this will depend also on the history of each of the catalyst pellets. Apart from this disadvantage, which could possibly by overcome by a careful start up of the reactor, there is nothing against operating within the non-unique region, provided that the pellets can be maintained at their lower steady state.

The interactive features of the reactor are extremely difficult to investigate, however, and it is possible that, even if one or two pellets were to exist at the upper steady state, the system would be stable since these pellets could reduce the concentration sufficiently for subsequent pellets to experience fluid conditions which lie well outside the non-unique region. The only problem which must then be examined is whether the reactor can withstand the large temperature gradients and the high temperature rise which would occur in this part of the reactor, since there would effectively be an adiabatic temperature rise.

The observations of transient effects have been discussed in an attempt to put the steady state criteria for stability in perspective. Again, they emphasize the importance of the upper arm of the curves defining the non-unique region. In these transient studies, each of the perturbations crossed the limit of non-uniqueness (i.e. the upper arm of the curve) by only a small amount, yet temperature runaway occurred in a relatively short time, usually within about twenty seconds, indicating that the steady state stability criteria are not overconservative. In the dynamic case, as for the steady state, it is impossible at the present time to say how individual pellets will interact, since it may be that the transient instabilities will propagate, but it is equally possible that one unstable pellet will merely stabilize other pellets downstream.

Because of the transient effects which occur in the reactor itself, a situation may arise where high concentration of reactant reach parts of the reactor which are already hot and which at the steady state would be receiving lower concentrations. This phenomenon has been discussed in detail in Chapter 8, and its relationship to the effects of non-uniqueness may be seen from Figure 9.16. It is apparent that although both the initial and final steady states are unique and stable, the transient profiles pass through the non-unique region and therefore lead to potential instability. Indeed it appears that great care must be taken if a reactor is to be operated under conditions giving profiles which pass anywhere near the non-unique region, and that all changes in operating conditions should, if possible, be carried out sufficiently slowly to give a monotonic change of profiles from one steady state to the other. Alternatively a more conservative limit on the inlet conditions might need to be imposed, such as restricting the value of B so that it is below the value obtained from Figure 9.5 for the

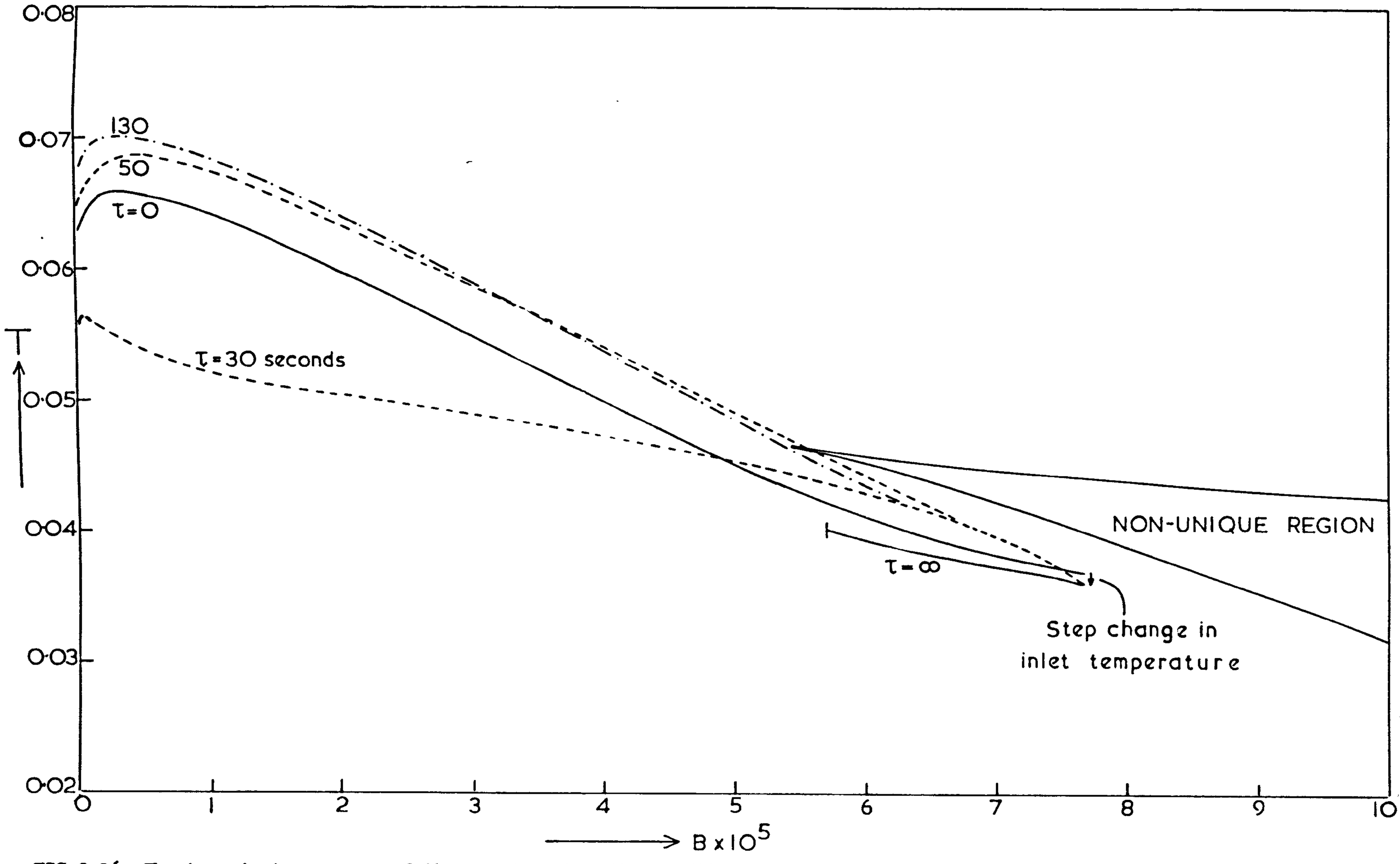

FIG.9.16 The transient response of the reactor when the profiles enter the non-unique region. Data as given in Table 9.2 . T_c=0.0353 which corresponds to 475°K for the given activation energy, E_1 .

given value of θ_1 and Sh'_A. This would ensure that all transient responses would be stable, with regard to non-uniqueness, since the operating conditions would always lie to the left of the non-unique region for the particular system under consideration.

CHAPTER 10

FINAL COMMENTS

10.1 Summary of the present work.

Consideration has been given to exothermic reactions where the kinetic scheme may be represented by: A ⟶ B ⟶ C. For this system, steady

state and dynamic models of the fixed bed catalytic reactor have been developed which specifically take into account the heterogeneous nature of the bed. This was accomplished by considering the performance of single catalyst pellets in which the reaction rate is not only controlled by the reaction kinetics, but may also be influenced by transport processes. A method has been proposed for determining regions of potential operating difficulties, with particular reference to the bounds on the fluid conditions within which the catalyst pellet may exhibit multiple steady states, and a means suggested by which the global stability of the reactor may be examined.

The models of the catalyst pellet have been developed in a way which takes account of the resistances to heat and mass transfer within and around the pellet. It was demonstrated, for the range of data which is possible in real systems, that the thermal resistance between the bulk fluid and the pellet centre is concentrated across the fluid film. This enables considerable simplifications of the model to be made, since the pellet is effectively isothermal, a relatively large temperature rise occurring between the bulk fluid and the pellet surface. If the rate of reaction for each step may be regarded as first order, with respect to the key reactant being consumed in that step, then the equations which describe the mass balances in and around the pellet may be solved analytically. In the general case, the computing time is reduced considerably by this simplification, to an

extent where it is possible to incorporate detailed descriptions of the catalyst pellet into models of the reactor.

Two steady state models of the reactor have been developed, both of which are continuum models, i.e. the transport of heat and mass is described by differential equations. Solution of the models shows that the differences between the behaviour of heterogeneous and quasi-homogeneous systems is often large. A notable example of this is that the quasi-homogeneous model commonly predicts temperature runaway when the heterogeneous model predicts a completely satisfactory temperature profile, since the reaction rate is significantly influenced (i.e. reduced) by mass transfer effects.

In one of the proposed models, the two-dimensional model, both radial and longitudinal profiles of concentration and temperature are evaluated, whereas, in the other, only longitudinal profiles can be obtained from solution of the differential equations. The latter is known as a one-dimensional model, even though it is based on an assumed form for the radial temperature profile and thus takes some account of the two-dimensional nature of the system. In the steady state, the one-dimensional model gives rise to ordinary differential equations and the two-dimensional model gives partial differential equations.

It has been shown that the one-dimensional model can predict results which are in excellent agreement with those obtained from the more comprehensive two-dimensional model, and since the computing time is considerably less, a significant saving in computer time may be made. In spite of this reduction in the computational effort required to obtain the solution, the time required is much too long to enable the model to be used for controlling the reactor and this might have been anticipated from an examination of the equations which are involved. For this reason the work described in this thesis has proceeded in phase with work on the development of model reduction

techniques.[61] If successful 'reduced' models are available, then the time for solution of the basic models is less critical, since these would only need to be solved occasionally as a standard against which the simpler models may be judged, or when working in critical regions, such as close to the optimum or near constraints. (This comment applies equally well to distributed models of the catalyst pellet, since these are the standards against which the lumped thermal resistance (i.e. reduced) models may be judged.)

The most important required features of the more complex models are that the solutions should be obtainable in a reasonable time and that the numerical methods should be very stable. Variations on the same basic numerical method have therefore been used to solve all the non-linear differential equations which arise in the models, since this satisfies both the above requirements. Although the method is not particularly elegant, the convergence characteristics are known to be excellent.

Very little information was previously available concerning the dynamic behaviour of fixed bed catalytic reactors, since the solutions of models proposed in the literature have required such an excessive computational effort that very few results could be obtained, and the work may therefore be regarded as being almost mathematical or computational exercises. In order to examine the general features of the dynamic response, therefore, a model of the reactor has been developed for which the computing time is short enough to conduct a case study. The proposed model is one-dimensional and, although the detailed description of the system cannot be guaranteed, several potential difficulties have been identified, which might become manifest if an inappropriate control strategy were selected. In particular, the inlet temperature is unsuitable as a manipulated variable, since, when this is reduced, very high peak temperatures may occur and an unstable response is possible. These effects are primarily due to the heterogeneous

nature of the system, again demonstrating unsatisfactory features of representing the reactor by a quasi-homogeneous model.

The method developed to determine the ranges of fluid conditions over which multiple solutions of the pellet model may occur enables the global stability of the reactor to be studied by plotting reactor trajectories on a single graph and examining their relationship to the non-unique region. The method is particularly well suited to automatic application on a computer, in a way which makes it possible to continuously monitor the profiles of concentration and temperature during solution of the reactor models, and any conditions which could lead to multiple solutions (i.e. potential instability) can thus be readily identified. All previous analyses of reactor stability have been concerned with quasi-homogeneous systems, where the multiple solutions arise as a result of axial dispersion terms. Except for very short reactors, axial dispersion is known to be unimportant and the method proposed here enables, for the first time, an assessment of non-unique profiles to be made for the reactor systems likely to be important in practice.

10.2 Suggestions for further work.

The present work has been entirely theoretical, but it is clear that the reliability of the models can only be finally established by comparing the predictions of the models with the results obtained from real systems. This must therefore be regarded as having a high priority in any future work.

Parametric tests on the reactor models indicated that some of the required data must be known accurately - more accurately in fact than is possible using the standard correlations in the literature, and this might prevent successful application in some circumstances, even if the models themselves were completely satisfactory. It is therefore necessary to be able to identify some of the system parameters, either from preliminary experiments or, alternatively, by using the correlations in the literature

as the basis of the reactor design and then updating the estimates using on-line identification techniques. The present state of the art in on-line identification is rather unsatisfactory, however, and efforts are required to improve the current techniques.

On the theoretical side, investigation of the system is by no means complete. Attention has been given exclusively to analysing results for first order reactions, although the majority of the models are also suitable for reactions of other orders. A comprehensive examination of the effect of reaction order is desirable, both in single pellet studies and in reactor modelling. In analysing the dynamic behaviour of the reactor, attention has been confined exclusively to step and ramp changes in the manipulated variables. A more complete understanding of potential control difficulties could probably be obtained by examining the response to oscillating input conditions or constant values with random 'noise' superimposed. It is also desirable to develop a two-dimensional dynamic model of the reactor in order to confirm the conclusions reached using the one-dimensional model and to enable an assessment of the accuracy to be made.

The stability analysis of the reactor requires further study, particularly with regard to the behaviour when parts of radial profiles pass through the non-unique region, and the interaction of the catalyst pellets needs to be examined in this case. The dynamic characteristics of the reactor when pellets are changing from one steady state to another could also profitably be examined, in order to see whether instabilities are damped down or propagated. A finite stage model of part of the packed bed would probably be best for carrying out this study, since this enables the true geometry of the system to be considered rather than arbitrarily considering catalyst pellets to be placed (or acting) at the nodes of the finite difference network.

Lastly, it is desirable to continue with the development of model reduction techniques, since, no matter what models of the reactor are developed, reductions in computational effort will always be welcome.

APPENDIX 1

THE FINITE DIFFERENCE SOLUTION OF THE GENERALISED SINGLE PELLET MODEL

A1.1 Formulation of the finite difference equations.

The differential equations describing the behaviour of the pellet have been developed in Chapter 3. Equations (3.9), (3.10) and (3.11) are similar and may be written as

$$\frac{d^2f}{dy^2} - \frac{2}{1-y}\frac{df}{dy} + R'f + R'' = 0 \qquad (A1.1)$$

where R' and R'' are functions of the point concentrations and temperature at a distance y from the pellet surface. The boundary conditions for these equations are:-

$$\frac{df}{dy} = 0 \qquad \text{at } y = 1 \qquad (A1.2)$$

$$\frac{df}{dy} = K(f - F) \quad \text{at } y = 0 \qquad (A1.3)$$

F is the value of f in the fluid surrounding the catalyst pellet.

The expressions for K, R' and R'' are given in the table below.

Equation	f	F	R'	R''	K
3.9	c_A	C_A	$-\phi_1^{*2} c_A^{n_1-1} - \phi_3^{*2} c_A^{n_3-1}$	0	$\frac{Sh'}{2}_A$
3.10	c_B	C_B	$-\delta\phi_2^{*2} c_B^{n_2-1}$	$\delta\phi_1^{*2} c_A^{n_1}$	$\frac{Sh'}{2}_B$
3.11	t	T	0	$H(\phi_1^{*2} c_A^{n_1} + H_2\phi_2^{*2} c_B^{n_2} + H_3\phi_3^{*2} c_A^{n_3})$	$\frac{Nu'}{2}$

TABLE A1.1. The expression for the general terms in equations (A1.1), (A1.2) and (A1.3) obtained from equations (3.9), (3.10) and (3.11).

Solution of the three equations represented by equation (A1.1) may be accomplished by replacing the derivatives by their central difference approximations and solving the resulting simultaneous non-linear algebraic

equations iteratively. It is found that in some cases very steep gradients occur near the pellet surface making it impossible, using a uniform finite difference grid, to obtain adequate representation of the derivatives. Storage limitations normally restrict the number of nodes in the network to around 400 which is inadequate over some ranges of the system parameters. This problem may be overcome using a finite difference network containing steps of two sizes as follows.

Consider the general point in the finite difference network as shown below.

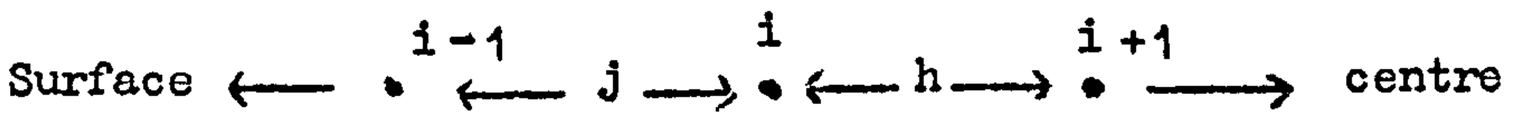

The derivatives in equation (A1.1) may be replaced by the following finite difference approximations:-

$$\frac{df}{dy} = \frac{f_{i+1} - f_{i-1}}{h + j}$$

$$\frac{d^2f}{dy^2} = \frac{2(jf_{i+1} - (h+j)f_i + hf_{i-1})}{hj(h+j)}$$

The general form of the equation is therefore

$$m_i f_{i+1} + p_i f_i + n_i f_{i-1} = a_i \qquad (A1.4)$$

where $m_i = \frac{2}{h+j}\left(\frac{1}{h} - \frac{1}{1-y}\right)$

$$n_i = \frac{2}{h+j}\left(\frac{1}{j} + \frac{1}{1-y}\right)$$

$$p_i = R'_i - \frac{2}{hj}$$

$$a_i = -R''_i \qquad (1 \leqslant i \leqslant N-1)$$

where nodes 0 and N are at the pellet surface and centre respectively.

When equation (A1.1) is combined with equation (A1.2), the boundary condition at the pellet centre, an indeterminate term is obtained. This term may be evaluated by applying Lhôpital's rule, giving

$$\lim_{y \to 1} \left(- \frac{2}{1-y} \frac{df}{dy} \right) = 2 \frac{d^2 f}{dy^2}$$

Substituting in equation (A1.1) gives

$$3 \frac{d^2 f}{dy^2} + R'f + R'' = 0 \qquad (A1.5)$$

In finite difference form obtained by putting $f_{N+1} = f_{N-1}$ and $j = h$, this becomes

$$p_N f_N + n_N f_{N-1} = a_N \qquad (A1.6)$$

where $n_N = \frac{6}{h^2}$

$$p_N = R'_N - \frac{6}{h^2}$$

$$a_N = - R''_N$$

Writing equation (A1.3), the boundary condition at the pellet surface, in finite difference form, we obtain

$$\frac{f_1 - f_{-1}}{2j} = K(f_o - F) \qquad (A1.7)$$

Eliminating the imaginary point f_{-1} between equations (A1.7) and (A1.4) and putting $j = h$

$$m_o f_1 + p_o f_o = a_o \qquad (A1.8)$$

where $m_o = \frac{2}{j^2}$

$$p_o = R'_o - \frac{2}{j^2} - 2K(\frac{1}{j} + 1)$$

$$a_o = -R''_o - 2KF(\frac{1}{j} + 1)$$

Equations (A1.4), (A1.6) and (A1.8) represent a system of simultaneous algebraic equations,

$$\underline{A} \ \underline{f} = \underline{a}$$

where

$$\underline{A} = \begin{bmatrix} p_o & m_o & & & \\ & \ddots & \ddots & \ddots & \\ & n_i & p_i & m_i & \\ & & \ddots & \ddots & \ddots \\ & & & n_N & p_N \end{bmatrix}$$

$\underline{A}$ is a tridiagonal matrix, and if the elements of $\underline{A}$ and $\underline{a}$ are known, then the equations which give rise to this type of matrix may be easily solved using the computationally efficient algorithm developed by Thomas, and described by Bruce et al.[63] (This algorithm is also given by Lapidus.[73])

However the non-linear terms R' and R'' which are involved in the elements of $\underline{A}$ and $\underline{a}$ are unknown, and an iterative procedure must be used. This may be done as follows: If the solution for $\underline{f}$ is assumed, R' and R'' may be calculated and after using these values to calculate the elements of $\underline{A}$ and $\underline{a}$, a new solution for $\underline{f}$ can be obtained. R' and R'' are again evaluated using the new $\underline{f}$, and so on until the solution becomes constant. For most purposes, the most convenient solution to assume initially is that $f_i = F$ for $0 \leqslant i \leqslant N$.

A1.2 Choice of the finite difference network.

The finite difference equations have been formulated in a way that will enable steps of more than one size to be used. Tables A1.3 and A1.4 show how the step sizes and the form of the grid affect the effectiveness factor and selectivity. These are calculated from equations (A1.10) and (A1.11) respectively. In section (a) of the tables, the step length is kept constant throughout the pellet. In section (b), the first 1% of the pellet near the surface is subdivided, doubling the number of steps in the interval each time, until there are 256. At this point the storage requirements are becoming excessive. The step size is further reduced by

halving y_I as seen in section (c), keeping the number of steps in the surface region at 256. In both sections (b) and (c) the interior of the pellet is divided into 100 increments. The data used are given in Table A1.2.

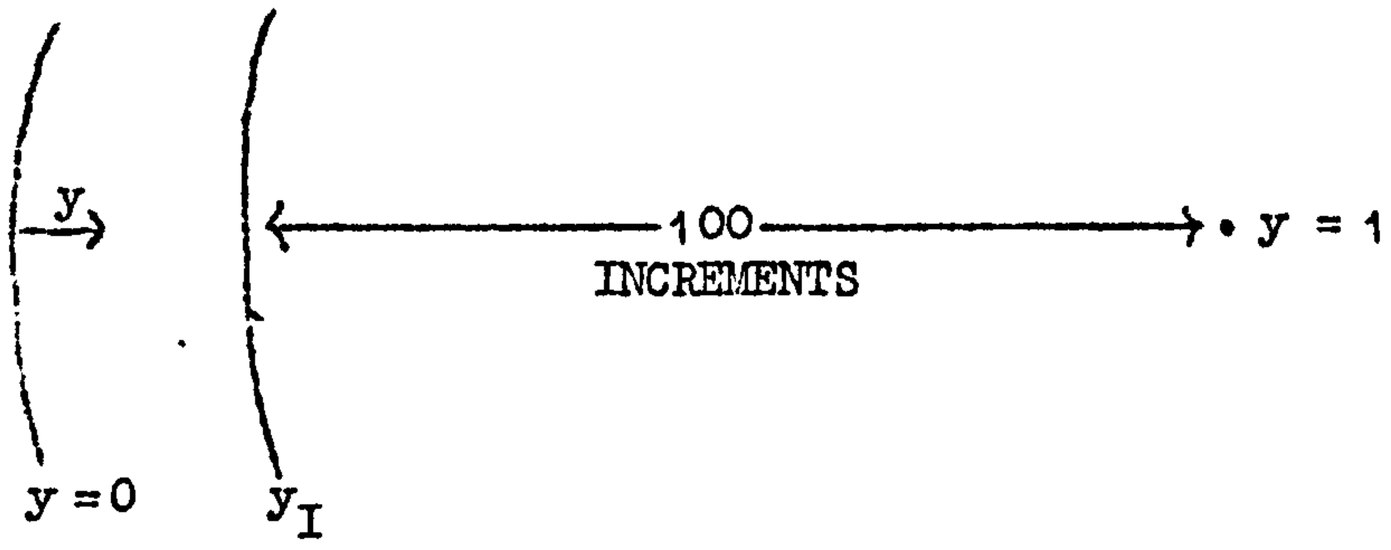

GROUP	VALUE
θ_1 , θ_2	2.2×10^4
θ_3	0.0
H	1.0×10^{-4}
E_2/E_1, H_2	1.0
Nu'	1.0
Sh'_A, Sh'_B	500
δ	1.0
c_B	0.0

TABLE A1.2 The values of dimensionless groups used to test convergence of the numerical procedures.

Figure A1.1 shows the effectiveness factor and selectivity as a function of temperature and indicates the controlling regions. From Tables A1.3 and A1.4 it may be seen that the region where convergence of the numerical procedure is easy to obtain, corresponds to kinetic control. As the region of interphase mass transfer control is approached, convergence becomes progressively more difficult to obtain. The reason may be easily

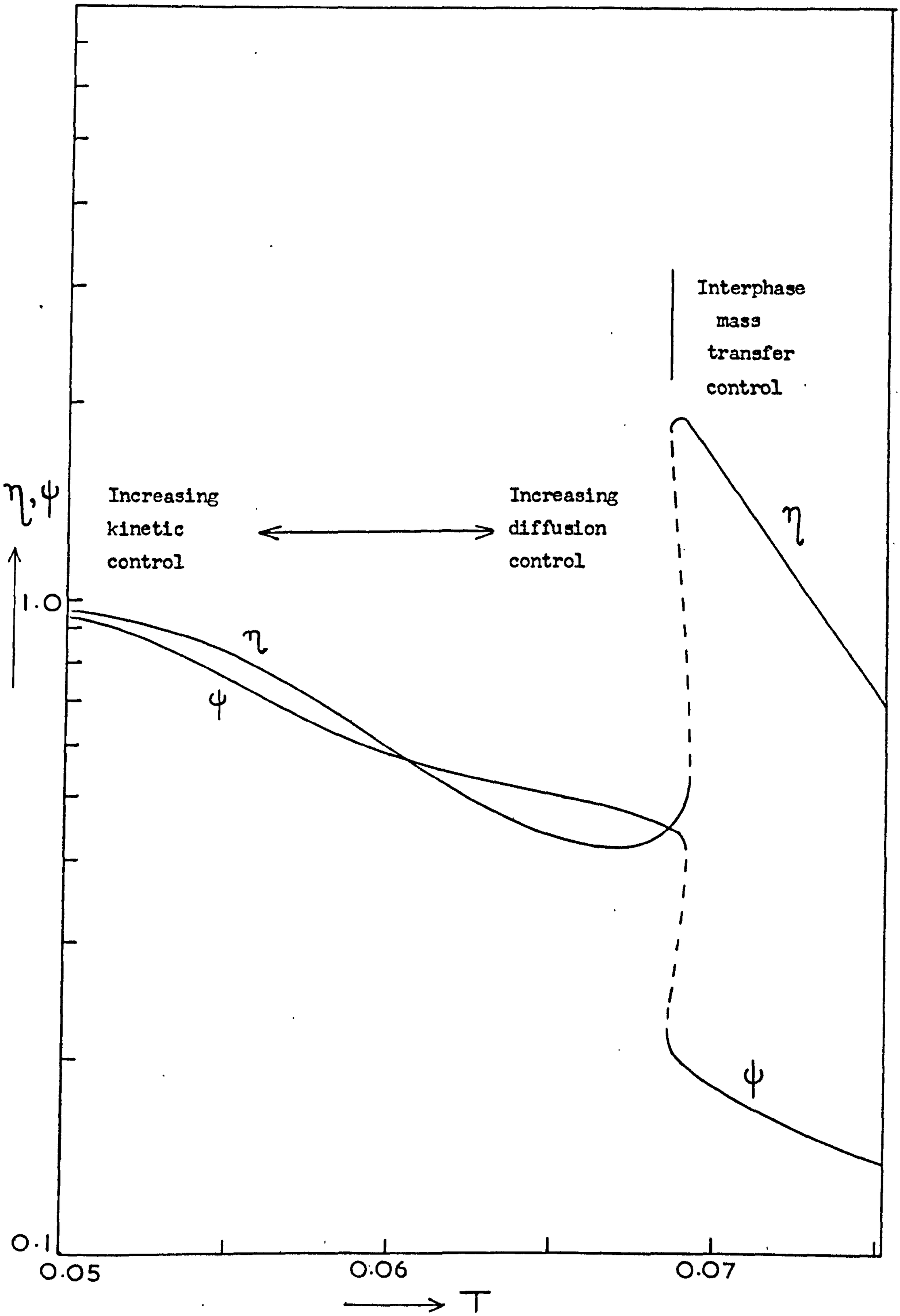

FIG. A1.1 Graph of effectiveness factor (η) and selectivity (ψ) against fluid temperature. This shows the range of conditions over which convergence of the finite difference network was tested. Data as given in Table A1.2 .

seen by examining the concentration and temperature profiles for various values of the fluid temperature, T, as shown in Figures A1.2, A1.3 and A1.4.

In the region of kinetic control (T = 0.05) the gradients are relatively shallow and the curvature gentle, allowing a fairly coarse grid to be used. As the region of diffusion control is approached (T = 0.55 → 0.65) the concentration gradients become steeper and the curvature increases, necessitating the use of smaller steps throughout the pellet. In the region of interphase mass transfer control, the gradients and curvatures in the concentration profiles are severe, but only near the external surface, enabling the use of a two step sized grid to be used with advantage. It may be seen from Figure A1.4 that the temperature profile is unlikely to present any convergence problems in itself, although it is high temperatures which are responsible for the steep concentration gradients which occur.

In Tables A1.3 and A1.4 the results for the diffusion controlled region begin to diverge in sections (b) and (c), to approach the values for a step size of 0.01. This is to be expected since, in the diffusion region, significant concentration gradients exist well into the pellet, while the smaller step size is only used near the surface.

The results discussed above indicate that the numerical solution of the equations is not as straightforward as has often been assumed in the literature. It is in fact necessary to solve the equations once with a relatively coarse grid to determine the step size and grid characteristics to be used for an accurate solution of the equations.

A1.3 Calculation of the effectiveness factor and selectivity.

The effectiveness factor and selectivity must be capable of accurate evaluation, since in a reactor, any small errors are likely to be magnified

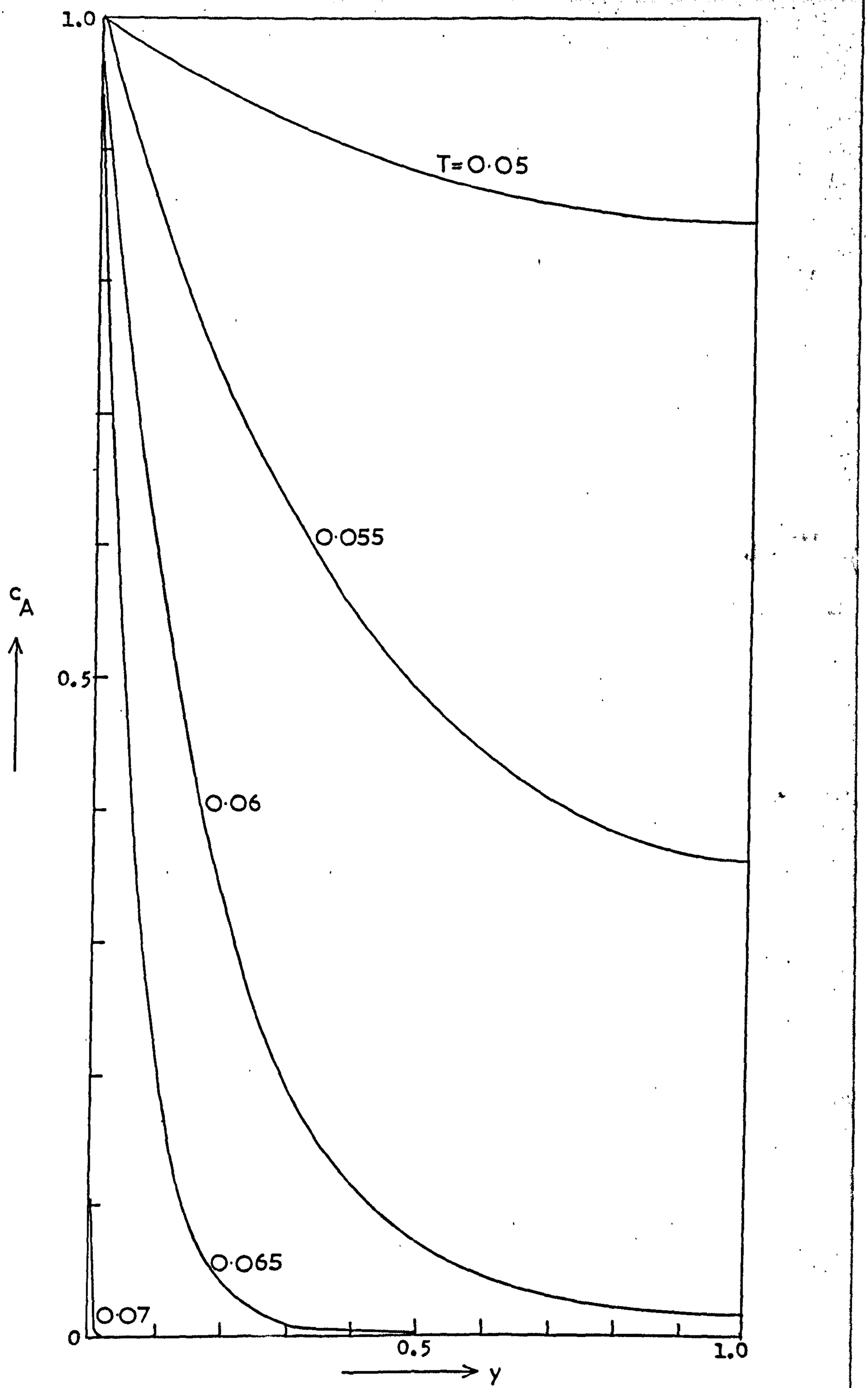

FIG. A1.2 Concentration profiles for species A within the catalyst pellet for various fluid temperatures. Data as given in Table A1.2 .

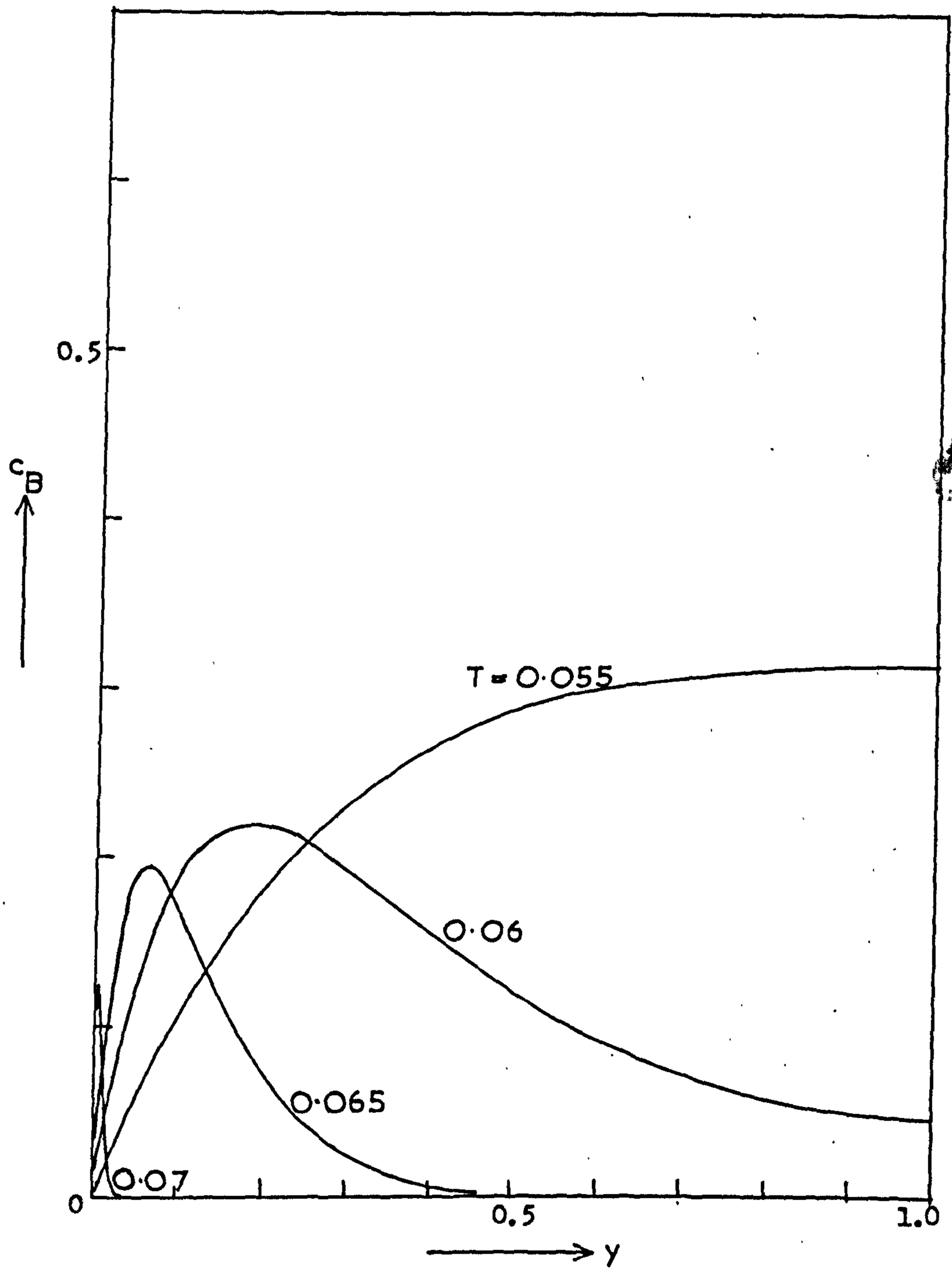

FIG. A1.3 Concentration profiles for species B within the catalyst pellet for various fluid temperatures. Data as given in Table A1.2 .

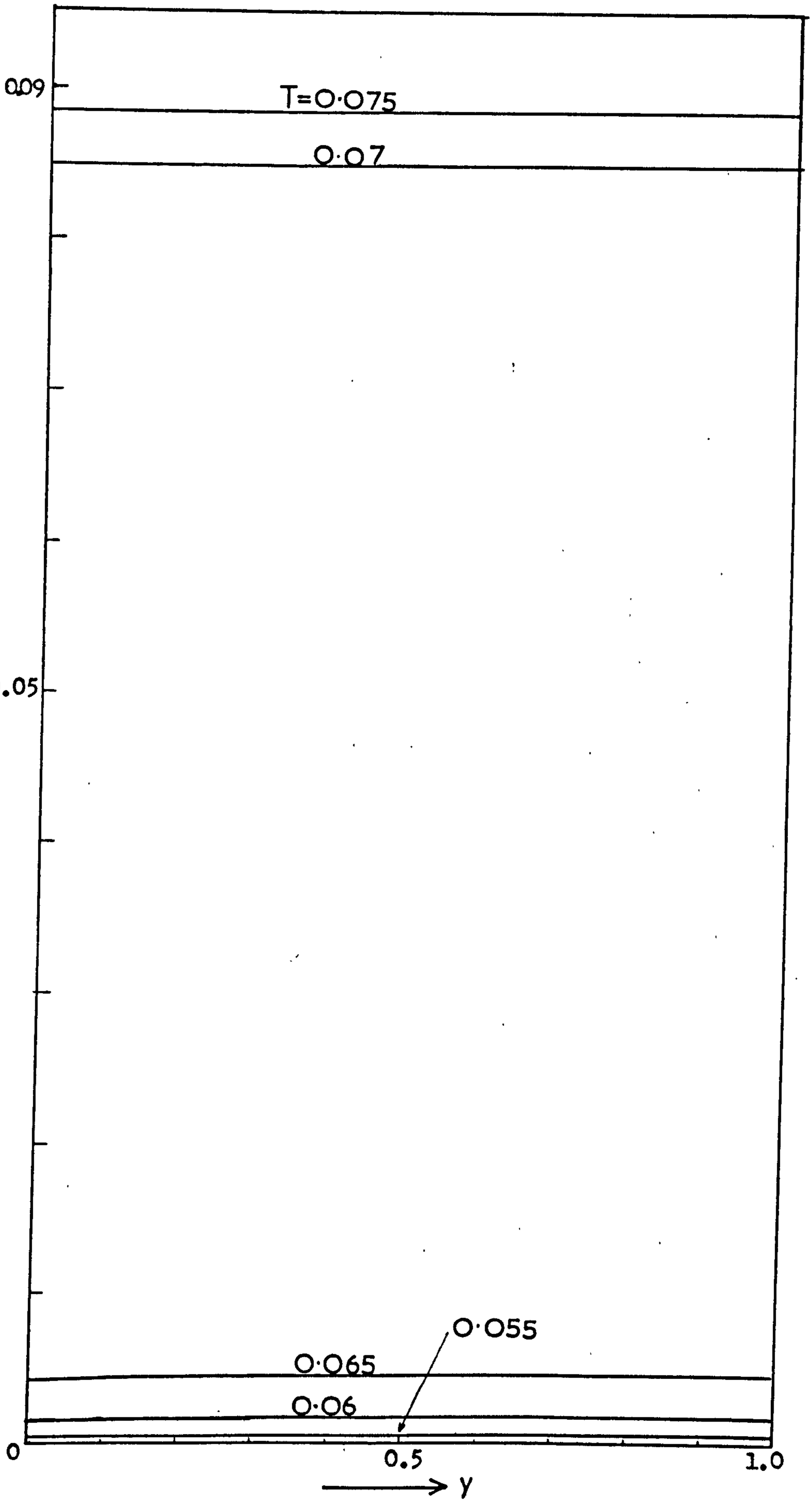

FIG. A1.4 Temperature profiles within the catalyst pellet measured relative to the temperature of the surrounding fluid (T). Data as given in Table A1.2 .

by the highly non-linear nature of the equations. Although the definitions of effectiveness factor and selectivity used by different authors may be essentially the same, the method of evaluation may vary, depending on which part of the boundary condition is used. For example, the boundary condition for component A is

$$2\left.\frac{dc_A}{dy}\right|_{y=0} = Sh'_A(c_{A_s} - C_A) \qquad (A1.9)$$

The effectiveness factor and selectivity are therefore defined by either:-

$$\eta = \frac{1.5\ Sh'_A(C_A - c_{A_s})}{(\phi_1^2 + \phi_3^2)\ C_A} \qquad (A1.10)$$

and $$\psi = \frac{Sh'_B(c_{B_s} - C_B)}{\delta Sh'_A(C_A - c_{A_s})} \qquad (A1.11)$$

or $$\eta = \frac{3\left.\frac{dc_A}{dy}\right|_{y=0}}{(\phi_1^2 + \phi_3^2)\ C_A} \qquad (A1.12)$$

and $$\psi = \frac{-\left.\frac{dc_B}{dy}\right|_{y=0}}{\delta\left.\frac{dc_A}{dy}\right|_{y=0}} \qquad (A1.13)$$

The form which has usually been used in the literature for the evaluation of η and ψ is that given by equations (A1.12) and (A1.13). Butt[31] used this method in his treatment of the reaction scheme A $\longrightarrow$ B $\longrightarrow$ C, calculating the derivatives by a three point backward difference formula.

$$\left.\frac{df}{dy}\right|_{y=0} = \frac{-3f_0 + 4f_1 - f_2}{2j}$$

It can be seen from Table A1.5 that the results calculated by the

two methods can give considerably different answers. The two methods agree when very small steps are used and it is apparent that for larger steps it is the method using gradient evaluation which gives the wrong answers. In some cases, especially in the evaluation of Ψ, the results calculated from the gradient form bear no relationship to the true values.

Throughout the work involving effectiveness factors and selectivity, η and Ψ are therefore evaluated from equations (A1.10) and (A1.11) using calculated values of the surface concentration.

STEP SIZE NEAR SURFACE	POSITION WHERE STEP SIZE CHANGES y_I	DIMENSIONLESS FLUID TEMPERATURE (T)						
		0.050	0.055	0.060	0.065	0.070	0.075	
		EFFECTIVENESS FACTOR (η)						
4.0×10^{-2}	CONSTANT STEP	0.964625	0.821882	0.586816	0.451499	2.44910	0.946470	a
2.0×10^{-2}	"	0.964593	0.821577	0.584454	0.434932	2.42323	0.938273	
1.0×10^{-2}	"	0.964592	0.821500	0.583861	0.430861	2.36437	0.920287	
5.0×10^{-3}	"	0.964590	0.821481	0.583713	0.429847	2.20971	0.877593	
2.5×10^{-3}	"	0.964590	0.821476	0.583676	0.429593	1.84181	0.786418	
1.28×10^{-3}	0.01	0.964648	0.821588	0.584009	0.430930	1.65135	0.719582	b
6.4×10^{-4}	"	0.964649	0.821589	0.584011	0.430931	1.60428	0.698799	
3.2×10^{-4}	"	0.964649	0.821589	0.584011	0.430931	1.59295	0.693555	
1.6×10^{-4}	"	0.964649	0.821589	0.584011	0.430931	1.59015	0.692243	
8.0×10^{-5}	"	0.964649	0.821589	0.584011	0.430931	1.58945	0.691915	
4.0×10^{-5}	"	0.964649	0.821591	0.584013	0.430933	1.58928	0.691834	

2.0×10^{-5}	0.005	0.964651	0.821602	0.584046	0.431155	1.61504	0.692746
1.0×10^{-5}	0.0025	0.944651	0.821576	0.584028	0.431234	1.72811	0.708804
5.0×10^{-6}	0.00125	0.964655	0.821784	0.584264	0.431572	1.89567	0.753385
2.5×10^{-6}	0.000625	0.964652	0.821628	0.584092	0.431393	2.06113	0.808285
1.25×10^{-6}	0.0003125	0.964657	0.821733	0.584215	0.431553	2.18924	0.854452
6.25×10^{-7}	0.00015625	0.964641	0.820987	0.583379	0.430552	2.27062	0.884756

} c

TABLE A1.3. The effect of step size and step size distribution on the effectiveness factor (η) over a range of controlling regimes (for data see Table A1.2).

The step sizes are considered in three groups as follows:

Part (a) Constant step size throughout the pellet
(b) y_I held constant and the region $y = 0$ to $y = y_I$ subdivided
(c) y_I varied with 256 steps in the region $y = 0$ to $y = y_I$

In (b) and (c) the region $y = y_I$ to $y = 1$ is divided into 100 increments.

STEP SIZE NEAR SURFACE	POSITION WHERE STEP SIZE CHANGES y_I	DIMENSIONLESS FLUID TEMPERATURE (T)						
		0.050	0.055	0.060	0.065	0.070	0.075	
		SELECTIVITY (Ψ)						
4.0×10^{-2}	CONSTANT STEP	0.937863	0.747647	0.580306	0.539308	0.0100047	0.00838087	a
2.0×10^{-2}	"	0.937827	0.747106	0.575659	0.510300	0.0203888	0.0169180	
1.0×10^{-2}	"	0.937818	0.746970	0.574481	0.502465	0.0434691	0.0352999	
5.0×10^{-3}	"	0.937816	0.746936	0.574185	0.500466	0.0975466	0.0753121	
2.5×10^{-3}	"	0.937815	0.746928	0.574111	0.499964	0.172661	0.133130	
1.28×10^{-3}	0.01	0.937827	0.747010	0.574523	0.501567	0.180745	0.143704	b
6.4×10^{-4}	"	0.937827	0.747011	0.574524	0.501555	0.179605	0.139941	
3.2×10^{-4}	"	0.937827	0.747011	0.574524	0.501552	0.179147	0.138352	
1.6×10^{-4}	"	0.937827	0.747011	0.574524	0.501552	0.179022	0.137911	
8.0×10^{-5}	"	0.937827	0.747011	0.574524	0.501552	0.178991	0.137798	
4.0×10^{-5}	"	0.937827	0.747010	0.574523	0.501551	0.178981	0.137769	

2.0×10^{-5}	0.005	0.927827	0.747014	0.574576	0.502126	0.168802	0.136204
1.0×10^{-5}	0.0025	0.937828	0.747023	0.574611	0.502475	0.131797	0.116402
5.0×10^{-6}	0.00125	0.937828	0.746981	0.574586	0.502626	0.089691 0	0.071 9161
2.5×10^{-6}	0.000625	0.937828	0.747014	0.574624	0.502751	0.0625942	0.0523281
1.25×10^{-6}	0.0003125	0.937828	0.746993	0.574607	0.502783	0.0505999	0.0409186
6.25×10^{-7}	0.00015625	0.937829	0.747148	0.574754	0.502940	0.0502940	0.0461805

c

TABLE A1.4. The effect of step size and step size distribution on the selectivity (Ψ) over a range of controlling regimes (for data see Table A1.2).

The step sizes are considered in three groups as follows:

Part (a) Constant step size throughout the pellet
(b) y_I held constant and the region $y = 0$ to $y = y_I$ subdivided
(c) y_I varied with 256 steps in the region $y = 0$ to $y = y_I$

In (b) and (c) the region $y = y_I$ to 1 is subdivided into 100 increments.

STEP SIZE NEAR SURFACE	POSITION WHERE STEP SIZE CHANGES y_I	η FROM FILM TRANSPORT	η BY BACKWARD DIFFERENCE	Ψ FROM FILM TRANSPORT	Ψ FROM BACKWARD DIFFERENCE	
4.0×10^{-2}	CONSTANT STEP	2.44910	0.00371365	0.0100047	-0.988349	a
2.0×10^{-2}	"	2.42323	0.0151515	0.0203888	-0.972750	
1.0×10^{-2}	"	2.36437	0.0648962	0.0434691	-0.926309	
5.0×10^{-3}	"	2.20971	0.297099	0.0975466	-0.755753	
2.5×10^{-3}	"	1.84181	1.03200	0.172661	-0.243555	
1.28×10^{-3}	0.01	1.65135	1.43195	0.180745	0.0561501	b
6.4×10^{-4}	"	1.60428	1.54598	0.179605	0.144875	
3.2×10^{-4}	"	1.59295	1.57764	0.179147	0.169776	
1.6×10^{-4}	"	1.59015	1.58621	0.179022	0.176571	
8.0×10^{-5}	"	1.58945	1.58845	0.178991	0.178363	
4.0×10^{-5}	"	1.58928	1.58903	0.178981	0.178822	

2.0×10^{-5}	0.005	1.61504	1.61497	0.168802	0.168759
1.0×10^{-5}	0.0025	1.72811	1.72808	0.131797	0.131782
5.0×10^{-6}	0.00125	1.89567	1.89565	0.089691	0.089685
2.5×10^{-6}	0.000625	2.06113	2.06112	0.0625942	0.0625922
1.25×10^{-6}	0.0003125	2.18924	2.18924	0.0505999	0.0505992
6.25×10^{-7}	0.00015625	2.27062	2.27062	0.0461805	0.0461803

c

TABLE A1.5. Comparison of typical values found when evaluating the effectiveness factor and selectivity from film transport and from surface concentration derivatives (for data see Table A1.2) T = 0.07.

The step sizes are considered in three groups as follows:

Part (a) Constant step size throughout the pellet
(b) y_I held constant and the region $y = 0$ to $y = y_I$ subdivided
(c) y_I varied with 256 steps in the region $y = 0$ to $y = y_I$

In (b) and (c) the region $y = y_I$ to $y = 1$ is divided into 100 increments.

APPENDIX 2

THE FINITE DIFFERENCE FORM OF THE TWO-DIMENSIONAL STEADY STATE MODEL OF THE REACTOR

Equations (5.6), (5.7) and (5.8) all have similar form and may be written as follows:-

$$\frac{\partial^2 f}{\partial r^2} + \frac{1}{r}\frac{\partial f}{\partial r} + K'\frac{\partial f}{\partial z} + R'f + R'' = 0 \qquad (A2.1)$$

subject to the boundary conditions

$$\frac{\partial f}{\partial r} = 0 \qquad \text{at } r = 0, \quad z > 0 \qquad (A2.2)$$

$$\frac{\partial f}{\partial r} + Kf + KK^{o} = 0 \qquad \text{at } r = 1, \quad z > 0 \qquad (A2.3)$$

and the initial condition

$$f = f(r) \text{ at } z = 0 \text{ for } 0 \geqslant r \geqslant 1$$

The parameters in these equations have the values shown in Table A2.1.

Equation	f	K'	R'	R''	K	K^o
5.6	C_A	$-G_1$	$-G_1 G_2 \eta (\phi_1^2 C_A^{n_1-1} + \phi_3^2 C_A^{n_3-1})$	0	0	0
5.7	C_B	$-G_1\Delta$	0	$G_1 G_2 \Delta\eta\psi (\phi_1^2 C_A^{n_1-1} + \phi_3^2 C_A^{n_3-1})C_A$	0	0
5.8	T	$-G_3$	$-G_3 G_4$	$G_3 G_4 t$	Nu_w	$-T_c$

TABLE A2.1 The expressions for the general terms in equations (A2.1), (A2.2) and (A2.3) obtained from equations (5.6), (5.7) and (5.8).

Equation (A2.1), together with its associated boundary conditions, may be solved by a finite difference method. In the method described here the gradients in the radial direction are replaced by their central difference approximations while those in the axial direction may be replaced by any first order finite difference approximation.

The terms in equation (A2.1) may be expressed as follows:-

$$\frac{\partial^2 f}{\partial r^2} = \frac{1}{h^2}\left(Q\left(f_{i+1} - 2f_i + f_{i-1}\right) + (1-Q)\left(xf_{i+1} - 2xf_i + xf_{i-1}\right)\right)$$

$$\frac{1}{r}\frac{\partial f}{\partial r} = \frac{1}{2hr}\left(Q\left(f_{i+1} - f_{i-1}\right) + (1-Q)\left(xf_{i+1} - xf_{i-1}\right)\right)$$

$$K'\frac{\partial f}{\partial z} = \frac{K'}{k}\left(f_i - xf_i\right)$$

$$R'f = QR'_i f_i + (1-Q)\,xR'_i\,xf_i$$

$$R'' = QR''_i + (1-Q)\,xR''_i$$

The prefix 'x' indicates the value of a variable at the previous axial position. This is a known value since the equations are initial valued in the axial direction. Q is a constant such that $0 \leqslant Q \leqslant 1$. When $Q = 0.5$ the equations reduce to the Crank-Nicholson form and the non-linear terms are averaged over the axial step.

Replacing the terms in equation (A2.1) by the expression given above, and rearranging, gives

$$m_i f_{i+1} + p_i f_i + n_i f_{i-1} = a_i \qquad \text{(A2.4)}$$

where $m_i = \frac{Q}{h^2} + \frac{Q}{2hr}$

$$n_i = \frac{Q}{h^2} - \frac{Q}{2hr}$$

$$p_i = -\frac{2Q}{h^2} + \frac{K'}{k} + QR'_i$$

$$a_i = -xf_{i+1}\left(\frac{1-Q}{h^2} + \frac{1-Q}{2hr}\right) - xf_i\left(-\frac{2(1-Q)}{h^2} - \frac{K'}{k} + (1-Q)\,xR'_i\right)$$

$$- xf_{i-1}\left(\frac{1-Q}{h^2} - \frac{1-Q}{2hr}\right) - QR''_i - (1-Q)\,xR''_i$$

These expressions hold for $1 \leqslant i \leqslant N-1$ where N and 0 are the numbers of the finite difference nodes at the tube wall and centre respectively.

At the tube centre $\frac{\partial f}{\partial r} = 0$ so $\frac{1}{r}\frac{\partial f}{\partial r}$ is indeterminate. Applying

L'Hôpital's rule, equation (A2.1) becomes

$$2\frac{\partial^2 f}{\partial r^2} + K'\frac{\partial f}{\partial z} + R'f + R'' = 0$$

and since $f_{-1} = f_1$ etc., the equation in finite difference form becomes

$$m_o f_1 + p_o f_o = a_o \qquad \text{(A2.5)}$$

where $m_o = \frac{4Q}{h^2}$

$$p_o = \frac{-4Q}{h^2} + \frac{K'}{k} + QR'_o$$

$$a_o = -xf_1\left(\frac{4(1-Q)}{h^2}\right) - xf_o\left(-\frac{4(1-Q)}{h^2} - \frac{K'}{k} - (1-Q)xR'_o\right) - QR''_o - (1-Q)xR'_o$$

At the tube wall, the boundary condition becomes, in difference form,

$$\frac{1}{2h}\left(Q(f_{N+1} - f_{N-1}) + (1-Q)(xf_{N+1} - xf_{N-1})\right) + K(Qf_N + (1-Q)xf_N) + KK^o = 0$$

This equation can be combined with equation (A2.4). This results in the elimination of the hypothetical function values f_{N+1} and xf_{N+1} giving

$$p_N f_N + n_N f_{N-1} = a_N \qquad \text{(A2.6)}$$

where $n_N = \frac{2Q}{h^2}$

$$p_N = -\frac{2Q}{h^2} + \frac{K'}{k} + QR'_N - 2Kh\left(\frac{Q}{h^2} + \frac{Q}{2h}\right)$$

$$a_N = -xf_N\left(-\frac{2(1-Q)}{h^2} - \frac{K'}{k} + (1-Q)xR'_N - 2Kh\left(\frac{1-Q}{h^2} + \frac{(1-Q)}{2h}\right)\right) - xf_{N-1}\left(\frac{2(1-Q)}{h^2}\right)$$

$$- QR''_N - (1-Q)xR''_N + KK^o\left(\frac{2}{h} + 1\right)$$

Equations (A2.4), (A2.5) and (A2.6) represent a system of simultaneous algebraic equations

$$\underline{A}\,\underline{f} = \underline{a} \qquad \text{(A2.7)}$$

where

$$\underline{A} = \begin{bmatrix} p_o & m_o & & & & \\ & \ddots & \ddots & & & \\ & & n_i & p_i & m_i & \\ & & & \ddots & \ddots & \ddots \\ & & & & n_N & p_N \end{bmatrix}$$

This matrix has the same form as that obtained for the pellet model in Appendix 1 and the solution for $\underline{f}$ can again be obtained using the Thomas method.[63]

APPENDIX 3

THE FINITE DIFFERENCE FORM OF THE FULLY DISTRIBUTED DYNAMIC MODEL OF THE CATALYST PELLET

For the A ⟶ B reaction, the heat and mass balances in the dynamic case are described by equations (7.1) and (7.2). These two equations have similar form and may be written as follows:-

$$\frac{\partial^2 f}{\partial y^2} - \frac{2}{1-y}\frac{\partial f}{\partial y} - K'\frac{\partial f}{\partial \Upsilon} + R'f + R'' = 0 \qquad (A3.1)$$

Subject to the boundary conditions

$$\frac{\partial f}{\partial y} = 0 \quad \text{at} \quad y = 1, \qquad \Upsilon > 0 \qquad (A3.2)$$

$$\frac{\partial f}{\partial y} = K(f - F) \quad \text{at} \quad y = 0, \qquad \Upsilon > 0 \qquad (A3.3)$$

$$f = f(y) \qquad \text{at} \quad \Upsilon = 0 \qquad 0 \leqslant y \leqslant 1$$

where K and F may be functions of time, Υ.

Equation	f	K'	R'	R''	K	F
7.1	c_A	K_c	$-\phi_1^{*2} c_A^{n_1 - 1}$	0	Sh'_A	C_A
7.2	t	K_T	0	$H\phi_1^{*2} c_A^{n_1}$	Nu'	T

TABLE A3.1. The expressions for the general terms in equations (A3.1) and (A3.3) obtained from equations (7.1) and (7.2).

Equation (A3.1) and its associated boundary conditions may be solved by a method very similar to that described in Appendix 2 for the two-dimensional steady state model of the reactor. The finite difference formulation is not quite the same, however, since F and K may be functions of time, and the finite difference grid must be non-uniform for the reasons discussed in Appendix 1 with reference to the steady state solution of the catalyst pellet model.

The derivatives and other terms in the general form of the equation may be replaced as follows:-

$$\frac{\partial^2 f}{\partial y^2} = \frac{2}{(h+j)hj}\left\{Q^*(jf_{i+1} - (j+h)f_i + hf_{i-1}) + (1-Q^*)(j\,of_{i+1} - (h+j)of_i + h\,of_{i-1})\right\}$$

$$\frac{\partial f}{\partial y} = \frac{1}{h+j}\left\{Q^*(f_{i+1} - f_{i-1}) + (1-Q^*)(of_{i+1} - of_{i-1})\right\}$$

$$R'f = Q^*R_i' f_i + (1-Q^*)\, oR_i'\, of_i$$

$$R'' = Q^*R_i'' + (1-Q^*)\, oR_i''$$

$$\frac{\partial f}{\partial \tau} = \frac{1}{l}\,(f_i - of_i)$$

These terms have been evaluated at the general point of the grid, i, which has a step size of j on one side and h on the other.

Pellet Surface ⟵ $i-1$ ⟵ j ⟶ i ⟵ h ⟶ $i+1$ ⟶ Pellet Centre

The prefix 'o' indicates the value of a variable at the previous time step (i.e. it is known).

l is the step length in the time direction

Q^* is a constant such that $0 < Q^* \leqslant 1$. When $Q^* = 0.5$ the equations reduce to the Crank-Nicholson form.

Replacing the terms in equation (A3.1) by their finite difference equivalents gives

$$m_i f_{i+1} + p_i f_i + n_i f_{i-1} = a_i \qquad \text{(A3.4)}$$

where $m_i = \frac{2Q^*}{h+j}\left(\frac{1}{h} - \frac{1}{1-y}\right)$

$$n_i = \frac{2Q^*}{h+j}\left(\frac{1}{j} + \frac{1}{1-y}\right)$$

$$p_i = -\frac{2Q^*}{hj} + Q^*R_i' - \frac{K'}{l}$$

$$a_i = \frac{2(1-Q^*)}{h+j}\left(-\frac{1}{h} + \frac{1}{1-y}\right)of_{i+1} + of_i\left(\frac{2(1-Q^*)}{hj} - (1-Q^*)\, oR_i' - \frac{K'}{l}\right)$$

(cont.)

$$- \frac{2(1-Q^*)}{h+j}\left(\frac{1}{j} + \frac{1}{1-y}\right) - Q^*R_i'' - (1-Q^*)\,oR_i''$$

for $1 \leqslant i \leqslant N-1$

The boundary conditions at $y = 0$ and $y = 1$ may be built into the finite difference formulation in the same way as for the steady state model (see Appendix 1).

At the centre ($i = N$)

$$p_N f_N + n_N f_{N-1} = a_N \qquad \text{(A3.5)}$$

where $n_N = \frac{6Q^*}{h^2}$

$$p_N = -\frac{6Q^*}{h^2} + Q^*R_N' - \frac{K'}{l}$$

$$a_N = of_N\left(\frac{6(1-Q^*)}{h^2} - (1-Q^*)oR_N' - \frac{K'}{l}\right) - \frac{6(1-Q^*)}{h^2}\,of_{N-1} - Q^*R_N'' - (1-Q^*)oR_N''$$

At the surface ($i = 0$) the finite difference form becomes

$$m_o f_1 + p_o f_o = a_o \qquad \text{(A3.6)}$$

where

$$m_o = \frac{2Q^*}{j^2}$$

$$p_o = -\frac{2Q^*}{j^2} + Q^*R_o' - \frac{K'}{l} - 2Q^*K\left(\frac{1}{j}+1\right)$$

$$a_o = \frac{-2(1-Q^*)}{j^2}\,of_1 + of_o\left\{\frac{2(1-Q^*)}{j^2} - (1-Q^*)oR_o' - \frac{K'}{l} + 2(1-Q^*)\,oK\left(\frac{1}{j}+1\right)\right\}$$

$$-QR_o'' - (1-Q^*)\,oR_o'' - 2Q^*FK\left(\frac{1}{j}+1\right) - 2(1-Q^*)\,oK\,oF\left(\frac{1}{j}+1\right)$$

Equations (A3.4) to (A3.6) represent a set of $N+1$ simultaneous algebraic equations which may be written

$$\underline{A}\,\underline{f} = \underline{b}.$$

The matrix of coefficients, $\underline{A}$, is tridiagonal, the elements being m_i, n_i and p_i. Using assumed values of R' and R'' the equations may be solved to find $\underline{f}$, by means of the Thomas algorithm discussed in Appendix 1.

APPENDIX 4

THE SOLUTION OF THE ONE-DIMENSIONAL TRANSIENT REACTOR MODEL

A4.1 The finite difference representation of the equations.

Equations (8.1), (8.2) and (8.3) have a similar form and may be written

$$\frac{\partial f}{\partial z} + K' \frac{\partial f}{\partial \tau} + K''f + K^* + R'f + R'' = 0 \qquad (A4.1)$$

where the parameters are defined in Table A4.1 for each of the equations under consideration.

In implicit finite difference form this equation may be written:

$$f\left(\frac{Q^*}{k} + \frac{K'Q}{j} + QQ^*(K'' + R')\right) = - xf\left(-\frac{Q^*}{k} + K'\frac{(1-Q)}{j} + (1-Q)Q^*(K'' + xR')\right)$$

$$- of\left(\frac{1-Q^*}{k} - \frac{K'Q}{j} + Q(1-Q^*)(K'' + oR')\right) - oxf\left(-\frac{1-Q^*}{k} - K'\frac{(1-Q)}{j} + (1-Q)(1-Q^*)(K'' + oxR')\right.$$

$$-QQ^*R'' - Q(1-Q^*)oR'' - (1-Q)Q^* xR'' - (1-Q)(1-Q^*)oxR'' - Q^*K^* - (1-Q^*)\, oK^*$$

where the prefix o indicates the value of a variable at the previous time position

x indicates the value of a variable at the previous axial position

ox indicates the value of a variable at the previous time and axial positions

j is the step size in the time (τ) direction

k is the step size in the axial (z) direction

Q and Q* are weighting factors defined by:-

$$0 < Q \leq 1$$

$$0 < Q^* \leq 1$$

A4.2 A check on the heat balance for an adiabatic reactor.

In order to have some check on the results computed by the transient reactor model, a heat balance over the reactor may be carried out. That

Equation	f	K'	K''	K*	R'	R''
8.1	C_A	$\frac{G_5}{G_1}$	0	0	$G_2 (\phi_1^2 C_A^{n_1 - 1} + \phi_3 C_A^{n_3 - 1}) \eta$	0
8.2	C_B	$\frac{G_5}{G_1}$	0	0	0	$-G_2 (\phi_1^2 C_A^{n_1} + \phi_3^2 C_A^{n_3}) \eta \psi$
8.3	T	$\frac{G_6}{G_3}$	$\frac{2Nu^*}{G_3 w} + G_4$	$\frac{-2Nu^*}{A_3 w} T_c$	0	$-G_4 t$

TABLE A4.1. The expressions for the general terms in equation (A4.1) obtained from equations (8.1), (8.2) and (8.3).

the heat balance should be confirmed is a necessary, but not sufficient, condition for the true solution, but in a highly non-linear system, such as the one studied here, it is very unlikely that any computational errors would give rise to a solution which satisfies the heat balance. The data used for the models are given in Table A4.2, and are such that they ensure complete conversion under all the conditions which arise.

ϕ_1	1.01×10^4	G_1, G_3	0.84
B_o	5×10^{-5}	G_2	0.0949
C_A	1.0	G_4	76.85
$\frac{K_T}{Nu'}$	1.55	G_5, G_6	0
Sh'_A	500	τ	142 seconds

TABLE A4.2. The data used for the heat balance on the adiabatic reactor.

The reaction scheme is confined to the A ——→ B step since this shows all the main dynamic characteristics of the more complex reaction scheme. The response of the reactor to a step increase in fluid temperature is shown in Figure A4.1. It is apparent that the same general characteristics as shown as for the non-adiabatic system when a similar change in temperature occurs. Rather surprisingly (at first sight) the outlet temperature falls, but this can be explained as being due to the following effects occurring in sequence.

(1) After the step change, some of the heat of reaction is used to heat the pellets in the inlet region, and less heat is available to heat the fluid. There is also heat transferred from the fluid to the pellets, and these effects cause the fluid temperature to

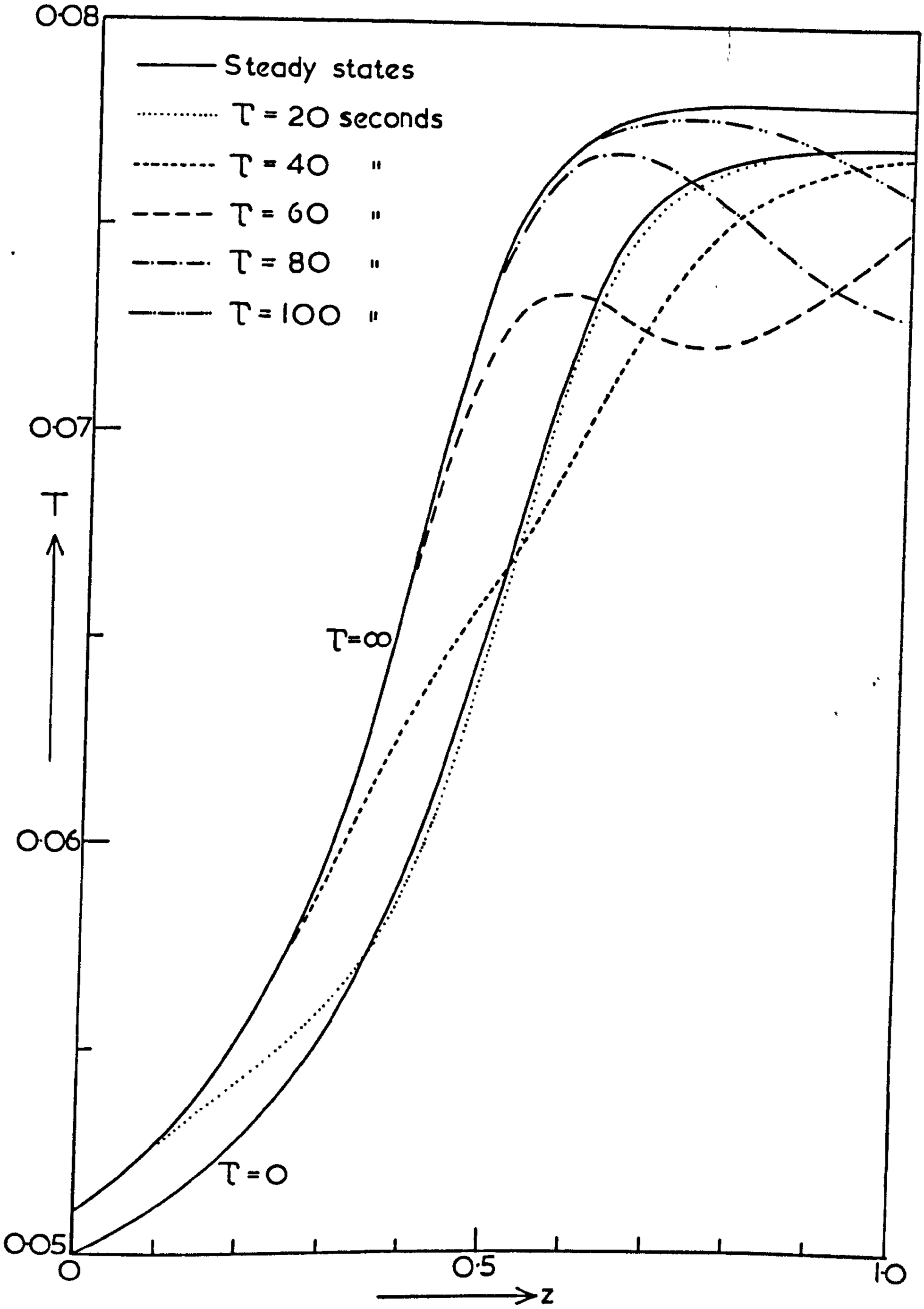

FIG. A4.1 The temperature profiles in an adiabatic reactor following a step increase of 0.001 in the dimensionless inlet temperature. Data as given in Table A4.2. For an activation energy of 32 Kcal./g.mole this change represents approximately 16°C.

fall below its initial value.

(2) In the outlet region of the reactor, there is no reaction and the pellet temperature begins to fall as the fluid temperature falls.

(3) Eventually as an increasing amount of the bed approaches its final steady state, the hot fluid begins to reach the pellets in the outlet region and the temperature in this region also rises towards final steady state.

Since the reaction goes to completion, the temperature rise through the bed would be constant in the absence of any capacitance effects. It is some time before the fluid at the outlet reaches its final steady state temperature and this 'loss' of heat should correspond to the increase in thermal energy within the bed.

The heat 'lost' from the fluid stream corresponds to the shaded area in Figure 4.2 and is given by

$$\rho u C_p \int_0^{\tau} (\text{final outlet temperature} - \text{outlet temperature})\, d\tau$$

The heat gained by the bed is given by

$$\rho^* (1-e) L C_p^* \int_0^1 (\text{final pellet temperature} - \text{initial pellet temperature})\, dz$$

These expressions should be equal and in the normal dimensionless form they may be written

$$(T_{\text{final outlet}} - T_{\text{mean outlet}})\tau = \frac{2}{3} \frac{K_T}{Nu'} G_4 (t_{\text{mean final}} - t_{\text{mean initial}}) \qquad (A4.2)$$

where the mean values must be obtained by carrying out the integrations above. The transient response has been examined over 142 seconds in 2-second steps and the integration carried out by the trapezoidal rule.

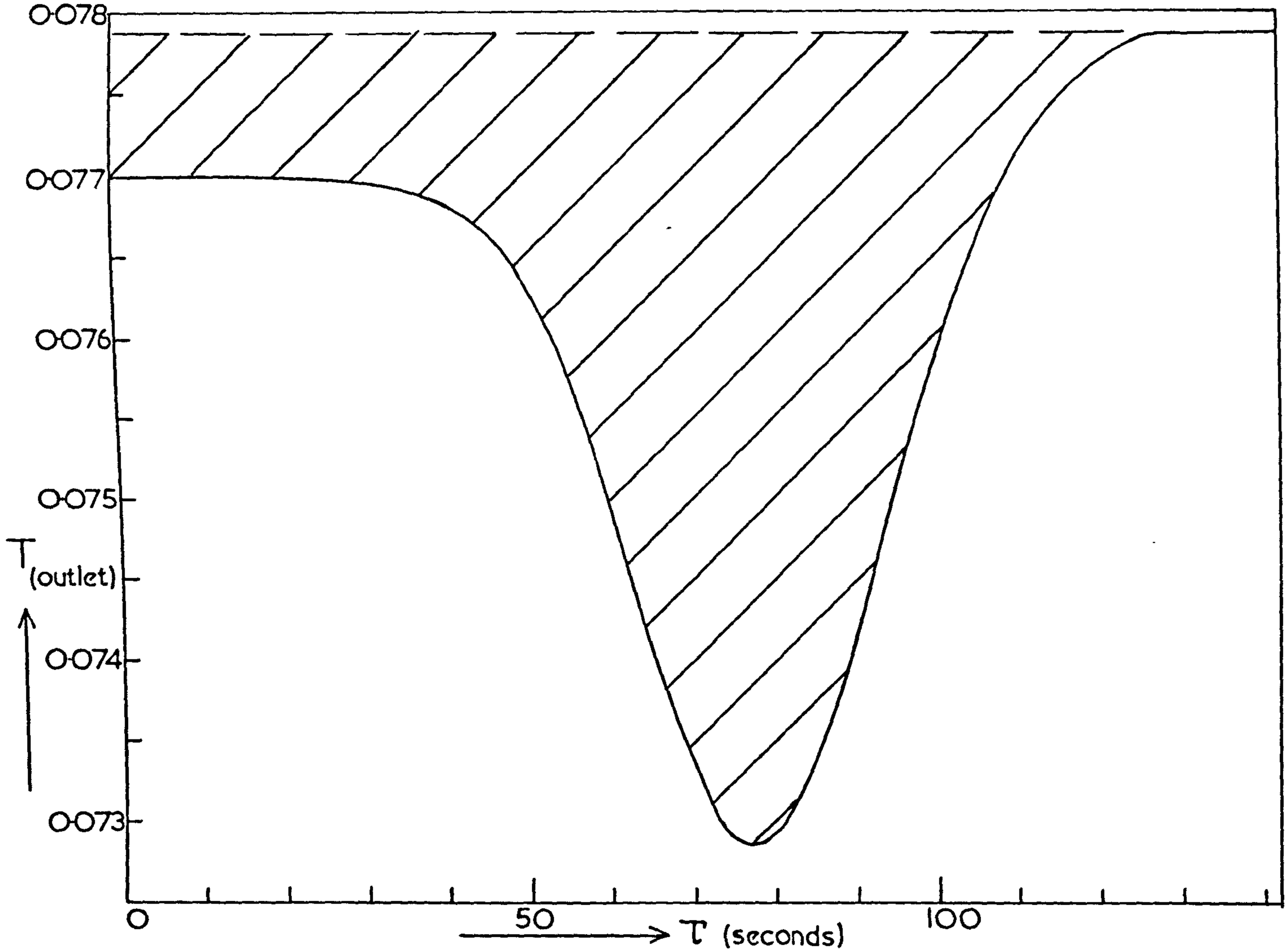

FIG. A4.2 The outlet temperature from an adiabatic reactor following a step increase of 0.001 in the dimensionless inlet temperature. Data as given in Table A4.2. For an activation energy of 32 Kcal./g.mole this change represents approximately 16°C.

Mean outlet temperature over 142 seconds = 0.0761435

Final outlet temperature = 0.0779860

142 x difference = 0.261787 (i.e. l.h.s. of equation A4.2)

Initial mean pellet temperatue in the reactor = 0.0654012

Final mean pellet temperature in the reactor = 0.0686983

$\frac{2}{3} \frac{K_T}{Nu'} G_4$ x difference = 0.261831 (i.e. r.h.s. of equation A4.2)

The heat balance is therefore excellent, agreement being to within 0.02%, indicating a high order of accuracy on the results of the solution of the transient equations.

APPENDIX 5

DETERMINATION OF THE BOUNDS ON NON-UNIQUENESS FOR COMPLEX AND NON-FIRST ORDER REACTIONS

A5.1 Complex reactions.

In Chapter 9, a method was developed for determining the bounds on non-unique solutions of the catalyst pellet model. The condition for the bound was shown to be $\frac{dT}{dt} = 0$, where T and t are the dimensionless fluid and pellet temperatures respectively.

For the complex reaction scheme, the same equation must be solved, but the relationship between T and t, given by the heat balance on the pellet, is more complicated than for the single reaction case. As was shown in Chapter 4, the heat balance may be written

$$T = t - B\left(Sh'_A\left(1 - \frac{c_{A_s}}{C_A}\right)\left(\frac{k_1^*}{k_1^* + k_3^*}(1 + H_2) + \frac{k_3^*}{k_1^* + k_3^*} H_3\right) - Sh'_B\left(\frac{c_{B_s}}{C_A} - \frac{C_B}{C_A}\right)H_2\right) \qquad (A5.1)$$

where $c_{A_s} = F_1$

$c_{B_s} = F_3 - F_2$ when $k_1^* + k_3^* \neq \delta k_2^*$

or $c_{B_s} = F_5 - F_4$ when $k_1^* + k_3^* = \delta k_2^*$

F_1 to F_5 are functions of the pellet temperature, t, and are given by equations (4.12), (4.20), (4.21), (4.24) and (4.25).

Differentiating equation (A5.1), the bounds on the non-unique region are obtained by solving the equation,

$$\frac{1}{B} \mp Sh'_A\left(1 - \frac{c_{A_s}}{C_A}\right)\left(\frac{d}{dt}\left(\frac{k_1^*}{k_1^* + k_3^*}\right)(1 + H_2) + \frac{d}{dt}\left(\frac{k_3^*}{k_1^* + k_3^*}\right)H_3\right) \mp \frac{Sh'_A}{C_A}\frac{dc_{A_s}}{dt}$$

$$\left(\frac{k_1^*}{k_1^* + k_3^*}(1 + H_2) + \frac{k_3^*}{k_1^* + k_3^*} H_3\right) \mp \frac{Sh'_B}{C_A}\frac{dc_{B_s}}{dt} H_2 = 0 \qquad (A5.2)$$

The expressions for c_{A_s} and c_{B_s} (i.e. the functions F_1 to F_5) are fairly complex functions of the pellet temperature, t, and the fully expanded form of equation (A5.2) is even more complex. Differentiation of the terms in this equation is basically straightforward, but the resulting expression comprises many relatively simple terms, the majority of which occur several times. Evaluation of the left hand side of the equation can therefore be broken down into a series of simple steps, and this form of calculation is ideally suited to a computer. Each of the derivatives needs to be evaluated once only for each value of t, and can then be stored and used as often as necessary. Clearly, this is extremely efficient when compared to writing out the fully expanded form of equation (A5.2) and evaluating each function of t as it occurs. The derivatives which occur during the differentiation of c_{A_s} and c_{B_s} are as follows:-

$$\frac{dk_i^*}{dt} = \frac{E_i}{E_1 t^2} k_i^* \qquad (i = 1, 2, 3)$$

$$\frac{d}{dt}\sqrt{k_1^* + k_3^*} = \frac{1}{2\sqrt{k_1^* + k_3^*}}\left(\frac{dk_1^*}{dt} + \frac{dk_3^*}{dt}\right)$$

$$\frac{d}{dt}\sqrt{\delta k_2^*} = \frac{\delta}{2\sqrt{k_2^*}}\frac{dk_2^*}{dt}$$

$$\frac{d}{dt}\left(\coth\sqrt{k_1^* + k_3^*}\right) = \left(1 - \coth^2\sqrt{k_1^* + k_3^*}\right)\frac{d}{dt}\sqrt{k_1^* + k_3^*}$$

$$\frac{d}{dt}\left(\coth\sqrt{\delta k_2^*}\right) = \left(1 - \coth^2\sqrt{\delta k_2^*}\right)\frac{d}{dt}\sqrt{\delta k_2^*}$$

$$\frac{d}{dt}\left(\tanh\sqrt{k_1^* + k_3^*}\right) = \left(1 - \tanh^2\sqrt{k_1^* + k_3^*}\right)\frac{d}{dt}\sqrt{k_1^* + k_3^*}$$

where $k_i^* = \theta_i^2 \exp\left(-\frac{E_i}{E_1 t}\right)$

Equation (A5.2) may be solved by the method of false position, and since the heat generation function represented by $Bx(Sh'_A$ ..... etc.) in equation (A5.1) is essentially the same shape as that for the single reaction,

no convergence difficulties should occur. As before, there are two roots of the equation, and the one to which the solution finally converges will depend on the initial value of t chosen.

For the simple reaction, the results were plotted in the T, B plane, and the locus of the bound on the non-unique region depends only on θ_1 and Sh'_A, which are constant for a given reactor operating at a fixed flowrate. The small number of parameters make it possible to construct graphs which cover all possible operating conditions, but this is not so for complex reactions. In this case, the majority of the parameters will also be fixed for a given reactor (such as θ_i, E_2/E_1, H_2 etc.) but C_B will not remain constant. This means that one curve is no longer sufficient to examine the performance of the reactor in terms of uniqueness, but at each point in the reactor it is necessary to choose the appropriate C_B curve to determine whether non-unique solutions are possible. This is illustrated in Figure A5.1 which shows a reactor profile of temperature against B (i.e. $B_o \times C_A$), with the values of C_B marked on it and the non-unique regions indicated. Initially, at the reactor inlet, the catalyst pellets are in a unique state since $C_B = 0$ and the point lies outside the non-unique region plotted for this value of C_B. Further down the reactor, however, C_B rises to 0.5 (point P on the diagram), and at this point it falls within the appropriate non-unique region. The concentration of B continues to rise to a maximum value and then falls as species B is consumed. When the concentration has fallen to 0.5 (point Q on the diagram), the state of the pellet is again unique, since Q lies outside the bounds for $C_B = 0.5$.

This procedure is slightly more laborious than that which is required for the single reaction, but presents no problems during solution of reactor models, since relatively little storage would be needed to retain the bounds on the non-unique region. This would be true even if several dozen curves were to be stored, since they are made up of very simple shapes which could be adequately represented by simple algebraic functions.

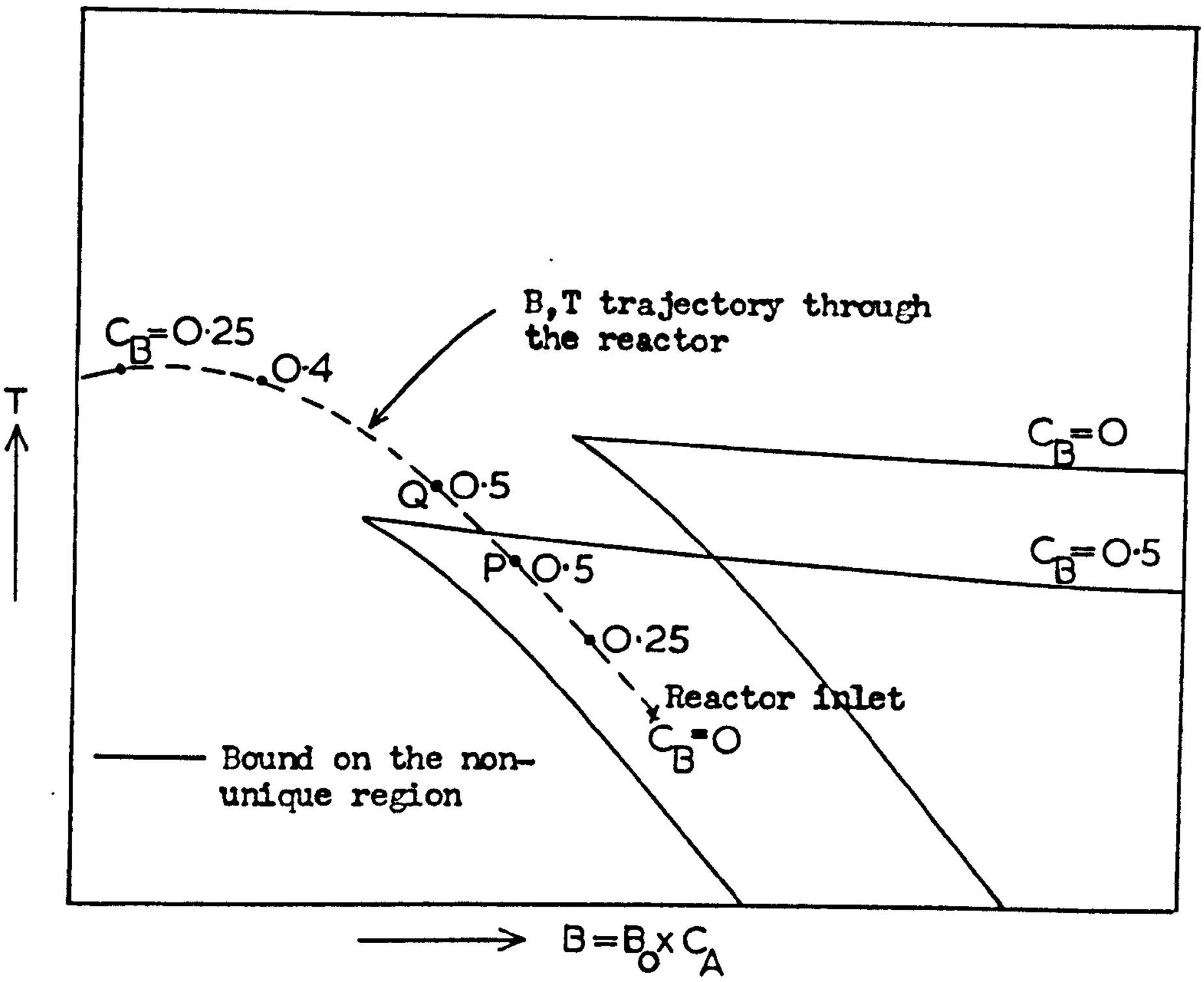

FIG. A5.1 Schematic diagram showing how an examination of global stability may be carried out for a complex reaction.

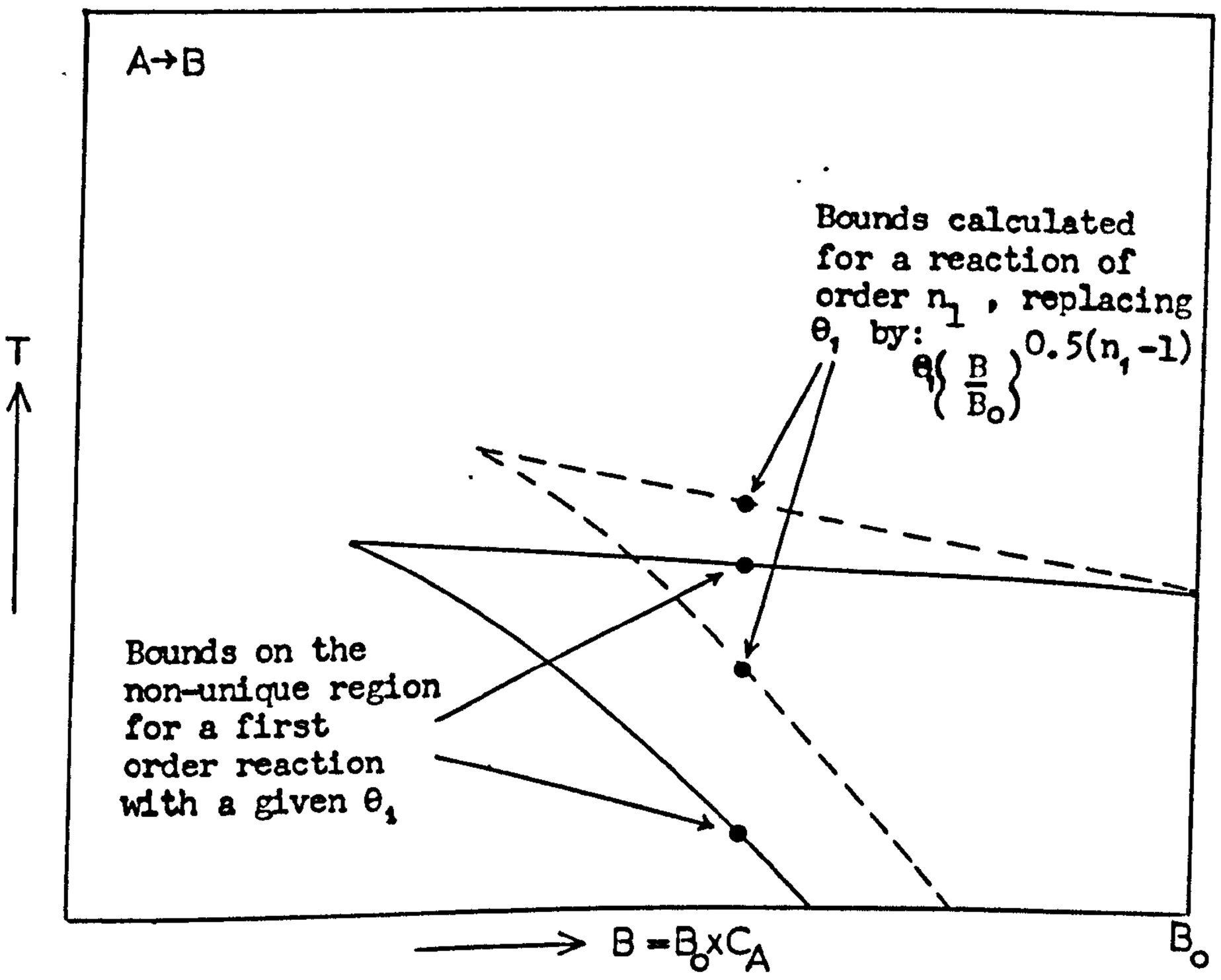

FIG. A5.2 Schematic diagram showing the change in the non-unique region for a non-first order reaction (assuming that both have the same initial value of θ_1 at B_o).

A5.2 Non-first order reactions.

For reactions other than first order, the analytic solution of the pellet equations is only possible if a pseudo-first order rate constant can be defined which is sufficiently accurate over the range of concentrations occurring between the pellet centre and the surrounding fluid. In dimensionless terms this is k_i^* where,

$$k_1^* = \theta_1^2 \exp(-\frac{1}{t})\ C_A^{n_1 - 1}$$

$$k_2^* = \theta_2^2 \exp(-\frac{E_2}{E_1 t})\ C_B^{n_2 - 1}$$

$$k_3^* = \theta_3^2 \exp(-\frac{E_3}{E_1 t})\ C_A^{n_3 - 1}$$

No problems arise with these reactions since the non-unique region can be plotted in terms of a modified θ_i, which will be written θ_i^*. For a given reactor, C_A is known for any value of B since $B = B_o \times C_A$. Therefore, when the bounds on non-uniqueness are calculated at a series of values of B (as for the first order reaction), it is only necessary to calculate a new value of θ_i^* and the bounds are evaluated as before. θ_i^* is given by

$$\theta_i^* = \theta_i\ C_A^{\frac{n_i - 1}{2}} = \theta_i (\frac{B}{B_o})^{\frac{n_i - 1}{2}} \qquad \text{for } i = 1 \text{ and } i = 3$$

This is illustrated in Figure A5.2, where the non-unique region for first order and non-first order reactions are indicated for the $A \longrightarrow B$ reaction. When the full set of complex reactions is occurring, a curve must be drawn for each value of C_B, as was the case for first order reactions. This time, however, not only C_B will change, but also θ_2^* where:

$$\theta_2^* = \theta_2^* C_B^{\frac{n_2 - 1}{2}}$$

Unlike θ_1^* and θ_3^* this remains constant all along the curve (since this is drawn for constant C_B). Having drawn the relevant curves, the reactor

trajectories can be examined in the same way as described for Figure (A5.1).

Under the conditions which occur in the region of temperature runaway, there may be some doubt about the validity of assuming that a sufficiently good pseudo-first order rate constant can be defined over the range of conditions existing within and around any one pellet. Under normal operating conditions, the concentration gradients across the boundary layer and within the pellet are small, but in the non-unique region one of the steady states gives rise to characteristically steep gradients. Nevertheless the proposed method will still give at least some clue that multiple solutions are likely to exist, and for many purposes, this will be sufficient.

NOMENCLATURE

a	Parameter in the expression for a parabolic radial temperature profile.
a_i	Matrix element in the finite difference formulation of differential equations.
A_i	Arrhenius pre-exponential factor for reaction i.
b	Pellet radius.
B_o	Dimensionless exothermicity factor $\frac{(-\Delta H_1)Dp_A C_o Rg}{2b\ hE_1}$
B	$B_o \times C_A$
c_A, c_B	Dimensionless concentrations within the catalyst pellet $\frac{Cp_A}{C_o}$, $\frac{Cp_B}{C_o}$
c_{A_s}, c_{B_s}	Surface values of c_A and c_B
C_A, C_B	Dimensionless concentrations within the fluid $\frac{Cf_A}{C_o}$, $\frac{Cf_B}{C_o}$
Cf_A, Cf_B	Concentrations in the fluid
Cp_A, Cp_B	Concentrations within the catalyst pellet
C_o	Reference concentration of reactant A
C_p, $C_p{}^*$	Specific heats of fluid and pellet respectively
Df_A, Df_B	Effective interstitial radial diffusivities in the fluid
Dp_A, Dp_B	Effective radial diffusivities within the catalyst pellet
e, e*	Porosity of the fixed bed and pellet respectively
E_i	Activation energy for reaction i
f	Dependent variable in the general form of the differential equations
F	Fluid phase state variable C_A, C_B or T
F_1 to F_8	Constants in the analytic solution of the single pellet model
g	$= \tanh(r^*) = \tanh\sqrt{k_1^*}$

G_1 to G_8 are parameters (dimensionless unless otherwise stated) used in the models of the reactor, and are defined as follows:-

G_1	$\frac{R^2}{2bL}\ Pe_M$
G_2	$\frac{(1-e)L\ Dp_A}{b^2\ ue}$

G_3 $\quad \frac{R^2}{2bL} \, Pe_H$

G_4 $\quad \frac{(1-e)3\,hL}{b\rho\, ueC_p}$

G_5 $\quad \frac{R^2 e}{2bu} \, Pe_M = G_1 \, \frac{Le}{u}$ seconds

G_6 $\quad \frac{R^2 e}{2bu} \, Pe_H = G_3 \, \frac{Le}{u}$ seconds

h — Step length in a finite difference grid

h — Pellet to fluid heat transfer coefficient

H — Dimensionless exothermicity factor $\frac{(-\Delta H_1) Dp_A C_o Rg}{Kp\ E_1}$

H_2, H_3 — Ratios of heats of reaction $\frac{(-\Delta H_2)}{(-\Delta H_1)}$, $\frac{(-\Delta H_3)}{(-\Delta H_1)}$ respectively

H* — The larger of H_3 and $(1 + H_2)$

i — Reaction number (1, 2 or 3)

i — Number of a node in a finite difference network

j — Step length in a finite difference grid

k — Step length in a finite difference grid

k_i — Rate constant at a point in the catalyst pellet for reaction i

k_i^* — Dimensionless first order (or pseudo-first order) rate constant evaluated at the pellet temperature = $\theta_i^2 \exp(-\frac{E_i}{E_1 t}) = \phi_i^{*2}$ (for a first order reaction).

k_i' — Dimensionless pseudo-first order rate constant evaluated at the fluid temperature = $\theta_i^2 \exp(-\frac{E_i}{E_1 t}) \, C_{(A,B)}^{n_i - 1} = \phi_i^2 \, C_{(A,B)}^{n_i - 1}$

K, K°, K', K'', K* — Parameters in the general formulations of differential equations (Appendices 1 to 4).

K_c — 'Capacitance' of the catalyst pellet to absorb mass $\frac{b^2 e^*}{Dp_A}$ seconds

K_T — 'Capacitance' of the catalyst pellet to absorb heat $\frac{\rho^* b^2 C_p^*}{Kp}$ seconds

k_{c_A}, k_{c_B} — Fluid to pellet mass transfer coefficients

Kf — Effective interstitial radial conductivity in the fluid phase

Kp — Effective radial conductivity within the catalyst pellet

l — Distance from the reactor inlet

l — Step size in a finite difference network

L	Reactor length
m_i	Element of the tridiagonal matrix in the finite difference formulation of differential equations
n_i	Order of reaction i
n_i	Element of the tridiagonal matrix in the finite difference formulation of differential equations
N	Number of radial steps in the finite difference grid (nodes are 0, 1 .... N)
Nu'	Modified Nusselt number for heat transfer between pellet and fluid = $\frac{2bh}{Kp}$
Nu_w	Nusselt number for heat transfer between fluid and tube wall = $\frac{RU}{Kfe} = \frac{RU\ Pe_H}{2b\rho\ ueC_p}$
Nu_w^*	Effective overall Nusselt number for heat transfer between fluid and tube wall. Used in the one-dimensional model.
of	The value of f at the previous time step (i.e. known).
oxf	The value of f at the previous time and axial step (i.e. known).
p_i	Element of the tridiagonal matrix in the finite difference formulation of differential equations
P	Cycle time (period) for a sinusodial perturbation
Pe_H	Radial Peclet number for heat transfer in the fluid phase = $\frac{2bu\rho C_p}{Kf}$
Pe_M	Radial Peclet number for mass transfer in the fluid phase = $\frac{2bu}{Df}$
Q, Q*	Weighting constants in the finite difference representation of differential equations such that $0 < Q, Q^* \leqslant 1$.
r	Dimensionless radial position in the reactor x/R
r*	$= \sqrt{k_1^*}$
R	Reactor radius
R', R''	Non-linear terms in the general forms of the differential equations (Appendices 1 to 4).
Rg	The gas constant
s	Distance from the centre of the catalyst pellet
Sh_A', Sh_B'	Modified Sherwood numbers $\frac{2bk_{cA}}{Dp_A}$, $\frac{2bk_{cB}}{Dp_B}$
t	Dimensionless pellet temperature $\frac{Tp\ Rg}{E_1}$

t_s	Surface value of t
T	Dimensionless fluid temperature $\frac{Tf\ Rg}{E_1}$
T_a	Value of T on the reactor axis
Tc	Coolant temperature
T_c	Dimensionless coolant temperature $\frac{Tc\ Rg}{E_1}$
Tf	Temperature of fluid
T_m	Radial mean value of T
Tp	Temperature of catalyst pellet
u	Interstitial fluid velocity
U	Fluid to coolant overall heat transfer coefficient
x	Distance from the reactor axis
xf	The value of f at the previous axial step (i.e. known)
y	Dimensionless pellet co-ordinate $1 - {}^{s}/_{b}$
y_I	The value of y where the step size changes in the finite difference network
z	Dimensionless axial position in the reactor $\frac{l}{L}$
z_A, z_B	Defined by equations (4.6) and (4.13)

Greek Symbols

β_i Exothermicity factor commonly used in the literature = $\frac{(-\Delta H_i) C_o Dp_A}{Kp\ Tf}$

γ_i Activation factor commonly used in the literature = $\frac{E_i}{RgTf}$

δ Ratio of diffusivities within the catalyst pellet = $\frac{Dp_A}{Dp_B}$

δ When used as a prefix indicates a small increment

Δ Ratio of diffusivities in the fluid $\frac{Df_A}{Df_B}$

η Effectiveness factor

θ_i Reaction-Diffusion modulus $b \sqrt{\frac{A_i}{Dp_A}} C_o^{n_i - 1}$

θ_i^* Parameter used in the analysis of multiple solutions to deal with non-first order reactions $\theta_i^* = \theta_i C_A^{(n_i - 1)/2}$ for $i = 1, 3$.
$\theta_2^* = \theta_2 C_B^{(n_2 - 1)/2}$

ρ, ρ^* Densities of fluid and catalyst pellet respectively

τ Time (seconds)

ϕ_i Thiele modulus evaluated at fluid conditions = $\theta_i \exp(-\frac{1}{2T} \frac{E_i}{E_1})$

ϕ_i^* Thiele modulus evaluated at pellet conditions = $\theta_i \exp(-\frac{1}{2t} \frac{E_i}{E_1})$

Ψ Selectivity for species B.

REFERENCES

1. Hougen, O.A., Ind. Eng. Chem., 53, 509 (1961).
2. Froment, G.F., Ind. Eng. Chem., 59 (2), 18 (1967).
3. Denbigh, K., Chemical Reactor Theory, C.U.P. (1965).
4. Bilous, O. and Amundson, N.R., A.I.Ch.E.Jl., 2, 117 (1956).
5. Barkelew, C.H., Chem. Eng. Progr. Symp. Ser., 55 (25), 37 (1959).
6. Coste, J. et al., A.I.Ch.E.Jl., 7, 124 (1961).
7. Liu, S. and Amundson, N.R., Ind. Eng. Chem. Fund., 1, 200 (1962).
8. Liu, S. and Amundson, N.R., Ind. Eng. Chem. Fund., 2, 183 (1963).
9. Liu, S. et al., Ind. Eng. Chem. Fund., 2, 12 (1963).
10. Carberry, J.J. and Wendel, M.M., A.I.Ch.E.Jl., 9, 29 (1963).
11. Vanderveen, J.W. et al., A.I.Ch.E.Jl., 14, 636 (1968).
12. Froment, G.F., Chem. Engng. Sci., 17, 849 (1962).
13. Mickley, H.S. and Letts, R.W.M., Can. J. Chem. Eng., 42, 21 (1964).
14. McGreavy, C. and Crosswell, D.L., 4th European Symposium on 'Chemical Reaction Engineering', Brussels, September 1968.
15. Deans, H.A. and Lapidus, L., A.I.Ch.E.Jl., 6, 656 (1960).
16. McGuire, M.L. and Lapidus, L., A.I.Ch.E.Jl., 11, 85 (1965).
17. Thiele, E.W., Ind. Eng. Chem., 31, 916 (1939).
18. Zeldowitsch, J.B., Acta Physicochim URSS, 10, 583 (1939).
19. Wheeler, A., Adv. in Catalysis, 3, 249 (1951).
20. Prater, C.D. and Weisz, P.B., Adv. in Catalysis, 6, 144 (1954).
21. Weisz, P.B., Z. Physik. Chem., 11, 1 (1957).
22. Weisz, P.B., Chem. Eng. Progr. Symp. Ser., 55 (25), 29 (1959).
23. Prater, C.D., Chem. Engng. Sci., 8, 284 (1958).
24. Schilson, R.E. and Amundson, N.R., Chem. Engng. Sci., 13, 226 (1961).
25. Schilson, R.E. and Amundson, N.R., Chem. Engng. Sci., 13, 237 (1961).
26. Carberry, J.J., A.I.Ch.E.Jl., 7, 350 (1961).
27. Beek, J., A.I.Ch.E.Jl., 7, 337 (1961).
28. Petersen, E.E., Chem. Engng. Sci., 17, 987 (1962).

29. Petersen, E.E., Chemical Reaction Analysis, Prentice Hall (N.J.) (1965).

30. Weisz, P.B. and Hicks, J.S., Chem. Engng. Sci., 17, 265 (1962).

31. Butt, J.B., Chem. Engng. Sci., 21, 275 (1966).

32. McGreavy, C. and Cresswell, D.L., Chem. Engng. Sci., 24, 608 (1969).

33. McGreavy, C. and Cresswell, D.L., Can. J. Chem. Eng., 47, 583 (1969).

34. Hutchings, J. and Carberry, J.J., A.I.Ch.E.Jl., 12, 20 (1966).

35. Cresswell, D.L., Ph.D. Thesis, University of Leeds (1969).

36. Kunii, D. and Smith, J.M., A.I.Ch.E.Jl., 6, 71 (1960).

37. Wei, J., Chem. Engng. Sci., 21, 1171 (1966).

38. Tinkler, J.D. and Metzner, A., Ind. Eng. Chem., 53, 663 (1961).

39. Aris, R., Chem. Engng. Sci., 24, 149 (1969).

40. Aris, R., Chem. Engng. Sci., 6, 262 (1957).

41. Gunn, J., Chem. Engng. Sci., 22, 1439 (1967).

42. Luss, D. and Amundson, N.R., A.I.Ch.E.Jl., 13, 759 (1967).

43. Rester, S. and Aris, R., Chem. Engng. Sci., 24, 793 (1969).

44. Rester, S. et al., Chem. Engng. Sci., 24, 1019 (1969).

45. Gavalas, G.R., Chem. Engng. Sci., 21, 477 (1966).

46. Luss, D., Chem. Engng. Sci., 23, 1249 (1968).

47. Drott, D.W. and Aris, R., Chem. Engng. Sci., 24, 541 (1969).

48. Stewart, W.E. and Villadsen, J., A.I.Ch.E.Jl., 15, 28 (1969).

49. Hlaváček, V. et al., Chem. Engng. Sci., 23, 1083 (1968).

50. Copelowitz, I. and Aris, R., Chem. Engng. Sci., 25, 906 (1970).

51. Marek, M. and Hlaváček, V., Chem. Engng. Sci., 21, 493 (1966), Ibid. 501.

52. Cresswell, D.L., Chem. Engng. Sci., 25, 267 (1970).

53. Frank-Kamenetskii, D.A., Diffusion and heat exchange in Chemical Kinetics, Princeton University Press (1955).

54. Thomas, J.M. and Thomas, W.J., Introduction to the principles of heterogeneous catalysis, Academic Press, London (1967).

55. Setterfield, C.N. and Sherwood, T.K., The role of diffusion in catalysis, Addison-Wesley, Mass. (1963).

56. Aris, R., Introduction to the analysis of chemical reactors, Prentice-Hall Inc., N.J. (1965).

57. Carberry, J.J., Ind. Eng. Chem., 58, 40 (1966).

58. Paris, J.R. and Stevens, W.F., 4th European Symposium on 'Chemical Reaction Engineering', Brussels, September 1968.

59. Calderbank, P.H. et al., 4th European Symposium on 'Chemical Reaction Engineering', Brussels, September 1968.

60. McGreavy, C. and Turner, K., Can. J. Chem. Eng., 48, 200 (1970).

61. Turner, K., Ph.D. Thesis, University of Leeds (1970).

62. Beek, J., Adv. in Chem. Eng., 3, 203 (1962).

63. Bruce, G.H. et al., Trans. A.I.M.E., 198, 79 (1953).

64. Petrovsky, I.G., Lectures on partial differential equations, Interscience, N.Y., 169 (1954).

65. Gunn, D.J., Chem. Engng. Sci., 21, 383 (1966).

66. Tinkler, J.D. and Pigford, R.L., Chem. Engng. Sci., 15, 326 (1961).

67. Sehr, R.A., Chem. Engng. Sci., 9, 145 (1958).

68. Vaidyanathan, K. and Doraiswamy, L.K., Chem. Engng. Sci., 23, 237 (1968).

69. Runge-Kutta-Merson algorithm, Library B3003, University of Leeds Computing Dept.

70. Yagi, S. and Kunii, D., Chem. Eng. (Japan), 18, 576 (1954).

71. Thierney, J.W. et al., A.I.Ch.E.Jl., 4, 460 (1958).

72. Valstar, J.M., A study of the fixed bed reactor with reference to the synthesis of vinyl acetate, Delftsche Uitgevers Maatschappij N.V., Delft (1969).

73. Lapidus, L., Digital Computation for Chemical Engineers, McGraw-Hill (1962).

74. Carberry, J.J. and White, D., Ind. Eng. Chem., 61, 27 (1969).

75. Wheeler, A., in 'Catalysis' Vol. 2, Reinhold, N.Y. (1955).

76. Paris, J.R. and Stevens, W.F., Can. J. Chem. Eng., 48, 100 (1970).

77. Crider, J.E. and Foss, A.S., A.I.Ch.E.Jl., 12, 514 (1966).

78. Beek, J. and Miller, R.S., Chem. Eng. Progr. Symp. Ser., 55 (25), 23 (1959).

79. Amundson, N.R., Ind. Eng. Chem., 48, 27 (1956), ibid. 35.

80. Selby, S.M. (ed.), Standard Mathematical Tables, The Chemical Rubber Co., Ohio (1967).

81. Hatfield, B. and Aris, R., Chem. Engng. Sci., 24, 1913 (1969).

82. Mingle, J.O. and Smith, J.M., A.I.Ch.E.Jl., 7, 243 (1962).

83. Carberry, J.J., A.I.Ch.E.Jl., 8, 557 (1962).

84. Carberry, J.J., Chem. Engng. Sci., 17, 675 (1962).

85. Cunningham, R.A. et al., A.I.Ch.E.Jl., 11, 636 (1965).

86. Miller, F.W. and Deans, H.A., A.I.Ch.E.Jl., 13, 45 (1967).

87. Irving, J.P. and Butt, J.B., Chem. Engng. Sci., 22, 1859 (1967).

88. Fulton, J.W. and Crosser, O.K., A.I.Ch.E.Jl., 11, 513 (1965).

89. Ramaswami, D., Ph.D. Thesis, University of Wisconsin (1961).

90. Hudgins, R.R., Chem. Engng. Sci., 23, 93 (1968).

91. Petersen, E.E., Chem. Engng. Sci., 23, 94 (1968).

92. Petersen, E.E., Chem. Engng. Sci., 20, 587 (1965).

93. Schneider, P. and Mitschka, P., Chem. Engng. Sci., 21, 455 (1966).

94. Reddy, K.A. and Doraiswamy, L.K., Chem. Engng. Sci., 24, 1415 (1969).

95. Copelowitz, I. and Aris, R., Chem. Engng. Sci., 25, 885 (1970).

96. Horn, F.J.M. et al., Chem. Eng. Jl., 1, 79 (1970).

97. Østergaard, K., Chem. Engng. Sci., 18, 259 (1963).

98. von Rosenberg, D.V. et al., Brit. Chem. Eng., 7, 186 (1962).

99. Feick, J. and Quon, D., Can. J. Chem. Eng., 48, 205 (1970).

100. van den Bleek et al., Chem. Engng. Sci., 24, 681 (1969).

101. Hawthorn, R. et al., A.I.Ch.E.Jl., 14, 69 (1968).

102. Rosenbrock, H.H. and Storey, C., Computational Techniques for Chemical Engineers, Pergamon Press, 148 (1966).

103. Crider, J.E. and Foss, A.S., A.I.Ch.E.Jl., 14, 77 (1968).

104. Agnew, J.B. and Narsimhan, G., Chem. Engng. Sci., 25, 685 (1970).